Western University
Scholarship@Western

Digitized Theses | Digitized Special Collections

1987

The Petrology, Mineral Chemistry And Tectonics Of Proterozoic Rift-related Igneous Rocks At Lake Nipigon, Ontario

Richard Harry Sutcliffe

Follow this and additional works at: https://ir.lib.uwo.ca/digitizedtheses

Recommended Citation
Sutcliffe, Richard Harry, "The Petrology, Mineral Chemistry And Tectonics Of Proterozoic Rift-related Igneous Rocks At Lake Nipigon, Ontario" (1987). *Digitized Theses*. 1643.
https://ir.lib.uwo.ca/digitizedtheses/1643

This Dissertation is brought to you for free and open access by the Digitized Special Collections at Scholarship@Western. It has been accepted for inclusion in Digitized Theses by an authorized administrator of Scholarship@Western. For more information, please contact tadam@uwo.ca, wlswadmin@uwo.ca.

National Library
of Canada

Canadian Theses Service

Ottawa, Canada
K1A 0N4

Bibliothèque nationale
du Canada

Services des thèses canadiennes

CANADIAN THESES

NOTICE

The quality of this microfiche is heavily dependent upon the quality of the original thesis submitted for microfilming. Every effort has been made to ensure the highest quality of reproduction possible.

If pages are missing, contact the university which granted the degree.

Some pages may have indistinct print especially if the original pages were typed with a poor typewriter ribbon or if the university sent us an inferior photocopy.

Previously copyrighted materials (journal articles, published tests, etc.) are not filmed.

Reproduction in full or in part of this film is governed by the Canadian Copyright Act, R.S.C. 1970, c. C-30.

THIS DISSERTATION
HAS BEEN MICROFILMED
EXACTLY AS RECEIVED

THÈSES CANADIENNES

AVIS

La qualité de cette microfiche dépend grandement de la qualité de la thèse soumise au microfilmage. Nous avons tout fait pour assurer une qualité supérieure de reproduction.

S'il manque des pages, veuillez communiquer avec l'université qui a conféré le grade.

La qualité d'impression de certaines pages peut laisser à désirer, surtout si les pages originales ont été dactylographiées à l'aide d'un ruban usé ou si l'université nous a fait parvenir une photocopie de qualité inférieure.

Les documents qui font déjà l'objet d'un droit d'auteur (articles de revue, examens publiés, etc.) ne sont pas microfilmés.

La reproduction, même partielle, de ce microfilm est soumise à la Loi canadienne sur le droit d'auteur, SRC 1970, c. C-30.

LA THÈSE A ÉTÉ
MICROFILMÉE TELLE QUE
NOUS L'AVONS REÇUE

NL-339 (r. 86/06)

Canada

THE PETROLOGY, MINERAL CHEMISTRY AND TECTONICS OF PROTEROZOIC RIFT - RELATED IGNEOUS ROCKS AT LAKE NIPIGON, ONTARIO

By

Richard Harry Sutcliffe
Department of Geology

Submitted in partial fulfillment
of the requirements for the degree of
Doctor of Philosophy

Faculty of Graduate Studies
The University of Western Ontario
London, Ontario
September 1986

© Richard Harry Sutcliffe 1986

Permission has been granted to the National Library of Canada to microfilm this thesis and to lend or sell copies of the film.

The author (copyright owner) has reserved other publication rights, and neither the thesis nor extensive extracts from it may be printed or otherwise reproduced without his/her written permission.

L'autorisation a été accordée à la Bibliothèque nationale du Canada de microfilmer cette thèse et de prêter ou de vendre des exemplaires du film.

L'auteur (titulaire du droit d'auteur) se réserve les autres droits de publication; ni la thèse ni de longs extraits de celle-ci ne doivent être imprimés ou autrement reproduits sans son autorisation écrite.

ISBN 0-315-36614-1

December 17, 1987

TO WHOM IT MAY CONCERN:

This is to permit the paper, "U-Pb ages from the Nipigon plate and northern Lake Superior" by D.W. Davis and R.H. Sutcliffe and published in Geological Society of America Bulletin, Vol. 96, 1572-1579, 1985, to be reprinted as an appendix in the thesis of R.H. Sutcliffe.

Donald W. Davis

D.W. Davis

ABSTRACT

The dominant tectonic event in the Lake Superior area was the development of the Keweenawan rift zone at approximately 1110 Ma. The Nipigon plate, which occurs north of a major flexure in the Keweenawan rift, hosted a failed arm during the main phase of rifting. The Nipigon area was also the site of periodic magmatic activity and deposition of sediments for at least 450 Ma prior to Keweenawan rifting.

Lithological sequences present within the Nipigon plate and the ages of these rocks are: passive granite and associated sub-aerial rhyolite (1536.7 +10/-2.3 Ma); alkali basalt and lamprophyre dikes (ca. 1500 Ma); epicontinental clastic sediments of the Sibley Group (<1536 Ma, >1108 Ma); and extensive tholeiitic diabase sills, dikes and cone sheets (1108+4/-2 Ma). These sequences form a shallow basinal structure which overlies Archean crust and is connected to the Lake Superior basin in the south by the Black Sturgeon Graben. An increase in intensity of rifting toward Lake Superior is suggested by the form of the igneous intrusions feeding diabase sills in the Nipigon plate. These feeders change from cone sheets in the north to a dike complex intruding the Black Sturgeon graben in the south.

The diabase and picritic intrusions both crystallized from fractionated magmas. The picrites are cumulate rocks derived at shallow crustal depths from a magma controlled by olivine fractionation. Picrite chills are in equilibrium with olivine phenocrysts of composition Fo_{80} and are interpreted to be the least evolved liquids observed. The diabase sills crystallized from an evolved basaltic liquid controlled by cotectic

crystallization of plagioclase and lesser olivine and pyroxene. The emplacement of dense olivine phyric picritic magmas early in the sequence followed by later voluminous, compositionally controlled magmas of lower density suggests the development of a crustal density filter effect as the igneous event progressed. Delamination of the crust mantle interface is proposed as a mechanism of achieving the density filter effect.

The diabase sills occur as two 150 to 200 m thick intrusions covering an area of 11,000 km^2. The sills were emplaced under conditions approaching hydrostatic equilibrium near the Archean/Proterozoic unconformity. The magma was emplaced as fingers which subsequently coalesced to form sills. At the time of emplacement, the lithostatic load was probably less than 0.4 kbars. Crustal loading of the sedimentary sequence with sills enabled later magmas to erupt as basalts. The sills crystallized over a temperature range of 1100°C to 800°C. Chemical variation within the sills reflects crystallization from multiple pulses of magma, minor crystal accumulation and movement of volatiles to late crystallizing parts of the sills. Variation in pyroxene crystallization sequences and the persistence of olivine during fractionation are a result of variations in a(SiO_2) in the magma. This variation may reflect the degree of contamination with siliceous crustal material.

Pre-Keweenawan passive granites and rhyolites are associated with a zone of ring faulting in northern Lake Nipigon. Alnoite and camptonite lamprophyres are interpreted to be of the same age as the granite. Partial melting of the lower crust with a heat source provided by mafic magmatism is suggested as a mechanism of producing the granites.

Acknowledgements

This work was made possible through the Ontario Geological Survey which provided the field support to map the Lake Nipigon area during the period 1981-1983. In addition, the survey provided analytical assistance and office support. J. Wood, P. Thurston and C.Blackburn are thanked for their interest in the project.

The Department of Geology at the University of Western Ontario provided an enjoyable learning atmosphere. I am grateful for the assistance of R. Greenwood who skillfully helped map parts of the area in 1982 and provided numerous late night discussions. R. Barnett patiently assisted me in the use of the microprobe and was a source of discussion on numerous wavelengths. W. Fyfe supervised the thesis and provided many inspiring ideas.

Discussion with R. Hodder, R. Tronnes, M. Arima, R. Sage and others are gratefully acknowledged. D. Walker, P. Dillon, D. Thompson and J. Hopper assisted in the field work. Tsai Way Wu is thanked for assistance with the XRF. J. Forth made many of the thin sections. E. Ambrose assisted with computing. Drafting was done by K. Gil, B. Moore and L. Radburn. Typing was done by P. Arora and A. Branicky.

Finally, I would like to thank Beth for her support and understanding which made completing this thesis a much easier task.

TABLE OF CONTENTS

Page
CERTIFICATE OF EXAMINATION ii
ABSTRACT iii
ACKNOWLEDGEMENTS iv
TABLE OF CONTENTS vi
LIST OF PHOTOGRAPHIC PLATES viii
LIST OF TABLES ix
LIST OF FIGURES x
LIST OF APPENDIX TABLES xiv

CHAPTER 1-INTRODUCTION 1
1.1 Purpose 1
1.2 Location and Access 1
1.3 Previous Work 2

CHAPTER 2 GENERAL GEOLOGY 4
2.1 General Statement 4
2.2 Archean 7
2.2.1 Archean Supracrustal Rocks 7
2.2.2 Archean Plutonic Rocks 12
2.3 Pre-Keweenawan 14
2.3.1 Felsic Subvolcanic and Volcanic Rocks 15
2.3.2 Alkaline Rocks 20
2.3.3 Sibley Group Sediments 22
2.4 Keweenawan 30
2.4.1 Picritic Rocks 31
2.4.2 Diabase Sills 38
2.4.3 Diabase Dikes, Cone Sheets, Sheets 53

CHAPTER 3-REGIONAL TECTONICS - LATE PROTEROZOIC RIFTING IN THE LAKE NIPIGON AND NORTHERN LAKE SUPERIOR AREA 57
3.1 Introduction 57
3.2 Keweenawan Rift Development 59
3.3 Nipigon Plate 64
3.3.1 Black Sturgeon Graben Structure 70
3.3.2 Feeder Zones of the Diabase Sills 75
3.4 Tectonic Summary 80

CHAPTER 4-PETROLOGY OF LATE PROTEROZOIC DIABASES AND PICRITES FROM LAKE NIPIGON 86
4.1 Introduction 86
4.2 Review of Geological Setting 87
4.3 Nipigon Diabase Sills 90
4.4 Picritic Rocks 95
4.5 Composition 97
4.6 Magma Fractionation 100
4.6.1 Variation in the Diabase Sills 109
4.6.2 Primary Magmas 113
4.7 Density relations and the Emplacement of Picritic and Diabasic Magmas 116
4.8 Summary 120

CHAPTER 5-EMPLACEMENT AND CRYSTALIZATION OF LATE PROTEROZOIC DIABASE SILLS AT LAKE NIPIGON 122
5.1 Introduction 122
5.2 Form of the Nipigon Sills 122
5.3 Contact Zones 125
5.4 Contact Metamorphism 127
5.5 Depth of Emplacement 128
5.6 Emplacement Mechanism 129
5.7 Magma Flow 135
5.8 Mineralogical Variation 137
5.8.1 Pyroxenes 138
5.8.2 Olivine 148
5.8.3 Feldspars 150
5.8.4 Oxides 154
5.8.5 Other phases 154
5.9 Cooling 157
5.10 Olivine compositions and silica activity 158
5.11 Pyroxene crystallization sequence 161
5.12 Differentiation Processes 165
5.13 Summary 167

CHAPTER 6-ASPECTS OF PRE-KEWEENAWAN MAGMATISM IN THE LAKE NIPIGON AREA 169
6.1 Camptonite Dikes and Associated Xenoliths: Implications for Bimodal Magmation 169
6.2.1 Petrography of the Xenoliths 172
6.2.2 Chemistry of Xenolith Phases 176
6.3 Origin of the Xenoliths 180
6.4 Summary 183

CHAPTER 7-SUMMARY AND CONCLUSIONS 185
7.1 Conclusions 185

APPENDIX 1-PUBLICATION 188
U-Pb Ages from the Nipigon Plate and Northern Lake Superior, Davis and Sutcliffe (1985)
APPENDIX 2-ANALYTICAL METHODS, PRECISION AND ACCURACY 197
APPENDIX 3 SAMPLE LOCATIONS, DESCRIPTIONS, AND SUMMARY OF ANALYTICAL WORK 208
APPENDIX 4 MODAL ANALYSES OF SELECTED SAMPLES 220
APPENDIX 5 WHOLE ROCK MAJOR AND TRACE ELEMENT ANALYSES 224
APPENDIX 6 RARE EARTH ELEMENT ANALYSES 252
APPENDIX 7 MINERAL ANALYSES 254

REFERENCES 303

VITA 324

LIST OF PHOTOGRAPHIC PLATES

PLATE 1 9
PLATE 2 17
PLATE 3 24
PLATE 4 34
PLATE 5 40
PLATE 6 46
PLATE 7 50
PLATE 8 174

LIST OF TABLES

Tables

2.1 Table of lithologic units 6

3.1 Rift related events in the Lake Nipigon and northern Lake Superior area 61

4.1 Representative analyses of diabase and picrites from the Lake Nipigon area 93

4.2 Representative mineral compositions from diabases and picrites of the Lake Nipigon area 94

4.3 Average analyses of basaltic rocks from Lake Nipigon, the Lake Superior area and continental basalt provinces 98

4.4 Results of major element subtraction model for diabase fractionation using XLFRAC 107

5.1 Representative analyses of diabase from the D'Alton Lake and Orient Bay sections, Lake Nipigon area 140

5.2 Representative pyroxene analyses 142

5.3 Representative olivine analyses 149

5.4 Representative feldspar analyses 151

5.5 Representative oxide analyses 155

6.1 Whole rock compositions of a camptonite dike and middle Proterozoic granitoids 177

6.2 Representative microprobe analyses of phases in the camptonite dike and xenoliths 179

LIST OF FIGURES

Figure

2.1 Location of the Nipigon plate showing provinces of the Canadian Shield 5

2.2 Geological map of the Nipigon area back pocket

2.3 Generalized cross-section of diabase sills in the Lake Nipigon area 44

3.1 Location of the Nipigon plate and major geological structures in the Great Lakes region. The Keweenawan rift and Nipigon plate are based on the outline of Keweenawan igneous rocks from Halls (1978). The Kapuskasing structural zone is based on a geological outline of the gravity high. 58

3.2 Generalized geology of the Lake Superior area. Based on maps of the Ontario Geological Survey and the geological map accompanying Geological Society of America, Memoir 156. 60

3.3 Geology of the Nipigon plate. Based on maps of the Ontario Geological Survey. Line AB refers to section shown in Figure 3.5. 65

3.4 Bouguer gravity map of the Nipigon plate. Gravity contours labelled in milligals. Based on gravity map accompanying the Geological Society of America, Memoir 156. Pattern shows area underlain by rocks of the Nipigon Plate and Keweenawan rift. 66

3.5 Cross section of the Black Sturgeon graben showing asymmetric structure of the graben and the location of the Fox Mountain dike. Line of cross-section AB is located on Figure 3.3. 72

3.6 Geology of the Kopka cone sheet. Based on maps of the Ontario Geological Survey. 76

3.7 Schematic diagram showing possible relationships between graben formation with axial dike and cone sheet formation. Modified from Koide and Bhattacharji (1975) and Bhattacharji and Koide (1975a, b). 81

4.1 Generalized geology of the Nipigon Plate and the northern Lake Superior area. Location of sampled sections of diabase sills are labelled. Geology from maps of the Ontario Geological Survey. 88

4.2 Mafic and ultramafic rocks of the Nipigon Plate 91 plotted on a) AFM diagram and b) alkalies vs silica diagram for weight % oxides. 91

4.3 Chondrite normalized REE patterns for selected samples from the Nipigon area compared with fields of olivine tholeiite and Fe-Ti tholeiite basalts of Lake Superior from Green (1982). 101

4.4 Basaltic rocks from Lake Nipigon plotted in projections of the basalt tetrahedron using the method of Irvine (1979). Curves separate liquidus fields for abyssal tholeiite glasses and Hawaiian tholeiites as defined by Irvine (1979). 103

4.5 Pearce-type diagrams for selected major elements (molecular % oxides) of basaltic rocks from the Lake Nipigon area. Regression lines with slope are given for comparison with predicted slopes for possible fractionated minerals in inset diagrams. 105

4.6 Assimilation-accelerated fractional crystallization model (atomic proportions) showing possible effect of contaminant approximated by rhyolite melt of the Osler group. 108

4.7 AFM diagram (weight % oxides) showing fields of variation for individual sample sections of diabase sills and the Kopka cone sheet. 110

4.8 Modal and chemical variation versus stratigraphic height for several sections of diabase from the Lake Nipigon area. Olivine and iddingsite are plotted in volume %. Major elements in weight % recalculated to 100% volatile free. Cr in ppm. Olivine data in D'Alton Lake section is from Kavanagh (1981). 112

4.9 MgO-FeO relationships between liquid compositions, model minimum melting relationships (Hanson and Langmuir, 1978) of an Fe-rich mantle composition (Carter, 1970), and a possible primary magma composition (molecular % oxides). 115

4.10 Liquid density versus fractionation (molar Fe/(Fe+Mg) relationships for rocks representative of liquids from the Nipigon area. Also shown is a picritic magma with 12% olivine of composition Fo_{80}. Densities were calculated using the method of Bottinga *et al*. (1982). All Fe was taken as FeO. Liquidus temperatures assumed to be 1100°C for diabase chills and estimated to be approximately 1250°C for the picritic chills using graphical method of Roeder and Emslie (1970). Liquid line of descent for MORB Suite recalculated using method of Bottinga *et al*. (1982) with data used by Stolper and Walker (1980). 117

4.11 Schematic cross-section of the crust-mantle interface showing possible evolution of crustal fracture system. a) Picritic magmas rise along fractures extending through the crust-mantle interface. Magma compositions are controlled by crystal settling and flowage differentiation in the conduits. b) Delamination results in a sub-crustal magma chamber. Evolved magmas are primarily controlled by the crustal density filter effect. 119

5.1 Form of the diabase sills in the vicinity of faults. a)Ring faults in northern Lake Nipigon, b)Black Sturgeon Fault 124

5.2 Hydrostatic relationship between column of magma and column of lithosphere after Bradley (1965). At equilibrium 2.65 h = 2.50 H, and f is the freeboard. 130

5.3 Modal variation in the D'Alton and Orient Bay sections. Minerals are plotted in volume percent. 139

5.4 Pyroxene and olivine chemistry in the Nipigon diabase. Atomic percent. 143

5.5 Details of pyroxenes from selected diabase samples:
a) augite with late pigeonite;
b) augite overgrowing olivine with late orthopyroxene;
c) ophitic augite and pigeonite;
d) pigeonite overgrowing olivine.
Numbered points refer to analyses in e). 146

5.6 Feldspar analyses in the Nipigon diabase. 152

5.7 T-f(O_2) diagram for compositions of coexisting magnetite and ilmenite from Nipigon diabase. Based on model of Spencer and Lindsley (1981). Buffer curves at 1 atm plotted for reference. Points are based on average of 2 to 6 analyses of a single grain of each phase. 156

5.8 Part of the equilibrium phase diagram of the system forsterite-diopside-silica after Kushiro (1972) and Morse (1980). Mantle derived magmas at point A fractionate along path ABCD, magmas mixed with siliceous crust move to point E and fractionate a~~long p~~ath EFCD (Longhi, 1980; Campbell, 1985). Different fractionation paths for rocks from Lake Nipigon are shown. Fo, forsterite; Pr, protoenstatite; Pg, pigeonite; Di, diopside; Si, silica. 163

6.1 Generalized geological map of the northern Lake 171

Nipigon area showing location of the sampled dike. 171

6.2 Chemical compositions of glasses and mineral phases in garnet granulite xenoliths. Ticks indicate direction in which melt should move if skeletal plagioclase crystals were re-dissolved. 182

LIST OF APPENDIX TABLES

Table

A1 Precision of major element analyses performed at the Geoscience Laboratories, Ontario Geological Survey 199

A2 Detection limits, optimum ranges and precision of Ba, Co, Cr, Cu, Ni, Pb and Zn analyses using atomic absorption at the Ontario Geological Survey 200

A3 Detection limits, and precision of Ga, Nb, Rb, Sr, V, Y, Zr analyses using XRF at the University of Western Ontario 201

A4 Detection limits, optimum ranges and precision of Rare Earth Element analyses at the Ontario Geological Survey 202

A5 Major element analyses of olivine YS15 with a MAC 400 electron microprobe, University of Western Ontario 204

A6 Major element analyses of kaersutite standard with a MAC 400 electron microprobe, University of Western Ontario 205

A7 Major element analyses of clinopyroxene BPX with a MAC 400 electron microprobe, University of Western Ontario 206

A8 Major element analyses of plagioclase An_{90} with a MAC 400 electron microprobe, University of Western Ontario 207

The author of this thesis has granted The University of Western Ontario a non-exclusive license to reproduce and distribute copies of this thesis to users of Western Libraries. Copyright remains with the author.

Electronic theses and dissertations available in The University of Western Ontario's institutional repository (Scholarship@Western) are solely for the purpose of private study and research. They may not be copied or reproduced, except as permitted by copyright laws, without written authority of the copyright owner. Any commercial use or publication is strictly prohibited.

The original copyright license attesting to these terms and signed by the author of this thesis may be found in the original print version of the thesis, held by Western Libraries.

The thesis approval page signed by the examining committee may also be found in the original print version of the thesis held in Western Libraries.

Please contact Western Libraries for further information:
E-mail: libadmin@uwo.ca
Telephone: (519) 661-2111 Ext. 84796
Web site: http://www.lib.uwo.ca/

CHAPTER 1

INTRODUCTION

1.1 Purpose

This thesis is a regional study of the tectonics and petrology of mafic igneous rocks in the Lake Nipigon area. These rocks provide a record of igneous activity during a late Proterozoic continental rifting event. The igneous activity and rifting at Lake Nipigon is associated with the much larger Keweenawan rift in Lake Superior to the south.

Prior to the initiation of this project, there was very little information available on the nature of the igneous rocks in the Nipigon area. This study, therefore, began with the undertaking of basic mapping of the igneous province. The purpose of the study is to:

a) document the nature of the Keweenawan and pre-Keweenawan tectonic history of the Nipigon area in order to provide a framework for understanding the mafic magmatism;

b) characterize the structure of the mafic igneous rocks and the conditions of their emplacment; and

c) document the petrology of the mafic igneous rocks.

1.2 Location and Access

Lake Nipigon is centered 150 km north of the city of Thunder Bay in northern Ontario. The area investigated is between latitudes 49°00' to 50°30'N and longitudes 88°00' to 90°00'W (see Figure 2.1). The area is covered by the 1:250 000 NTS topographic maps 52H (Nipigon) and 52I (Armstrong). During the study the Proterozoic rocks were investigated over an area of approximately 20,000km².

Access to the central part of the area is provided by Lake Nipigon which covers an area of approximately 4,300 km². Access points to Lake Nipigon are maintained at Humboldt Bay and Poplar Point in the east, Orient Bay and South Bay in the south and Gull Bay in the west. Northern parts of Lake Nipigon are reached by float equipped aircraft which can be chartered in Armstrong. Logging roads branching off highway 527 in the west and highway 11 in the east provide access to parts of the area away from Lake Nipigon.

1.3 Previous Work

Until the present study, the only regional mapping of the Lake Nipigon area was reported by Wilson (1910) in Memoir 1 of the Geological Survey of Canada which is titled "Geology of the Nipigon Basin, Ontario". Subsequent to the work of Wilson, mapping emphasis was placed on the Archean metamorphic rocks which underlie the Proterozoic igneous rocks. This work includes mapping by Pye (1968) and Mackasey (1970, 1975) east of Lake Nipigon and Pye (1965) and Kaye (1969) west of Lake Nipigon. Sage et al. (1974) mapped and compiled geological data over a large area on the western side of Lake Nipigon as part of the regional reconnaissance mapping of northwestern Ontario. One of the few studies which emphasized the Proterozoic rocks was that of Coates (1972) who mapped the area of Sibley group sediments south of Lake Nipigon.

As a result of the mapping for this study eight 1:50,000 preliminary geological maps have been published (Sutcliffe, 1982; Sutcliffe and Greenwood, 1985). Summaries of this field work are reported by Sutcliffe (1981) and Sutcliffe and Greenwood (1982).

Other work which is relevant to this thesis includes a study of the metallogeny of the Thunder Bay area by Franklin (1970) and a study of the stratigraphy of the Middle Proterozoic Sibley Group sediments south of Lake Nipigon by Franklin et al. (1980). Cheadle (1986) has reported on further analysis of the sedimentary rocks of the Sibley Basin. Investigations of diabase sills south and southwest of the present study area have been made by Pye (1953) and Blackadar (1954). Paleomagnetic studies of igneous rocks at Lake Nipigon have been reported by Palmer (1970) and summarized by Halls and Personen (1982). The ages of igneous rocks in the Lake Nipigon area have been determined by the U-Pb zircon method in conjunction with this thesis (Davis and Sutcliffe, 1985). Previous dating attempts are reported by Silver and Green (1963), Franklin (1970), Hanson and Malhotra (1971), and Hanson (1975).

CHAPTER 2

GENERAL GEOLOGY

2.1 General Statement

The Proterozoic rocks within the area form the Nipigon plate which is part of the Southern Province of the Canadian Shield (Stockwell et al. 1970) (Figure 2.1). The Nipigon plate consists of a 200 to 800 meter thick sequence of late Proterozoic (Helikian) sediments and mafic intrusive rocks which overlie Archean rocks of the Superior Province. In addition, late Proterozoic mafic to ultramafic rocks intrude the Archean basement in the vicinity of the plate. In northern Lake Nipigon, a Middle Proterozoic subvolcanic intrusion and related volcanic rocks occur at the base of the sedimentary sequence.

The rocks of the Nipigon plate form a broad, shallow, structure extending north for 160 km from Lake Superior. In this study the term "Nipigon plate" as defined by Stockwell et al. (1970) is retained. It should be noted, however, that the term "plate" is not used in a global tectonic sense. Wilson (1910) originally referred to the structure as the Nipigon basin, a term which may have been more appropriate.

A table of lithologic units in stratigraphic order is given in table 2.1. The plutonic rock classification follows that of Streckeisen (1976). The following sections describe the occurrence of these lithologies in the Lake Nipigon area. In the descriptions emphasis is placed on the Proterozoic igneous rocks which are the focus of the study. Place names and lithological units referred to in the text are labelled on the geological map

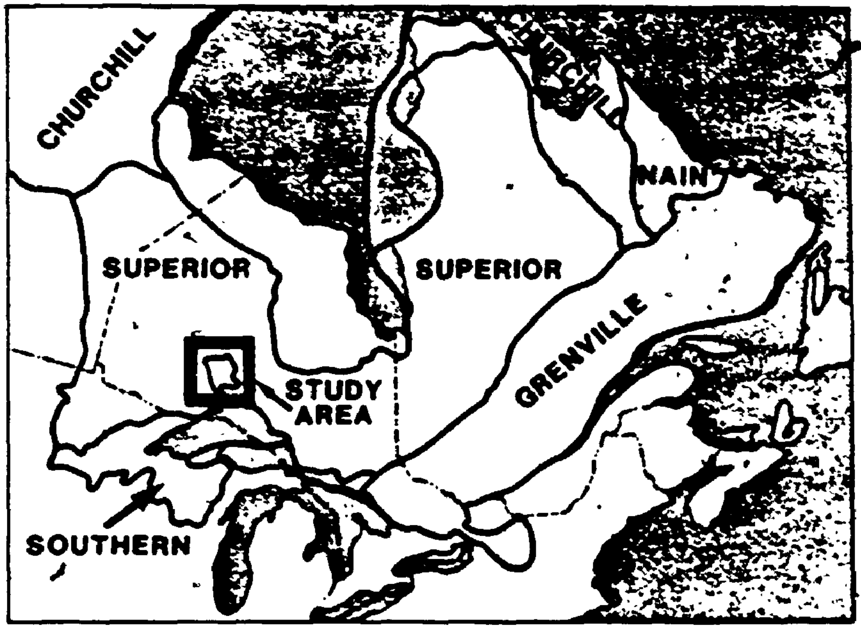
CHURCHILL
CHURCHILL
NAIN
SUPERIOR
SUPERIOR
GRENVILLE
STUDY AREA
SOUTHERN

2.1 Location of the Nipigon plate showing provinces of the Canadian Shield

Table 2.1 Lithologic units in the Lake Nipigon area

- PRECAMBRIAN
    - PROTEROZOIC
        - HELIKIAN
            - KEWEENAWAN (NEO HELIKIAN)
                - Diabase Sills, Sheets and Dikes: diabase; minor granophyre
                - Picritic Intrusions: periodotite; olivine melagabbro; olivine gabbro
            - PRE-KEWEENAWAN (PALEOHELIKIAN?)
                - Sibley Group Sedimentary Rocks: quartz arenite; arkose; conglomerate; calcareous mudstone; dolomitic limestone
                - Felsic Subvolcanic to Volcanic Rocks: quartz-feldspar porphyry; granite; welded tuff and tuff-breccia; volcanic conglomerate
                - Mafic to Ultramafic Lamprophyre Dikes: camptonite; ultramafic alnoite
    - ARCHEAN
        - Felsic to Intermediate Plutonic Rocks: hornblende-biotite tonalite; hornblende diorite; microcline megacrystic granodiorite; biotite granite; biotite-muscovite granite; pegmatite
        - Mafic Intrusive Rocks: amphibolite dikes; pyroxene amphibolite
        - Metasedimentary Rocks: conglomerate; wacke; argillite; biotite schist; migmatized metasedimentary gneiss; chert; ironstone
        - Intermediate Metavolcanic Rocks: tuff breccia; schist
        - Mafic Metavolcanic Rocks: pillowed flow; massive flow; flow breccia; porphyritic flow, plagioclase-hornblende gneiss; foliated to schistose flow

in Figure 2.2.

2.2 Archean

The study area includes Archean supracrustal and plutonic rocks of the Wabigoon and Quetico Subprovinces (Stockwell _et al._, 1970). The Archean rocks are exposed around the margin of the Nipigon plate and locally within the plate underlying the late Proterozoic diabase and sediments.

South of Lake Nipigon, in the Quetico Subprovince the Archean rocks consist of metasediments which increase in metamorphic grade southward and eventually become migmatized. Rocks of the Wabigoon subprovince underlie most of Lake Nipigon. These consist of mafic to intermediate metavolcanic rocks with minor metasediments which are intruded by dioritic, tonalitic and granitic plutons.

Insufficient outcrop of Archean rock occurs within the Nipigon plate to trace the sub-province boundary through Lake Nipigon. A pronounced linear magnetic high (ODM-GSC, 1962) associated with iron formation in the boundary zone indicates that the approximate position of the boundary passes from the east shore of Nipigon, south of Shakespeare Island, through McIntyre Bay to Black Sturgeon Lake (Figure 2.2).

2.2.1 Archean Supracrustal Rocks

Archean mafic metavolcanics of the Wabigoon Subprovince are exposed mainly on the east shore of Lake Nipigon between Humboldt Bay in the north and Lion Bay in the south. These rocks are part of the Geraldton-Beardmore supracrustal belt. Smaller areas of mafic metavolcanics are also exposed east of Black Sturgeon Lake and on the islands between Shakespeare Island and the east shore of Lake Nipigon.

Excellent exposures of mafic metavolcanic rocks are present on the southeast shore of Lake Nipigon. These have been previously described by Mackasey (1975). Along this section, the metavolcanics range from weakly to strongly deformed but massive, pillowed, amygdaloidal and flow breccia textures are preserved (Plate 1). Field examination and limited petrographic study indicates that these rocks are of low metamorphic grade.

In the Humboldt Bay and East Bay area in the northeastern part of Lake Nipigon the metavolcanics are predominately of medium grade. Despite the higher metamorphic grade these rocks are relatively well preserved and also display relict pillow, flow breccia and porphyritic textures.

Mafic metavolcanics occurring in an inlier of Archean rocks in the Black Sturgeon Lake area are also of medium grade. In this area however, the mafic metavolcanics are strongly deformed and have gneissic to schistose textures.

Intermediate to felsic metavolcanic rocks also outcrop on the east side of Lake Nipigon north of Mungo Park Point and between Bish Bay and Poplar Point. The later section is described by Mackasey (1975). These metavolcanics, which are probably andesitic flow breccias and debris flows, consist of poorly sorted angular lapilli to breccia sized fragments in a green chloritic matrix (Plate 1). Minor units of metawacke and

Plate 1

a) Pillow lavas in Archean mafic metavolcanics at Poplar Point on the east shore of Lake Nipigon.

b) Well preserved interbedded wacke and pelite in Archean metasediments on the east shore of Lake Nipigon, south of Poplar Point.

c) Deformed tuff breccia in Archean metavolcanics on the east shore of Lake Nipigon north of Mungo Park Point.

d) Archean plutonic rocks on the northwest shore of Lake Nipigon, north of Wabinosh Bay. The biotite tonalite is strongly foliated to gneissic and contains deformed amphibolite enclaves which are visible at the top of the photo.

e) Archean amphibolite dikes intruding gneissic tonalite on the Britannia Islands, northern Lake Nipigon. The dikes are discordant to gneissosity but have subsequently been deformed. The tonalite at this location was dated by Davis and Sutcliffe (1985).

f) Archean dioritic rocks on the east shore of Ombabika Bay, northeastern Lake Nipigon. The hornblende diorite contains numerous hornblende rich enclaves of varying composition.

argillite are intercalated with the northern sequence.

Metasedimentary rocks are exposed on the east shore of Lake Nipigon south of Poplar Lodge (Plate 1) and immediately east of Lake Nipigon. These rocks are associated with the boundary zone between the Wabigoon and Quetico Subprovinces. The metasediments, which consist of conglomerate, arenite, wacke and argillite have been described by Mackasey (1975). These sediments are of low metamorphic grade and display well preserved primary sedimentary structures.

On the northeastern shore of Humboldt Bay a unit of deformed metaconglomerate with tonalite clasts occurs at the inferred base of the supracrustal belt. The tonalite clasts are texturally similar to tonalite outcropping on the northwestern shore of Humboldt Bay. This relationship suggests that the supracrustal rocks unconformably overlie the tonalite in this area, however, the possible unconformity is obscured by intrusion of late megacrystic granodiorite.

Metasediments exposed east of Black Sturgeon Lake are biotite schists derived from wacke and pelite and have metamorphic assemblages consisting of biotite + quartz + plagioclase ± garnet ± amphibole. Relict bedding is the only primary texture preserved. This sequence of predominantly clastic rocks has local units of ferruginous metasediments containing variable proportions of quartz, biotite garnet, magnetite and gedrite and quartz-magnetite ironstone. The sequence is probably stratigraphically equivalent to the metasediments exposed south of Poplar Lodge.

argillite are intercalated with the northern sequence.

Metasedimentary rocks are exposed on the east shore of Lake Nipigon south of Poplar Lodge (Plate 1) and immediately east of Lake Nipigon. These rocks are associated with the boundary zone between the Wabigoon and Quetico Subprovinces. The metasediments, which consist of conglomerate, arenite, wacke and argillite have been described by Mackasey (1975). These sediments are of low metamorphic grade and display well preserved primary sedimentary structures.

On the northeastern shore of Humboldt Bay a unit of deformed metaconglomerate with tonalite clasts occurs at the inferred base of the supracrustal belt. The tonalite clasts are texturally similar to tonalite outcropping on the northwestern shore of Humboldt Bay. This relationship suggests that the supracrustal rocks unconformably overlie the tonalite in this area, however, the possible unconformity is obscured by intrusion of late megacrystic granodiorite.

Metasediments exposed east of Black Sturgeon Lake are biotite schists derived from wacke and pelite and have metamorphic assemblages consisting of biotite + quartz + plagioclase ± garnet ± amphibole. Relict bedding is the only primary texture preserved. This sequence of predominantly clastic rocks has local units of ferruginous metasediments containing variable proportions of quartz, biotite garnet, magnetite and gedrite and quartz-magnetite ironstone. The sequence is probably stratigraphically equivalent to the metasediments exposed south of Poplar Lodge.

In the Quetico Subprovince, south of Lake Nipigon and Black Sturgeon Lake, the metasedimentary sequence increases in metamorphic grade. With the increase in grade, the metasediments are progressively migmatized and contain a higher proportion of granitic leucosome.

2.2.2 Archean Plutonic Rocks

Felsic to intermediate plutonic rocks are the most widespread Archean lithologies in the Nipigon area. These rocks are well exposed underlying diabase sills in the northern part of Lake Nipigon. In the southern part of Lake Nipigon and south of the lake, outcrops of Archean plutonic rocks are more isolated but are locally exposed both underneath and on top of the diabase sills.

In the northern part of Lake Nipigon, biotite tonalite and hornblende-biotite tonalite are widespread. The tonalite occurs in several phases ranging from gneissic to massive and commonly contains amphibolite and pyroxene amphibolite enclaves (Plate 1). The tonalite is medium grained and typically contains 5 to 15% mafic minerals. Leucocratic medium grained biotite granite and granite pegmatite dikes intrude the tonalite throughout the area. East of Armstrong, biotite granite forms a late massive pluton which is intrusive into tonalite.

A minor intrusion of microcline megacrystic granodiorite forms a sheet peripheral to the supracrustal belt on Humboldt Bay. The granodiorite contains megacrysts of microcline to 2 cm.

On the east shore of Ombabika Bay of Lake Nipigon, inhomogeneous hornblende diorite intrudes the tonalite. The intrusion contains numerous fragments of hornblende rich xenoliths with compositions ranging from hornblende diorite to hornblendite (Plate 1). This intrusion is also associated with a small unit of metamorphosed gabbro, which consists of 30%euhedral amphibole crystals to 2 cm in a medium grained matrix of clinopyroxene and plagioclase.

Mafic amphibolite dikes intrude the tonalite at several locations. On the Britannia Islands of Lake Nipigon (Plate 1), the mafic dikes discordantly intrude gneissic tonalite and have subsequently been deformed. Several mafic dikes are also observed to intrude foliated tonalite on the South Peninsula. This phase of the tonalite is also present as clasts in the conglomerate on Humboldt Bay suggesting that the tonalite is the basement to the supracrustal sequence. The dikes may therefore be feeders for the overlying mafic metavolcanics. Most dikes range in width from 10 cm to 3 meters, however, a large 30 m wide dike is well exposed east of Two Mountain Island.

North of Lake Nipigon, a garnet syenite intrusion occurs on the Pikitigushi River south of Pikitigushi Lake. The intrusion, which is poorly exposed, probably has a diameter of approximately 1 km. The syenite exhibits modal layering and consists of andradite garnet, aegirine-augite, microcline, minor nepheline and oxides. The intrusion is interpreted to be Archean because it is intruded by medium grained granitic dikes similar to other Archean granites in the vicinity.

Granitoid rocks of the Quetico Subprovince, south of Lake

Nipigon consist predominantly of muscovite biotite granite and pegmatite and appear to be derived from anatexis of sediments. Associated zoned pegmatite dikes in the Forgan Lake area contain minor spodumene, tourmaline, garnet and beryl. Breaks (1980) considers that the beryl and spodumene bearing pegmatites of this region may be related to an anatectic center further to the south in the Quetico Subprovince.

Dating of an Archean gneissic tonalite from the Britannia Islands by the U-Pb Zircon method indicates a minimum age of 2716 Ma (Davis and Sutcliffe 1985). This suggests that the Archean basement underlying much of the Nipigon plate formed during the Kenoran event.

2.3 Pre-Keweenawan

In the study area, pre-Keweenawan rocks include: 1)a granite pluton and related volcanic rocks; 2) minor alkali basalt and lamprophyre dikes and 3) sedimentary rocks of the Sibley Group. As with the Archean rocks, these lithologies are exposed mainly beneath the diabase sills but are locally found on top of the sills.

The granite pluton is a passive intrusion which is part of a group of plutons which were intruded into the mid-continent area during the time interval from 1.4 to 1.5 Ga. (Silver _et al._ 1977, Anderson, 1983).

Extensive mid-Proterozoic red bed sequences such as the Baraboo, Barron and Sioux quartzite are also common in the mid-continent region. They are considered to be part of a period of epicontinental deposition known as the Baraboo interval (Greenberg and Brown, 1984). There has been speculation as to whether the Sibley Group is part of this interval, however, data presented by Davis and Sutcliffe (1985) suggest the Sibley is part of a younger sequence.

2.3.1. Felsic subvolcanic and volcanic rocks

Felsic subvolcanic and volcanic rocks of pre-Keweenawan age were first reported from the Nipigon area by Sutcliffe and Greenwood (1982). These rocks are best preserved in the northeast part of Lake Nipigon near English Bay where a quartz-feldspar porphyry to equigranular granite pluton is exposed. The pluton is intruded by picritic dikes and diabase sills and inclusions of porphyry are also locally present in the diabase sills. Most of the exposed pluton is preserved as a basin shaped structure surrounded and underlain by diabase. The granitic pluton outcrops over an area of approximately 30 km^2. A sample of the granite from Redstone Point has an age of 1536.7 + 10/-2.3 Ma. by the U-Pb zircon method (Davis and Sutcliffe, 1985).

The pluton ranges in texture from medium grained, massive, equigranular granite to quartz-alkali feldspar porphyry with an aphanitic groundmass. A distinctive feature of the rock in the field is a brick red weathered and fresh surface due to pervasive hematization. In thin section, the granitic rocks contain 3 to 4 mm tabular orthoclase (30-60%), 3 to 4 mm euhedral oligoclase (0 to 30%), quartz (30%) and chloritized biotite (5%). The mafic minerals are ragged and occur as interstitial grains. Porphyritic phases have euhedral anorthoclase to 6 mm and euhedral to partially resorbed quartz to 4 mm in in a very fine groundmass of quartz, altered feldspar and oxides. In general, feldspars exhibit moderate sericite alteration. Locally feldspars and the matrix are pervasively altered to micaceous minerals and the rock weathers grey to white. Minor carbonate is locally present as an alteration of feldspar and matrix. Significant euhedral zircon and euhedral to interstitial fluorite are present in most samples.

The quartz-alkali feldspar porphyry and granite locally contain numerous inclusions of felsite and porphyry and lesser flow banded and pumiceous fragments (Plate 2). The felsite inclusions are subrounded and up to 10 cm in diameter. Good exposures of the inclusions are present in the islands in the center of English Bay. The presence of inclusions with volcanic textures and the mineralogical similarities between the pluton, inclusions and volcanic rocks suggest that the pluton is the centre of volcanism.

Volcanic rocks exposed in northern Lake Nipigon include debris flow, welded tuff and tuff breccia. Only sparse remnants of the volcanic rocks are preserved, possibly due to erosion during volcanism. Outcrops of volcanic rocks occur on the western shore of Lake Nipigon south of Castle Bay (Plate 2) and on the eastern shore of Lake Nipigon in Humboldt Bay. Numerous large blocks of tuff-breccia occur on the Mountain Islands and are probably not far removed from source.

Plate 2.

a) Proterozoic quartz-feldspar porphyry from the islands in English Bay of Lake Nipigon. The porphyry contains numermous inclusions of felsite and pumiceous rhyolite.

b) Proterozoic volcanic conglomerate, south of Castle Bay, northeast shore of Lake Nipigon. The conglomerate contains subrounded clasts of felsite and clasts of amygdaloidal basalt with bleached rims.

c) Proterozoic volcanic breccia from the Mountain Islands in Lake Nipigon. Angular flow banded clasts of rhyolite are contained in an arkosic matrix. The photograph is taken of a large block which is not in situ.

d) Photomicrograph of welded tuff from Humboldt Bay on the east shore of Lake Nipigon. The tuff forms a thin rind overlying outcrops of Archean rocks. Quartz and biotite phenocrysts in a matrix of devitrified glass shards are visible in the thin section. Plane light, sample 82-92.

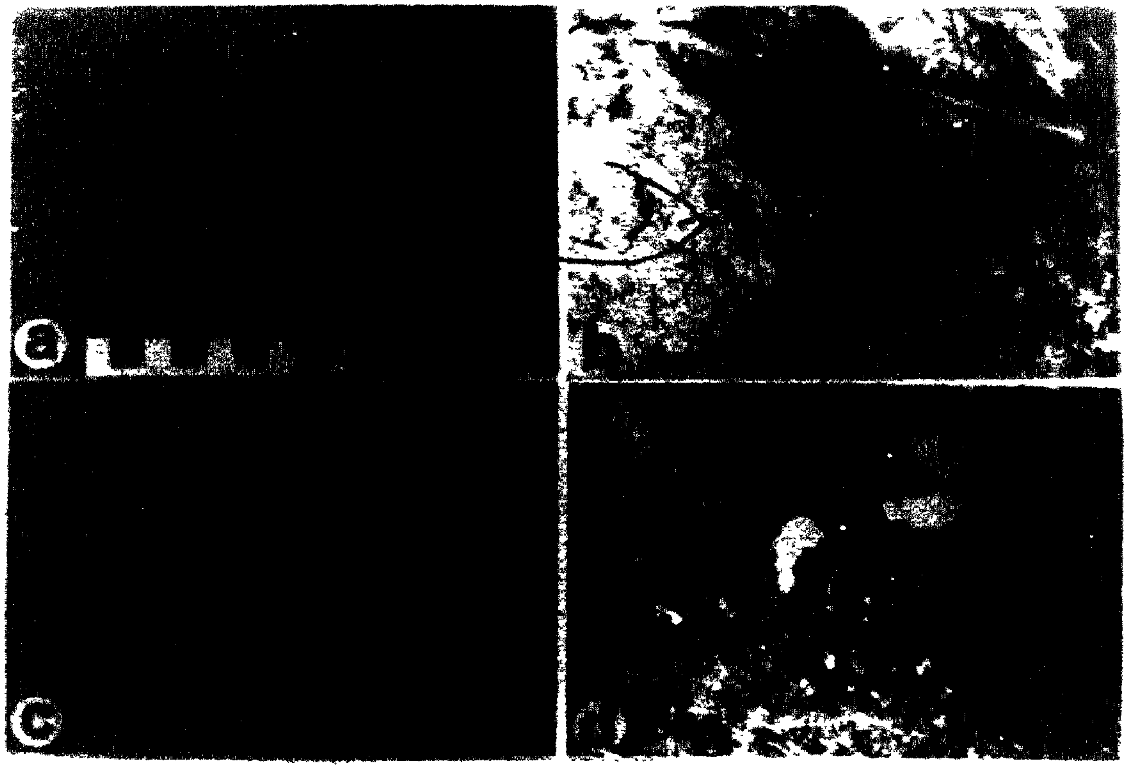
a
c

The exposure of debris flow on the western shore of Lake Nipigon consists of sub-rounded to sub-angular fragments of amygdaloidal basalt with trachytic texture and red felsite in a matrix of immature arkosic sandstone (Plate 2). The basalt fragments are aphanitic, weather dark red-brown and have 1 cm thick bleached rinds. In thin section, the basalt fragments consist of devitrified glass with quench-textured plagioclase crystallites and sparse altered mafic microphenocrysts. The debris flow is overlain by quartz arenite with poorly sorted rounded to sub-angular grains.

On Humboldt Bay, a thin (1 to 2 cm thick) rind of welded tuff (Plate 2) is attached to the surface of outcrops of Archean supracrustal rocks. The tuff is overlain by cross bedded quartz arenite. The association of welded tuff and cross bedded quartz arenite suggests that both were deposited in a sub-aerial environment.

The best examples of pre-Keweenawan felsic volcanics occur as large blocks on Mountain Island in Lake Nipigon (Plate 2). These consist of red to pink weathering, well bedded, tuff breccia and volcanic conglomerate with angular flow banded fragments in a matrix of arkosic sandstone. In thin section, the volcanic rocks are generally highly altered. The volcanic conglomerate contains fragments of quartz porphyry with euhedral phenocrysts of quartz in a groundmass of interlocking fine grained oxidized quartz and feldspar. The matrix of the breccia is a poorly sorted arkose with 60% rounded to subangular quartz, 10% altered feldspar and 30% fine sericite. A thin section of tuff breccia shows that angular fragments consist of quartz porphyry and flow banded felsite to several centimeters. The tuff matrix consists of angular 0.1 mm chips of quartz (20%), altered feldspar (5%), minor muscovite, and granular to sparry carbonate (75%). The volcanic rocks contain accessory zircon.

2.3.2 Alkaline Dikes

The pre-Keweenawan igneous rocks in the Lake Nipigon area consist predominantly of the previously described subvolcanic granite and felsic volcanics, however, numerous minor dikes of ultrabasic lamprophyre, camptonite and trachyte are also present. In the Caribou Lake area, 30 km northwest of Lake Nipigon approximately 40 of these dikes ranging in width from a few centimeters to 3 meters have been observed during detailed mapping (Sutcliffe, 1984). All of the dikes are intrusive into Archean basement consisting of tonalitic granitoid and mafic metavolcanics. These rocks have not been dated but are considered to be pre-Keweenawan because they are not observed to intrude Keweenawan diabase. In addition, the ultramafic lamprophyres at Caribou Lake are petrographically similar to alnoitic lamprophyres dated at 1653±122 Ma in the Marathon area (Platt and Mitchell, 1982).

Alnoitic, phlogopite-olivine lamprophyre dikes occur along the shores of Caribou Lake. The dikes are generally less than 0.5 m in width and also occur as the matrix of narrow breccia zones. The lamprophyres weather bright red to orange brown and have dark to pale grey fresh surfaces. In thin section (Plate 4) these dikes are seen to contain 30 to 50 percent 0.5 mm to 1 cm pseudomorphed olivine phenocrysts and fragments. The olivine is now replaced by serpentine and carbonate. Pale brown pleochroic, fresh, phlogopite phenocrysts range in size from 0.5 to 3 mm are locally bent and fractured and account for up to 25% of the rock. A fine grained matrix of phlogopite, opaques and carbonate forms 40 to 50% of the rock. The opaques consist of blocky grains of chromite, rimmed by magnetite and as atoll spinel structures (Pasteris, 1981). Apatite is present in some specimens.

Camptonite dikes (Plate 4) are porphyritic with an aphanitic to fine grained matrix and usually weather reddish brown. The dikes contain sparse megacrysts to 1 cm of kaersutite, anorthoclase, andesine, augite and ilmenite. Smaller 1 to 3 mm phenocrysts of augite and plagioclase are fresh with oscillatory zoning and resorbed edges. Apatite and relict olivine phenocrysts are observed in one sample.

The matrix of the camptonite dikes consists of tabular 0.1 to 0.2 mm plagioclase, 0.1 mm augite and fine opaques. Carbonate and biotite, locally altered to chlorite, occur as interstitial phases. Some rocks contain sanidine in addition to plagioclase. Sub-spherical miarolitic cavities 2 to 5 mm are filled with carbonate, chlorite and epidote.

Minor trachyte dikes are present within the area. These dikes are bright red on the weathered and fresh surface and contain approximately 90% 0.5 mm laths of orthoclase which displays a well defined trachytic texture. Minor sericite, hematite and chlorite are also present. The trachyte dikes may be genetically related to the subvolcanic granites at English Bay.

2.3.3. Sibley Group Sediments

The Sibley Group is a Helikian red bed sequence (Franklin _et al._, 1980) which forms a northwesterly trending basin from Lake Superior to Lake Nipigon. Within the area the Sibley Group unconformably overlies Archean granitoid and supracrustal rocks and Proterozoic felsic subvolcanic rocks. The Sibley Group rocks are intruded and are locally thermally metamorphosed by the diabase sills.

Franklin _et al._ (1980) have subdivided the Sibley Group in to three formations which consist of a lower unit of quartz arenite with conglomerate lenses (Pass Lake Formation) overlain by red, fine grained arenaceous and clayey dolomite (Rossport Formation) passing upwards to red shale and mudstone (Kama Hill formation). Within the Lake Nipigon area, the sediments are of the Pass Lake and Rossport Formations and include calcareous mudstone, carbonate, quartz arenite and locally conglomerate. Most of the sections examined in the southern part of the area have a high carbonate content which suggests that they are part of the Rossport Formation. In the northern part of the area, quartz arenite predominates and is probably part of the Pass Lake Formation.

A pre-Keweenawan age of deposition of the Sibley Group is indicated by available geochronology. Outliers of quartz arenite in northern Lake Nipigon are interpreted as correlative with the lower formation of the Sibley Group (Franklin et al., 1980; Sutcliffe and Greenwood, 1982). These are interbedded with fragmental rocks related to the granitic rocks on English Bay. If the correlation of these quartz arenites with the Sibley group is valid then the 1536.7 + 10/-2.3 Ma age of the granite dates the initiation of Sibley Group sedimentation. Franklin et al. (1980) obtained a Rb/Sr whole rock isochron of 1339±33 Ma for argillaceous sediments in the Sibley Group which is also substantially older than Keweenawan igneous activity. Furthermore, Ojakangas and Morey (1982) report rounded clasts of Sibley sandstone in conglomerate at the base of the Keweenawan Osler Group.

Exposures of the Archean-Sibley group unconformity are present on Highway 11, 14 km southwest of Beardmore (Plate 3), on the east shore of Frazer Lake and on the west shore of Lake Nipigon south of Livingstone Point. Exposures of the unconformity between the Sibley Group and pre-Keweenawan granite are found in the vicinity of English Bay.

At the Highway 11 exposure, Sibley metasediments overlie Archean metasediments. The Archean metasediments dip at approximately 70o northwest and consist of wacke and pelite injected by conformable quartz veins and pods. The unit shows no extensive weathering or alteration. The Sibley rocks dip at approximately 25o southeast and are in direct contact with the metasediments. A white carbonate, 5 to 25 cm thick is the basal Sibley unit. The carbonate bed, which has up to 50% angular

Plate 3

a) Outcrop of Proterozoic Sibley sandstone of the Rossport Formation, unconformably overlying Archean metasediments on Highway 11, west of Beardmore. The sub-horizontally dipping sediments consist mainly of quartz arenite and overlie sub-vertically dipping biotite schists.

b) Cooke Point, Lake Nipigon showing a section of metamorphosed Rossport Formation (white) beneath the upper diabase sill.

c) Proterozoic stromatolites of the Rossport Formation of the Sibley Group, west of Disraeli Lake. This block which is not *in situ* shows longitudinal sections of the stromatolites.

d) Cross bedded quartz arenite the Sibley Group on the north shore of Livingstone Point in northwestern Lake Nipigon. The sandstones consist of well sorted quartz arenite and are exposed underneath a diabase sill.

clasts of Archean metasediments, is irregular and fills cracks and hollows in the metasediment. This is overlain by a lens of conglomerate 0 to 25 cm thick which contains angular clasts of metasediment, feldspar and quartz in a quartz arenite matrix. The conglomerate is overlain by massive buff coloured quartz arenite with some quartz and feldspar granules.

At the exposure on the east shore of Frazer Lake, the Sibley Group overlies Archean pegmatite. The pegmatite weathers red and is fractured but is not highly altered. The surface is irregular and the sediment fills cracks in the pegmatite. The Sibley sandstone dips at approximately 10° to the west and consists of arkose with angular fragments and pieces of pegmatite. The sandstone appears to have been metamorphosed by the nearby diabase as the matrix contains prismatic pale green amphibole crystals.

On the south shore of Livingstone Point, Sibley sediments overlie Archean tonalites which are highly altered and hematized. At this location the actual contact of the tonalite and sediment was not observed.

Sediments overlying the granite at English Bay include quartz arenite and locally conglomerate with granules and cobbles of felsite and porphyry. The quartz arenite is moderately well sorted with subrounded grains of quartz and minor altered feldspar. At this location the underlying granite is strongly hematized. Fractures filled with hematite and clay minerals form concentric circular structures 0.5 to 1 m in diameter, which may be a result of weathering during the time of sedimentation.

East of Black Sturgeon Lake along the Black Sturgeon fault, outcrops of Sibley sandstone and conglomerate occur in close proximity to Archean granitoids but the actual unconformity was not observed. The Sibley sandstone is massive grey quartz arenite with pebbly layers of quartz and feldspar clasts. The underlying granite is very highly fractured and is chloritized and hematized. Breccia with angular fragments of granitoid rock in a sandstone matrix locally occurs near the granite-sediment contact. Fracturing of the granitoids appears to be associated with the Black Sturgeon Fault and the fault may be contemporaneous with Sibley sedimentation.

In the southern part of the area, most of the exposures of Sibley sediments consist of well bedded calcareous mudstone to carbonate with minor interbedded sandstone. The sediments are found between the upper and lower diabase sills and underlying the lower sill. In close proximity to the diabase sills, the sediments are white to pale green, but away from the contact zone the sediments are brick red. The transition from white to red coloured sediments, however, was not observed in a single section.

A good exposure of Sibley sediment underlying the lower diabase sheet is exposed on a lumber road near Gorge Creek. At this location, a 10 [illegible] vertical exposure of horizontally bedded white calcareous mudstone is overlain by diabase.

At Cooke Point (Pipestone Point) a 10 m section of white calcareous mudstone and carbonate is exposed between the upper and lower diabase sheets (Plate 3). The bedding is generally conformable to the sheet and dips gently north. Intrusion of diabase however, has locally caused minor buckle folding of the sediment. The sediment weathers chalky white and has bedding defined by alternating massive and fissile sections 10 to 20 cm thick. Within 2 m of the diabase, the development of contact metamorphic minerals is evident.

Within the map area, a good exposure of unaltered red calcareous mudstone typical of the Rossport formation is present on the west bank of the Black Sturgeon River near Nonwatin Lake. The exposure is 3 m thick and consists of red calcareous mudstone with green reduction spots and lenses up to 1 cm thick. Beds up to 0.5 m thick are defined by massive layers and shaley fissile layers. The mudstone has a crumbly texture and readily breaks into chips. Sparse carbonate filled vugs are present. Some exposures of Rossport Formation in the area exhibit intraformational breccia. The breccia is composed of angular mudstone clasts up to 10 cm long in a finer mud matrix. The clasts are best distinguished on the weathered surface where they weather in various shades of red.

In the Disraeli Lake area well preserved stromatolites (Plate 3) are present in the Rossport Formation. These have been described by Franklin et al. (1980).

Contact metamorphism of the calcareous sediments adjacent to the diabase sheets occurs over a zone several meters thick. Bleaching of the sediments to a white colour appears to be the most widespread effect. Bleaching occurs over a minimum thickness of 10 m adjacent to major sills. The contact metamorphic minerals are generally fine grained and therefore cannot usually be identified in the field. Several metamorphic calc-silicate minerals are recognized in thin section. These are, in order of increasing metamorphic grade: talc, tremolite, serpentine, and diopside. Serpentine is secondary after forsterite.

At Cooke Point and at the Tchiatang Bluffs, serpentine is visible in hand specimen as radiating clusters to 2 mm and occurs within about 0.5 m of the contact. The other minerals are visible only as a light green colour in the hand specimen and are present for at least 2 m from the contact.

Along the Tchiatang Bluffs within approximately 1 m of the contact with the diabase, rounded nodules to 4 cm are developed within the carbonate rich rock. The nodules are composed mainly of epidote with minor talc, tremolite and serpentine in a matrix of carbonate and quartz.

In the northern part of Lake Nipigon, sedimentary rocks are exposed underneath the diabase sheet and consist predominately of quartz arenite. The quartz arenite reaches a maximum thickness of 25 m as indicated by sections on Humboldt Bay of Lake Nipigon and Castle Lake.

Ripple marks and crossbeds are a conspicuous feature of the quartz arenite. Well developed crossbeds are exposed on the north shore of Livingstone Point and in Humboldt Bay (Plate 3). At the former location crossbeds are up to 1.8 m thick.

In thin section, the quartz arenite is observed to be well sorted and well rounded with medium sized sand grains. The sediment varies from friable to well indurated and is cemented by quartz overgrowths.

2.4 Keweenawan

Keweenawan igneous rocks in the Nipigon area consist of two suites. A series of picritic intrusions form an early and volumetrically minor sequence. The majority of the igneous rocks are tholeiitic diabases which occur largely as sills and probably originally covered an area of over 25,000 km2.

The picrites are cumulates derived by accumulation of olivine at shallow crustal depths. The picritic rocks occur as sills, dikes, ring dikes and plugs which are intrusive into the Archean basement and Sibley Group sediments.

In addition to the extensive diabase sills, the diabase occurs as dikes, cone sheets and other discordant sheets. The diabase sills at Lake Nipigon have been dated at 1108.8+4/-2 Ma (Davis and Sutcliffe, 1985) by the U-Pb zircon method. This indicates that the diabase was intruded at an early stage of Keweenawan rifting.

The diabase sills in the Nipigon area have previously been informally referred to as the Logan sills (Stockwell et al, 1972). During the original mapping of the area, Wilson (1910) referred to the sills as the Nipigon traps. In this study, the term Logan sill has been avoided for the Nipigon diabase. Logan intrusions has been used as a general term for Keweenawan sills and dikes along the north shore of Lake Superior from Thunder Bay to Duluth (Weiblen et al. 1972). Field, geochemical, and paleomagnetic studies, however, indicate that there are several types and ages of diabase intrusion. Geul (1970) distinguished two major cross-cutting petrogenetic types in the Thunder Bay district: early mafic intrusions; and Pigeon River intrusions. Weiblen et al. (1972) noted that diabase sills in Cook Country Minnesota appear to be equivalent to Geul's (1970) early mafic intrusions and are characterized by high abundances of K,P,Ti and low Mg. Weiblen et al. (1972) proposed that the term Logan sills be applied informally to intrusions having these characteristics, a requirement which is not met by the sills at Lake Nipigon.

Paleomagnetic studies indicate that the Nipigon sills are probably correlative with the Thunder Bay sills and at both Thunder Bay and Nipigon the sills are characterized by reversed magnetic polarity (Palmer, 1970; Robertson and Fahrig, 1971). In Minnesota, however, intrusions that have been referred to as Logan sills in Cook County have both normal and reversed magnetic polarity (Halls and Pesonen, 1982) indicating that the sills were emplaced at different stages of Keweenawan rifting. The term Logan sill therefore includes Keweenawan sills of different chemistry and ages, and has not been used in this study.

2.4.1 Picritic Rocks

Three areas of picritic ultramafic to mafic intrusions within the Nipigon area were delineated during this study. These occur in the Disraeli Lake - Leckie Lake area, on the east shore of Lake Nipigon in Eva and Kitto Townships and the Jackfish Island area in northern Lake Nipigon. Ultramafic rocks had previously been reported by Franklin (1970) in the Disraeli Lake area, but the intrusions on Lake Nipigon were first documented during the field work for this study (Sutcliffe, 1981; Sutcliffe and Greenwood, 1985).

The picritic intrusions are determined to be Proterozoic in age because they cross cut Archean structural trends and Proterozoic granitoid rocks in English Bay. The intrusions are considered to be Keweenawan because they appear to post date Sibley Group sediments. No contacts with the sediments were observed, however, picritic intrusions are surrounded by sediments (eg. Leckie Lake intrusion) and outcrop at higher elevation than the sediments (Disraeli Lake Intrusion) suggesting that they probably intruded the Sibley Group. The picritic rocks are known to be older than the diabase since the diabase is observed to intrude the picritic intrusion at Disraeli Lake and the Eva Township ring dike. At both of these locations, the diabase is chilled against the picritic rocks.

The intrusions are all composed of similar rock types and range from lherzolite and wehrlite to olivine gabbronorite. The intrusions range in form from elliptical plugs 1 to 2 km in diameter at Disraeli and Leckie Lake to the Eva-Kitto Townships intrusion which is a circular ring structure. A well exposed picritic dike 8 to 10 m wide striking at 135° and inclined at 45° to the south occurs at Redstone Point south of English Bay on Lake Nipigon. Possible picritic sills are observed at Disraeli and Leckie Lake and on Jackfish Island beneath these diabase sill. In general, the structures of the picritic rocks are less well defined than the diabase partly because the picrites are overlain and intruded by diabase.

The intrusion in Eva-Kitto Townships consists of a ring of ultramafic rocks 6 km in diameter (Figure 2.2). The center of the ring is underlain by Archean metavolcanics and metasediments which strike at 070° parallel to the strike of the Archean rocks outside of the structure. The ultramafic rocks are intruded by an outer ring of diabase. Inside of the ultramafic ring is a small intrusion of medium grained olivine gabbro. Due to poor exposure of the contact of the intrusive rocks with the Archean rocks the geometry of dip surface the ring structure could not be obtained. The chilled surface of the outer diabase against the ultramafic however was observed to dip vertically.

In handspecimen, the ultramafic picritic rocks are massive, fine to medium grained and equigranular. Orthopyroxene oikocrysts to 1 cm are locally present. Olivine (light green), clinopyroxene (dark green) and orthopyroxene (dark brown) are visible on fresh and weathered sufaces. Serpentinized fractures, spaced at 10 to 20 cm intervals and occurring as orthogonal sets, weather more readily than the unaltered rock and result in a blocky appearance(Plate 4). The picritic gabbroic rocks are massive, fine to medium grained and exhibit greater than 10% interstitial poikilitic plagioclase to 1 cm. The olivine gabbro intrusion occurring in the Eva-Kitto Township Intrusion is medium to coarse grained with tabular plagioclase and subhedral mafic minerals.

In thin section, the ultramafic picritic rocks (Plate 4) are

Plate 4

a) Photomicrograph of zoned augite phenocrysts (aug) in a camptonite dike. Crossed polars, sample 80-337. The dike is from Caribou Lake and contains deep crustal xenoliths. The matrix consists of plagioclase, sanadine, pyroxene, biotite, oxides and carbonate.

b) Photomicrograph of olivine phenocrysts, pseudomorphosed by serpentine and calcite, in a lamprophyre dike from Caribou Lake. Crossed polars, sample 80-1099. The matrix consists of phlogopite, carbonate and opaques. The dike is approximately 0.5 cm wide.

c) Outcrop of peridotite on the east shore of Lake Nipigon, south of Lion Bay in Kitto Township. Serpentinized fractures result in the characteristic blocky weathering.

d) Photomicrograph is peridotite cumulate from the Eva-Kitto Township ring dike on the east shore of Lake Nipigon. Crossed polars, sample 81-273. Note the adcumulate texture displayed by olivine and pyroxene with minor interstitial plagioclase.

e) Photomicrograph of olivine gabbro from Jackfish Island, Lake Nipigon. Plane light, sample 82-34. Large olivine (ol) primocrysts have zoning defined by opaque inclusions, fine olivine grains are poikilitically enclosed by plagioclase (pl). Augite (aug) is relatively minor. Euhedral chromite (chr) is enclosed by plagioclase.

f) Photomicrograph of resorbed olivine (ol) phenocrysts in picritic chill of dike on English Bay, Lake Nipigon. Plane light, sample 83-251.

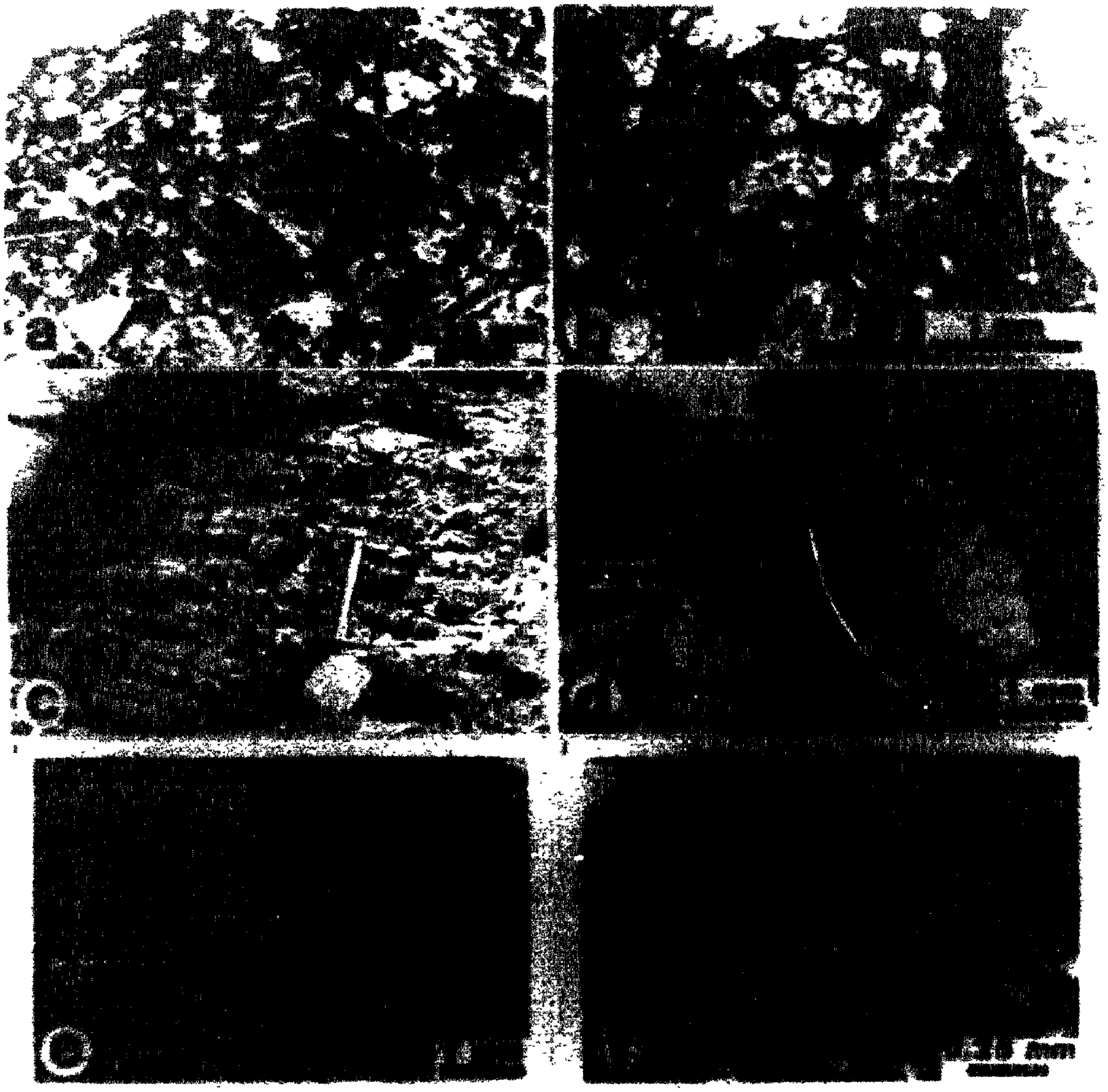
a
c
e
mm

seen to contain 40 to 70 percent euhedral olivine, 15 to 40 percent clinopyroxene, 0 to 15 percent orthopyroxene, 0 to 10 percent plagioclase with minor chromite, ilmenite, amphibole and biotite. Olivine occurs as 0.1 millimeter to 3 millimeter euhedral to subhedral rounded grains. The grains are generally fresh, but fractures with iddingsite and serpentine alteration are present. Clinopyroxene occurs as fresh 0.1 to 2 millimeter subhedral to anhedral grains. The habit of clinopyroxene varies from discrete cumulate grains to an interlocking mosaic of anhedral grains which are interstitial to olivine. Orthopyroxene occurs as large poikilitic plates to 1 centimeter which enclose clinopyroxene and olivine. The orthopyroxene appears to have reacted with the enclosed olivine grains. Plagioclase occurs as anhedral interstitial to poikilitic grains up to 1 cm. The plagioclase is well twinned, fresh and has a composition of approximately An_{72}. Chromite occurs ~~as~~ 0.1 millimeter euhedral grains which are enclosed in pyroxene and olivine. Late phases are biotite, which occurs as anhedral interstitial grains and as fine grains rimming opaques, and interstitial brown pleochroic amphibole which appears to have been in reaction with olivine. Biotite, hornblende and iddingsite alteration are particularly abundant in the Disraeli Lake intrusion where they may account for up to 25 percent of the rock. This alteration occurs as overgrowths on primary phases and as cross cutting veinlets.

The texture of the ultramafic picrite is medium grained, allotriomorphic to hypidiomorphic, equigranular. A well defined crystallization sequence of olivine, clinopyroxene, orthopyroxene, and plagioclase is indicated by textural relations. Cumulate phases are olivine and some clinopyroxene, while orthopyroxene, plagioclase and some clinopyroxene occur as intercumulate phases.

Olivine melagabbro from the picritic intrusions (Plate 4) are texturally similar to the ultramafics except for the presence of 10 to 35% plagioclase. In these rocks, the plagioclase also occurs as anhedral poikilitic grains enclosing cumulus olivine and clinopyroxene. Some rocks contain two generations of olivine with large early formed primocrists and fine euhedral grains in the matrix. The olivine gabbronorite in the Eva-Kitto Township intrusion contains up to 50% anhedral grains of fresh plagioclase enclosing subhedral to euhedral pyroxenes and olivine. The sample contains traces of quartz associated with myrmekitic intergrowth in plagioclase.

A glassy chill approximately 8 mm thick is observed on the picrite dike in the English Bay area (Plate 4). The chill contains 12% olivine phenocrysts in a matrix of opaque devitrified glass. The euhedral, elongated phenocrysts are embayed and range in length from 0.5 to 3 mm. The phenocrysts in the glassy chill are altered to serpentine and iddingsite but fresh euhedral olivine, phenocrysts are preserved in the fine grained chill. A zone of flow banding and olivine accumulation occurs at the interface between the glassy chill and the fine grained chill.

Medium grained picritic rocks from the dike interior contain fresh 0.1 to 2 mm euhedral fresh olivine. Augite occurs as

7

fresh, subhedral to euhedral prismatic 1 to 2 mm grains with hourglass sector zoning. Pigeonite occurs as equant to tabular grains which enclose relict resorbed olivine grains. Fresh plagioclase occurs as interstitial to poikitic grains.

2.4.2. Diabase Sills

Diabase sills are the most extensive rock type in the area. The sills are intruded in to the Sibley Group sediments near the Archean-Proterozoic unconformity. Locally the sills are observed to cross cut Proterozoic granitoids in the English Bay area and the picritic rocks.

At least two major sills appear to be present. The lower sill is interpreted to occupy most of the Nipigon area. Diabase from each of the two sills is petrographically indistinguishable, and therefore the recognition of two sills is based on establishing stratigraphy in the diabase and sediments.

The upper sill is exposed as erosional remnants in the Gros Cap area, on the islands in McIntyre Bay, at Otter Head, and Cooke Point of Lake Nipigon and west of Krug Lake. This upper sheet is locally separated from the lower sheet by Sibley sedimentary rocks.

The relationship between sills is well exposed at Cooke Point where approximately 10 meters of metamorphosed sediment are found between the sills. At other locations the upper sill rests directly ~~on the~~ lower, since the direct contact was observed on the east side of Three Mount Point.

Near complete sections of the lower sill are exposed in the vicinity of Highway 11 in the Nipigon Palisades area and at Livingstone Point and indicate that the sill is approximately 200 meters thick. The lower contact of the lower sill was only observed in northern Lake Nipigon at Humboldt Bay and Livingstone Point. In the southern part of the area the lower contact can be defined to within approximately 3 meters in the Nipigon Palisades area where Sibley sediments and Archean rocks underlying the sill are exposed. Numerous exposures of the top of the lower sill are present in the area south of Grand Bay, McIntyre Bay and South Bay of Lake Nipigon and in northern Lake Nipigon along the east and west shores of the Lake.

The most complete section of the upper sill appears to be exposed at Otter Head where the sill is at least 150 meters thick. At this location, however, the top of the sill is not exposed. Greater than 100 meter thick sections of the upper sill are also present in the Gros Cap area.

The topography of Brown Island in McIntyre Bay suggests that a possible third and uppermost sill may be present which dips to the south. No contact relationships to support this relationship were observed.

Typically the diabase forms mesas and cuestas with the upper section forming cliffs with columnar jointing and the lower parts of the section being covered by talus (Plate 5). A vertical igneous stratigraphy which appears to be similar in both the upper and lower sills can be established in the field from composite sections. This stratigraphy was used during mapping in order to establish approximate positions within the sill. The

Plate 5

a) Typical exposure of diabase section, north of Castle Lake in the northwestern part of the area. Diabase exposed at the top of the chill shows weakly developed columnar jointing. Extensive diabase talus forms at the base of the chill, often obscuring the lower contact.

b) Typical exposure of lower contact of diabase sheet on the south shore of Berry Lake, west of Armstrong. Lower contact of sheet is polygonally fractured and dips at approximately 30°. Tonalite country rock is visible in lower part of the photograph.

c) Diabase chill showing polygonal fractures from the west shore of Black Sturgeon Lake, south west of Lake Nipigon. This is the upper chill of the lower diabase sill. Fractures are defined by epidote alteration (light coloured) with an indistinct outer zone of amphibole.

d) Diabase chill with round vesicles exposed on th Eagle Egg Islands in central Lake Nipigon. Vesicles are lined with amphibole (dark) and wollastonite (white).

e) Elongated vesicles in diabase chill on Dawson Island in central Lake Nipigon. Epidote alteration occurs around the vesicles.

f) Cusp shaped grooves in the upper chill surface of diabase on the east shore of Lake Nipigon, south of Wabinosh Bay. These grooves locally contain deformed remnants of sediment. The grooves are interpretted to result from coalescing diabase fingers. Brunton compass for scale.

Plate 5 continued)

g) Cross-section of a diabase finger intrusive into Rove shale near the Great Lakes Nickel deposit, southwest of Thunder Bay. This is not from the Nipigon area, but is a good example of a diabase finger.

h) Diabase fingers intrusive into Sibley sediments at the lower contact of the upper sheet at Cooke Point, Lake Nipigon. Several fingers have coalesced and have wedges of deformed sediment in between.

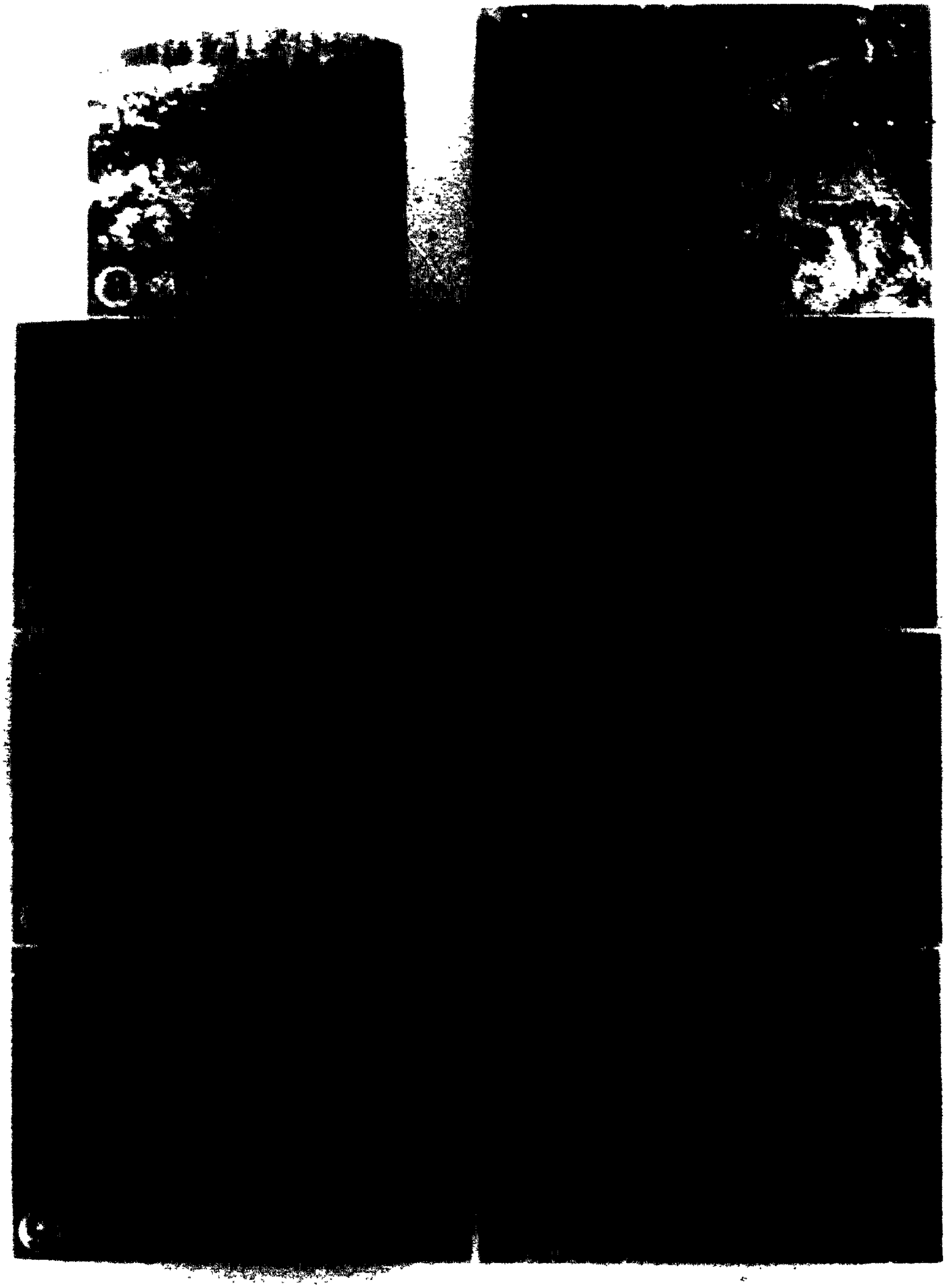

stratigraphy is summarized in figure 2.3.

The chill has a glassy rind approximately 1 cm thick which contains skeletal crystals of plagioclase, olivine and locally augite microphenocrysts in a devitrified glass groundmass. The glassy rind grades upwards to very fine grained isogranular diabase with plagioclase, pyroxene and magnetite. The lower 10 to 15 cm of the chill zone is polygonally fractured with epidote alteration along the fractures (Plate 5).

At the lower contact of the sill on Cooke Point, elliptical fingers of diabase with a long axis of approximately 1 m are observed to intrude the Sibley sediments (Plate 5). The intrusion of fingers appears to have caused buckling of the host sediments. Similar particularly well exposed diabase fingers were also observed in Keweenawan diabase intruding shales south west of Thunder Bay (Plate 5). The fingers at Cooke Point show evidence of having coalesced and have cusps of sediments partially separating them. The coalescing of fingers appears to be a mechanism of generating cusp-shaped grooves on the upper surface of diabase sills (Plate 5).

At approximately 5 to 50 m above the base, the diabase is medium grained and becomes ophitic in texture. The ophitic diabase is recognized in the field by a distinctive, knobby weathering texture (Plate 6). Individual oikocrysts of pyroxene are typically 1 to 2 cm in diameter in this zone of the sill. The ophitic diabase is easily weathered and often forms gravel deposits of rounded granules at the base of the outcrops.

The middle portion of the diabase sill (50 to 150 m) is

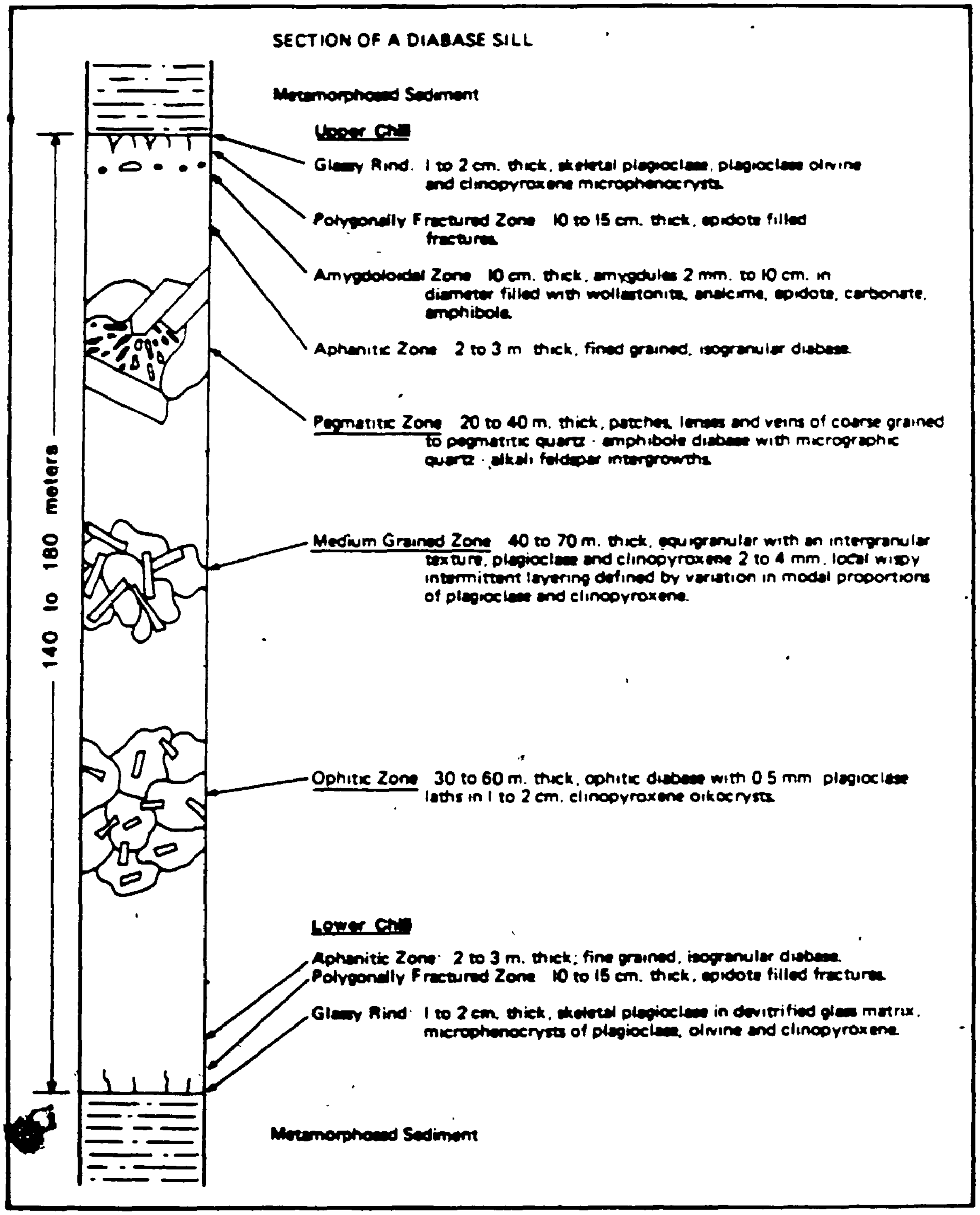
SECTION OF A DIABASE SILL
Metamorphosed Sediment
Upper Chill
Glassy Rind. 1 to 2 cm. thick, skeletal plagioclase, plagioclase olivine and clinopyroxene microphenocrysts.
Polygonally Fractured Zone 10 to 15 cm. thick, epidote filled fractures.
Amygdoloidal Zone 10 cm. thick, amygdules 2 mm. to 10 cm. in diameter filled with wollastonite, analcime, epidote, carbonate, amphibole.
Aphanitic Zone 2 to 3 m thick, fined grained, isogranular diabase.
Pegmatitic Zone 20 to 40 m. thick, patches, lenses and veins of coarse grained to pegmatitic quartz - amphibole diabase with micrographic quartz - alkali feldspar intergrowths.
Medium Grained Zone 40 to 70 m. thick, equigranular with an intergranular texture, plagioclase and clinopyroxene 2 to 4 mm. local wispy intermittent layering defined by variation in modal proportions of plagioclase and clinopyroxene.
140 to 180 meters
Ophitic Zone 30 to 60 m. thick, ophitic diabase with 0 5 mm plagioclase laths in 1 to 2 cm. clinopyroxene oikocrysts.
Lower Chill
Aphanitic Zone 2 to 3 m. thick; fine grained, isogranular diabase.
Polygonally Fractured Zone 10 to 15 cm. thick, epidote filled fractures.
Glassy Rind 1 to 2 cm. thick, skeletal plagioclase in devitrified glass matrix, microphenocrysts of plagioclase, olivine and clinopyroxene.
Metamorphosed Sediment

2.3 Generalized cross-section of diabase sills in the Lake Nipigon area characterized by medium-grained equigranular diabase. The middle parts of the sills locally show weakly developed subhorizontal modal layering defined by wispy 1 to 2 cm wide bands enriched in mafic material contrasting with leucocratic diabase bands 2 to 5 cm wide (Plate 6). Well developed layering is present on the east shore of Murchison Island and in the vicinity of Kelvin Island. Locally, such as on Logan Island the medium grained diabase contains anorthositic schlieren (Plate 6).

Towards the top of the sill, patches of coarse grained diabase appear in the medium grained diabase. The patches, which are irregular in shape and average approximately 10 cm in diameter, grade sharply with the medium grained host (Plate 6). In some patches, amphibole replaces pyroxene and interstitial quartz is present. In the zone of the sill which contains the coarse patches, large lenses of coarse grained to pegmatitic quartz-amphibole diabase are locally present.

Within a few meters of the top of the sill, the coarse patches diminish to clusters of coarse crystals and the rock has a speckly texture. Above this, the rock becomes progressively finer grained. The upper chill zone of aphanitic diabase is approximately 1 m thick and has a thin 1 to 2 cm rind of very fine to glassy diabase.

Exposures of polygonally fractured upper chill zone are common in the region between Black Sturgeon Lake and Forgan Lake and the south part of Lake Nipigon. These exposures characteristically form flat outcrop surfaces with slopes that parallel the dip of the sill. The exposures display regular

Plate 6

a) Ophitic diabase at the base of the lower sill on the east shore of Lake Nipigon in Pijitiwabik Bay. Dark spots are augite oikocrysts which result in a knobby weathered surface. Pen magnet is approximately 12 cm long.

b) Wispy modal layering in medium grained part of diabase sill on the east shore of Murchison Island in northern Lake Nipigon. Layering is defined by concentration of mafic minerals. Compass is approximately 18 cm long.

c) Anorthositic schlieren in medium grained part of diabase sill on Logan Island in northern Lake Nipigon.

d) Pegmatitic patches in the upper part of diabase sill on the west shore of Lake Nipigon near Spruce Point. Patches contain fayalite, quartz, augite, plagioclase, amphibole, magnetite and ilmenite.

e) Medium grained granophyre intruding diabase on Dog Island near the west shore of Lake Nipigon.

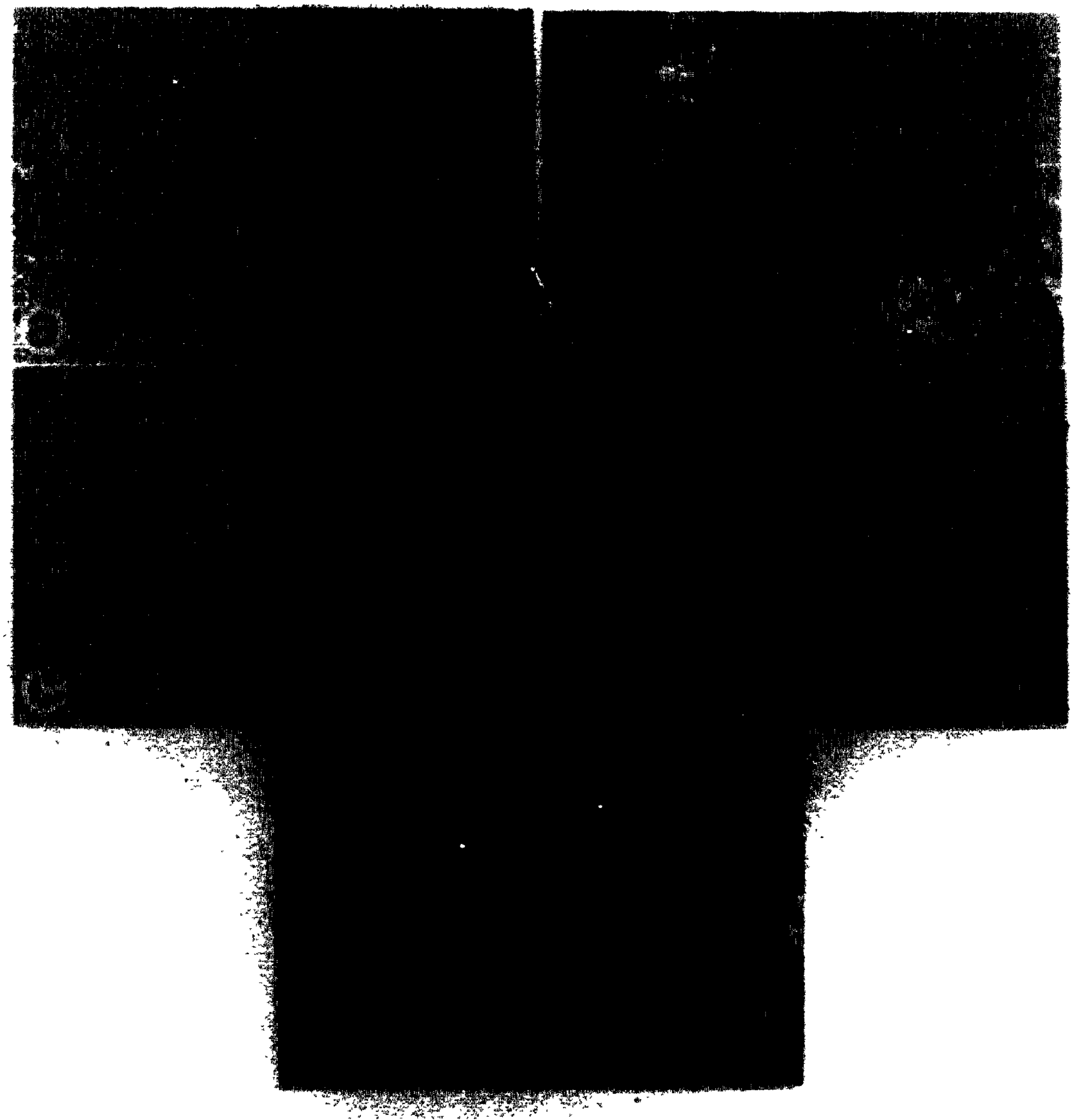

polygonal fracturing which is developed on a 10 cm scale. The fractures vary from rectangular to crudely hexagonal and are accentuated by epidote alteration along them (Plate 5).

Approximately 10 to 20 cm below the upper chilled rind, a zone of amygdaloidal diabase is locally present. The amygdaloidal layer is approximately 5 cm thick. The amygdules vary from 1 to 2 mm in diameter to several centimeters. The smaller amygdules are sub-spherical while the larger ones are bell shaped to discoid with flat bottoms. In some locations, the amygdules are stretched and define a lineation in a plane parallel to the contact of the sill (Plate 5). Wollastonite, analcime, amphibole, epidote, magnetite and carbonate are observed as phases filling the amygdules.

Locally the upper surface of the sill may be brecciated. The breccia consists of angular 1 to 10 cm chilled diabase fragments with epidotized rims in a matrix of vuggy carbonate, epidote, amphibole and wollastonite. The breccia resembles a hyaloclastic breccia due to the angular fragments and appears to be due to brecciation of the polygonally fractured top of the sill by volatiles from the magma and surrounding sediments.

Alteration veins are common in the upper and lower parts of the diabase sill. The veins are generally less than 3 cm wide but locally up to 8 cm. Particularly good exposures of wollastonite veins are exposed in the diabase in the Pijitawabik Bay area. The veins here are composed of white acicular wollastonite which form radiating bundles roughly perpendicular to the vein walls. Minor euhedral, creamy white analcime crystals to 1 cm diameter are present within the wollastonite in some veins.

In thin section, the diabase consists of plagioclase (labradorite), clinopyroxene (augite and subordinate pigeonite), olivine, magnetite and ilmenite. Accessory constituents are quartz, biotite, hornblende, iddingstite and apatite. The grain size varies from less than 0.1 mm in the chilled margin to 1 cm in th pegmatitic lenses. In general, the grain size is 2 to 3 mm and becomes coarser towards the top of the sill.

Textures are most commonly sub-ophitic to ophitic in the main part of the sill. Intergranular textures occur in the upper parts of some sills (Plate 7). In the well developed ophitic textures, fresh augite and pigeonite oikocrysts are up to 1 cm and enclose plagioclase with minor olivine. Magnetite, olivine, minor biotite and altered pyroxene are primarily restricted to zones between the oikocrysts. Plagioclase grains enclosed in the oikocrysts are generally finer grained than those interstitial to them.

Fine grained diabases display intergranular to isogranular textures. Microphenocrysts and glomeroporphyritic aggregates of olivine, pyroxene and plagioclase are commonly present (Plate 7). Glassy rinds of the chill zone are composed of devitrified glass with altered olivine, plagioclase and pyroxene microphenocrysts. Well developed skeletal plagioclase crystals showing "swallow-tail" longitudinal and "hollow-box" cross sections are usually present. Microphenocryst assemblages are:

Plate

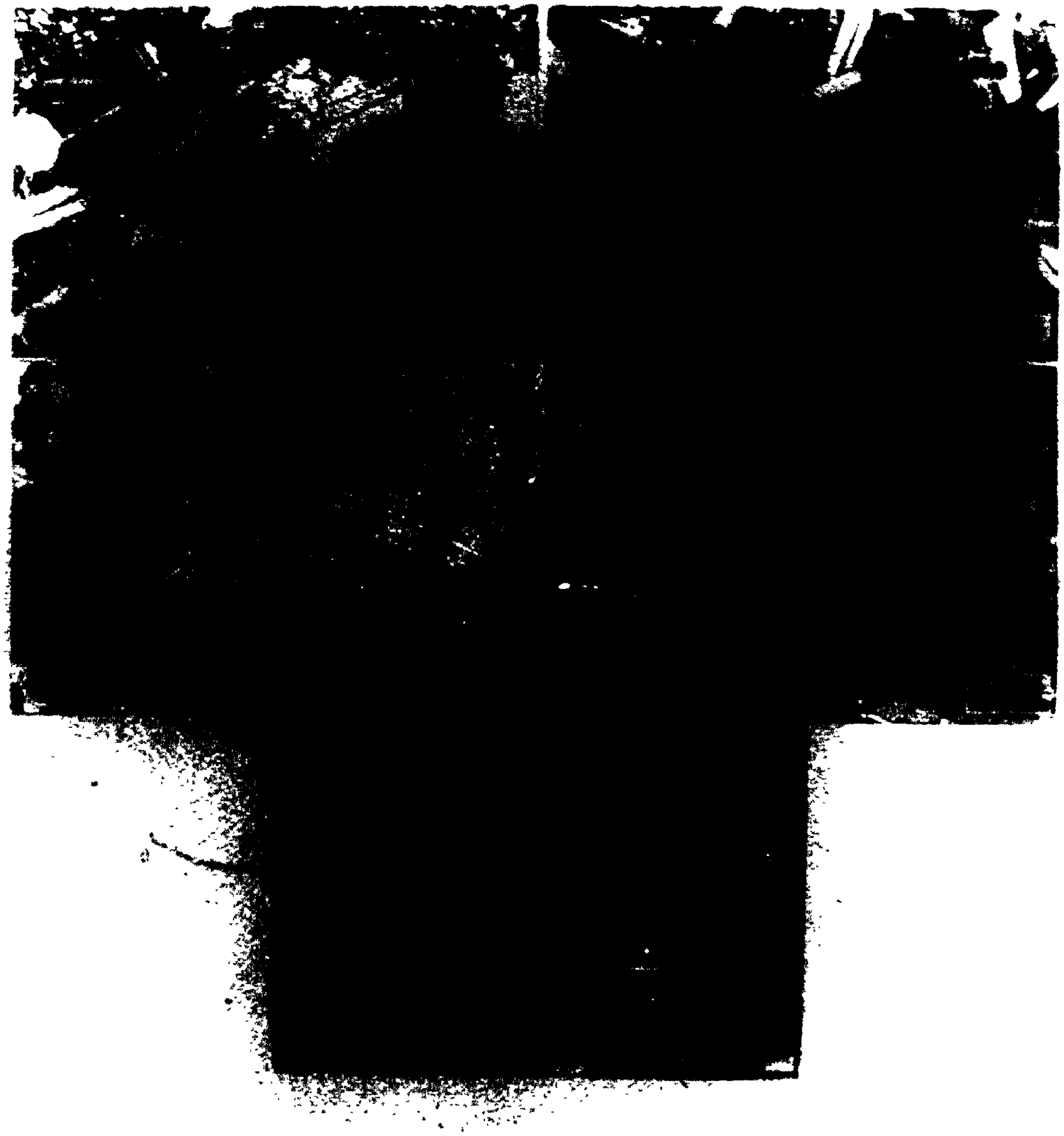

plagioclase; plagioclase and olivine; plagioclase, olivine and augite.

In the medium grained diabase, plagioclase (labradorite to calcic-andesine) occurs as lath shaped crystals with an average length of 1 to 2 mm. The grains are usually fresh and show well developed albite and Carlsbad twinning with less well developed pericline twinning. Weak normal and oscillatory zoning is locally developed.

The habit of the pyroxene varies from elongated prismatic crystals in the coarse grained pegmatitic diabase, to subhedral equant grains in the isogranular diabase, to anhedral grains in the sub-ophitic and ophitic diabase. Planar exsolution lamellae parallel to 001 and bleb-like lamellae parallel to 100 are developed in the medium to coarse grained rocks.

Olivine occurs as subhedral grains to 1.5 mm which are commonly partially altered to or rimmed by iddingsite. In some sections olivine is interstitial to plagioclase. Olivine is concentrated in the lower parts of the sill where it reaches a maximum of 10% of rock. The upper parts of some sill sections are olivine free.

Micrographic intergrowth of quartz in feldspar is present toward the top of the sills (Plate 7). The intergrowth is associated with the coarse grained patches and pegmatitic diabase.

Magnetite and ilmenite are present as subhedral to euhedral grains from 0.1 mm to 4 mm. Biotite and hornblende occur as deuteric alteration of pyroxene. Hornblende also occurs as dendritic crystals to 4 mm in coarse grained and pegmatitic diabase. Minor apatite is present as discrete prismatic crystals.

Late granophyre dikes intrude the diabase and locally intrude the Sibley Group (Plate 5). Good examples are exposed on Dog Island, and Grand Bay of Lake Nipigon and Forgan Lake. The dikes are up to 30 cm wide. They have brick red fresh and weathered surfaces and are fine grained with miarolitic cavities. Flakes of specular hematite to 1 centimeter are locally observed within the dikes. One thin section of a granophyre shows that it is composed of perthite (60%), quartz (35%), hematite (5%), and a trace of altered biotite. The feldspars in the granophyre dikes are hematized.

Most granophyre dikes have sharp contacts with the diabase host. A granophyre dike exposed on the northwest arm of Forgan Lake has a gradational contact with diabase. Adjacent to the dike, the diabase becomes coarser grained, which suggests that granophyre was emplaced prior to complete crystallization of the diabase.

2.4.3. Diabase Dikes, Cone Sheets, Sheets

Diabase intrusions described in this section occur as discordant units intrusive into Archean basement, Sibley Group sediments, picritic intrusions and locally into the diabase sills. These intrusions are locally observed or interpreted to feed the diabase sills.

In the northwestern part of the area, west of the town of

Armstrong, two intersecting cone sheet structures 30 to 40 km in diameter intrude the Archean basement (Figure 2.2). The cone sheets are observed to dip inward at 45o to vertical. The sheet has a minimum thickness of approximately 30 m at Kenakskaniss Lake. In the western part of the structure the cone sheets become thicker and grade upward into to subhorizontal diabase sills. East of Lake Nipigon in the vicinity of Beardmore, a second cone sheet structure of comparable dimensions has been mapped but there is limited data on the dip of the sheets. An inward dipping structure is indicated by a cross section of the sheet exposed in the Leitch gold mine (Mackasey,1970).

North of Lake Nipigon, several inclined sheets of diabase up to 200 m thick discordantly intrude the Archean basement. These sheets are irregular and have sinuous outcrop patterns at the surface. The sheets may be have been feeders for the sills but this relationship was not established during mapping.

A detailed section of an inclined sheet at D'Alton Lake was studied by Kavanagh (1981). This section is composite having formed from at least two magma pulses as indicated by an internal sub-chilled contact. The section is weakly differentiated in a similar manner to the sill sections. The most noteable features of the differentiation are a zone of olivine accumulation near the base and a zone with coarse grained to pegmatitic patches near the top.

Diabase dikes are relatively sparse within the area. A minor swarm 10 to 15 km wide and 30 to 40 km long trends north along the east side of Lake Nipigon. Mapping by Pye (1965) indicates 10 to 12 dikes of up to 50 m width are present in this swarm to the southeast of Lake Nipigon. The relationship between these dikes and the sills was not established during mapping for the present study. Halls (1978) however, indicates that at least some of these dikes have normal magnetic polarity suggesting that they postdate the sills. A north trending dike 3 to 10 m wide along the east shore of Lake Nipigon in the Vint Bay and Humboldt Bay area is probably associated with this swarm.

South of Lake Nipigon in the Disraeli Lake area, the Fox Mountain dike extends for approximately 6 km in a northerly direction and is 400 m wide. To the north of Disraeli Lake the dike is interpreted to intrude Sibley group sediments but the contact with sediments was not identified. To the south, the dike is interpreted to be overlain by a diabase sill which forms the escarpment at Wolf Mountain. East of Disraeli Lake, the Fox Mountain dike intrudes picritic rocks of the Disraeli Lake intrusion.

Several dikes up to 10 to 20 m in width and traceable for several km intrude Archean rocks in the vicinity of Caribou Lake north of Lake Nipigon (Sutcliffe, 1984). These trend in a north to northwesterly direction. A sample from a dike at the west end of Caribou Lake has a reversed magnetic polarity (Halls, personal communication, 1982) and therefore is probably of similar age to the diabase sills. A large northwesterly trending dike, known as the Ogoki dike, outcrops north of Lake Nipigon and may be continuous for over 250 km on a basis of aeromagnetic expression. This dike possibly represents the northern most extension of the Nipigon structure, however the dike was not examined in the present survey.

Numerous small, discontinuous, aphanitic dikes approximately 1 meter in width were observed throughout the area. These dikes locally intrude the diabase sills. No preferred orientation was recognized.

In handspecimen and in the thin section the diabase in the dikes and sheets is generally similar to the diabase of the sills. In most cases the mineralogy is the same, however, the dikes and sheets are characterized by sub-ophitic to intergranular textures as opposed to the sub-ophitic to ophitic textures of the sills. The dikes and sheets have polygonally fractured chill margins, but lack miarolitic cavities. Microphenocrysts assemblages in the chills are similar to those of the sills except in some samples of north trending dikes on the east shore of Lake Nipigon. These dikes contain pigeonite as a microphenocryst phase in addition to olivine and plagioclase (Plate 7). In most other rocks, pigeonite crystallized after augite.

CHAPTER 3

REGIONAL TECTONICS - ~~LATE PROTEROZOIC~~ RIFTING IN THE LAKE NIPIGON AND NORTHERN LAKE SUPERIOR AREA

3.1 Introduction

The 1.2 to 1.0 Ga Keweenawan or Midcontinent rift system (King and Zietz, 1971; Chase and Gilmer, 1973; Ocola and Meyer, 1973) occupies an arcuate belt over 2,000 km long in the central part of the North American continent. The rift is only exposed in the Lake Superior region and is covered by Cambrian and younger sediments to the west and east. The Lake Superior area therefore provides most of the basis for the understanding of the lithologies and tectonics of the entire Keweenawan rift.

The subsurface extent of the Keweenawan rift has been clearly shown by gravity studies, summarized by Halls (1978). This data, shown schematically in Figure 3.1, demonstrates that the rift system changes strike abruptly from a northeast trend in western Lake Superior to a southeast trend in eastern Lake Superior. Burke and Dewey (1973) suggested that this geometry, characterized by two limbs meeting at approximately 120° may have been accommodated by a rift-rift-rift junction on the north shore of the lake. The association of 1.1 to 1.0 Ga alkalic-and-carbonatite complexes combined with a prominent gravity high led Burke and Dewey (1973) to suggest that the Kapuskasing Structural Zone was a failed rift arm and that a triple junction formed near the

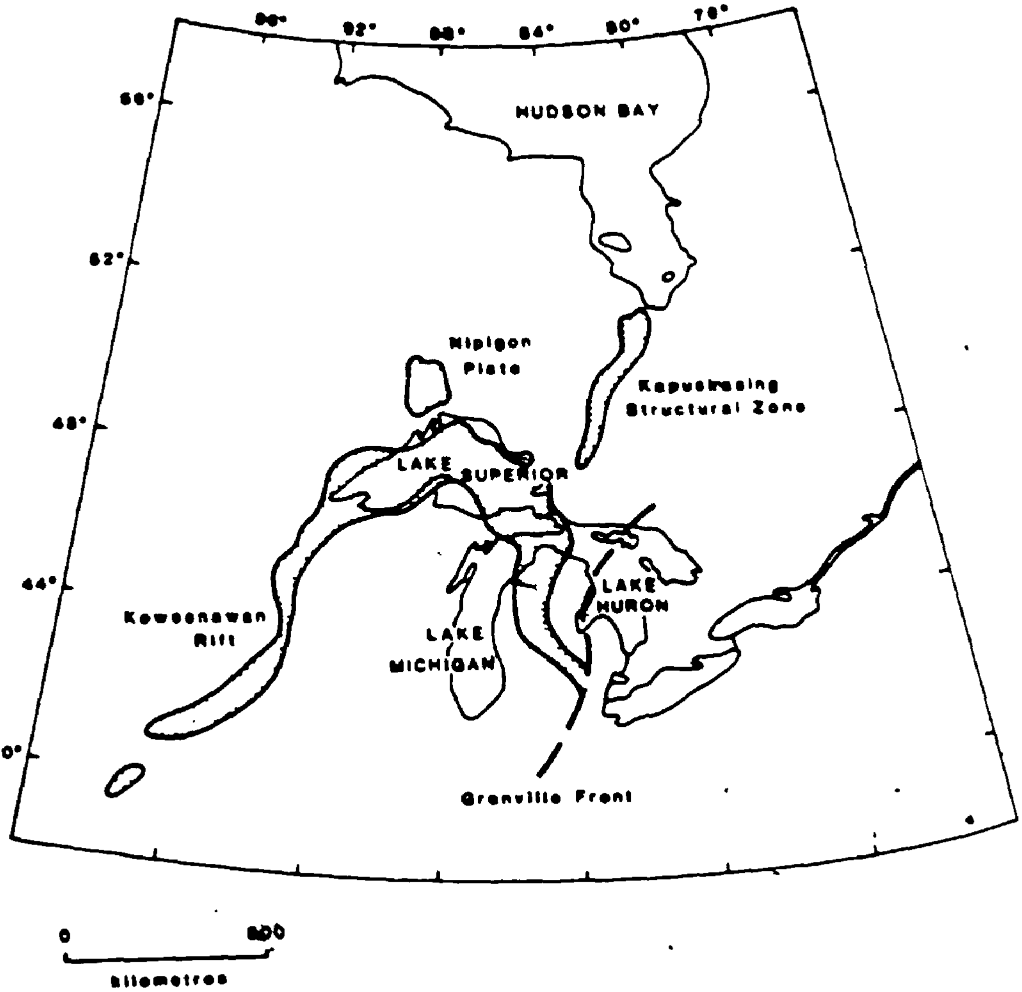
96°
92°
88°
84°
80°
76°
56°
52°
48°
44°
40°
HUDSON BAY
Nipigon
Plate
Kapuskasing
Structural Zone
LAKE SUPERIOR
Keweenawan
Rift
LAKE
MICHIGAN
LAKE
HURON
Grenville Front
0
800
kilometres

3.1 Location of the Nipigon plate and major geological structures in the Great Lakes region. The Keweenawan rift and Nipigon plate are based on the outline of Keweenawan igneous rocks from Halls (1978). The Kapuskasing structural zone is based on a geological outline of the gravity high.

Mamainse Point area, Ontario (Figure 3.2). Recently, Percival and Card (1983) have shown that the Kapuskasing structure is a section of the Archean crust uplifted along a northwest dipping thrust fault. Although the structure has been activated during the Proterozoic, its origin as a thrust appears incompatible with rifting. As an alternative, Card *et al*. (1972) and Franklin *et al*. (1980) have suggested that the sediments of the Sibley basin and mafic igneous rocks of the Nipigon plate occupy a failed arm.

This chapter presents geological evidence to show that the lithosphere underlying the Nipigon plate fractured in an extensional tectonic regime to allow emplacement of mantle derived magmas during the main phase of Keweenawan rifting. These features indicate that the Nipigon plate fits the broad definition of a rift (Neumann and Ramberg, 1978) and therefore can be considered as a failed arm of the Keweenawan rift in Lake Superior. The nature of the feeder zones for the extensive diabase sills on Lake Nipigon also provide an insight to the processes by which rifting took place and suggests that the rift formed by active mechanisms.

3.2 Keweenawan Rift Development

Tectonic events in the Lake Superior and Lake Nipigon area are summarized in table 3.1. Evidence that the Lake Superior basin (Figure 3.2) is a rift structure has been summarized by Halls (1978) and includes 1) dimensional similarity of the Keweenawan belt to global rift systems; 2)

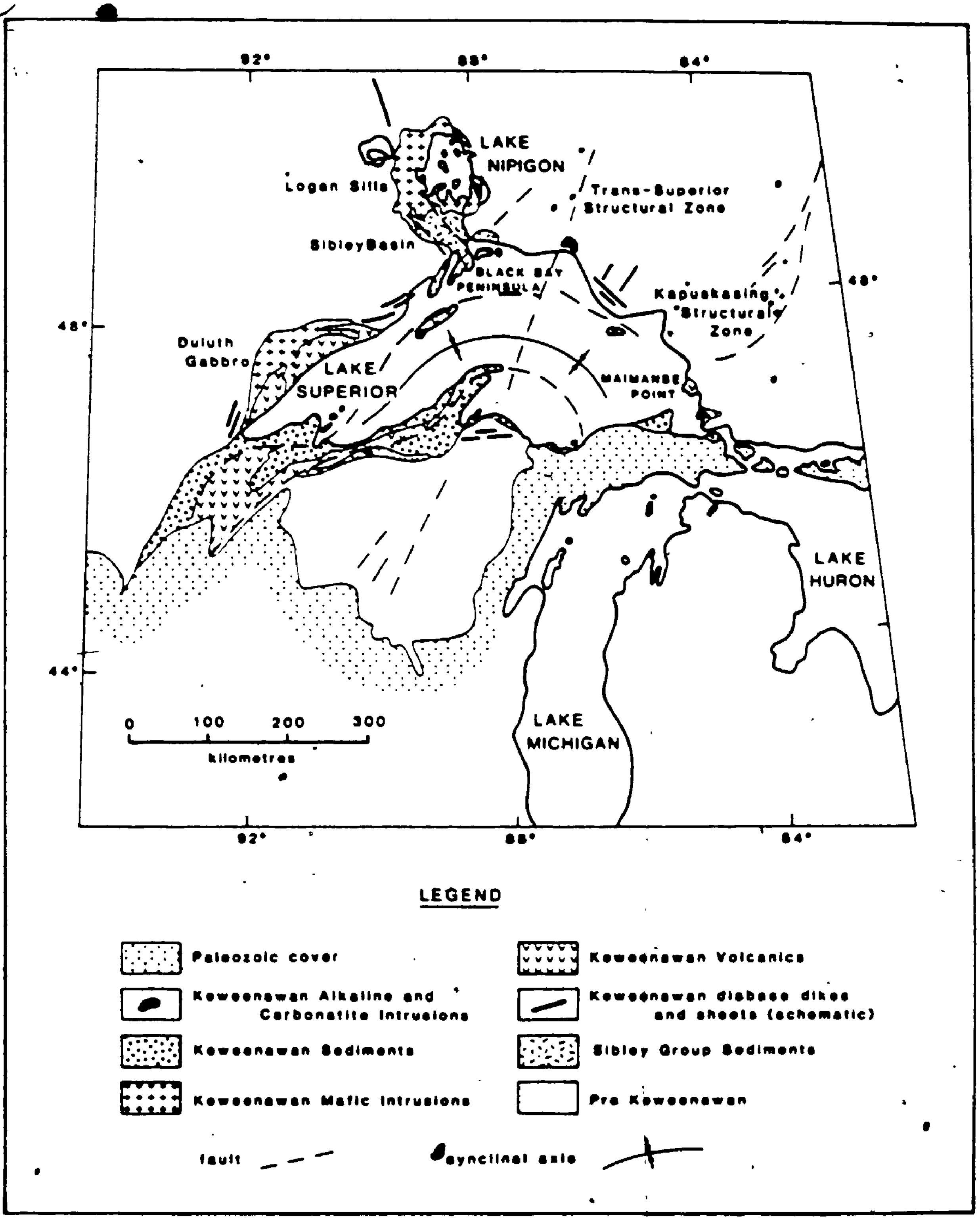
92°
88°
84°
48°
44°
LAKE NIPIGON
Logan Sills
Trans-Superior Structural Zone
Sibley Basin
BLACK BAY PENINSULA
Kapuskasing Structural Zone
Duluth Gabbro
LAKE SUPERIOR
MAIMANSE POINT
LAKE HURON
LAKE MICHIGAN
0
100
200
300
kilometres
LEGEND
Paleozoic cover
Keweenawan Alkaline and Carbonatite Intrusions
Keweenawan Sediments
Keweenawan Mafic Intrusions
Keweenawan Volcanics
Keweenawan diabase dikes and sheets (schematic)
Sibley Group Sediments
Pre Keweenawan
fault
synclinal axis

3.2 Generalized geology of the Lake Superior area. Based on maps of the Ontario Geological Survey and the geological map accompanying Geological Society of America, Memoir 156.

Table 3.1 Rift related events in the Lake Nipigon and northern Lake Superior area.

	Event	Constrained by	Timing	Method	Reference
Lake Superior Rift	Initial rifting	Age of diabase dikes in Sudbury area	1225±50	Rb-Sr	Van Schmus et al. (1982).
		Age of Powdermill Group volcanics in Michigan	1209±36	Rb-Sr	Wilbrand et al. (1984)
	Main igneous activity	Age of normal and reversed igneous rocks	1110±10	U-Pb	Silver and Green (1963, 1972).
Nipigon Plate	Lamprophyre dikes	Similar to lamprophyres dated at Marathon, Ontario	1653±122	Rb-Sr	Platt and Mitchell (1982)
	Anorogenic granitoids and volcanics	Age of English Bay intrusion	1536.7+10 -2.3	U-Pb	Davis and Sutcliffe (1985).
	Alkaline dikes, syenite dikes	Not dated. Conglomerate with clasts of this unit overlain by Sibley			
	Deposition of Sibley Group	Age of dolomites and shales. Overlies anorogenic granitoids.	1339+33	Rb-Sr	Franklin et al. (1980)
	Formation of Black Sturgeon Graben	Age of U-mineralized veins. Fault disturbs Sibley but not diabase.	1090±20	U-Pb	Ruzicka and Le Cheminant (1984)
	Intrusion of diabase sills	Age of lower sill	1108.8+4-2	U-Pb	Davis and Sutcliffe (1985)

the occurrence of flood basalts fed by fissure systems oriented more or less parallel to the belt axis; 3) presence of dense crust beneath the central part of the belt, and 4) apparent offsets in pre-Keweenawan geology due to crustal spreading. The Keweenawan rift apparently lacks bounding normal faults, although these may have been obscured by subsequent compressional tectonism.

The rift formed at a high angle to the generally east-north-east trend of the older Precambrian basement. In detail, the Keweenawan rift is composed of a number of segments offset by northeast or northwest trending faults (Halls, 1978). Klasner _et al_ (1982) have found that there is a significant correspondence between the geometry of the rift and older linear features in the Precambrian rocks surrounding the rift; suggesting the shape of the rift is controlled by pre-existing structures.

Keweenawan volcanics were erupted from fissures in a sub-aerial environment during rifting. The timing of initial rifting is poorly constrained. Rifting may have begun at approximately 1200 Ma as indicated by Rb-Sr isochron ages of 1225+/-50 Ma for diabase dikes in the Sudbury area (Van Schmus _et al_. 1982) and 1209±36 Ma for the Powdermill Group lavas (Wilbrand _et al_. 1984).

A major paleomagnetic reversal (Palmer, 1970; Books, 1972) within the mafic rocks has been an important tool for correlation of sequences within the Lake Superior basin and surrounding areas, although possible complications in this stratigraphy may exist (Massey, 1979). The lower part of the Keweenawan sequence has a reverse magnetic polarity and the upper part has a normal polarity. Both sequences contain subordinate rhyolitic volcanics and interflow sediments (Wallace, 1981). A variety of lithologies from both the reverse and upper normal magnetic sequences have been dated by the U-Pb zircon method and indicate that the main phase of Keweenawan igneous activity took place at 1110 +/-10 Ma (Silver and Green, 1963; 1972).

Dominant basalt types include high-Al olivine tholeiite (characterized by low K, P, Ti, high Al, and enriched LREE) and transitional, weakly alkaline, Fe-Ti basalts (higher K, P, Ti, Fe and lower Mg, Al) (Green, 1982). The olivine tholeiites are considered to resemble midocean ridge basalts except for enrichment in LREE and higher Al_2O_3 (Green, 1982). Numerous intrusive bodies, the largest of which is the Duluth Gabbro, are associated with the volcanic rocks of the Lake Superior basin. Parts of the feeder system for the volcanics are now represented by diabase dike swarms which occur around the basin and trend parallel to the basin axis. In a general way, the older magnetically reversed feeders occupy more marginal positions than younger ones, consistent with a model of crustal spreading (Halls, 1978).

Coarse, immature clastic rocks occur interbedded with the Keeweenawan lava flows. Paleocurrent measurements in the interflow sediments show transport to the rift axis and indicate continual subsidence of the rift during volcanism

(Ojakangas and Morey, 1982). With cessation of volcanism, basin subsidence continued and red clastic detritus was deposited in the basin (Ojakangas and Morey, 1982). During or after the final stages of infilling, crustal compression led to steepening of the basin limbs and the formation of major faults with the uplift of a central horst block along the rift axis (Halls, 1978).

3.3 Nipigon Plate

The Nipigon plate (Stockwell et al. 1972) (Figure 3.3) primarily consists of a sequence of late Proterozoic (Helikian) sediments and diabase sills which overlie Archean rocks of the Superior Province and define a broad basinal structure extending north for 160 km from Lake Superior. The plate is indicated geophysically by a subdued gravity high which extends north from Lake Superior (Figure 3.4). Analysis of the gravity data in Northern Lake Superior led Chandler et al. (1982) to favour the Nipigon plate - Sibley basin, rather than the Kapuskasing Structural Zone as a possible failed arm. The gravity high associated with the Kapuskasing structure is considered to be due to granulites uplifted along a west dipping thrust (Percival and Card, 1983) and is not continuous with the Superior basin to the south.

Franklin et al. (1980) have interpreted the Sibley Group sediments as a red-bed sequence deposited in a fault bounded basin elongated in a northerly direction and deepening to the east and south. Drilling has indicated the sequence has a

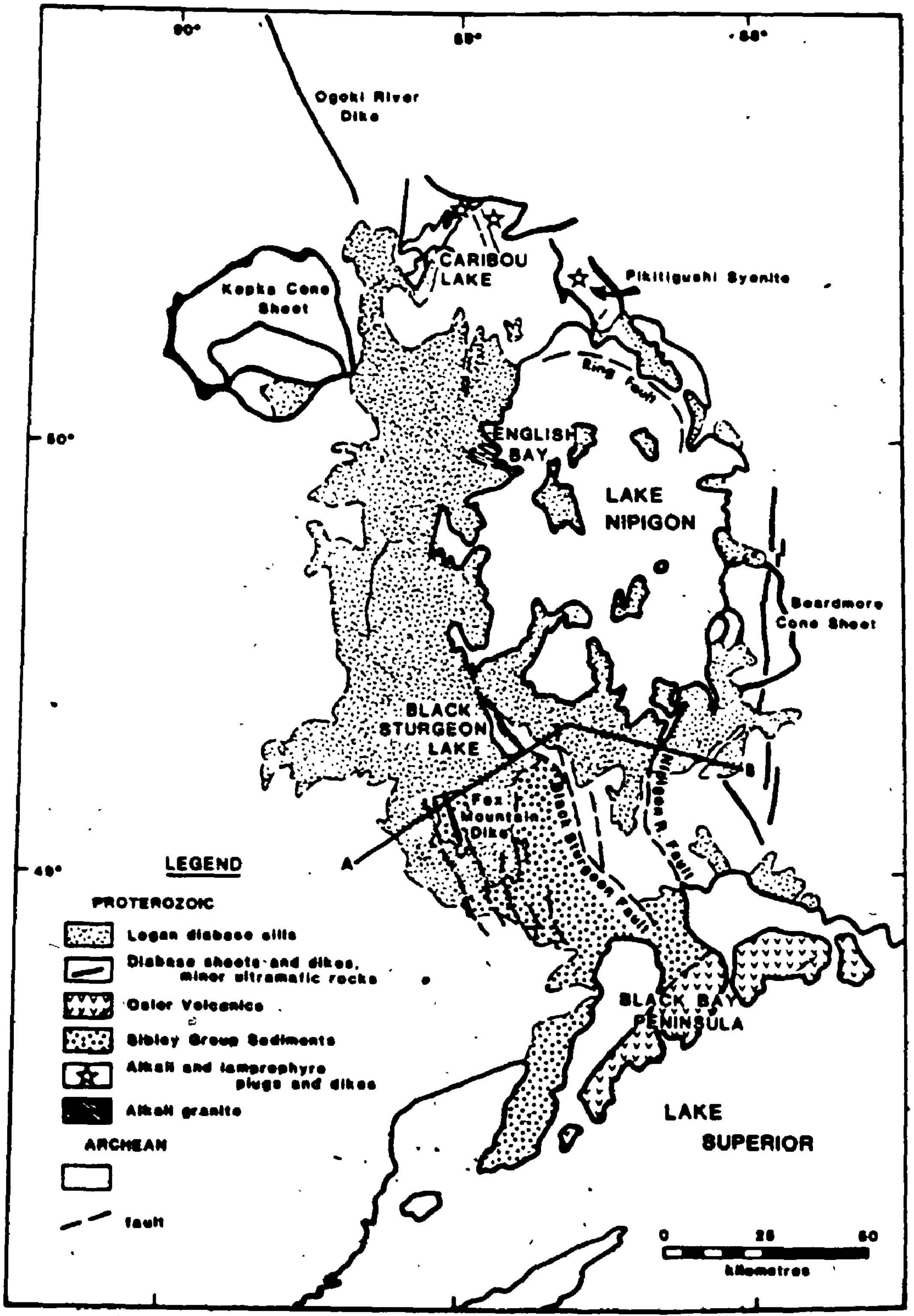
90°
89°
88°
Ogoki River Dike
CARIBOU LAKE
Kopka Cone Sheet
Pikitigushi Syenite
Ring Fault
50°
ENGLISH BAY
LAKE NIPIGON
Beardmore Cone Sheet
BLACK STURGEON LAKE
B
Nipigon R. Fault
Fox Mountain Dike
Black Sturgeon Fault
A
49°
LEGEND
PROTEROZOIC
Logan diabase sills
Diabase sheets and dikes, minor ultramafic rocks
Osler Volcanics
Sibley Group Sediments
Alkali and lamprophyre plugs and dikes
Alkali granite
ARCHEAN
fault
BLACK BAY PENINSULA
LAKE SUPERIOR
0
25
50
kilometres

3.3 Geology of the Nipigon plate. Based on maps of the Ontario Geological Survey. Line AB refers to section shown in Figure 3.5.

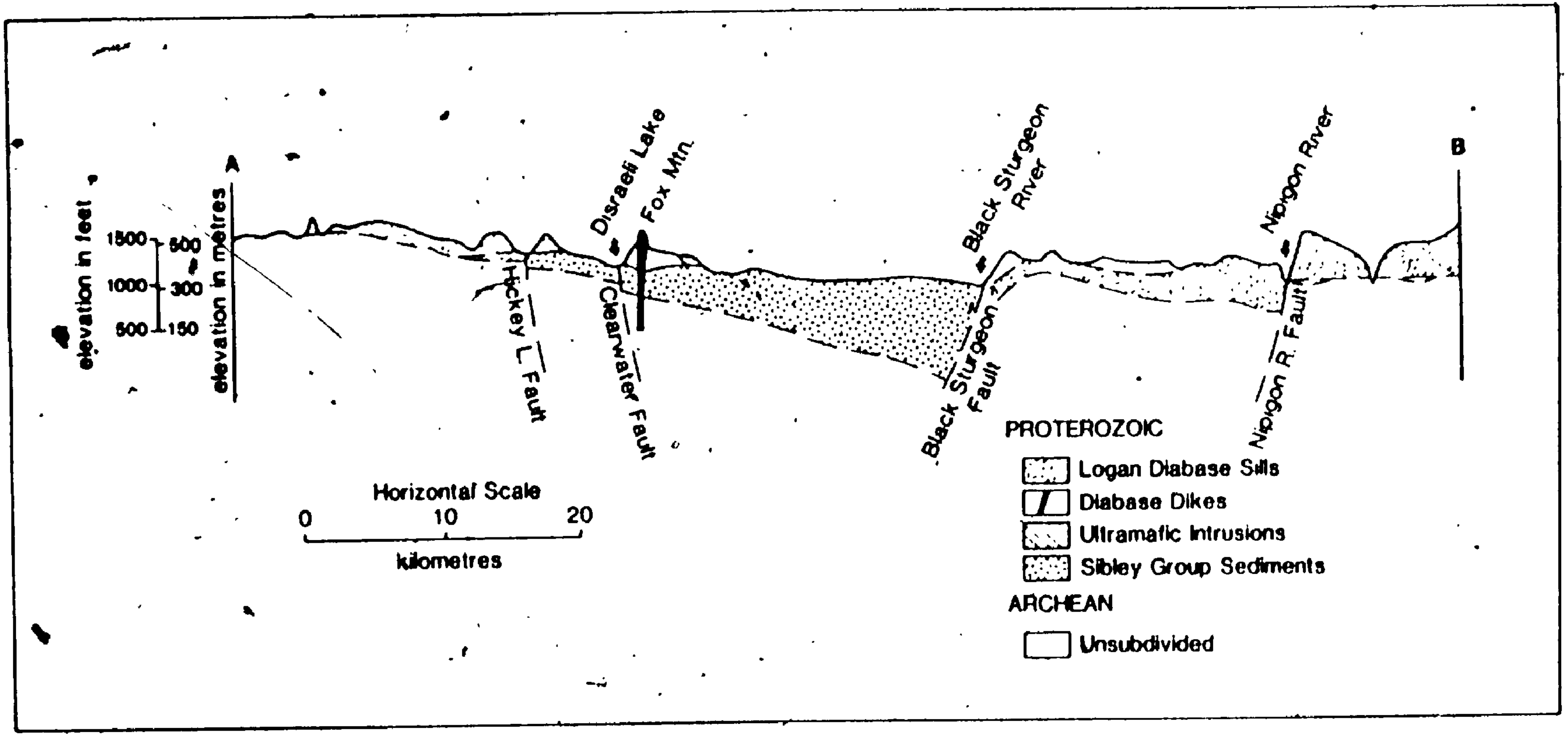
A
B
elevation in feet
1500
1000
500
500
300
150
elevation in metres
Disraeli Lake
Fox Mtn.
Hickey L. Fault
Clearwater Fault
Black Sturgeon River
Black Sturgeon Fault
Nipigon River
Nipigon R. Fault
Horizontal Scale
0
10
20
kilometres
PROTEROZOIC
Logan Diabase Sills
Diabase Dikes
Ultramafic Intrusions
Sibley Group Sediments
ARCHEAN
Unsubdivided

3.5 Cross section of the Black Sturgeon graben showing asymmetric structure of the graben and the location of the Fox Mountain dike. Line of cross-section AB is located on Figure 3.3.

maximum thickness of 420 meters (Ojakangas and Morey, 1982) and consists of a lower unit of quartz arenite with conglomerate lenses (Pass Lake Formation) overlain by red, fine grained arenaceous and clayey dolomite (Rossport Formation) passing upwards to red shale and mudstone (Kama Hill Formation) (Franklin et al. 1980).

An Rb-Sr whole rock isochron on dolomites and shales gives an age of 1339 +/-33 Ma for the Sibley Group (Franklin et al. 1980) and indicates that the sediments are at least 150 Ma older than the volcanic rocks of the Lake Superior Basin. This age difference is further supported by the presence of rounded clasts of Sibley sandstone in conglomerates at the base of the volcanic sequence which indcates that the Sibley was lithified prior to volcanism (Ojakangas and Morey, 1982). Cheadle (1986) has suggested a genetic connection between the formation of the Sibley basin and later Keweenawan subsidence based on the similarities in tectonic regimes (ie. broad crustal subsidence). Due to the difference in ages and the protracted crustal instability in the Nipigon- Superior area, a dynamic connection between the Sibley basin and Lake Superior basin is considered tenuous and the two basins may have developed as discrete events.

Diabase, occurring as sills, cone sheets and minor dikes, is the predominant igneous rock of the Nipigon plate. Recent mapping by Sutcliffe (1981) and Sutcliffe and Greenwood (1982) has indicated that one major diabase sill approximately 200 meters thick is exposed over most of the Lake Nipigon area, however, there are local remnants of another sill of approximately equal thickness overlying this. The present volume of the lower sill is approximately 5000 km3, but in excess of 10,000 km3 of magma was probably emplaced if the upper sill was as extensive as the lower sill. Compositionally the diabase is an olivine tholeiite with low abundances of K, P, Ti and is similar to the olivine tholeiite basalt flows (Green, 1982) of Lake Superior. Minor picritic intrusions and peridotite to olivine melagabbro cumulate rocks are associated with the diabase sills.

U-Pb dating of zircon and baddelyite indicates that the sills are 1108.8 +4/-2 Ma (Davis and Sutcliffe, 1985) which is within error of the age of 1110 +/-10 Ma determined by Silver and Green (1972) for the main phase of Keweenawan igneous activity.

Geological mapping has shown that the Nipigon plate has been the location of granitic and alkaline magmatic events which predate the Keweenawan rifting event. On English Bay of Lake Nipigon, an alkali feldspar granite to subvolcanic rhyolite porphyry dated at 1536.7 +10/-2.3 Ma (Davis and Sutcliffe 1985) is overlain by quartz arenites and conglomerates of the Sibley Group. This pluton is the intrusive source of now poorly exposed rhyolitic volcanics underlying diabase sills in the northern part of Lake Nipigon (Sutcliffe and Greenwood, 1982). Some of the volcanics exhibit welded textures and are associated with cross bedded sandstones suggesting that they were deposited in a subaerial environment. This plutonic-volcanic event is probably related to, although somewhat older than, the 1.4 to 1.5 Ma passive granitoid plutonic event (Anderson 1983), which was widespread over the North American continent but has not been previously reported in northwestern Ontario.

Alkaline rocks of the Nipigon plate include a series of alkali-basalt and olivine-phlogopite lamprophyres with affinity to carbonatite in the Caribou Lake area, 30 km northwest of Lake Nipigon. The age of these alkaline rocks is not certain, but they are probably of similar age to the granitoid-volcanic event at 1537 Ma. Volcanic conglomerate containing alkali basalt fragments is overlain by quartz arenite of the Sibley Group on the northwest shore of Lake Nipigon. This suggests that the alkali basalt magmatism, like the granitoid-volcanic event is older than or approximately the same age as the Sibley Group. The lamprophyre dikes on Caribou Lake are petrographically similar to alnoitic lamprophyres dated at 1653 +/-122 Ma by Platt and Mitchell (1982) in the Marathon area, approximately 200 km south east of Caribou Lake. The alkaline rocks and lamprophyres in the Nipigon area therefore appear to be older than the main phase of Keweenawan rifting in the Lake Superior basin.

Franklin et al. (1980) in a study of the Sibley Group sediments expanded on the earlier suggestions of Card et al. (1972) that the Sibley basin - Nipigon plate is the failed arm of a triple junction located near the Black Bay Peninsula of Lake Superior. They suggested that Sibley Group sedimentation may have been controlled by a rift valley and that the diabase sills were intruded into the same failed arm during a reactivation of the structure 150 to 200 Ma later in the Keweenawan rift event. Franklin et al. (1980) noted that it is also possible that the Sibley basin may have been preserved in a failed arm which formed after deposition of the sediments. This latter possibility is supported by Cheadle (1986) who considers that the sediments were not deposited in a failed arm but may have been preserved by faulting. Green (1983) previously questioned the failed arm origin, for the Sibley Group based on the greater age of the sediments relative to Keweenawan rift related rocks and lack of contemporaneous igneous activity. The present data however indicate granitic and alkaline magmatism which is older than, and may be in part contemporaneous, with Sibley sedimentation and in part, discounts this latter argument.

Since the Sibley Group sediments are not clearly related to the Keweenawan rift event, the failed arm model is difficult to constrain on sedimentological grounds. The model, however, can be more fully evaluated by examining the mechanism of intrusion of the diabase sills and related tectonic features which were developed during the main phase of Keweenawan rifting.

3.3.1 Black Sturgeon Graben Structure

The Black Sturgeon fault which extends northwest from the Black Bay Peninsula of Lake Superior to Lake Nipigon

(Coates, 1972) is a major tectonic feature of the Nipigon plate. The fault system is a series of en echelon northwest trending faults which form the eastern margin of an asymetrical graben structure approximately 20 km wide (Figure 3.3).

The uplifted eastern block of the fault zone forms the eastern boundary of a thick prism of Sibley Group sediments. Exposure of westerly dipping mylonite north of Black Sturgeon Lake on Lake Nipigon and a prominent vertical to west dipping fracture set in the Archean rocks parallel to the fault suggest that the Black Sturgeon Fault dips west and indicate that it is a normal fault. The western margin of the Sibley sediment prism is not clearly fault bounded but a series of northwest trending lineaments suggest that faults may underlie this part of the basin (Coates, 1972). The prism of sediments appears to be preserved in an asymetric graben with a well defined eastern margin and a less strongly developed western margin (Figure 3.5).

In the southern part of the area, the Black Sturgeon fault forms a prominent escarpment. Exposures of Archean rocks on the elevated eastern block contrast with the 400 meter thick prism of Sibley sediments preserved in the western block and indicate a minimum vertical displacement of approximately 500 meters. Further north in the southern part of Lake Nipigon the fault is evident as an offset in the magnetic anomalies associated with the east trending iron formation which passes under the lake. The data indicate that

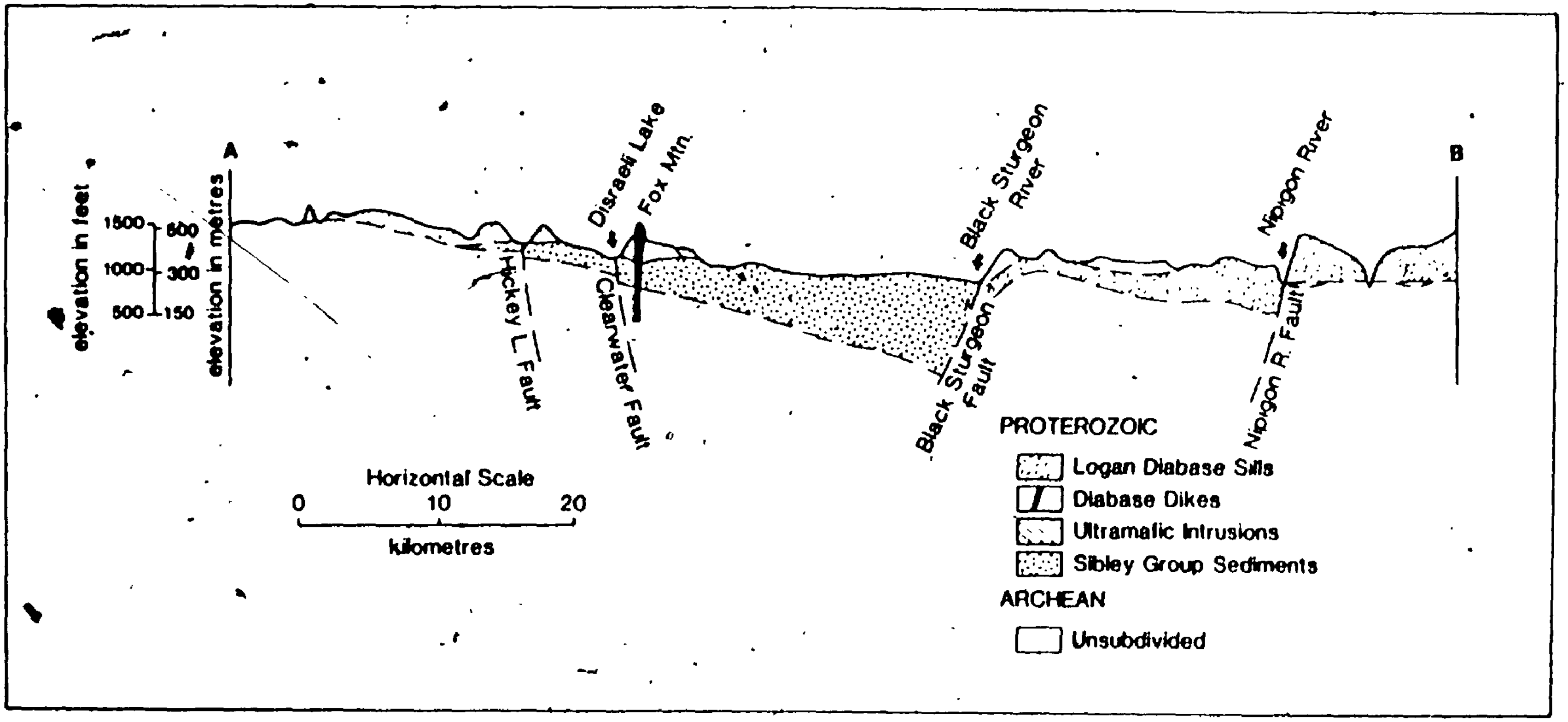
A
B
elevation in feet
elevation in metres
1500
1000
500
600
300
150
Disraeli Lake
Fox Mtn.
Hickey L. Fault
Clearwater Fault
Black Sturgeon River
Black Sturgeon Fault
Nipigon River
Nipigon R. Fault
Horizontal Scale
0
10
20
kilometres
PROTEROZOIC
Logan Diabase Sills
Diabase Dikes
Ultramafic Intrusions
Sibley Group Sediments
ARCHEAN
Unsubdivided

3.5 Cross section of the Black Sturgeon graben showing asymmetric structure of the graben and the location of the Fox Mountain dike. Line of cross-section AB is located on Figure 3.3.

the fault has a major horizontal component with a sinistral offset of approximately 4 km.

Another zone of faulting occurs along the Nipigon River (Wilson, 1910). Displacement along this fault is considerably less than the Black Sturgeon Fault and no horizontal displacement has been recognized. Vertical movement along the Nipigon River Fault has a similar sense to the Black Sturgeon Fault.

A zone of dislocation has not been traced north of Lake Nipigon, however, alkalic and lamprophyre dikes on Caribou Lake, and the Ogoki River diabase dike (Figure 3.3) may represent an extension of the fault zone. Although these rocks have not been dated, other Proterozoic alkaline intrusions north of Lake Superior are clearly related to major structural zones (Klasner et al. 1982; Percival and Card, 1983). Several northwest trending lineaments and minor faults in the Caribou Lake area may also be related to graben development (Sutcliffe, 1984).

Brecciation and folding of Sibley sediments in the vicinity of the Black Sturgeon fault (Wilson, 1910; Coates, 1972) indicates fault movement has occurred after deposition of the sediments. There is no evidence for significant movement along the Black Sturgeon fault after emplacement of the diabase sills. This brackets development of the graben structure between 1339 +/-33 and 1108.8 +4/-2 Ma. One kilometer east of Black Sturgeon Lake, pitchblende-hematite veins occur in northwest trending fractures which have the same orientation as, and are therefore considered to be related to, the Black Sturgeon Fault. This mineralization has been dated at 1090 +/-20 Ma by the U-Pb method (Ruzicka and Le Cheminant, 1984). This age is similar to the diabase sills and suggests that extensional tectonism leading to graben formation and diabase intrusion are contemporaneous.

The relationship between graben formation and mafic magmatism is further supported by the emplacement of a differentiated mafic to ultramafic dike complex within the graben structure south of Lake Nipigon (Figure 3.3). The 0.4 km wide by 10 km long Fox Mountain gabbro dike is associated with olivine gabbro to peridotite intrusions and is intrusive into Sibley sediments. Parallelism of the dike complex with the Black Sturgeon fault system suggests emplacement of the mafic magma under the extensional tectonic conditions that were responsible for graben formation.

The geological evidence indicates that faulting and graben formation in the southern part of the Nipigon plate is associated with the main Keweenawan rift-related igneous event at [illegible]0 +/-10 m.y. and postdates sedimentation in the Sibley basin. The development of this failed rift in the Nipigon area during the Keweenawan event may have reactivated older rift related structures. These structures may have developed at 1.3 b.y. controlling Sibley Group sedimentation (Franklin et al. 1980) and at approximately 1.5 b.y. associated with alkalic and granitic magmatism.

3.3.2 Feeder Zones of the Diabase Sills

The feeder zones of the diabase sills of the Nipigon plate provide data on the strain within the lithosphere during the main phase of Keweenawan magmatism. Cone sheets and dikes are the two major forms of feeder zones which have been recognized. Ring faulting also controls some mafic magmatism in the northern part of Lake Nipigon.

In the northwestern part of the plate a large cone sheet structure (Figure 3.6) 30 to 40 km in diameter dips inward at 45° to vertical and changes abruptly into a horizontal diabase sill. East of Lake Nipigon, near Beardmore, a second cone sheet of comparable dimensions has been recognized but limited data on the dip of the sheets are available. The cone sheets are intrusive into Archean plutonic and metamorphic rocks.

A broad gravity high approximately 30 milligals above the background is coincident with the cone sheet structure northwest of Nipigon and is one of the most prominent gravity features of the Nipigon Plate (Figure 3.4). This anomaly suggests that the mafic rocks extend to depth and are distinct from the diabase sills exposed to the east which are not associated with a significant gravity expression.

The cone sheets flank a region of ring faulting and subsidence in the northern part of Lake Nipigon. Reverse faulting is observed to post-date Sibley sedimentation in this area, but the diabase sheets post-date the development of the fault. Minor picrite and diabase dikes were intruded parallel to the ring fault suggesting that the structure has

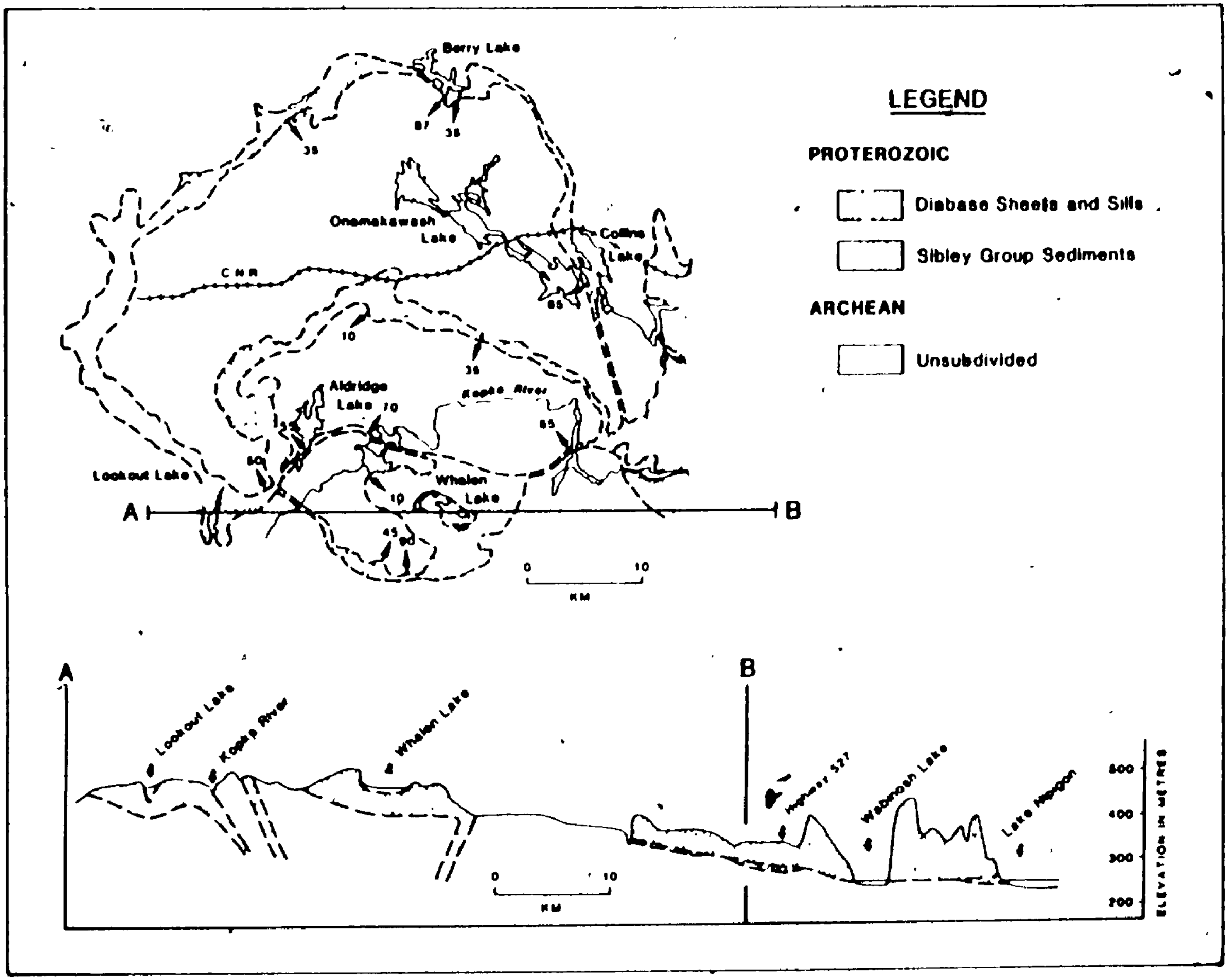
LEGEND
PROTEROZOIC
Diabase Sheets and Sills
Sibley Group Sediments
ARCHEAN
Unsubdivided
Berry Lake
Onamakawash Lake
Collins Lake
CNR
Aldridge Lake
Kopka River
Whalen Lake
Lookout Lake
A
B
0
10
KM
Lookout Lake
Kopka River
Whalen Lake
Highway 527
Wabinosh Lake
Lake Nipigon
500
400
300
200
ELEVATION IN METRES

3.6 Geology of the Kopka cone sheet. Based on maps of the Ontario Geological Survey.

controlled the emplacement of some mafic magmas.

In the southern part of the plate within the Black Sturgeon graben, the Fox Mountain dike discussed previously has been identified as a probable feeder zone. Other than the Fox Mountain dike, no other dikes are recognized as feeders for the diabase sills. A swarm of dikes along the eastern margin of the plate has a positive magnetic polarity (Halls, 1978) and therefore do not appear related to the sills which have reverse polarity. Several large northwest trending dikes of reversed polarity are present in the Caribou Lake area and extend north toward the Ogoki River. These may potentially be feeders for the sills, but the relationship has not been demonstrated.

Examples of cone sheets as feeder zones for diabase sheets are not commonly described in the literature. The best examples appear to have been documented by Carey (1958a) and Spry (1958) in the Jurassic Tasmanian dolerites. Annular outcrop patterns of diabase with inward dips of 20° to 25° in the Karoo dolerites were originally considered to be cone sheets but subsequently have been identified as shallow basins (Walker, 1958).

In the Tasmanian dolerites, cone sheets are intruded into a sequence of Triassic and older sediments and grade upward into horizontal sills. The structures are of comparable form to those observed at Nipigon although somewhat smaller, have been modified by subsequent faulting, and in the case of the Tasmanian Huon Cone sheet, contain a central syenite complex.

In both the Tasmanian and Nipigon structures, cone sheets issuing from different centers merge into a sill at one stratigraphic level.

In the Nipigon plate the radially symetrical cone sheet structures indicate that the sheets must be emplaced under conditions of equal horizontal stress (Roberts, 1970). Hebridean cone sheets have been modelled by Anderson (1937) as being emplaced into tension fractures generated by the upward push of magma, by Robson and Barr (1964) as occupying shear fractures which occur as conical normal faults above a magma body under pressure and by Phillips (1974) as occupying shear fractures formed as a result of dynamic stresses arising from rapid expansion of magma undergoing retrograde boiling. A feature common to all of these models is that the sheets are intruded above a magma which is expanding or rising upwards.

Cone sheets of the Nipigon diabase are larger and lack the associated granitic rocks of the Hebridean cone sheets on which much of the previous work is based. However, in both provinces the cone sheets are predominantly mafic. In the Hebridean province, cone sheets occur where doming has taken place although some subsidence may be associated with the emplacement of cone sheets (Walker, 1975). Although doming can not readily be demonstrated in the Nipigon structures, uplift of the central block appears to have occurred based on the higher elevation of the basal contact of the diabase sill toward the center of the structure.

The dimensions and inferred focus of the Nipigon cone sheets suggest that fracturing has occurred on a scale which has affected the entire thickness of the continental crust. Since cone sheets form over upward rising magma, fracturing on this scale may have been induced by upwelling zones of melting or hot spots beneath the lithosphere in the region of the plate.

Koide and Bhattaoharji (1975) have developed a model for the origin of cone sheets and calderas based on the stress distribution around a prolate magma body intrusive into an elastic lithospheric plate which provides a theoretical basis for the Nipigon structures. Their interpretation differs from Anderson's (1937) model but is similar to the Robson and Barr (1964) model in that caldera subsidence and cone sheet emplacement may result from excess magma pressure due to horizontal extension above a magma body.

The Bhattacharji and Koide (1975a) model was originally developed to explain the origin of rift valleys based on the intrusion of an oblate magma body into the lithospheric plate. The model provides a basis for a continuum between the development of cone sheets and graben development with axial dikes, based on the geometry of the a magma chamber intrusive into the lithosphere. Bhattacharji and Koide (1975 a,b) suggest that the origin of a rift structure is initiated by wide domal or antiformal uplift over an asthenospheric upwell. The stress from doming is not sufficient to produce axial collapse which requires that a magma body wedges higher in the crust. Under these conditions, inward dipping, normal, funnel shaped faults develop and a central area of subsidence occurs in the domal uplift. A graben develops over an oblate magma body and may later be accompanied by intrusion of axial dikes. Caldera collapse and cone sheets may form over a prolate magma body (Figure 3.7). Within the Nipigon plate, these intrusive forms may be represented by the Fox Mountain dike within the Black Sturgeon graben in the southern part of the plate and by the cone sheets in the north. According to the model, individual cone sheets may have formed over secondary diapirs from the larger asthenospheric upwell. The zone of ring faulting and caldera collapse in the northern part of Lake Nipigon may have occurred over the first order upwell, however, the model predicts that subsidence is associated with inward dipping or conical fractures and therefore does not fully account for this structure.

3.4 Tectonic Summary

On a global scale, major provinces of diabase sills and sheets are associated with sedimentary basins of moderate thickness which had not been folded significantly at the time of intrusion (Carey, 1958b). Within this category are the Triassic-Jurassic dolerite sheets of Tasmania, Antarctica, South Africa, Brazil and northeastern United States (Carey 1958b). These provinces may be related to a period of major Triassic-Jurassic rifting which resulted in the break up of Pangea in a series of presumed hot spot related events (Burke and Dewey, 1973).

2

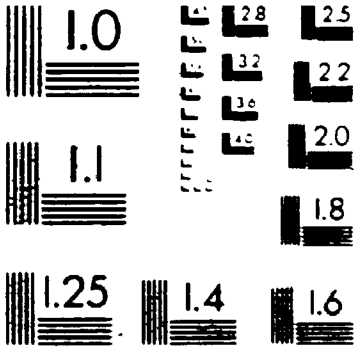
1.0
2.8
2.5
3.2
2.2
3.6
4.0
2.0
1.1
1.8
1.25
1.4
1.6

MicroD

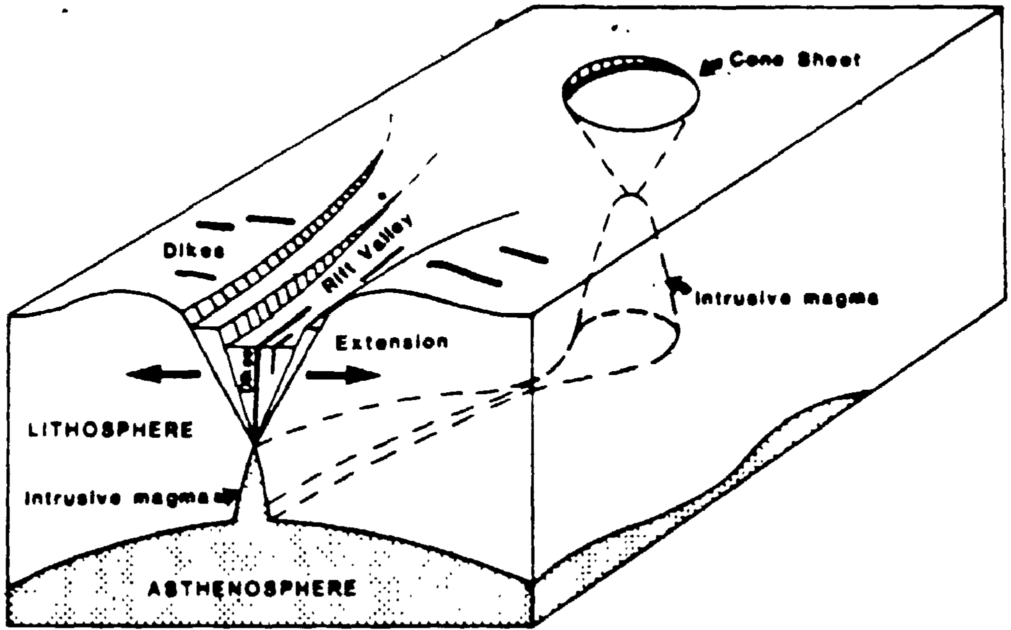
Cone Sheet
Dikes
Rift Valley
Intrusive magma
Extension
LITHOSPHERE
Intrusive magma
ASTHENOSPHERE

3.7 Schematic diagram showing possible relationships between graben formation with axial dike and cone sheet formation. Modified from Koide and Bhattacharji (1975) and Bhattacharji and Koide (1975a, b).

Sawkins (1976) has noted that the geological record on several continents indicates a late Proterozoic event of widespread rifting. This time period between 1,200 and 1,000 Ma is characterized by sequences of continental clastic and contemporaneous basaltic rocks which are related to tensional tectonic regimes. Several late Proterozoic provinces of diabase sills such as the Jotnian sills of Scandinavia and Cuddapahs of India are related to rifting events (Sawkins, 1976). The tectonic setting and lithologies of the Nipigon plate appear similar to these other late Proterozoic sequences.

The main phase of rift related igneous activity at 1109 Ma within the Nipigon plate is related to a failed arm extending north from the Keweenawan rift. This failed arm may have reactivated older rift-related structures, associated alkali basalt and lamprophyre magmatism, passive granite plutonism at 1537 Ma (Davis and Sutcliffe, 1985) and Sibley sedimentation at 1339 +/-33 Ma (Franklin _et al_. 1980). Repeated activation is a characteristic feature of tectonic zones marginal to the Keweenawan rift (Klasner _et al_. 1982) and many rift zones record a history of tensional tectonic activity for about 200 Ma prior to rifting. For example in the Gardar Province, which overlaps in age with the Keweenawan, three episodes of faulting and alkali magmatism at 1300, 1250, and 1170 Ma have been recognized (Upton and Blundell, 1970). These repeated tensional phases may be incidental to large scale Late Proterozoic plate motions

(Burke and Dewey, 1973).

The cause of Keweenawan rifting is not well defined and several hypotheses have been proposed. These include: a) rifting due to dextral shearing along the Grenville Front (Donaldson and Irving, 1977); b) rifting due to the Grenville collisional event with the Keweenawan opening as an impactogen (Burke, 1978; Gordon and Hampton, 1986); c) active rifting generated by plumes beneath the Keweenawan rift (Burke and Dewey, 1973; Franklin et al. 1980) and d) rifting related to opening of the Grenville proto-Atlantic with a plume located southeast of the Grenville Front and the Keweenawan opening as an aulacogen (Burke and Dewey, 1973).

In these hypotheses, a crucial problem is that although the age of Keweenawan rifting is relatively well constrained, the age of deformation in the Grenville province is not. This makes it difficult to evaluate models a) and b) in which Keweenawan rifting occurs during Grenville deformation and c) and d) in which rifting may predate Grenville deformation. Anderson and Burke (1983) have observed that the timing of Keweenawan rifting and the beginning of the Grenville orogeny, based on a small number of U-Pb and Rb-Sr dates suggest that the Keweenawan is not an aulacogen of a rifting event related to the opening of the Grenville proto-Atlantic.

Gordon and Hampton (1986) have suggested that the Keweenawan rift formed as a result of convergence related to the Grenville orogeny. They suggest that the rift formed as a result of northwest trending strike slip faults in the foreland of the Grenville front. In the model, offsets in the strike slip faults caused the development of pull-apart basins which subsequently evolved into a rift. In order to explain offsets in the mid-continent gravity anomaly, they suggest that these faults had a left lateral offset. The Black Sturgeon Fault in the Nipigon area would potentially satisfy the requirements for the proposed faults since a sinistral offset of several km along the Black Sturgeon Fault is indicated by displacement of Archean structures identified on a basis of aeromagnetics.

Most of the observations in the Nipigon area, however, support an active rifting model in which the Nipigon plate hosted a failed arm during the main phase of rifting in the Lake Superior basin. Intrusion of basaltic rocks in the Nipigon plate at 1109 Ma was coeval with the igneous activity in the Superior basin. The evidence for rifting in the Nipigon plate includes: the geometry of the Nipigon structure with respect to a flexure in the Keweenawan rift of Lake Superior; a weak gravity high extending north from Lake Superior; development of the Black Sturgeon graben in the southern part of the Nipigon plate and emplacement of basaltic magma into the graben. A progression in the intensity of rifting from north to south is indicated by the nature of the feeder zones of the diabase sills. In the northern part of the plate, cone sheets indicate lithospheric doming over an upwelling asthenosphere under conditions of hydrostatic horizontal strain. In the southern part of the plate, the emplacement of mafic magma is controlled by the graben structure and represents a stronger manifestation of rifting. There is no indication that mafic magmatism was due to pull-apart basins. Furthermore, the development of the Nipigon arm may be superimposed on earlier rift related structures controlling deposition of the Sibley Group an alkali granite plutonic-volcanic event, and alkali basalt-lamprophyre magmatism.

CHAPTER 4

PETROLOGY OF LATE PROTEROZOIC DIABASES AND PICRITES FROM LAKE NIPIGON

4.1 Introduction

Recent studies of continental basalt petrogenesis have stressed the importance of lower crustal processes in the evolution of the mantle derived magmas. The recognition of a density filter effect in which the continental crust restricts the upward rise of dense picritic and MORB-like basaltic magmas (Stolper and Walker 1980, Sparks et al. 1980) has lead to a model of underplating and ponding of basalt melts at the crust-mantle interface (Cox, 1980). These studies show that in a subcrustal magma chamber, mantle derived magma may assimilate a lower crustal component, mix with fresh injections of primitive magma, and fractionate to a density minimum prior to eruption at the earth's surface. Recent studies (eg. Francis et al. 1983) have documented how these processes evolve during continental rifting resulting in distinct tectonic control on the type of magma erupted.

This chapter presents an account of the magmatic chemistry of the late Proterozoic diabases and picritic rocks in the Nipigon plate adjacent to the Keweenawan rift. The compositional variation of these rocks is interpreted as representing two magma series, which are fractionated to different degrees as a consequence of the development of crustal filtering during the igneous event. Early magmas in the sequence are picritic.

Density relations suggest that picritic magmas may pass through the crust along fractures which extend through the crust-mantle interface. The later magmas are more fractionated and were probably temporarily ponded at the base of the crust where they fractionated along an olivine-plagioclase cotectic prior to eruption. These magmas are intruded as diabase sills. Compositional variation within the sills reflects the composite nature of the intrusions which crystallized from episodic injections of magma.

4.2 Review of Geological Setting

The mafic rocks at Lake Nipigon (Figure 4.1) are intruded into an undeformed flat lying succession of late Precambrian epicontinental clastic sediments named the Sibley Group (Franklin et al. 1980). These sediments overlie an Archean and Middle Proterozoic basement in the Lake Nipigon area. The sediments and sills have a combined maximum thickness of 600 to 800 m and form a broad, shallow basinal structure named the Nipigon plate (Stockwell et al. 1972) which extends 160 km north from the Keweenawan rift of Lake Superior. Zircon dating of the diabase sills (Davis and Sutcliffe, 1985) indicates that mafic magmatism in the Nipigon plate took place at 1108.8+4/-2 Ma and is contemporaneous with basaltic magmatism associated with Keweenawan rifting. During this rift event the Nipigon plate hosted a failed arm. This is indicated primarily by graben development in the southern part of the plate.

Feeders for the diabase sills change in geometry from north

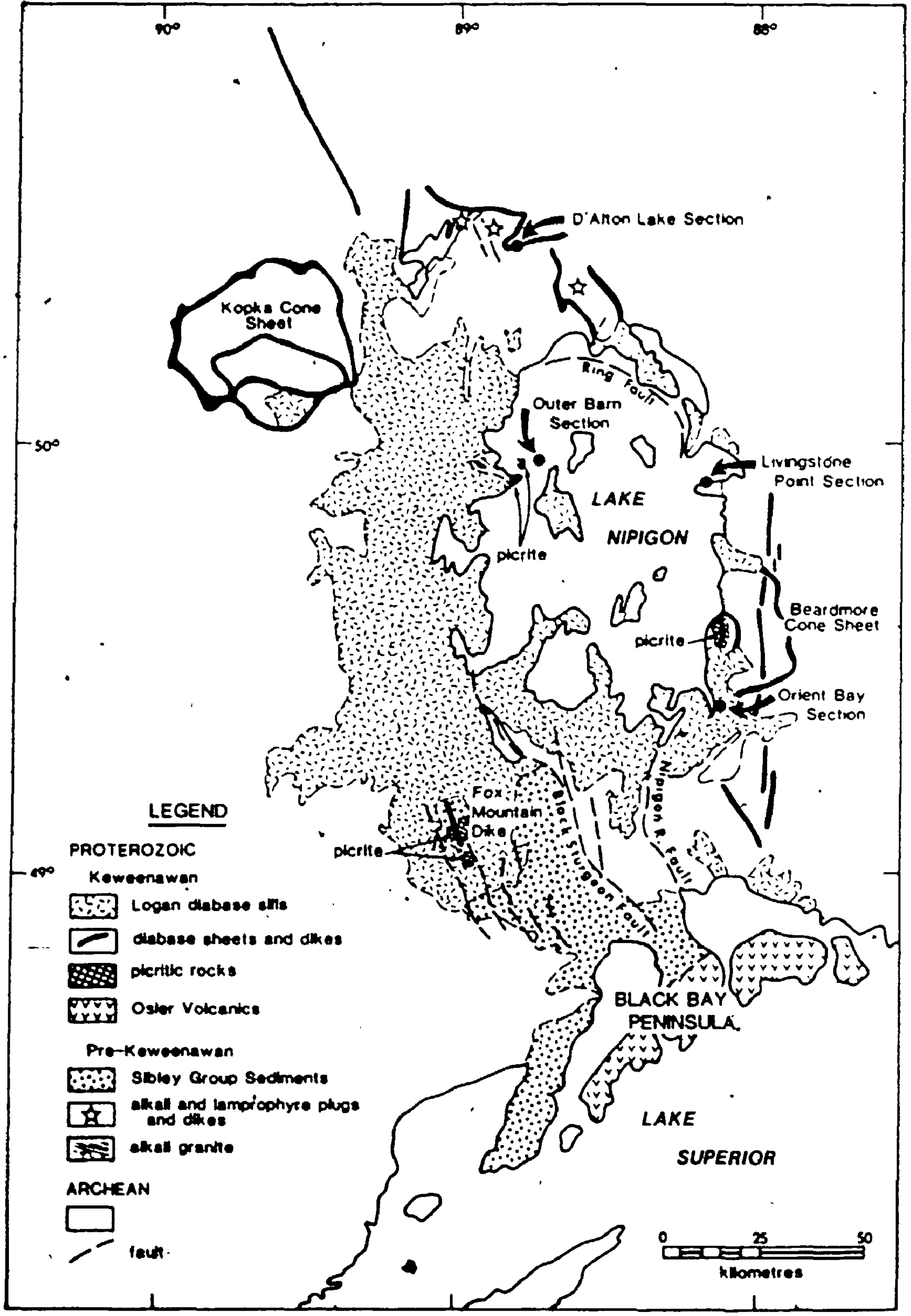
90°
89°
88°
50°
49°
D'Alton Lake Section
Kopka Cone Sheet
Ring Fault
Outer Barn Section
Livingstone Point Section
LAKE NIPIGON
picrite
Beardmore Cone Sheet
picrite
Orient Bay Section
Fox Mountain Dike
picrite
Black Sturgeon Fault
Nipigon R. Fault
BLACK BAY PENINSULA
LAKE SUPERIOR
LEGEND
PROTEROZOIC
Keweenawan
Logan diabase sills
diabase sheets and dikes
picritic rocks
Osler Volcanics
Pre-Keweenawan
Sibley Group Sediments
alkali and lamprophyre plugs and dikes
alkali granite
ARCHEAN
fault
0
25
50
kilometres

4.1 Generalized geology of the Nipigon Plate and the northern Lake Superior area. Location of sampled sections of diabase sills are labelled. Geology from maps of the Ontario Geological Survey.

to south, reflecting the intensity of rifting in the failed arm. In the south, a large composite feeder dike intrudes the Black Sturgeon graben, while in the north, under conditions of low horizontal stresses circular ring dikes and cone sheets feed the diabase sills (Figure 4.1).

Mafic rocks in the Nipigon plate consist of two suites. An early and volumetrically minor, sequence of picritic rocks forms dikes, ring dikes, and locally sills of olivine gabbro and peridotite. The picritic rocks are associated with magmatic centers which later become feeder zones for the diabase. The majority of the igneous rocks are tholeiitic diabase sheets, sills and dikes which cover an area of approximately 11,000 km^2. The total volume of basaltic rocks in the Nipigon plate is estimated to be in excess of 10,000 km^3. This represents a minimum figure since an unknown amount of diabase has been removed by erosion. The volume however is comparable to recent plume related igneous events such as the Hawaiian volcanic centers which have volumes of 3,000 to 40,000 km^3 (Carmichael _et al._ 1974).

Mafic volcanic rocks associated with the sills are not observed in the Nipigon plate, however to the south the sills dip under the Keweenawan flood basalts of the Osler Group. It is possible that volcanic rocks, once overlying the sills in the Nipigon plate are now removed by erosion. Geochronology and field relations suggest that the sills were intruded early in the igneous event and may have contributed to crustal loading facilitating later eruption of the volcanics (Davis and

Sutcliffe, 1985).

Except for minor granophyre dikes, felsic rocks associated with the diabase are absent. To the south, however, rhyolite flows and intrusions are associated with the Osler basalts. Zircon data (Davis and Sutcliffe, 1985) indicate that these rhyolites formed by melting of older crust during the Keweenawan igneous event.

The diabases and picritic rocks of Lake Nipigon are sub-alkalic tholeiites. Rock compositions plotted in figure 4.2, show a well developed iron-enrichment trend although it is important to note that many of the magnesium rich picritic rocks formed by crystal accumulation and do not represent liquid compositions.

4.3 Diabase Sills

One major diabase sill approximately 150 to 200 m thick is exposed over most of the Nipigon Plate (Sutcliffe, 1981; Sutcliffe and Greenwood, 1982). Erosional remnants of an upper sill at least 150 m thick locally overlie this. The two sills are separated by a septa of Sibley Group sediments up to 10 m thick although the chilled margins of the two sills were observed in direct contact at one locality on Lake Nipigon. In general the lower sill is characterized by shallow dips of less than 10° which define undulating basins and arches. Steeper dips are characteristic of areas with major structures extant prior to sill emplacement such as the circular ring fault in northern Lake Nipigon and the Black Sturgeon graben in the south.

Detailed mapping permitted a textural stratigraphy to be

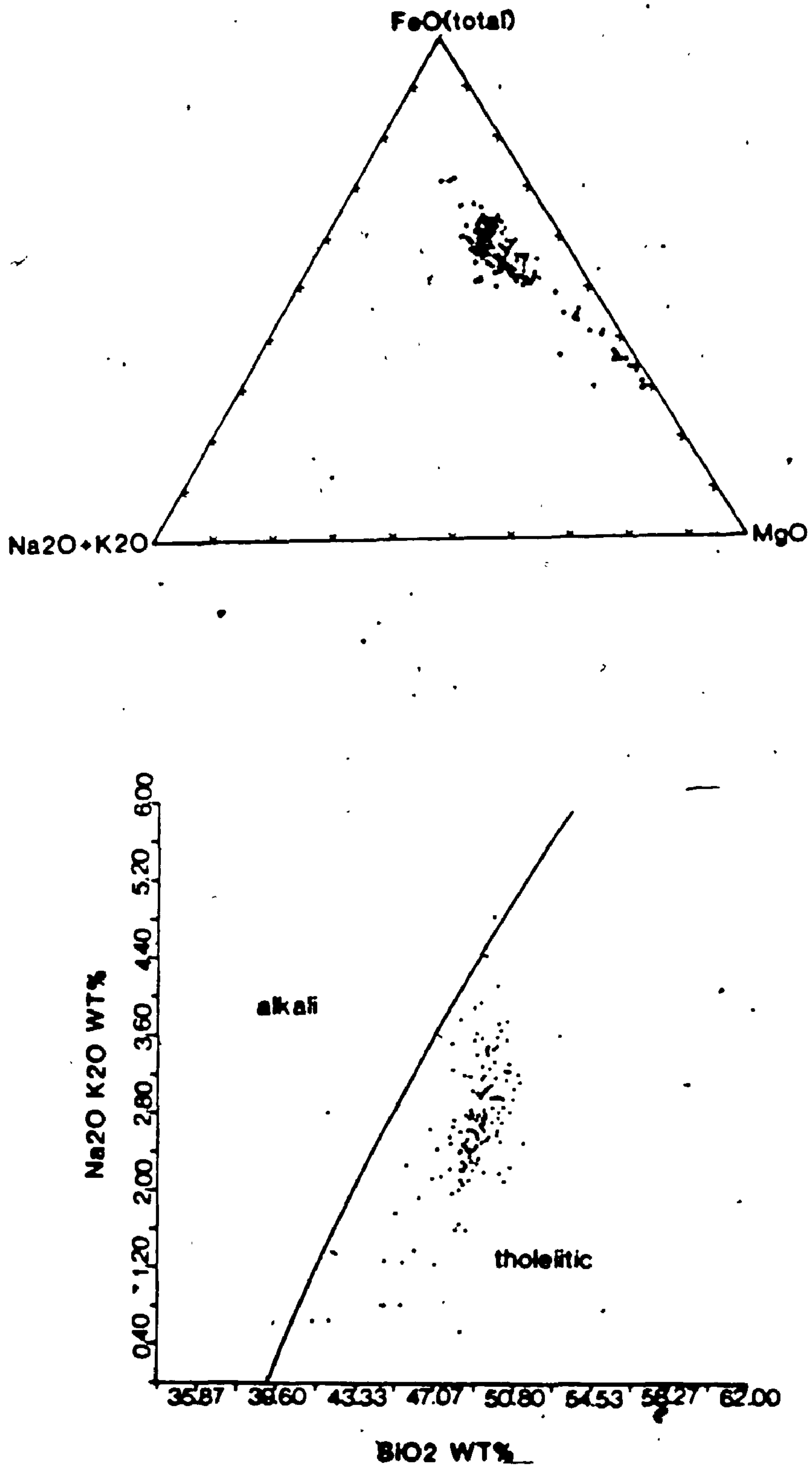

4.2 Mafic and ultramafic rocks of the Nipigon Plate plotted on a) AFM diagram and b) alkalies vs silica diagram for weight % oxides.

established in the lower sill. The stratigraphy, (see figure 2.3), demonstrates that in most cases the diabase sills represent a single cooling unit. An internal chill contact is only found in one isolated case, in the D'Alton Lake section, north of Lake Nipigon.

Representative whole rock analyses and mineral compositions for the diabase are given in tables 4.1 and 4.2. The diabase consists of euhedral, tabular plagioclase (An_{75-44}), anhedral, interstitial to oikocrystic clinopyroxene ($Wo_{30-40}En_{32-54}$-Fs_{14-37}), rounded to subhedral olivine (Fo_{70-32}), interstitial anhedral magnetite and ilmenite. Minor late pigeonite ($Wo_{12}En_{45}$-Fs_{43}) rims earlier augite. Accessory constituents are biotite, hornblende, iddingsite, chalcopyrite and apatite. Biotite and hornblende occur as interstitial phases rimming clinopyroxene. Typical grain sizes of plagioclase and clinopyroxene vary depending on the diabase texture and are indicated in figure 2.3. Olivine ranges in size from 0.1 to 1.5 mm. The upper coarse grained to pegmatitic zones of the sill have grain sizes in excess of 1 cm and contain well developed micrographic intergrowths of quartz-albite and quartz-orthoclase. In most samples alteration of plagioclase and pyroxene is minimal while olivine shows minor to complete alteration to iddingsite.

Fine grained chilled diabases commonly have an isogranular to intergranular texture with 5 to 10% microphenocrysts and glomeroporphyritic aggregates of microphenocrysts, although some chills are aphiric. The microphenocryst assemblages observed in the chills are plagioclase, plagioclase-olivine, plagioclase-

Table 4.1: Representative analyses of diabases and picrites from the Lake Nipigon area.

	1	2	3	4	5	6	7	8	9
SiO_2	41.00	44.60	47.10	48.50	50.10	49.00	48.90	50.10	48.60
TiO_2	0.71	1.88	2.68	1.50	1.10	0.91	0.88	1.44	2.89
Al_2O_3	2.88	7.72	11.50	15.50	13.50	15.30	14.70	14.40	10.20
$Fe_2O_3{}^t$	17.50	17.30	15.30	13.40	12.70	12.10	12.90	14.80	20.70
MnO	.23	0.21	.21	0.15	0.19	.17	.18	.20	.24
MgO	30.20	17.10	8.82	5.61	7.96	7.53	8.75	5.91	3.99
CaO	4.05	7.98	9.32	10.80	12.00	11.70	10.80	9.80	8.36
Na_2O	.20	1.32	2.53	3.30	2.26	2.27	1.92	2.25	2.72
K_2O	.43	0.41	0.66	.22	0.32	.36	0.61	0.69	0.80
P_2O_5	.06	0.14	0.20	.14	0.09	.07	0.06	0.06	0.20
LOI	2.30	0.41	0.25	.95	0.10	.11	.08	.15	0.04
Total	99.56	99.07	98.57	100.07	100.32	99.52	99.78	99.80	98.74
ppm									
Ni	871	755	305	-	106	115	157	128	57
Cr	2549	1000	430	-	167	243	240	120	78
Zr	134	-	-	-	97	79	81	132	184
Y	74	-	-	-	30	26	26	30	44
La	8	-	-	-	7	5	6	12	18
Ce	15	-	-	-	14	11	11	26	40
Nd	8	-	-	-	8	6	7	12	23
Sm	ND	-	-	-	3	3	3	4	7
Eu	0.8	-	-	-	1.0	0.9	0.9	1.2	1.9
Gd	3	-	-	-	3	3	3	4	8
Dy	1.5	-	-	-	3.5	2.9	2.7	4.3	8.0
Yb	0.5	-	-	-	1.7	1.5	1.4	2.7	4.2

1) Picrite cumulate sa 81-273. Beardmore ring dike.
2) Picrite dike sa.83-260. (Same dike as sa.83-251)
3) Picrite dike chill sa.83-251.
4) Diabase chill from D'Alton Lake section sa.80-1116.
5) Diabase from Orient Bay section sa.81-286. Near top of section.
6) Diabase from Orient Bay section sa.81-288. Middle of section.
7) Diabase fro Orient Bay section sa.81-289. Base of section.
8) Diabase from Kopka cone sheet sa.82-75.
9) Pegmatitic diabase from top of sill sa.81-285.

ND - not detected

Table 4.2 Representative mineral compositions from diabases and picrites from the Lake Nipigon area

	Olivine Analyses			
	1	2	3	4
SiO_2	39.53	38.71	38.00	34.59
TiO_2	0.00	.05	.03	.16
Cr_2O_3	.04	.18	.17	0.00
FeO	18.79	18.70	27.03	46.45
MnO	.23	.22	.34	.86
NiO	.37	.45	.25	.36
MgO	41.73	40.71	33.17	17.90
CaO	.12	.27	0.72	.30
Sum	100.81	99.31	99.71	100.62
Si	1.003	1.000	1.016	1.015
Ti	.000	.000	.001	.004
Cr	.001	.004	.004	.000
Fe	.399	.402	.605	1.140
Mn	.005	.004	.008	.021
Ni	.008	.008	.005	.008
Mg	1.578	1.566	1.322	.783
Ca	.003	.008	.021	.009
O	4.000	4.000	4.000	4.000

	Pyroxene Analyses					
	5	6	7	8	9	10
SiO_2	55.13	54.35	51.72	49.93	51.46	51.79
TiO_2	.42	.27	0.54	.66	.33	.36
Al_2O_3	.89	.65	2.64	1.51	2.61	1.12
Cr_2O_3	.27	.19	.46	.05	.28	.11
FeO	12.01	5.41	9.79	17.55	14.02	22.19
MnO	.23	.04	.22	.31	.26	.42
MgO	29.42	16.54	16.07	12.95	21.26	18.81
CaO	1.55	21.42	18.35	16.31	9.74	5.32
Na_2O	.30	.62	.49	.15	.02	.00
K_2O	.00	.00	.01	.00	.00	.00
Sum	100.22	99.49	100.29	99.42	99.98	100.12
Si	1.959	1.998	1.916	1.927	1.901	1.956
Aliv	.037	.002	.084	.069	.099	.044
Alvi	.000	.026	.032	.000	.014	.006
Ti	.011	.007	.015	.019	.009	.010
Cr	.008	.006	.013	.002	.008	.003
Fe	.357	.166	.303	.567	.433	.701
Mn	.007	.001	.007	.010	.008	.013
Mg	1.558	.906	.887	.745	1.170	1.059
Ca	.059	.844	.728	.675	.385	.215
Na	.021	.044	.035	.011	.001	.000
K	.000	.000	.000	.000	.000	.000
O	6.000	6.000	6.000	6.000	6.000	6.000

	Plagioclase Analyses	
	11	12
SiO_2	51.07	53.34
Al_2O_3	30.47	29.85
FeO	.66	.54
CaO	14.46	11.59
Na_2O	3.45	4.68
K_2O	.13	.21
Sum	100.24	100.21
Si	9.33	9.643
Aliv	6.547	6.357
Alvi	.000	.003
Fe	.101	.082
Ca	2.825	2.245
Na	1.220	1.640
K	.030	.048
O	32.000	32.000

1) Olivine primocryst core in picrite cumulate (sa.81-273)
2) Olivine phenocryst core in picrite dike (sa.83-251)
3) Olivine phenocryst core in diabase chill (sa.80-1116)
4) Olivine in diabase (sa.82-75)
5) Poikilitic orthopyroxene in picrite cumulate (sa.81-273)
6) Augite core in picrite cumulate (sa.81-273)
7) Augite phenocryst core in diabase chill (sa.80-1116)
8) Augite oikocryst in diabase (sa.82-75)
9) Pigeonite phenocryst core in diabase chill (sa.82-201)
10) Pigeonite rim on oikcryst in diabase (sa.82-75)
11) Plagioclase phenocryst in diabase chill (sa.1116)
12) Poikilitic plagioclase core in picrite cumulate (sa.81-273)

olivine-clinopyroxene and indicate the crystallization sequence of silicate phases is plagioclase, olivine, clinopyroxene. The presence of 5-10% microphenocrysts indicates that the diabase sills cooled from sub-liquidus temperatures and were close to being multiply saturated with the major silicate phases at the time of intrusion. The matrix of the chills contain crystallites which vary in habit from tabular 0.1 mm grains in the fine grained chill to skeletal in the glassy rinds. As determined by Lofgren (1980) these habits probably reflect an increase in the degree of supercooling towards the sill margin.

The crystallization sequence determined from the phenocrysts in chills is supported by textural relations in medium grained diabase. Olivine occurs as rounded grains interstitial to plagioclase or as anhedral grains which locally enclose plagioclase indicating that olivine crystallized after plagioclase. In the ophitic lower zone of the sills, clinopyroxene oikocrysts enclose both plagioclase and olivine. If ophitic textures are interpreted as developing as a result of early nucleation of plagioclase followed by simultaneous crystallization of plagioclase and clinopyroxene (Cox et al. 1979; Lofgren, 1980), then these features suggest a liquid close to cotectic composition in which early crystallization was dominated by plagioclase and olivine and followed by later crystallization of plagioclase and clinopyroxene.

4.4 Picritic Rocks

Picritic rocks in the Lake Nipigon area occur as dikes, ring dikes, small plugs and sills. The structures of the picritic rocks are less well defined than in the diabase, due to the difficulty in observing contacts in these rocks. This is partly because the picrites are often overlain and intruded by the diabase. All of the areas in which picritic rocks outcrop (Figure 4.1) have subsequently become magmatic centers associated with feeders for the diabase sills, although no picritic rocks have been found in the Kopka River cone sheet, the major feeder zone for the diabase west of Lake Nipigon.

The picritic rocks contain variable amounts of cumulate euhedral olivine (Fo_{82-69}) ranging in size from 0.1 to 3.0 mm and lesser euhedral to subhedral clinopyroxene ($En_{44-54}Fs_{7-14}Wo_{38-46}$) ranging in size from 0.1 to 2 mm. Anhedral interstitial to poikilitic orthopyroxene ($En_{76-80}Fs_{17-21}Wo_{2-4}$) up to 1 cm and plagioclase (An_{70}) are the principal intercumulus phases. Minor Fe-Cr spinel is included in olivine. Hornblende and biotite occur as interstitial phases rimming clinopyroxene. The rocks have a mesocumulate to orthocumulate texture which defines a crystallization sequence olivine, clinopyroxene, orthopyroxene, plagioclase.

A glassy chill approximately 7 mm thick observed on a picrite dike on the west shore of Lake Nipigon has 12% olivine phenocrysts (Fo_{80}) up to 2 mm in a matrix of devitrified glass. The chill contains 8.82% MgO and has an Mg'(see table 4.3 for definition) of 0.56. The medium grained parts of the dike contain up to 24.2% MgO with an Mg' of .73 and texturally appear to have accumulated olivine relative to the chill. Since the dike is inclined at 45° gravity settling could explain the olivine accumulation but flow differentiation is also an alternative and by analogy with picritic rocks of the Scottish Hebrides (Bowen, 1928; Simkin, 1967) may be the preferred mechanism. These rocks are close analogues in texture and field relations to the peridotite dikes of Skye described by Bowen (1928).

The absence of aphyric chills and ubiquitous cumulate textures of the picritic rocks indicate that the intrusions were formed by accumulation of olivine at shallow crustal depths from a magma with olivine crystals at the time of emplacement.

4.5 Composition

In order to determine the compositional nature of the Nipigon igneous rocks and to examine the compositional relationship between these rocks and the Keweenawan basalt flows of the Lake Superior rift, 26 chills from dikes and sills were analysed. These rocks can be divided into two types: 1) The majority of samples (24) taken from diabases are olivine normative to marginally quartz normative tholeiites. This group has Mg' ranging from .54 to .46. The rocks are characterized by moderately high Al_2O_3 (avg. 13.78 wt%) and contain plagioclase as a common microphenocryst phase. The group has moderately low TiO_2 (avg. 1.51 wt%), K_2O (avg. 0.56 wt%) and P_2O_5 (avg. 0.09 wt %) in comparison to other typical continental provinces (Table 4.3). 2) Two samples from the chills of picritic dikes have a distinct chemical composition. They are characterized by slightly higher Mg' (avg. 0.55), distinctly higher TiO_2 (avg. 2.70 wt %), K_2O (avg. 0.84 wt %) and P_2O5 (avg. 0.19 wt %)

Table 4.3 Average analyses of basaltic rocks from Lake Nipigon, the Lake Superior area, and continental basalt provinces.

	1	2	3	4	5	6	7	8	9	10	11	12
SiO_2	48.49	50.05	50.38	49.99	49.89	49.61	50.46	51.73	48.79	51.21	49.80	51.90
TiO_2	2.79	1.55	1.51	1.63	1.39	1.01	1.64	1.84	1.24	2.28	2.24	2.39
Al_2O_3	11.96	14.12	14.43	13.58	14.58	15.14	13.99	14.06	17.57	16.16	15.50	14.72
Fe_2O_3	1.61	1.54	1.36	1.66	1.50	1.32	1.60	1.42	1.13	1.34	1.38	1.39
FeO	13.03	12.44	11.04	13.54	12.12	10.64	12.96	11.45	9.15	10.90	11.11	11.24
MnO	.23	.20	.18	.23	.20	.18	.22	.21	.14	.17	.21	.22
MgO	8.78	6.55	7.09	6.38	7.05	8.35	6.06	6.04	7.10	4.70	5.44	5.34
CaO	9.32	10.30	9.91	10.43	10.48	11.06	10.18	10.26	10.59	8.04	9.94	9.03
Na_2O	2.72	2.58	3.17	2.04	2.24	2.19	2.27	2.41	3.54	3.58	3.00	2.77
K_2O	.87	.57	.85	.43	.47	.43	.53	.59	.61	1.31	.97	.55
P_2O_5	.20	.09	.09	.07	.07	.07	.08	[illegible]	.13	.30	.38	.46

1) Picritic chills, Lake Nipigon (n=2)
2) All diabase chills, Lake Nipigon area (N=24)
3) Diabase chills with Mg' .53 to .55, Lake Nipigon area (n=5)
4) Diabase chills with Mg' .45 to .49, Lake Nipigon area (n=6)
5) All diabases, Lake Nipigon area (n=56)
6) Diabases with Mg' .55 to .60, Lake Nipigon area (n=10)
7) Diabases with Mg' .43 to .47, Lake Nipigon area (n=15)
8) Osler group basalts; Lake Superior (n=52) (Wallace, 1972)
9) North Shore Volcanic Group olivine tholeiites (n=8) (Basaltic Volcanism, Study Project, 1981)
10) North Shore Volcanic Group Fe-Ti basalts (n=4) (Basaltic Volcanism Study Project, 1981)
11) Deccan Upper Traps (n=65) (Ghose, 1976)
12) Columbia River reference suite (n=10) (Basaltic Volcanism Study Project, 1981)

Mg' = mol MgO/(mol MgO + 0.9 mol FeO_t)

FeO adjusted to 0.9 FeOt.
Analyses recalculated to 100% volatile free

and by lower Al_2O_3 (avg. 14.55 wt %) than the diabase chills. These rocks are olivine normative and contain olivine microphenocrysts.

The diabase chills are very similar in major element composition to the average Osler basalt flow determined by Wallace (1972) except for the marginally higher MgO, FeO and Mg' of the chills. The Osler basalt ranges from olivine tholeiite to quartz tholeiite but most flows are quartz normative. They appear to be equivalent to the more fractionated diabase chills. This similarity in composition is not unexpected since a possible genetic relationship between the diabase and Osler flows is implied by the temporal and spatial association.

Green (1982) has subdivided the Keweenawan basalts into two chemical types based primarily on work in the North Shore Volcanic group (Table 4.3). Most abundant are olivine tholeiite flows characterized by low K_2O, P_2O_5, TiO_2 and high Al_2O_3 (16 to 19%) with Mg' ranging from 0.68 to 0.43. The most primitive of these resemble mid-ocean ridge basalts (MORB) except for the high Al_2O_3 and light rare earth element (REE) enrichment. Transitional (weakly alkaline) Fe-Ti basalts merge compositionally with the olivine tholeiites, but in general are characterized by higher K_2O, P_2O_5, TiO_2, FeO^t, incompatible trace elements and REE and by lower Al_2O_3 and MgO. These basalts are considered to be similar to modern mantle plume basalts on a basis of major and trace elements (Weiblen, 1982) and are more typical of continental flood basalts.

Geochemically the Nipigon diabase chills most resemble the olivine tholeiites of Green (1982), particularly with respect to K_2O, P_2O_5, TiO_2 and Mg'. REE (Figure 4.3), and other incompatible trace elements are similar. However, the higher FeO^t and lower Al_2O_3 of the chills are more characteristic of the transitional basalts. Green (1979) has noted that olivine tholeiite lavas of the Osler group have more evolved compositions with lower Mg', TiO_2 and Al_2O_3 than typical Keweenawan high-Al olivine tholeiites. The geochemical nature of the Nipigon diabase may represent an extension of these Osler Group characteristics, and represent a different composition to some of other the Keweenawan volcanic plateaus.

The picrite chills with high TiO_2, K_2O and P_2O_5 have a similarity with the transitional Fe-Ti basalt type (Green, 1982). The higher Mg' of these chills is anomalous, since the Fe-Ti basalts generally have lower Mg' than the olivine tholeiites. These chills could represent a parental magma for the Fe-Ti suite and may be related to olivine cumulate Fe-Ti lava flows which erupted early in the Keweenawan sequence (Basaltic Volcanism Study Project (BVSP), 1981). The transitional Fe-Ti basalts generally occur early in the Keweenawan sequence (Green, 1982; Weiblen, 1982) and this relationship appears to be consistent at Lake Nipigon.

4.6 Magma Fractionation

Primary basalt magmas in equilibrium with residual mantle olivine compositions of Fo_{88} (Carter, 1970) to Fo_{94} (BVSP, 1981) should have Mg' ranging from 0.68 to 0.83 using the olivine-melt

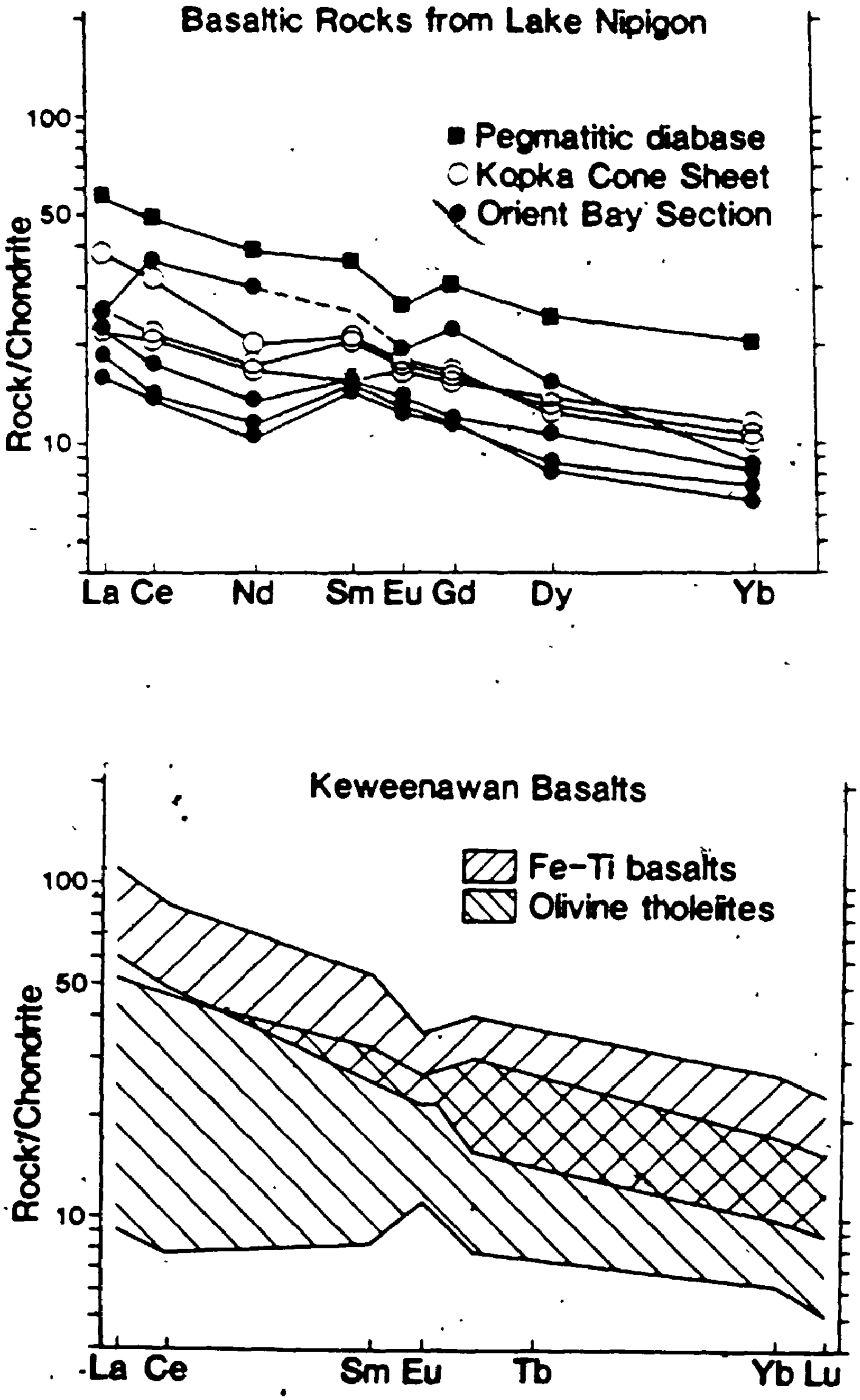

4.3 Chondrite normalized REE patterns for selected samples from the Nipigon area compared with fields of olivine tholeiite and Fe-Ti tholeiite basalts of Lake Superior from Green (1982).

partition coefficient of Rocder and Emslie (1970). All of the Nipigon diabase and picrite chills are too low in Mg' to be in equilibrium with even the most Fe-rich of proposed mantle compositions and therefore represent magmas which have fractionated since segregation from the upper mantle. Although the picritic magmas are more primitive than the diabase and have comparable Mg' to the most primitive basalts in the Keweenawan sequence (BVSP, 1981), they do not appear to be parental to the diabase.

As a first step in examining the fractionation of the Nipigon basaltic rocks, compositions of picritic rocks and diabase chills are plotted in projections of the basalt tetrahedron (Figure 4.4) using the method of Irvine (1979). On these diagrams, most of the picritic rocks plot in the olivine liquidus field and show olivine control. A few samples plot in the clinopyroxene field and may represent olivine and clinopyroxene control. The picrite chills are the only rocks in this suite which approach liquid compositions and these plot in the olivine field near the olivine-clinopyroxene cotectic. The diabase chill analyses show no well developed control lines in keeping with the near liquid compositions. Most plot within the plagioclase field close to the plagioclase-olivine-clinopyroxene cotectic. More evolved compositions are quartz normative and plot near the 4 phase cotectic. These relationships are in agreement with those deduced from petrographic observations. The picrites were derived from olivine phyric magma which accumulated olivine and to a lesser extent clinopyroxene. The diabases were emplaced as

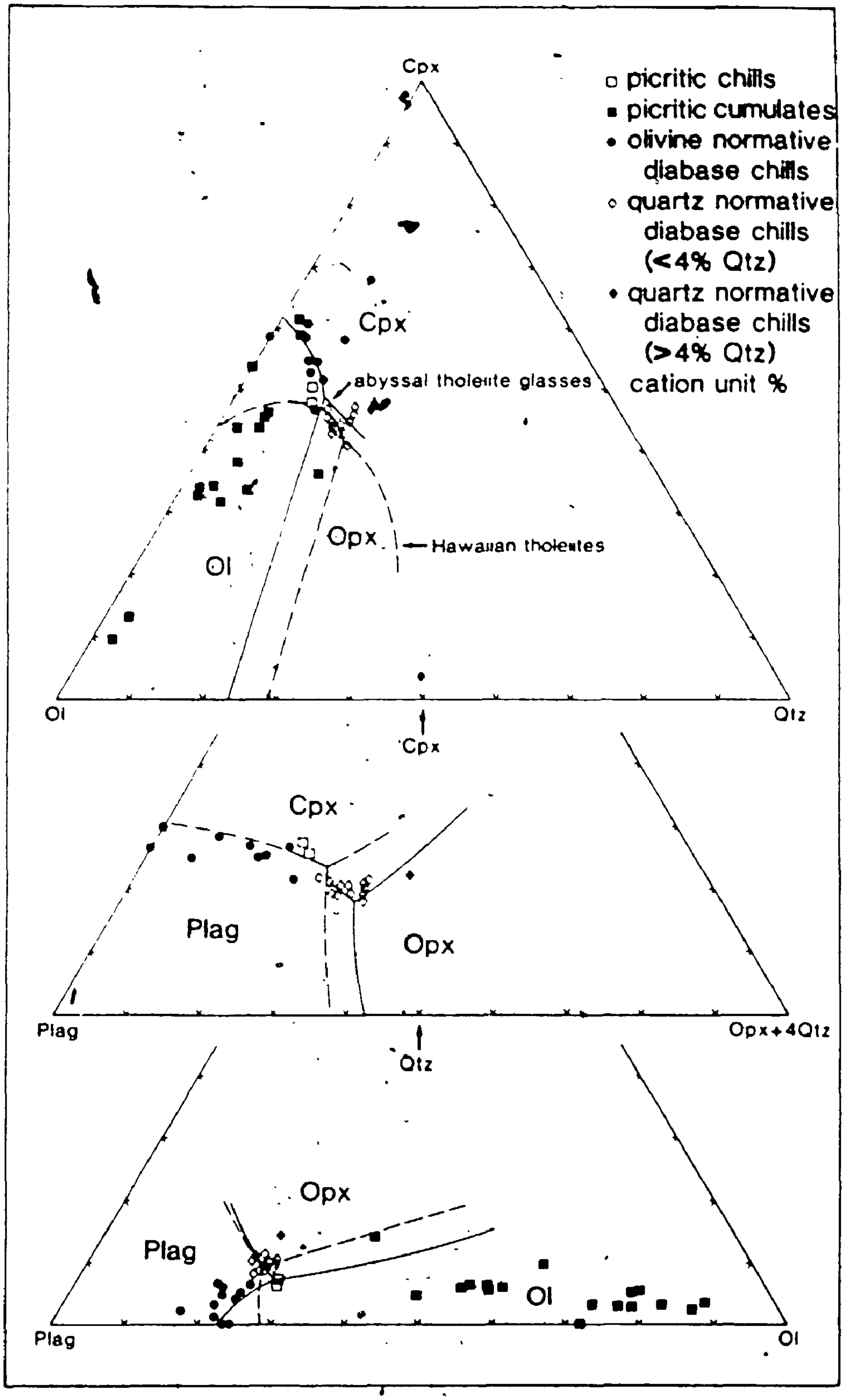

4.4 Basaltic rocks from Lake Nipigon plotted in projections of the basalt tetrahedron using the method of Irvine (1979). Curves separate liquidus fields for abyssal tholeiite glasses and Hawaiian tholeiites as defined by Irvine (1979).

evolved liquids close to cotectic composition in which plagioclase and olivine were the early crystallizing phases.

The relative proportions of olivine, plagioclase and clinopyroxene involved in fractionation of the two suites are evaluated graphically using Pearce-type diagrams (Pearce, 1970) (Figure 4.5). These diagrams use TiO_2, an oxide which is only a minor component in the phases to be considered, as a common denominator for both ordinate and abscissa. This technique is used because of the restricted range in SiO_2 displayed by the diabase suite.

Variation in Al_2O_3 vs SiO_2 and MgO vs SiO_2 (Figure 4.5) clearly show that the diabase and picrite suites are controlled by different fractionation processes and that the picrite suite is not parental to the diabases. The Al_2O_3 vs SiO_2 variation indicates that fractionation of plagioclase is important in the diabase suite where as an aluminous phase is not fractionated in the picrite suite. The MgO vs SiO_2 variation illustrates that both suites involve the fractionation of a magnesian phase. Using average mineral and phenocryst compositions observed in the suites (Table 4.2), the chemical variation of the picrites can be explained by fractionation of predominately olivine (Fo_{80}) with lesser clinopyroxene ($En_{50}Fs_{10}Wo_{40}$). Fractionation of a Ca-poor pyroxene is considered to be of minor importance since it is a late crystallizing subordinate phase. Chemical variation in the diabase is dominated by fractionation of plagioclase and to a lesser extent mafic phases.

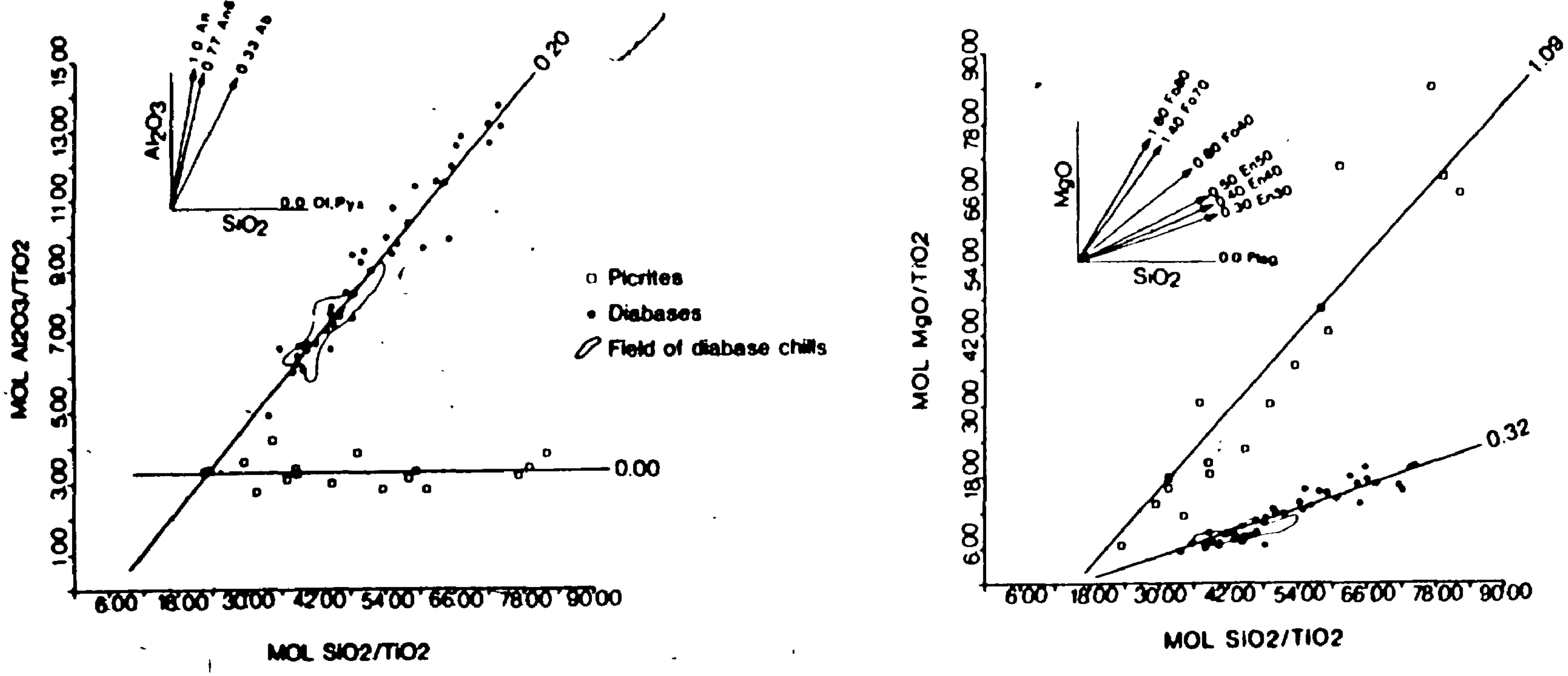

4.5 Pearce-type diagrams for selected major elements (molecular % oxides) of basaltic rocks from the Lake Nipigon area. Regression lines with slope are given for comparison with predicted slopes for possible fractionated minerals in inset diagrams.

Major element modeling using XLFRAC (Stormer and Nicholls, 1978) (table 4.4) shows that the variation in the diabases is best approximated by removal of plagioclase (An_{69}), olivine (Fo_{69}) and clinopyroxene ($En_{46}Fs_{16}Wo_{38}$) in the proportions 53:21:26. Fractionation of plagioclase and olivine without clinopyroxene is less able to account for the chemical variation between the most primitive and most fractionated diabases.

Since both the picritic and diabasic magmas have been implaced into granitoid crust, contamination is a possible complication in these fractionation processes. In the absence of isotopic data, a problem in assessing the degree of contamination is that the effects of assimilation tend to produce the same assemblages of crystals and major element compositions as result from spontaneous fractionation (Bowen, 1928; McBirney, 1979). An assimilation accelerated fractionation model as applied by Francis et al. (1983) is illustrated in figure 4.6 and shows the effect of assimilation of a contaminant approximated by Osler Group rhyolite volcanics. The addition of the contaminant forces crystallization of a thermally equivalent amount of basaltic magma and moves the residual liquid along the plagioclase-olivine-pyroxene cotectic (Bowen, 1928). In order to maintain the liquid on the cotectic, the fractionating assemblage is enhanced in plagioclase because the contaminant lies on the plagioclase side of the cotectic. The net result of this contamination is that the observed spectrum of magmas could be produced by lower degrees of crystallization involving small changes in Mg' as determined by Frances *et al.* (1983) in the

Table 4.4 Results of major element subtraction model for diabase fractionation using XLFRAC (Stormer and Nicholls, 1978).

	INITIAL	FINAL	MODEL A-USING THE PHASES Fo69. An69 1	2	3	4	5	MODEL B-USING THE PHASES Fo69, An69, Cpx 1	2	3	4	5
SiO2	49.67	50.51	46.68	0.831	1.293	-0.461	51.20	48.46	0.831	0.896	-0.064	50.62
TiO2	1.01	1.65	0.00	0.638	0.556	0.082	1.52	0.14	0.638	0.660	-0.022	1.68
Al_2O_3	15.16	14.00	20.15	-1.166	-2.080	0.914	12.62	16.77	-1.166	-1.214	0.049	13.91
FeO^t	11.85	14.49	9.61	2.642	1.647	0.995	12.98	8.69	2.642	2.539	0.103	14.30
MnO	0.18	0.22	0.12	0.042	0.037	0.005	0.22	0.13	0.042	0.042	0.000	0.22
MgO	8.37	6.07	11.26	-2.296	-1.755	-0.542	6.89	11.28	-2.296	-2.282	-0.014	6.09
CaO	11.07	10.09	9.81	-0.886	0.128	-1.014	11.72	12.51	-0.886	-1.018	0.132	9.95
Na_2O	2.19	2.27	2.28	-0.080	-0.005	0.085	2.14	1.95	0.080	0.140	-0.060	2.38
K_2O	0.43	0.53	0.09	0.104	0.150	-0.047	0.60	0.07	0.104	0.201	-0.098	0.70
P_2O_5	0.07	0.08	0.00	0.011	0.028	-0.017	0.11	0.00	0.11	0.036	-0.025	0.13

SUM of the Squares of the Residuals=3.3761

Phase	Amount as wt % of Initial Magma	Amount as wt% of subtracted phase
Fo69	-11.39	33.70
An69	-22.40	66.30

SUM of the Squares of the Residuals=0.0491

Phase	Amount as wt% of Initial Magma	Amount as wt% of subtracted phase
Fo69	-9.37	21.39
An69	-23.18	52.94
Cpx	-11.24	25.67

INITIAL	- average of diabases with Mg' .55 to .60 recalculated to 100%
FINAL	- average of diabases with Mg' .43 to .47 recalculated to 100%
1	- Bulk composition of Subtracted material
2	- Observed difference between initial and final magma
3	- Calculated difference between initial and final magma
4	- Residuals (observed difference - calculated difference)
5	- Model final magma composition

Phase compositions are given in table 2 and are Fo69 (analyses 3), An69 (analysis 11), Cpx (analysis 7).

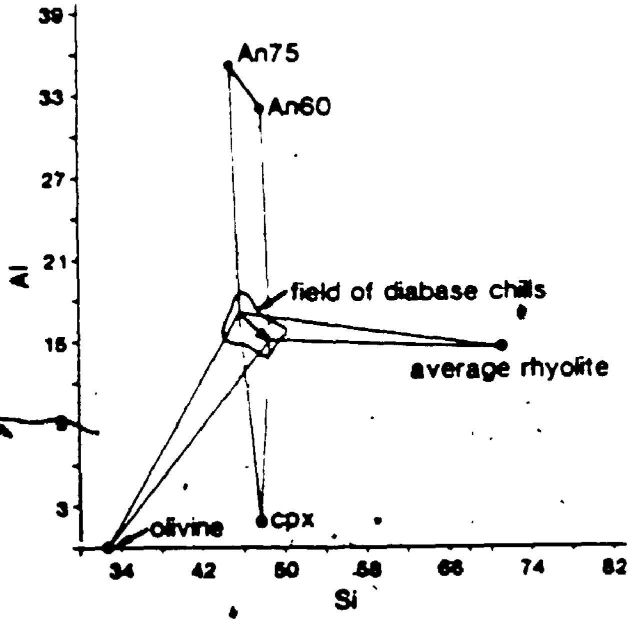

4.6 Assimilation-accelerated fractional crystallization model (atomic proportions) showing possible effect of contaminant approximated by rhyolite melt of the Osler group.

Povungnituk volcanics.

4.6.1 Variation in the Diabase Sills

In order to examine the nature of differentiation in the Nipigon diabase, suites of samples were collected from three well exposed sections of the lower sill at Orient Bay, Livingstone Point and Outer Barn Island of Lake Nipigon. Other suites were taken from a section of a diabase sheet which intrudes Archean rocks at D'Alton Lake north of Lake Nipigon and from the Kopka River cone sheet west of Lake Nipigon (Figure 4.1). The petrography of the D'Alton Lake section was previously studied by Kavanagh (1981).

The AFM diagram (Figure 4.7) shows that these is a regional variation in the major element chemistry of the sill sections despite the interpretation that the Orient Bay, Livingstone Point and Outer Barn sections represent the same sill. The diabase sheet at D'Alton Lake and the Kopka River Cone sheet are more Fe rich than the sill sections. The variation in chemistry between the sill sections is interpreted as reflecting the composite nature of the sills. Although it is observed that in general the sills form a single cooling unit, each appears to be composed of several pulses of magma. The variation within sample sections is small compared to the regional variation. Hence all of the regional variation is unlikely to be attributed to in situ fractional crystallization.

The variations of modal mineral abundances and major element chemistry with stratigraphic height are summarized in figure

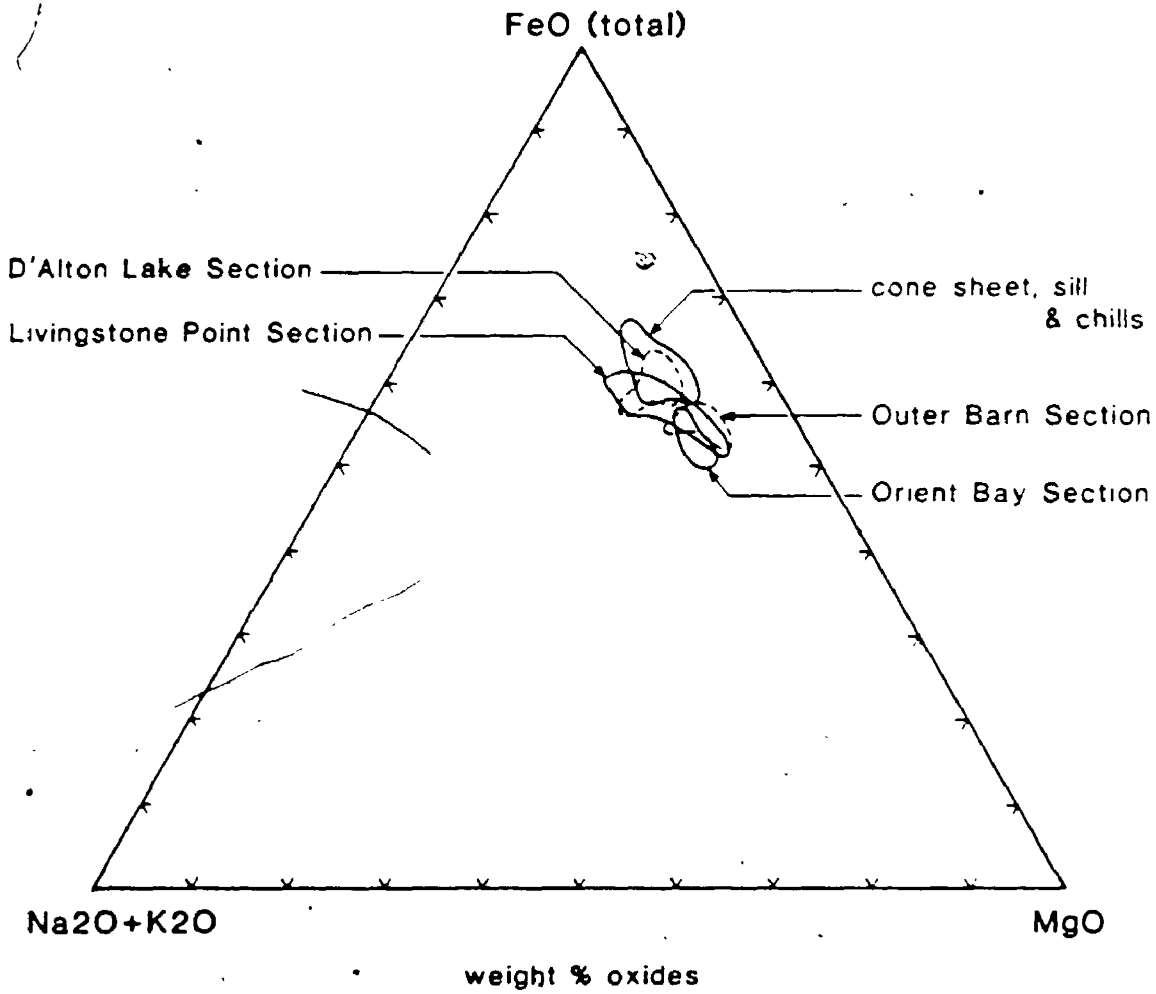

4.7 AFM diagram (weight % oxides) showing fields of variation for individual sample sections of diabase sills and the Kopka cone sheet.

4.8. The data show fluctuations in mineral and elemental abundances that are best explained by multiple magma injection coupled with minor crystal accumulation. In the case of the D'Alton Lake section, multiple injection is evident in the field as an internal chilled contact 60 m from the base of the section, however, there is no field textural evidence for multiple magma pulses in the other sections. In these sections multiple pulses are recognized on a basis of the sawtoothed distributions of MgO, SiO_2, MgO/(MgO + FeO^t) and Cr in several of the sections. The increases of MgO, Cr, MgO/(MgO + FeO^t) and decrease of SiO_2 can largely be correlated with increase in modal abundance of olivine. This variation is attributed to the input of several pulses of basaltic magma of varying degrees of fractionation and olivine content. In some sections there is a tendency for the most magnesium rich rocks to occur toward the top of the section.

Olivine accumulation occurs at the base of the second magma pulse of the D'Alton Lake section and may be present in other sections. This may be due to gravitational setting as in the Mg-olivine layer of the Palisade sill (Walker, 1970) or by flowage differentiation (Bhattacharji and Smith, 1964; Simkin, 1967). The later possibility is favored due to the problem of early crystallizing plagioclase impeding the sinking of olivine. In either case, the presence of olivine phenocrysts and chain like aggregates of olivine suggest that olivine was present in the magma at the time of intrusion.

Enrichment of alkalis toward the top of the sections is minor and is associated with the development of micrographic inter-

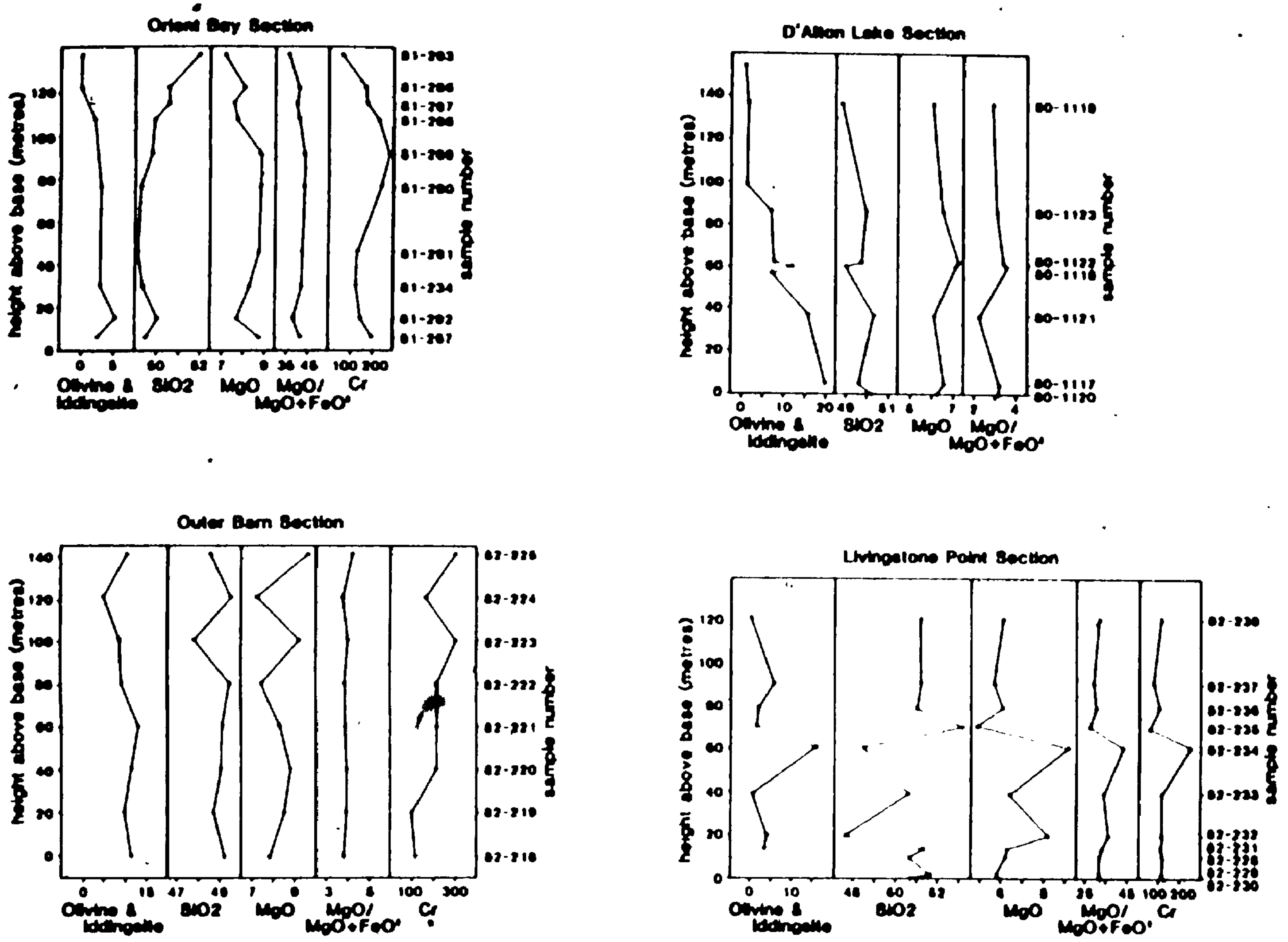

4.8 Modal and chemical variation versus stratigraphic height for several sections of diabase from the Lake Nipigon area. Olivine and iddingsite are plotted in volume %. Major elements in weight % recalculated to 100% volatile free. Cr in ppm. Olivine data in D'Alton Lake section is from Kavanagh (1981).

growth and the development of coarse grained and pegmatitic diabase.

4.6.2 Primary Magmas

The most primitive basaltic rocks from the Nipigon area which are likely to be representative of near liquid compositions are the picrite chills. The least altered chill is from a picrite dike and has an Mg' of 0.56. Although this rock contains 12% olivine microphenocrysts of composition Fo_{80}, modification of the liquid by olivine accumulation is probably minimal. This is because the calculated equilibrium olivine composition ($Fo_{79.2}$) using the method of Roeder and Emslie (1970) is close to the observed composition.

As determined in the preceding discussion the picrite suite is primarily controlled by olivine with minor clinopyroxene fractionation. With the assumption that the picrite chills have only been affected by olivine fractionation it is possible to make some inferences as to the nature of the primary magma of this suite (Figure 4.9). Although the figure is calculated for 1 atm., the data are considered to be a reasonable approximation of relationships at high pressure (Hanson and Langmuir, 1978). The diagram shows that the picrite chill represents a liquid which has fractionated approximately 25% olivine from a minimum melt in equilibrium with an iron-rich model mantle composition of Carter (1970). The most magnesium rich olivine observed in the suite is Fo_{82}. This olivine would crystallize from a liquid which has fractionated appoximately 20% olivine from the model primary liquid.

Fractionation of magnesian olivine (Fo>80) results in a large decrease in MgO content of the remaining liquid but does not significantly affect FeO concentration. This suggests that the picrite suite is derived from an unusually Fe-rich parental magma in comparison to the Nipigon diabases, other Keweenawan high-Al olivine tholeiites and recent mid-ocean ridge basalts. Note, however, that the assumption that the picrite chills have only been affected by olivine fractionation results in a high estimate of the Fe content of the primary magma since the effect of clinopyroxene fractionation is to move the residual liquid to more iron-rich compositions. From Figure 4.9 the parental magma for the diabase suite is likely to be derived by similar degrees of partial melting at lower temperature or by higher degrees of melting.

The anomalously high K_2O, P_2O_5, and TiO_2 in the picrite chills relative to the diabase chills suggests that that parent magma of the picrites was enriched in incompatible elements relative to the diabases or that the picrites have assimilated crustal material. Sparks (1986) has shown that the latter alternative may be more probable in primitive magmas because of the high temperature, large crystallization interval and high heat of fusion of olivine. Campbell (1985) furthermore, has shown that magma flow in picritic dikes is likely to be turbulent and capable of assimilating large volumes of crustal material.

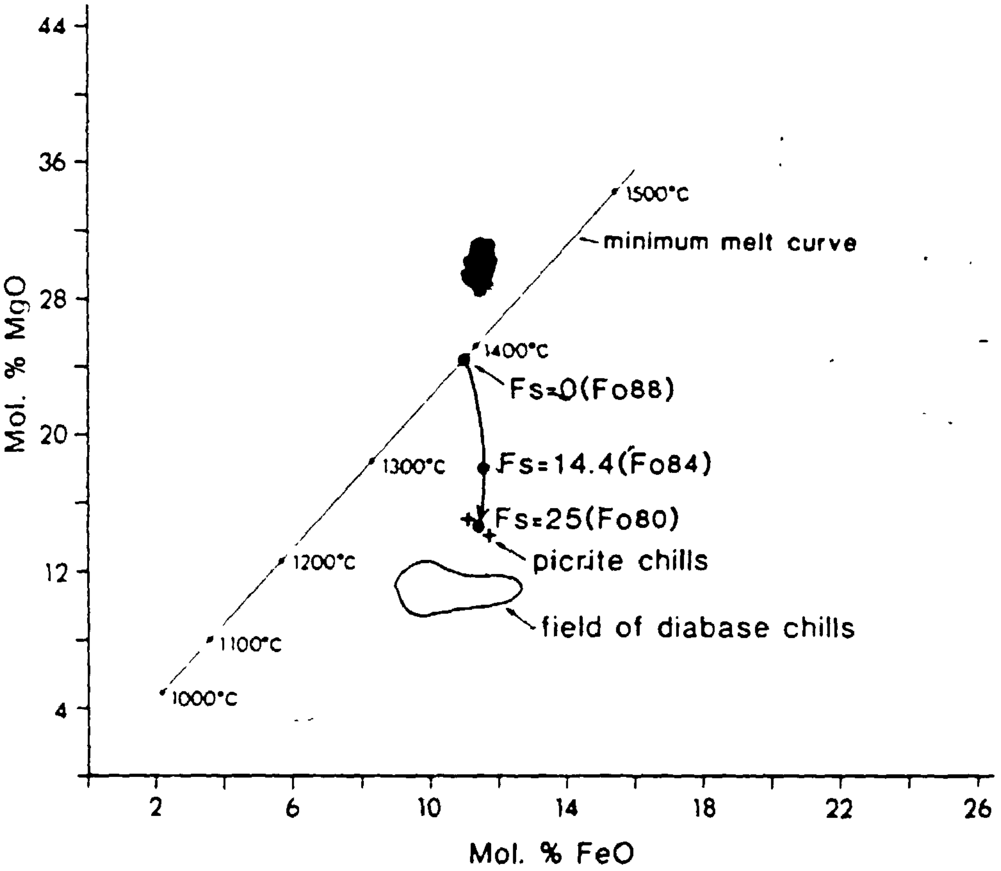

4.9 MgO-FeO relationships between liquid compositions, model minimum melting relationships (Hanson and Langmuir, 1978) of an Fe-rich mantle composition (Carter, 1970), and a possible primary magma composition (molecular % oxides).

4.7 Emplacement of Picritic and Diabasic Magmas

In Phanerozoic continental basalt provinces such as West Greenland-Baffin Island (Clarke, 1970), Deccan (Cox, 1978) and the Karoo (Cox et al. 1965) picritic magmas are erupted along linear zones and were not preceeded by significant low Mg-basalts (Cox, 1978). In this respect the Nipigon suite is similar to Phanerozoic continental basalt sequences, although the Nipigon picrites do not represent high Mg'-liquids they do represent dense olivine phyric magmas (Figure 4.10).

Stolper and Walker (1960), Sparks et al.(1980) and Herzberg et al. 1983 have shown that the continental crust with an average density of 2.75 gm/cm^3 is able to act as a density filter restricting the emplacement of dense magmas such as komatiites, picrites and MORB-like tholeiites. Stolper and Walker (1980) show that during fractionation of olivine from a primitive liquid the density of the residual liquid decreases until pyroxene and plagioclase join the crystallization sequence (Figure 4.10). The average composition of continental basalts coincides with the density minimum of approximately 2.65 gm/cm^3.

These density relationships suggest that basaltic magmas are underplated at the base of the crust and fractionate olivine until a density minimum is reached and evolved basaltic magmas can erupt (Cox 1980; Stolper and Walker, 1980). Herzberg et al. (1983) suggest that basaltic magmas will form a stable fluid layer beneath granitic material of lower density as long as the plastic nature of the buoyant layer can seal fractures and prevent the formation of a hydraulic head via extrusion. A

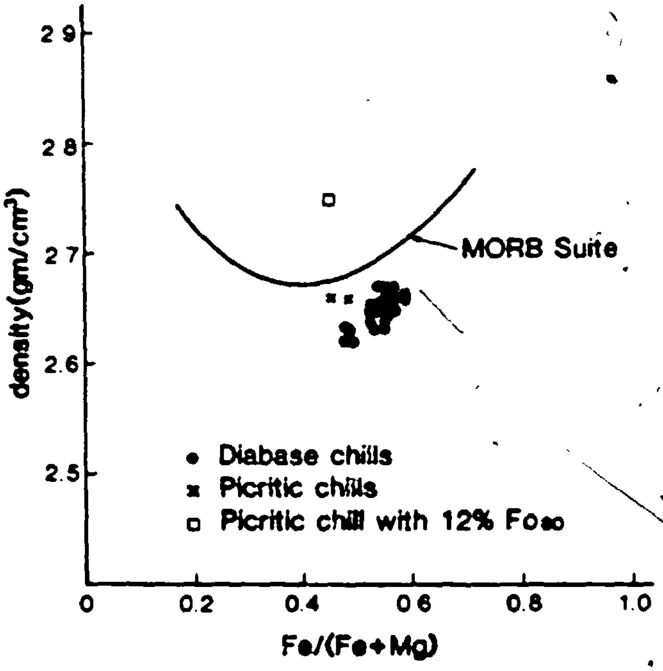

4.10 Liquid density versus fractionation (molar Fe/(Fe+Mg) relationships for rocks representative of liquids from the Nipigon area. Also shown is a picritic magma with 12% olivine of composition Fo_{80}. Densities were calculated using the method of Bottinga et al. (1982). All Fe was taken as FeO. Liquidus temperatures assumed to be 1100°C for diabase chills and estimated to be approximately 1250°C for the picritic chills using graphical method of Roeder and Emslie (1970). Liquid line of descent for MORB Suite recalculated using method of Bottinga et al. (1982) with data used by Stolper and Walker (1980).

breakdown of this layer may only occur if the underplated magma evolves and gains volatiles.

The scarcity of picritic rocks is partially accounted for by the high density of the magmas and the density filter effect. Cox (1980) estimates that the density of a picrite liquid is approximately 2.8 gm/cm3 and the density of a picritic magma with 20% olivine crystals is up to 3.0 gm/cm3. Picritic magmas therefore may rise by hydraulic head if the lithostatic load of the rock column is greater than the hydrostatic pressure of the column of magma. The implication of this mechanism is that unless some form of tectonic overpressure occurs, the fractures along which the picritic magma rises must extend through the continental Moho into the subcontinental mantle, with the continental crust strongly coupled across the Moho interface, in order to generate a lithostatic load in excess of the hydrostatic pressure of a column of primitive magma.

These relationships suggest that picritic magmas are most likely to reach the surface early in an igneous event. As the event progresses and the source plume reaches the crust-mantle interface ponding of basaltic melt at the interface is an additional factor which would effectively prevent the eruption of picritic magmas. Once ponding of melt at the crust-mantle interface is established the density filter effect then controlled the composition of erupted rocks (Figure 4.11).

Decoupling of the crust-mantle interface has been suggested as a consequence of the rise of less dense asthenosphere into the dense mantle portion of the lithosphere (Bird, 1979). This

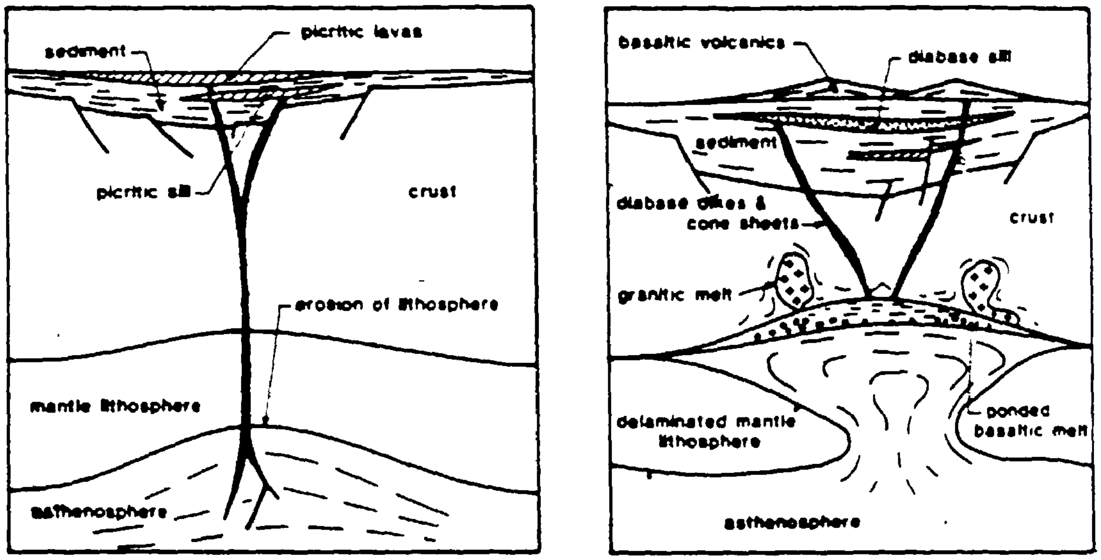
sediment
picritic lavas
picritic sill
crust
erosion of lithosphere
mantle lithosphere
asthenosphere
basaltic volcanics
diabase sill
sediment
diabase dikes &
cone sheets
crust
granitic melt
delaminated mantle
lithosphere
ponded
basaltic melt
asthenosphere

4.11 Schematic cross-section of the crust-mantle interface showing possible evolution of crustal fracture system. a) Picritic magmas rise along fractures extending through the crust-mantle interface. Magma compositions are controlled by crystal settling and flowage differentiation in the conduits. b) Delamination results in a sub-crustal magma chamber. Evolved magmas are primarily controlled by crustal density filter effect.

process in which the mantle portion of the subcontinental lithosphere sinks into and is replaced by the rising asthenosphere may promote the ponding of basaltic magma. Decoupling may also contribute to several tectonic processes which affect continental tectonics ranging from regional uplift, mafic dike and diabase emplacement, crustal melting and emplacement of passive granitoids (Bird 1979, Fyfe 1978). In the case of continental basaltic volcanism, decoupling may result in a change of style of magmatism from early picritic magmas to later evolved basalt compositions with a density-compositional control.

The large volumes of compositionally homogeneous evolved magma in the diabase sills also implies the presence of large magma reservoirs which buffered the composition of rising mantle magma (Robson and Cann, 1982). Each sill contains several pulses of magma tapped from the reservoir. The emplacement of these pulses may be determined by the interplay of variables such as the influx of pristine liquid into the chamber and the fractionation of olivine to produce residual liquids of a minimum density.

4.8 Summary

Two suites of igneous rocks were formed during the Proterozoic rifting event at Lake Nipigon. These are an early picritic cumulate suite which crystallized from a magma controlled by olivine and clinopyroxene fractionation and a later suite of diabases with evolved compositions. These suites were derived from separate magma sources. Parental magmas of the picritic suite were probably enriched in iron relative to the parental magma of the diabases. A high concentration of incompatible elements in the picrite suite may reflect crustal contamination.

Most of the difference between the two suites of rocks, however, can be attributed to the ability of the crust to filter the density of the magmas. Since the evolved rocks were formed during the main phase of the igneous event filtering may only become an important process as the igneous event reaches its peak. Delamination of the crust-mantle interface in response to an impinging mantle plume is suggested as a mechanism for establishing magma underplating and the filtering process.

CHAPTER 5

EMPLACEMENT AND CRYSTALLIZATION OF LATE PROTEROZOIC DIABASE SILLS AT LAKE NIPIGON

5.1 Introduction

Continental tholeiitic diabase sills and dikes provide an ideal situation to examine the mechanisms of emplacement and crystallization of basalt magma under geological conditions that can be comparatively well constrained. Recent studies show that although diabases often appear superficially homogenous, mineralogical compositional and textural variations may provide sensitive indications of processes of magma evolution, emplacement and crystallization (eg. Kretz *et al*. 1985; Hall *et al*. 1985).

This chapter reports field evidence for the mechanism of emplacement, documents mineralogical variation and characterizes the conditions of emplacement for Proterozoic diabase sills in the Lake Nipigon area of northwestern Ontario. The study shows that pyroxene chemistry and crystallization sequences are highly variable in the sills which otherwise display limited compositional variation. These differences are attributed to variation in $a(SiO_2)$ which in light of recent arguments by Longhi (1981) and Campbell (1985) may reflect varying degrees of crustal contamination.

5.2 Form of the Nipigon Sills

In previous chapters it has been explained that one major diabase sill 140 to 200 m thick is interpreted to be exposed over most of the Nipigon Plate and locally erosional remnants of an upper sill overlie this. A few minor sills approximately 1 m thick were observed but there appears to be no cases of thicknesses intermediate between these and the major sills.

From field mapping, a textural stratigraphy was established in the lower sill (Figure 2.3). This stratigraphy enabled the approximate position within the section to be established in areas of low relief. The stratigraphy demonstrates that in most cases the diabase sills represent single cooling units.

The upper chilled contact and to a lesser extent the lower contact of the diabase sills are well exposed in the Lake Nipigon area and measurement of the strike and dip of these surfaces enabled the structure of the sills to be determined. In general the lower sill is characterized by shallow dips of less than 10o which define gently undulating basins and arches. Steeper dips up to 80o are characteristic of areas with major fault structures extant prior to sill emplacement. The most important of these structures are the ring fault in northern Lake Nipigon and the Black Sturgeon Fault in the south. Even though the diabase sills show no evidence of significant deformation along these fault zones and therefore post date faulting, the upper contact of the sill is displaced in the direction of vertical displacement across the fault (Figure 5.1).

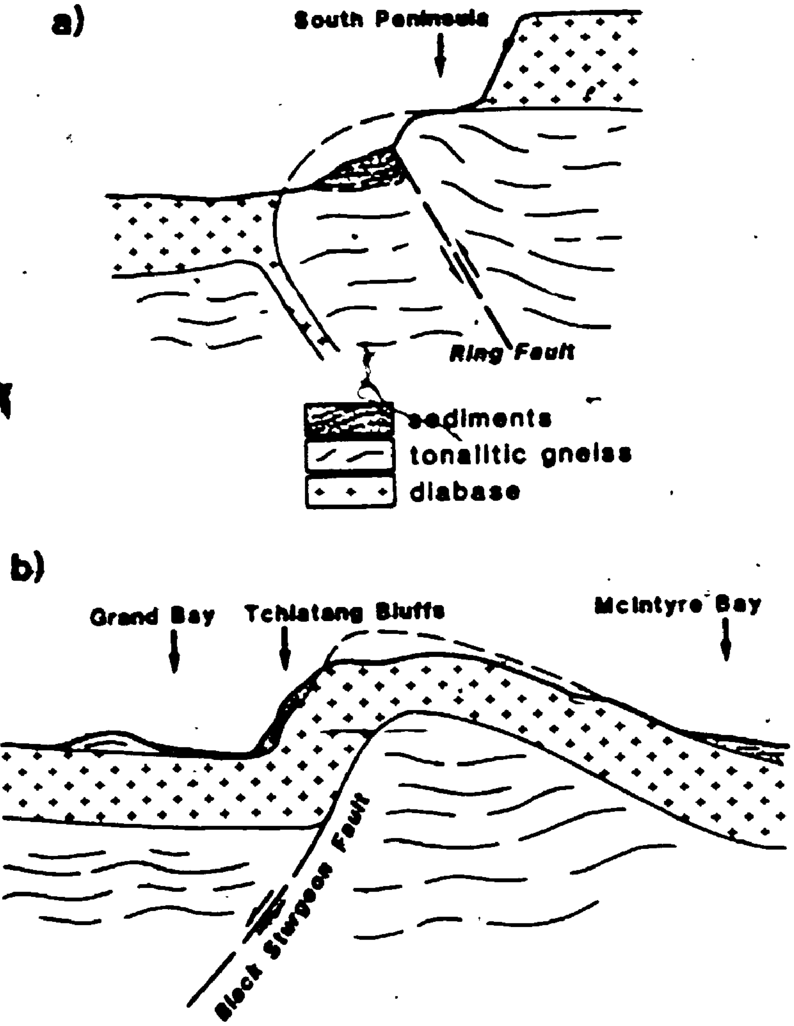
a)
South Peninsula
Ring Fault
sediments
tonalitic gneiss
diabase
b)
Grand Bay
Tchiatang Bluffs
McIntyre Bay
Black Sturgeon Fault

5.1 Form of the diabase sills in the vicinity of faults. a)Ring faults in northern Lake Nipigon, b)Black Sturgeon Fault

Diabase sheets intruded into Archean granitoid basement have a more irregular form, however, these are a relatively minor component of the diabase exposed in the area. The D'Alton Lake section which is examined in this study is an example of an inclined sheet intruded into Archean tonalite and metavolcanics.

5.3 Contact Zones

The contacts of the Nipigon diabase sills with the country rock are very sharp. The upper chill of the lower diabase is well exposed. This surface shows that inclusions of host rock are rare and that there is very little evidence of assimilation of either Sibley sediments or Archean granitoids by the diabase at the present erosional level.

The chilled margins of the diabase (Figure 2.3) are aphyric to porphyritic with 5-10% microphenocrysts to 2 mm and contain tabular 0.1 mm plagioclase crystallites which show flow alignment. The outermost 1 to 2 cm thick rind of very fine grained diabase contains skeletal plagioclase and fine polygonal fractures spaced at 1 to 2 cm. Inside of the outermost chill is a 10-15 cm thick zone of fine grained diabase with polygonal fractures at 10 to 15 cm spacings. These polygonal fractures are defined by alteration of the diabase to hydrous assemblages, primarily epidote and amphibole. The innermost part of the chill is a 2 to 3 m wide zone fine grained isogranular diabase which show wider spaced polygonal fractures defined by jointing.

The upper chill zone of the diabase contains a 5 to 10 cm thick zone containing up to 15% miarolitic cavities approximately 30 cm below the top of the sill. These cavities range in size from 1 - 2 mm to 20 cm. The cavities range in shape from spherical to prolate elliptical to bell shaped. Minerals contained in the cavities are hornblende, wollastonite and analcite.

Abundant exposures of the upper surface of the lower diabase sill enable details of the nature of the sill surface to be evaluated. Large areas of the surface (100 m^2 to hectares) are gently undulating to sub-horizontal planar. However, dipping chill surfaces are usually accomplished by stepped contacts, which resemble a stair case with runs on the order of 1 meter and 20 to 30 cm rises. Pieces of sediment commonly adhere to the angles in the staircase.

Another feature of the upper surface of the diabase chills are cusp-like grooves (see Plate 5), which are often filled with remnants of deformed sediment which are typically in excess of 1 meter in length, 10 to 15 cm wide and spaced at 1 to 2 m. These cusps are generally developed parallel to the axis of the staircase structures and are also parallel to lineated amygdules within the chill.

The termination of sills are not well exposed in the Lake Nipigon area due to erosion. Pollard _et al._ (1975) have documented fingers of igneous rock intruding sediments at the outer termination of the Shonkin Sag Laccolith. Similar fingers (see Plate 5) were observed at Lake Nipigon intruding sedimentary rocks below the lower contact of the upper sill at Cooke Point. The fingers are elliptical with a long axis of 1.5 m. Wedges of sheared and buckled sedimentary statra occur between the fingers.

5.4 Contact Metamorphism

In the Lake Nipigon area where diabase intrudes the argillaceous dolomite of the Rossport Formation a variety of metamorphic minerals are observed. Within approximately 10 m of major sills, the Rossport Formation, which is normally red weathered is bleached white. Contact metamorphic minerals are found in fine grained hornfelsic rocks within approximately 2 m of major sills and 10 samples of these were studied by XRD and petrography to identify the metamorphic phases.

Two common assemblages as defined by Winkler (1976) were observed. These are calcite+tremolite+forsterite and at higher grade, calcite+diopside+forsterite. In both assemblages forsterite is altered to serpentine. No dolomite and only minor quartz were locally observed in these assemblages. The former assemblage occurs with clinochlore and possibly reflects the aluminous nature of the sediments.

A review of metamorphic reactions in carbonate rocks at 1 kbar by Winkler (1976) provides approximate constraints on minimum temperatures at which these assemblages form provided that the fluid phase present has a medium to high XCO_2. An invariant point at 490°C determines the minimum temperature for the first appearance of tremolite or diopside for X_{CO_2} >0.2. The paragenesis calcite + tremolite + forsterite reacts to diopside + forsterite + calcite by the reaction:

$$3 \text{ tr} + 5 \text{ cc} = 11 \text{ diopside} + 2 \text{ forsterite} + 5CO_2 + 3H_2O. \quad (1)$$

An invariant point at 540°C determines the minimum temperature for the latter assemblage provided that X_{CO_2} >0.6 in the fluid phase.

5.5 Depth of Emplacement

Features such as apharitic chilled margins and miarolitic cavities indicate that the Nipigon sills were emplaced at a high crustal level. Estimates of the overburden into which the sills were emplaced can be made from a stratigraphic reconstruction of the thickness of Sibley Group which originally covered the Nipigon area. Geochronological evidence (Sutcliffe and Davis, 1985) indicates that the Osler Group basalts south of Lake Nipigon are younger than the Nipigon sills and therefore the basalts probably did not contribute to the overburden at the time of sill emplacement.

Franklin *et al*. (1980) estimated the complete thickness of the Sibley Group to the base of the Osler Group on Black Bay Peninsula to be 235 m from measuring of stratigraphic sections. Drilling in the Black Sturgeon Graben has subsequently indicated thicknesses up to 420 m. A stratigraphic reconstruction of the Sibley Group from Red Rock to Black Bay Peninsula using an average dip of 5° suggests a maximum possible thickness of approximately 1700 m.

Using an average density of 2.5 gm/cm^3 for the sediments, estimates of overburden pressure range from a mimimum of approximately 0.06 kbar to a maximum of 0.43 kbar. Since the

Sibley Group appears to be anomalously thick in the Black Sturgeon Graben. Franklin et al.'s (1980) estimate of Sibley group thickness is probably most appropriate for most of the Nipigon area and therefore the lowest estimate of pressure may be most appropriate.

5.6 Emplacement Mechanism

Diabase sills are characteristically emplaced into relatively undeformed sedimentary sequences less than 6 km thick which overlie crystalline basements (Carey 1958; Bradley 1965). Mechanisms which have been advanced to explain sill emplacement from dike feeders are largely based on the relationship between hydrostatic pressure of a column of magma and the lithostatic pressure of a corresponding column of lithosphere (Bradley, 1965). This relationship, reviewed by Francis (1982) is illustrated diagramatically in figure 5.2. As the total lithostatic pressure is unknown, it is not possible to specify the potential magma pressure. The magma pressure at the point of sill intrusion, however, can be estimated. This is somewhat lower than the potential pressure due to the effects of friction, compressibility and viscosity (Leaman, 1975). Willams and McBirney (1979) emphasize that the model does not apply to moving magma which requires an additional pressure to drive it through the conduit. The condition of static equilibrium is however closely approached at the instant intrusion is complete (Bradley, 1965).

In principle, the optimum level for sill intrusion is the

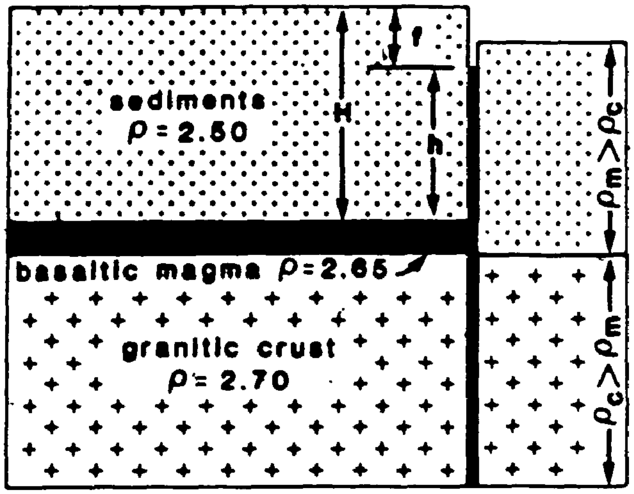
f
sediments
ρ = 2.50
H
h
basaltic magma ρ=2.65
granitic crust
ρ = 2.70
ρm > ρc
ρc > ρm

5.2 Hydrostatic relationship between column of magma and column of lithosphere after Bradley (1965). At equilibrium $2.65\ h = 2.50\ H$, and f is the freeboard.

point at which the density of the country rock becomes less than that of the magma. At this point the excess magma pressure is maximized. Effectively, the low density roof floats on the higher density magma (Bradley, 1965). Sill initiation may also be influenced by the state of stress in the country rocks and is favoured by regions of compression (Roberts, 1970) but this factor may be more important at deeper crustal levels than those discussed here.

The lower and apparently oldest Nipigon sill is intruded within approximately 20 meters of the Proterozoic/Archean unconformity. This is in agreement with the observation from the hydrostatic model that the optimum level for sill emplacement is at the depth at which the density of the country rock becomes less than that of the magma.

The consistent thickness of the Nipigon sills relates to magma pressure required to lift the roof. The pressure required to lift the load of Sibley sediments was probably approximately 60 bars. If the roof was lifted a further 200 meters to accommodate the maximum thickness of the sills then the magma pressure at a source underneath the sill must have been a minimum of approximately 110 bars. This estimate neglects injection pressure required to overcome viscosity, tensile pressure required to split strata and pressure required to bend the roof. These components however, are considered to be small (Bradley, 1965). This intrusion pressure would have been sufficient for the diabase magma to rise through approximately 410 meters of Sibley sediment and erupt. However, while the density of the sedimentary column remains low, little or no magma is able to reach the surface.

Another application of the hydrostatic model is to evaluate the potential of crustal loading to enable successive magmas to rise higher in the crust. This can be used to evaluate the sequence in the Nipigon area in which there is two major sills intruded into the thin sequence of Sibley sediments. Subsequently, basaltic magmas erupted as indicated by the Osler Group basalts, south of Lake Nipigon.

The intrusion pressure can be represented as the hydrostatic head in a feeder dike which extends above the sill (Figure 5.2). At hydrostatic equilibrium, for a magma density of 2.65 and a sediment density of 2.50 the height of the compensating columns of magma and sediment must bear the same ratio (Bradley, 1965). The margin between the level to which the magma rises and the surface is called the freeboard (Bradley 1965). If the Sibley sediments were 235 m thick at the time of intrusion the freeboard is approximately 14 meters.

Loading of the sedimentary column with diabase sills will have the effect of increasing the magma pressure and reducing the amount of freeboard. Once magma erupts at the surface the effect will be to rapidly prevent the intrusion of further sills and promote further volcanism.

The presence of more than one sill implies multiple episodes of intrusion with a separation of at least the crystallization time. Bradley (1965) has demonstrated that in a hydrostatic flotational enviroment, only one major sill may develop in a column from a given episode of magma injection. The main intrusion will develop at the highest stratigraphic point, even when several contemporaneous injections from more than one source are present, providing that hydraulic connections between the intrusions are made (Bradley, 1965; Leaman, 1975). This relationship may explain why single composite sills, composed of several magma pulses, form as opposed to multiple single phase sills. Provided new injections of magma occur before the first pulse is fully crystallized, a composite intrusion is formed.

Evidence for the mechanism of horizontal propagation of sills is best obtained at the edges of the sills. Diabase sills are generally considered to wedge apart sedimentary strata which have low tensile strength. Several authors (Bradley, 1965; Francis, 1982) have suggested that steam may play an important role in the wedging process.

In a study of the edges of the Shonkin Sag Laccolith, Pollard et al. (1975) have documented fingers of igneous rock emanating from the laccolith and elaborated on the mechanism of wedging. These fingers have a thickness of 0.6 to 1.2 m by 3 to 5 m wide and are up to 100 m long. Pollard et al. (1975) show that energy expanded by magma to dilate and flow through a finger is greater than that for a sheet. The initiation of fingers is attributed to the instability of the advancing liquid interface. After the initial propagation of fingers they tend to subsequently coalesce and form a sill.

The fingers are very similar to features observed in cross-section at the edges of sills in the Nipigon area described in Plate 5. The propagation of the Nipigon sills by the finger mechanism over a wide area is also indicated by the presence of cusp-shaped grooves filled with deformed sediment in the upper chilled surface of the diabase. The grooves are similar to those which Pollard et al. (1975) have shown as being remnants of deformed host rock occurring where fingers have coalesced and formed a sill. Another feature of the fingers is the tendency for systematic offsets of coalescing fingers to develop offsets resulting in the formation of staircase structures. Offsets develop as the intrusion propogates through a region where the stess changes direction (Pollard et al. 1975) and this is compatible with the occurrence of offsets at Lake Nipigon near regions of faulting.

Shearing and buckling of sedimentary strata occurs between the fingers and this observation indicates that the fingers grow in width and deform the host rock. At the leading edge of fingers, Pollard et al. (1975) observed that the host rock is wedged apart and that wedge shaped pieces of host rock are moved ahead with the advancing fingers. This mechanism of wedging and host rock deformation by buckling does not appear to be in accordance with a phreatic mechanism such as proposed by Bradley (1965) and Grapes et al. (1972) where the advancing diabase magma occupies a steam filled extension space. Field evidence for phreatic activity observed at Lake Nipigon is minimal.

This includes the large vuggy cavities observed in sandstones near the upper contact of the sill on the east shore of Lake Nipigon. These occur along a zone of reverse faulting in the sediment which would be a likely zone of groundwater access at the time of intrusion. Fissures cutting diabase which are filled with wollastonite, analcime and calcite may also have been avenues of phreatic activity by analogy with similar fissures observed by Grapes et al (1972) in Antarctic dolerites.

5.7 Magma Flow

Pollard et al. (1975) have determined that the direction of magma flow is parallel to the orientation of fingers and cusps in the Shonkin Sag laccolith. Data on the orientation of these features, particularly cusps, and of strongly elongated vesicles (which were observed to parallel cusps) were measured in the Lake Nipigon area. The data (see Figure 2.2) although restricted to the northwest part of Lake Nipigon indicate that the direction of magma flow during finger propagation was radial to the center of the lake. This suggests the possibility of a magma source underneath Lake Nipigon, possibly occupying the ring fracture system in the north end of the lake.

The nature of the flow in a sill can be predicted from the Reynolds number. For a volume rate of flow in a dike or sheet, the equation for Reynold's number is given by Shaw (1965).

$$Re = \frac{4 r_h \rho Q}{S_1 S_2 \eta} \quad (2).$$

where: ρ is the magma density; Q is the flow rate; η is the magma viscosity, S_1 is the height of the sill, S_2 is the width of the sill and r_h is the hydraulic radius ($r_h = S_1S_2/2S_1 + 2S_2$)). The flow is turbulent if Re exceeds a critical value of approximately 2000. Several assumptions must be made to evaluate the Reynolds number. These are $\rho = 2.65$ gm/cm3 and η = 790 poise as calculated by the method of Shaw (1972). S_1 is taken as 1 m which is the initial height of the finger propogating the sill and S_2 is taken as 5000 m which is selected as a minimum front over which the sill propogates. The flow rate Q is the most difficult to evaluate, but flow rates of other basalt fissure eruptions provide a reasonable basis for an estimate.

An example of an eruption with a high flow rate is the Lakagigar 1783 fissure eruption in Iceland (Cox _et al._ 1979). This volcano erupted at an average flow rate of 0.08 km3/day for 145 days, but taking into account pauses in eruption the flow rate during eruption was 0.14 km3/day over 85 days (Thorarenson, 1970). Assuming this is a reasonable estimate of flow rates at Lake Nipigon, a 5000 km3 sill could have been emplaced in approximately 98 years.

The flow rate suggests Re approximately 15.6 which is well within the field of laminar flow even at the initiation of sill spreading. As the sill becomes thicker, spreads over a greater area and becomes more viscous, laminar flow is favoured. This estimate of Reynolds number is also consistent with the observation that recent basalts flow by laminar shear and have low Reynolds numbers (Huppert et al., 1984).

5.8 Mineralogical Variation in the Sills

In order to assess mineralogical variation in the Nipigon sills, samples from two sections of diabase plus additional specific rock types were selected for microprobe analysis. Samples were chosen in order to examine the maximum range in composition indicated by a reconnaissance study of petrography and chemistry.

The Orient Bay section is a typical complete section of diabase intrusive into Rossport Formation sediments from the southern part of Lake Nipigon. The D'Alton Lake section is from an inclined sheet which is intrusive into Archean granitoid rocks north of Lake Nipigon. The relationship between the sheet at D'Alton Lake and the sill which covers most of the area represented by the Orient Bay Section is not known, but the former sheet might possibly be a feeder to the overlying sill.

Typical petrographic aspects of the Nipigon sills have been outlined in chapter 2. In detail, however, there are significant differences between the suites mainly due to pyroxene variation and these are outlined below.

Phenocryst assemblages in chilled margins of diabase consist of plagioclase, plagioclase + olivine, plagioclase + olivine + augite. These assemblages indicate a crystallization sequence of plagioclase, olivine, augite for the major silicate phases. This sequence is supported by petrographic textures such as olivine which is interstitial to plagioclase and ophitic augite enclosing plagioclase and olivine.

A study of the major element chemistry in chapter 4 indicates that within sill variation is small compared to regional variation. The origin of this variation is attributed to fractionation of olivine and plagioclase at depth. The major source of chemical variation within sections of diabase is mainly due to injection of multiple pulses of magma. In the case of the D'Alton Lake section there is an internal sub-chilled contact. In other sections however no field evidence for multiple intrusion was observed. Blackadar (1956) also concluded that variation in the Logan sills in the Thunder Bay area southwest of Lake Nipigon was due to the multiple intrusion. The Logan sills are the same age as, and may be correlative with the Nipigon sills.

Olivine accumulation is locally evident near the base of sills and olivine becomes less abundant to absent toward the top of sills. The upper portion of sills are enriched in micrographic quartz-alkali feldspar intergrowths.

Modal and major element variations for the sill sections are shown in Figure 5.3 and in Table 5.1.

5.8.1 Pyroxenes

Pyroxenes analyzed from the Orient Bay and D'Alton Lake

D'ALTON LAKE SECTION

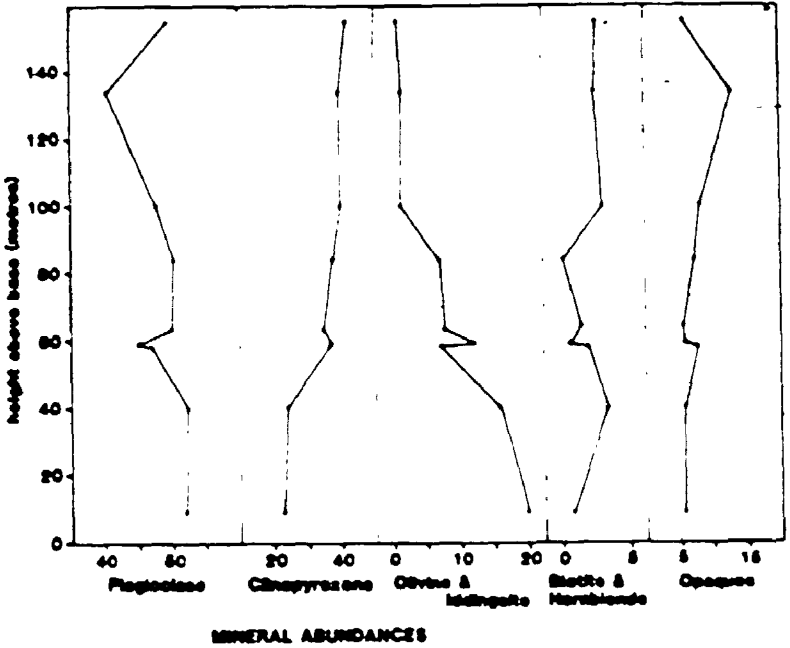

ORIENT BAY SECTION

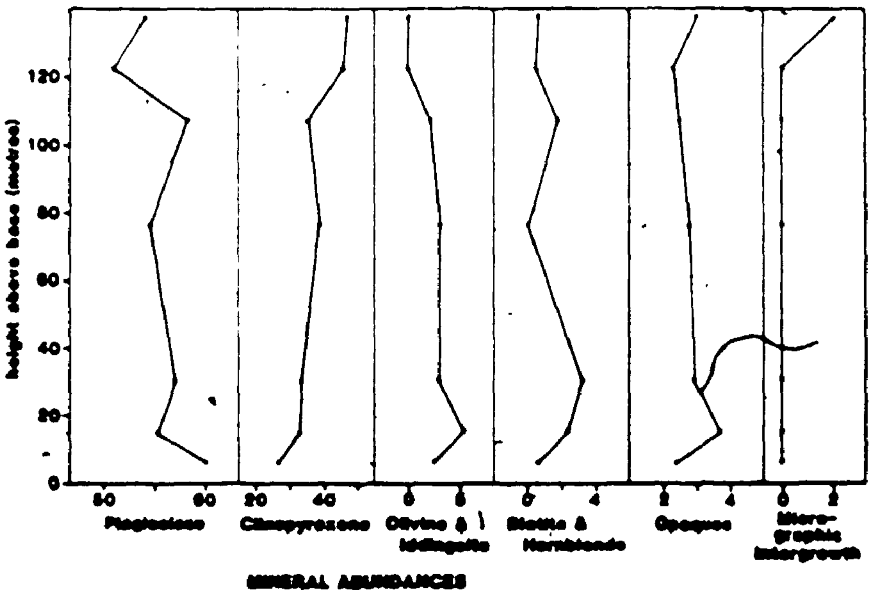

5.3 Modal variation in the D'Alton and Orient Bay sections. Minerals are plotted in volume percent.

Table 5.1: Major element chemistry of the diabase

	D'Alton Lake Section							Orient Bay Section								Others	
	1	2	3	4	5	6	7	8	9	10	11	12	13	14	15	16	17
SiO_2	48.50	48.80	48.90	47.90	48.40	49.00	47.90	49.10	48.30	48.60	48.90	49.00	49.80	50.10	51.20	49.20	48.60
TiO_2	1.50	1.46	1.56	1.32	1.40	0.91	1.79	1.27	.97	.88	.88	0.91	.92	1.10	1.05	1.69	2.89
Al_2O_3	15.50	14.80	13.40	15.90	13.80	15.30	15.50	14.60	15.50	15.40	14.70	15.30	14.80	13.50	13.20	14.00	10.20
Fe_2O_3t	13.40	15.30	15.80	14.40	15.20	12.10	15.90	13.50	13.20	12.70	12.90	12.10	12.10	12.70	13.90	15.70	20.70
MnO	0.15	.22	.22	.20	.21	.17	.22	.19	.18	.18	.18	.17	.17	0.19	.23	.21	.24
MgO	5.61	6.42	5.91	6.91	7.06	7.53	5.97	7.50	8.51	8.66	8.75	7.53	7.41	7.96	7.14	6.20	3.99
CaO	10.80	10.00	10.30	9.87	10.30	11.70	9.77	10.30	10.20	10.80	10.80	11.70	11.70	12.00	10.60	9.69	8.36
Na_2O	3.30	2.37	2.10	2.27	2.06	2.27	2.26	2.34	2.10	2.11	1.92	2.27	2.29	2.26	2.16	1.96	2.72
K_2O	.22	.40	.39	.32	.33	.36	.40	.42	.42	.52	.61	.36	.32	0.32	.33	.78	.80
P_2O_5	.14	.15	.15	.14	.13	0.07	.15	.09	.07	.06	0.06	.07	.06	0.09	.06	.06	.20
LOI	.95	.30	.13	.22	.12	.11	.32	.12	.10	.06	.08	.11	.08	0.10	.12	.32	.11
Total	100.07	100.22	98.86	99.45	99.01	99.52	100.18	99.43	99.55	99.97	99.78	99.52	100.26	100.32	99.99	99.81	99.81

D'Alton Lake Section

1	80-1116	Diabase chill
2	80-1117	Medium grained diabase, 4 m. above base
3	80-1121	Sub-chilled diabase from internal contact, 35 m.
4	80-1118	Medium grained diabase, 60 m.
5	80-1122	Medium grained diabase, 62 m.
6	80-1123	Medium grained diabase, 85 m.
7	80-1119	Medium grained diabase with pegmatitic patches, 140 m.

Orient Bay Section

8	81-292	Medium grained, ophitic diabase, 15 m. above base
9	81-291	Medium grained, ophitic diabase, 46 m.
10	81-290	Medium grained diabase, 77 m.
11	81-289	Medium grained diabase, 93 m.
12	81-288	Medium grained diabase, 109 m.
13	81-287	Medium grained diabase, 112 m.
14	81-286	Medium grained diabase, 125 m.
15	81-293	Medium grained diabase with pegmatitic patches, 140 m.

Others

16	82-201	Fe-rich diabase dike, Vint Bay, Lake Nipigon
17	81-285	Pegmatitic diabase from top of sill, Spruce Point, Lake Nipigon

sections, Fe-rich diabase and pegmatitic diabase (Table 5.2) show a wide ranges in chemistry in terms of the variables Mg, Fe, and Ca (Figure 5.4). Augite typically occurs as coarse, well developed sub-ophitic to ophitic grains, composed of complex chemically zoned sub-grains in which the axes of individual crystals are nearly parallel. These textures are similar to those reported in other diabase suites such as the Grenville Swarm (Kretz et al. 1985). Ca-poor pyroxenes vary from late forming interstitial grains, to sub-ophitic grains which co-precipitate with augite, to early forming phenocrysts. In general, exsolution textures are not well developed in these rocks, however, some samples of diabase from lower parts of the sills have prominant blebby exsolution textures.

The Nipigon pyroxenes exhibit an overall trend typical of tholeiitic rocks as defined by Deer et al. (1978). The pyroxenes are Ca-poor in comparison to the Skaergaard trend (Figure 5.4) but occupy a similar range in composition to pyroxenes from Hawaiian tholeiites (Fodor et al. 1975). In most samples Al_2O_3 varies between 1.5 and 2.5 and decreases with increasing Fe/Fe+Mg+Ca.

The complex relationships make determination of coexisting phases difficult. Furthermore, since in many rocks the Ca-poor phase is late forming, the determination of coexisting phases is of limited significance. Pairs of augite and pigeonite which are interpreted to represent co-existing phases are plotted on the Lindsley (1984) graphical pyroxene thermometer (Figure 5.4). Most of these analyses are from

Table 5.2: Representative pyroxene analyses

	Augite Analyses									Ca-poor Pyroenes		
	1	2	3	4	5	6	7	8	9	10	11	12
SiO_2	51.72	49.09	51.78	50.03	50.22	51.27	52.56	51.90	50.05	52.22	52.22	52.58
TiO_2	.54	1.12	.51	.71	.65	.51	.31	.63	.62	.34	.39	.34
Al_2O_3	2.64	4.36	2.15	2.14	1.25	3.06	1.63	2.02	1.19	.87	.95	2.70
Cr_2O_3	.46	.18	.24	.28	.10	.27	.13	.00	.02	.15	.04	.19
FeO^*	9.79	12.96	10.52	16.13	20.30	8.75	9.94	13.37	20.18	22.34	20.33	13.65
MnO	.22	.33	.28	.34	.48	.02	.06	.21	.45	.45	.40	.18
MgO	16.07	14.18	15.78	12.96	11.30	16.11	18.37	15.45	11.01	19.36	20.32	21.13
CaO	18.35	17.01	18.13	16.33	15.26	19.42	16.58	17.26	15.81	5.07	4.48	9.05
Na_2O	.49	.56	.13	.10	.08	.00	.00	.00	.44	.00	.00	.09
K_2O	0.1	.02	.00	.00	.00	.00	.00	.00	.00	.01	.00	.00
Sum.	100.29	99.81	99.52	99.02	99.64	99.41	99.58	100.84	99.77	100.81	99.13	99.91
Si	1.916	1.855	1.935	1.925	1.952	1.908	1.945	1.932	1.948	1.958	1.968	1.929
AlIV	.084	.145	.065	.075	.048	.092	.055	.068	.052	.038	.032	.071
AlVI	.032	.049	.030	.022	.009	.043	.016	.020	.002	.000	0.011	.046
Ti	.015	.032	.014	.021	.019	.014	.009	.018	.018	.010	.011	.009
Cr	.013	.005	.007	.009	.003	.008	.004	.000	.001	.004	.001	.006
Fe	.303	.409	.329	.519	.660	.272	.308	.416	.657	.700	.641	.419
Mg	.887	.798	.879	.743	.655	.894	1.013	.857	.639	1.082	1.142	1.156
Mn	.007	.011	.009	.011	.016	.001	.002	.007	.015	.014	.013	.006
Ca	.728	.689	.726	.673	.635	.774	.657	.688	.659	.204	.181	.356
Na	.035	.041	.009	.007	.006	.000	.000	.000	.033	.000	.000	.006
K	.000	.001	.000	.000	.000	.000	.000	.000	.000	.000	.000	.000
O	6.000	6.000	6.000	6.000	6.000	6.000	6.000	6.000	6.000	6.000	6.000	6.000
Wo	37.95	36.31	37.54	34.78	32.59	39.91	33.23	35.09	33.73	10.25	9.21	18.43
En	46.24	42.10	45.46	38.40	33.57	46.06	51.22	43.70	32.67	54.48	58.15	59.87
Fs	15.81	21.59	17.00	26.82	33.84	14.04	15.55	21.22	33.60	35.27	32.64	21.70

1 80-1116 (73) Diabase chill, D'Alton Lake, augite phenocryst core.
2 80-1116 (75) Diabase chill, D'Alton Lake, augite in matrix
3 80-1123 (161) Medium grained diabase, D'Alton Lake, intersertal augite, sector core.
4 80-1123 (169) Medium grained diabase, D'Alton Lake, intersertal augite, sector rim.
5 80-1123 (166) Medium grained diabase, D'Alton Lake, intersertal augite, extreme sector.
6 81-292 (40) Medium grained diabase, Orient Bay, ophitic augite, core.
7 81-292 (41) Medium grained diabase, Orient Bay, ophitic augite.
8 81-292 (43) Medium grained diabase, Orient Bay, ophitic augite, rim.
9 81-285 (76) Pegmatitic diabase, Spruce Point, augite rim.
10 80-1123 (163) Medium grained diabase, D'Alton Lake, pigeonite rim on intersertal augite.
11 81-234 (108) Medium grained diabase, Orient Bay, ophitic pigeonite.
12 82-201 (120) Fe-rich diabase dike, chill, pigeonite overgrowth on olivine.

D'Alton Lake Section

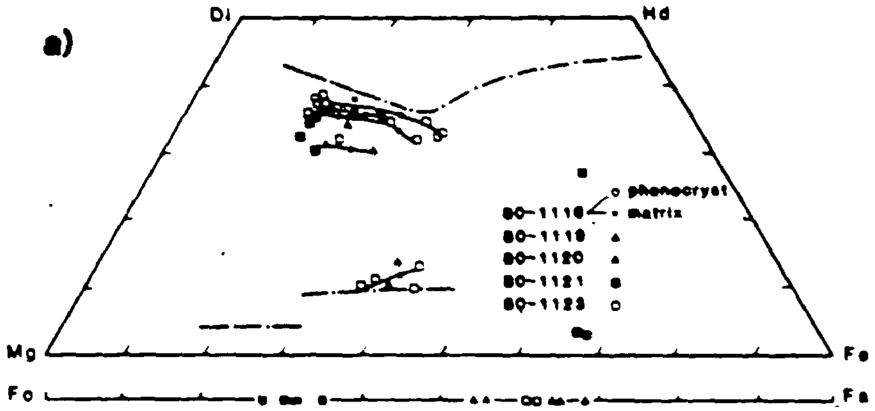

Orient Bay Section

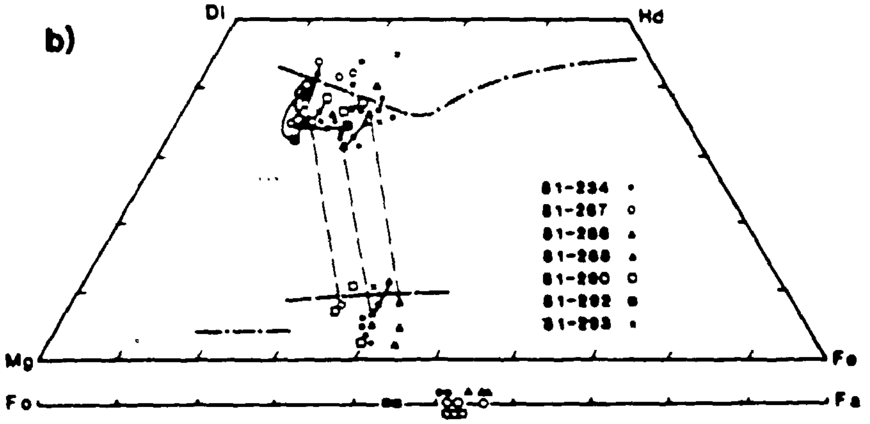

Fe–Dikes and Pegmatitic Diabase

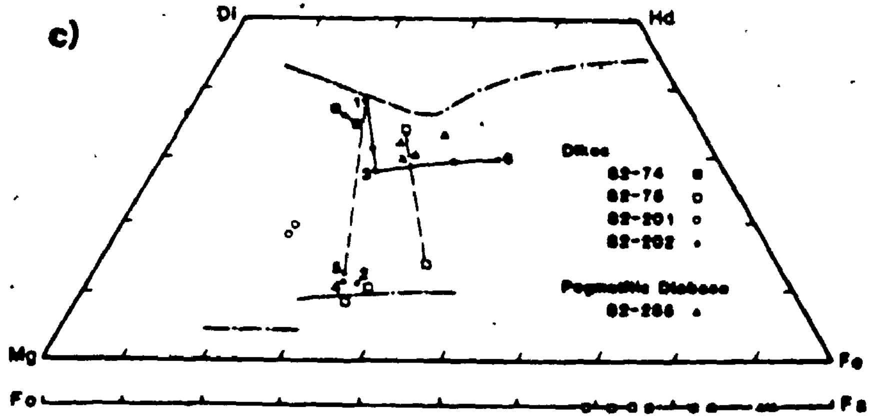

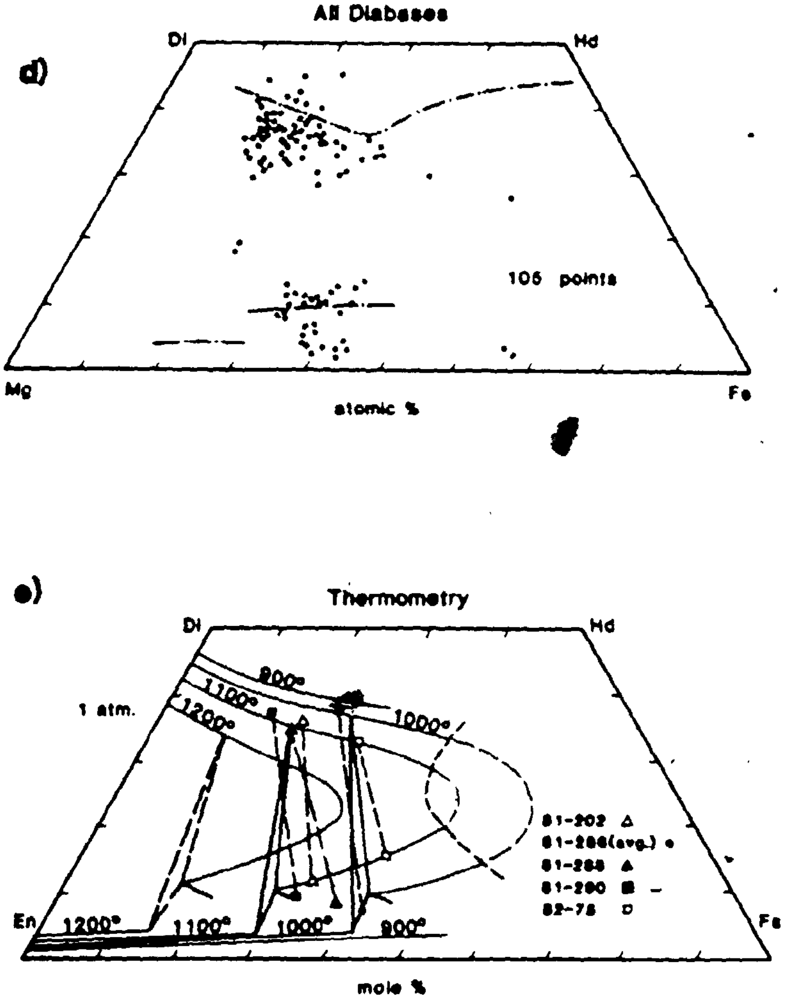

5.4 Pyroxene and olivine chemistry in the Nipigon diabase. a), b), c), d), in atomic percent. Dash - dot line is Skaergaard pyroxene trend. Solid lines with arrows indicate core to rim zoning. Dashed lines indicate coexisting Ca - poor and Ca - rich phases. In e) isotherms are from Lindsley (1983).

cores of co-existing sub-ophitic grains except for samples 82-75 and 82-202 which are from co-existing pigeonite and augite phenocrysts in chilled diabase. These pairs suggest that pyroxene crystallized over a temperature range of approximately 1100-1000oC.

In the D'Alton Lake Section (Figure 5.4) the most primitive augite ($Wo_{38}En_{46}Fs_{16}$) is from a phenocryst in a chill. This composition is closely approached by the cores of some sub-ophitic grains. Ca-poor pyroxenes are late forming and occur at the edges of augite grains as sectors or rims. Pyroxenes from the D'Alton Lake section show no significant compositional variation with stratigraphic height.

Marked variation in complex single sub-ophitic grains parallels the Mg-rich augite trend of the Skaergaard (Deer et al. 1978). Variation in single 1 mm grains shows chemical variation in Mg:Fe which is as great as the variation over the entire section. These sub-ophitic grains (Figure 5.5) consist of several sectors in near optical continuity which show zoning to Fe-enrichment at the sector edges. Sectors toward edges of grains show a further Fe-enrichment relative to sectors near the center of the composite grain. The trend of increasing Fe:Mg in composite grains suggests that earlier formed augite failed to react with remaining melt on the scale of single ophitic grains.

In the Orient Bay section (Figure 5.4), both augite and pigeonite occur as sub-ophitic grains which texturally appear to have crystallized together. The augite and pigeonite

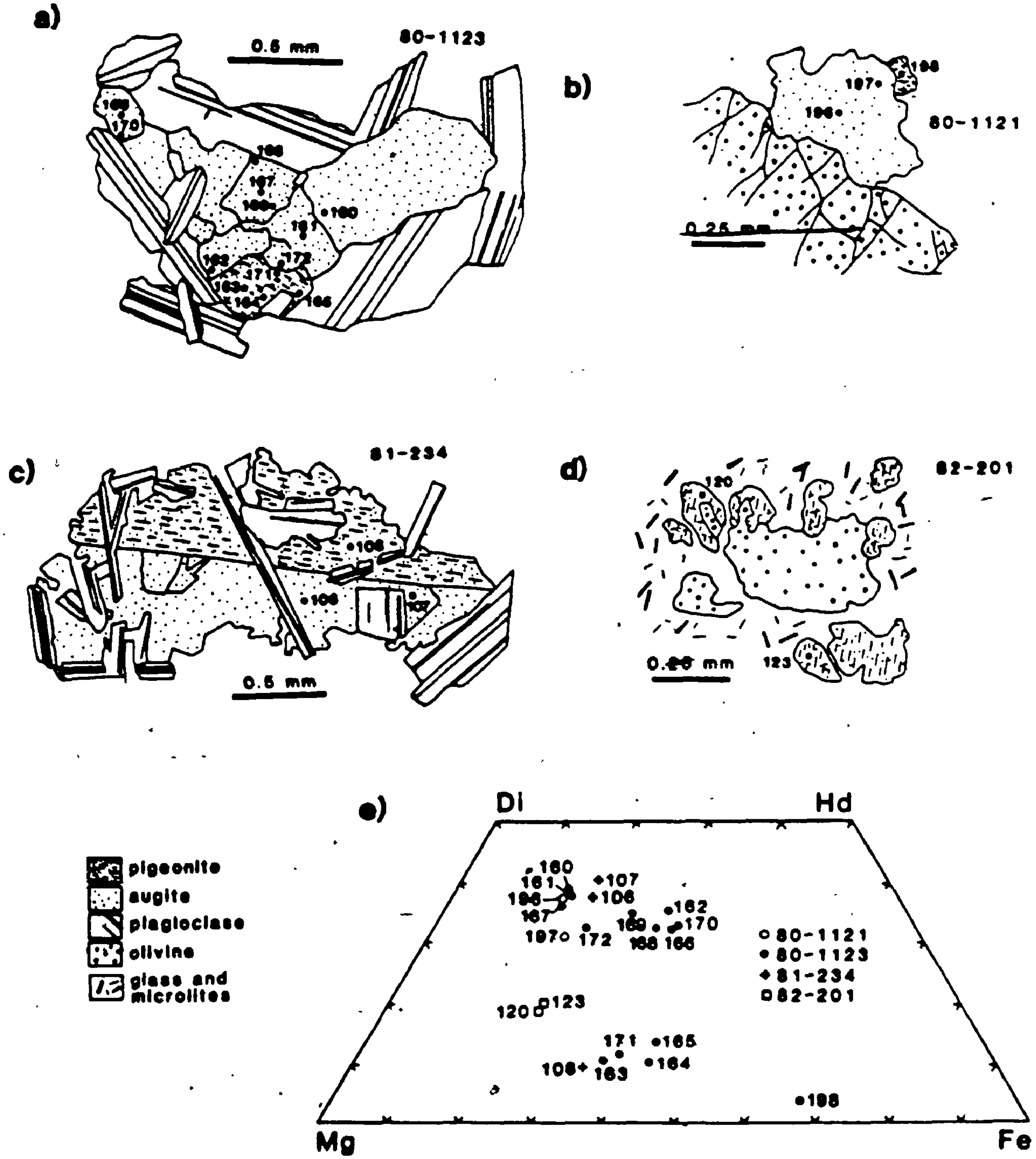
a)
0.5 mm
80-1123
b)
80-1121
0.25 mm
c)
81-234
0.5 mm
d)
82-201
0.25 mm
120
123
e)
Di
Hd
Mg
Fe
160
161
196
167
197
172
107
106
162
170
169
168
166
120
123
171
165
108
163
164
198
○ 80-1121
● 80-1123
◆ 81-234
□ 82-201
pigeonite
augite
plagioclase
olivine
glass and microlites

5.5 Details of pyroxenes from selected diabase samples:
- a) augite with late pigeonite;
- b) augite overgrowing olivine with laté orthopyroxene;
- c) ophitic augite and pigeonite;
- d) pigeonite overgrowing olivine.

Numbered points refer to analyses in e).

commonly form composite grains in which the crystallographic axes are nearly parallel. These composite grains have complex chemical zonations, but unlike the D'Alton Lake Section there is only a limited trend to Fe enrichment in the augite. Instead, the augite has varying Ca content. Several grains show an initial trend to lower Ca resembling the quench trend of Smith and Lindsley (1971), but then subsequently move to higher Ca. Individual samples from the Orient Bay section show a weak trend toward increasing Fe:Mg which corresponds with stratigraphic height, although there is considerable overlap due to within sample variation.

Tie lines between co-existing pyroxene pairs in the Orient Bay section show that the Ca-poor pyroxene phase is Fe-rich relative to experimentally determined tie lines (Lindsley, 1983) and tie lines from pyroxenes of other typical tholeiitic suites (Deer et al. 1978). The slopes of the tie lines are comparable to those determined by Konda (1970) for the Keweenawan Beaver Bay complex in Minnesota. In the Beaver Bay complex the Fe-rich nature of pigeonite co-existing with augite is attributed to the late crystallization of pigeonite from interstitial liquid. Fe-rich orthopyroxene (Wo_{03} En_{30} Fs_{67}) occurs as a late crystallizing phase in some samples. Fe-rich diabase dikes display complex pyroxene compositional variation (Figure 5.4). In sample 82-201, pigeonite with a composition plotting in the metastable field is observed as a phenocryst phase. The pigeonite clusters around small corroded olivine phenocrysts (Figure 5.5) suggesting that the reaction olivine + melt to form pigeonite has taken place. This reaction is significant because in most other samples olivine appears to be in equilibrium with phenocrystic augite. Sample 82-202, from the same suite, contains hourglass zoned augite with piegeonite sectors and cores. Irregular ragged cores of pigeonite observed in these grains suggest the reaction pigeonite + melt = augite. Compositional variation in a zoned augite for these rocks is shown in figure 5.4.

5.8.2 Olivine

Olivine is found in most diabases from the Lake Nipigon area examined, the exception being in the upper part of the Orient Bay section. A wide range in composition (Fo_{72-09}) is observed (Table 5.3) (Figure 5.4). In rocks containing olivine ranging in composition from Fo_{56-32}, the olivine occurs as fine rounded 0.1 to 1.5 mm grains which are usually enclosed by oikocrystic augite. A few samples exhibit olivine as anhedral grains which are interstitial to plagioclase.

Fayalite (Fo_{09}) occurs as anhedral grains to 2 mm in association and apparently in equilibrium with quartz-albite granophyric intergrowths in pegmatitic diabase (sample 81-285). This is the most Fe-rich olivine observed in the suite. A medium grained diabase with pegmatitic patches (sample 80-1119) from the D'Alton Lake section contains olivine of composition Fo_{32-36}. This olivine comes from the medium grained diabase containing quartz-alkali feldspar

Table 5.3: Representative olivine analyses

	1	2	3	4	5	6	7	8	9
SiO_2	38.29	34.98	34.19	33.73	36.30	35.02	34.01	34.15	30.73
Al_2O_3	.00	.03	.03	.00	.00	.00	.00	.02	.00
TiO_2	.01	.04	.09	.00	.00	.02	.00	.13	.03
Cr_2O_3	.07	.17	.05	.00	.04	.00	.11	.02	.00
FeO	24.61	41.95	47.66	49.69	36.92	41.55	44.22	47.80	63.95
NiO	.32	.00	.02	.00	.15	.10	.16	.53	.02
MgO	36.39	21.85	17.70	15.38	25.68	22.39	19.96	16.32	3.72
MnO	.23	.66	.84	.64	.50	.58	.66	.82	.91
CaO	.19	.20	.14	.29	.22	.10	.16	.38	.38
Total	100.11	99.88	100.72	99.84	99.81	99.76	99.28	100.17	99.74
Si	1.007	1.009	1.007	1.015	1.018	1.009	1.002	1.017	1.010
AlIV	.000	.001	.001	.000	.000	.000	.000	.001	.000
AlVI	.000	.000	.000	.000	.000	.000	.000	.000	.000
Ti	.000	.001	.002	.000	.000	.000	.000	.003	.001
Cr	.001	.004	.001	.000	.001	.000	.003	.000	.000
Fe	.541	1.012	1.174	1.251	.866	1.001	1.090	1.190	1.757
Ni	.007	.000	.000	.003	.003	.002	.004	.013	.001
Mg	1.426	.939	.777	.690	1.074	.961	.877	.724	.182
Mn	.005	.016	.021	.016	.012	.014	.016	.021	.025
Ca	.005	.006	.004	.009	.007	.003	.005	.012	.013
O	4.000	4.000	4.000	4.000	4.000	4.000	4.000	4.000	4.000
Fo	72.49	48.14	39.84	35.55	55.35	48.99	44.58	37.83	90.61

1	80-1161	(26)	Diabase chill, D'Alton Lake, olivine phenocryst core.
2	80-1120	(24)	Medium grained diabase D'Alton Lake, olivine core.
3	80-1123	(29)	Medium grained diabase D'Alton Lake, olivine
4	80-1119	(34)	Medium grained diabase with pegmatitic patches, D'Alton Lake, olivine core.
5	81-292	(45)	Medium grained diabase, Orient Bay, olivine core.
6	81-290	(41)	Medium grained diabase, Orient Bay, olivine core.
7	81-288	(37)	Medium grained diabase, Orient Bay, olivine core.
8	82-75	(10)	Medium grained Fe-diabase dike, olivine core.
9	81-285	(30)	Pegmatitic diabase, Spruce Point, olivine with quartz.

granophyric intergrowths, but is not in contact with the intergrowths.

The most magnesian olivine Fo_{69-72} occur as phenocrysts in chilled phases of the D'Alton Lake section. Olivine in medium grained diabases from the D'Alton Lake and Orient Bay sections respectively show the ranges in composition of Fo_{32-46} and Fo_{44-56}. Both sections show decreases in Fo content which correspond with stratigraphic height. The magnesian olivine in the Orient Bay section reflect a slightly more magnesian bulk composition in this section.

All of the olivines have low Cr_2O_3 which ranges from 0.21 in phenocrysts to less than 0.05 in the medium grained diabase.

5.8.3 Feldspar

Plagioclase analyzed from Nipigon diabases have a wide range in anorthite content (Table 5.4) (Figure 5.6). In medium grained diabase the plagioclase occurs as medium to coarse 1.5 to 4 mm euhedral tabular to lath shaped grains which have well developed albite Carlsbad and pericline twinning. Alteration of plagioclase is minimal in most rocks.

In the D'Alton Lake section (Figure 5.6) the most calcic plagioclase (An_{71}) occurs in phenocrysts in chilled diabase. The phenocrysts generally have normal core to rim variation in the range An_{70-68}. Some oscilatory zoning occurs with compositions ranging from An_{71} to An_{65}. Plagioclase in the matrix is less calcic than the phenocrysts and in the range

Table 5.4: Representative feldspar analyses

	1	2	3	4	5	6	7	8	9	10	11	12
SiO_2	52.20	51.91	51.57	52.10	51.05	52.90	51.09	55.36	53.76	58.50	64.36	65.89
Al_2O_3	30.38	29.22	29.77	29.31	29.49	29.77	29.77	26.81	28.36	25.21	18.72	20.77
FeO	.80	.80	.48	.60	1.34	.54	.55	.71	.37	.32	.48	.21
Na_2O	3.43	3.64	4.50	4.34	3.42	4.07	3.67	5.68	4.21	6.60	2.55	11.04
CaO	14.12	13.44	13.04	12.96	14.24	12.89	14.00	10.21	12.44	8.79	.23	1.48
K_2O	.18	.11	.16	.23	.54	.25	.22	.23	.17	.43	12.66	.95
Total	101.06	99.12	98.52	99.54	100.08	100.42	99.30	99.00	99.31	99.85	99.00	100.34
Si	9.420	9.538	9.451	9.540	9.373	9.574	9.397	10.105	9.803	10.521	11.903	11.612
AlIV	6.460	6.327	6.429	6.324	6.381	6.349	6.452	5.767	6.094	5.343	4.080	4.313
AlVI	.000	.000	.000	.000	.000	.000	.000	.000	.000	.000	.000	.000
Fe	.121	.123	.074	.092	.206	.082	.085	.108	.056	.048	.074	.031
Ca	2.730	2.646	2.560	2.542	2.801	2.500	2.759	1.997	2.430	1.694	.046	.279
Na	1.200	1.297	1.599	1.541	1.217	1.428	1.309	2.010	1.488	2.301	.914	3.772
K	.030	.026	.037	.054	.126	.058	.052	.054	.040	.099	2.986	.214
O	32.000	32.000	32.000	32.000	32.000	32.000	32.000	32.000	32.000	32.000	32.000	32.000
Ab	30.30	32.68	38.10	37.24	29.37	35.83	31.77	49.51	37.60	56.22	23.17	88.44
An	68.94	66.67	61.01	61.46	67.58	62.72	66.98	49.18	61.40	41.37	1.15	6.55
Or	.76	.65	.89	1.30	3.05	1.45	1.25	1.32	1.00	2.41	75.68	5.01

1 80-1116 (83) Diabase chill, D'Alton Lake, phenocryst core.
2 80-1116 (85) Diabase chill, D'Alton Lake, phenocryst rim.
3 80-1120 (90) Medium grained diabase, D'Alton Lake, plagioclse core.
4 80-1119 (117) Medium grained diabase with pegmatitic patches, D'Alton Lake, plagioclase core.
5 81-292 (23) Medium grained diabase, Orient Bay, plagioclase core.
6 81-290 (32) Medium grained diabase, Orient Bay, plagioclase core.
7 81-288 (17) Medium grained diabase, Orient Bay, plagioclase core.
8 81-288 (19) Medium grained diabase, Orient Bay, plagioclase rim.
9 81-286 (15) Medium grained diabase, Orient Bay, plagioclase core.
10 81-286 (16) Medium grained diabase, Orient Bay, plagioclase rim.
11 80-1119 (115) Medium grained diabase with pegmatitic patches, D'Alton Lake, K-spar in intergrowth.
12 81-285 (95) Pegmatitic diabase, Spruce Point, albite in intergrowth.

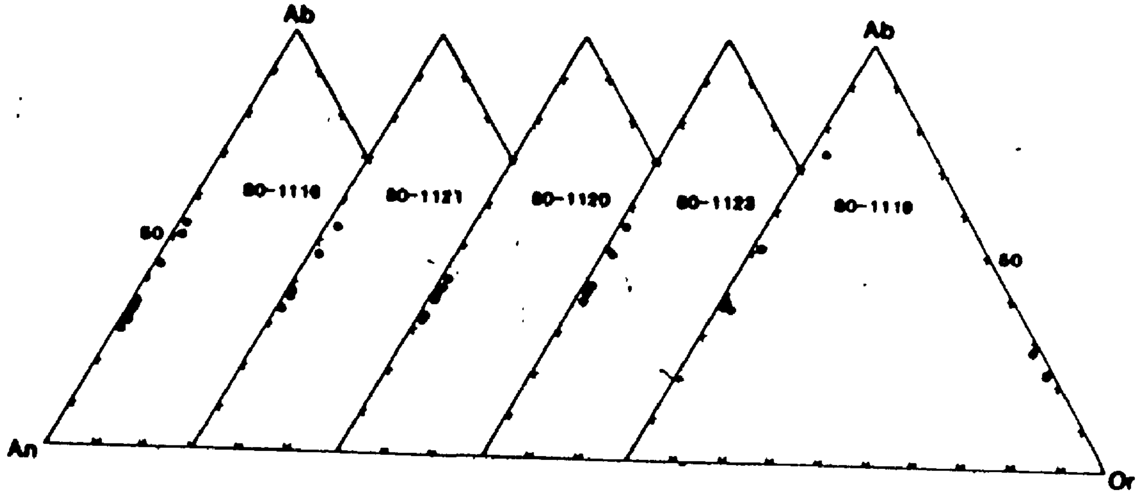

D'Alton Lake Section

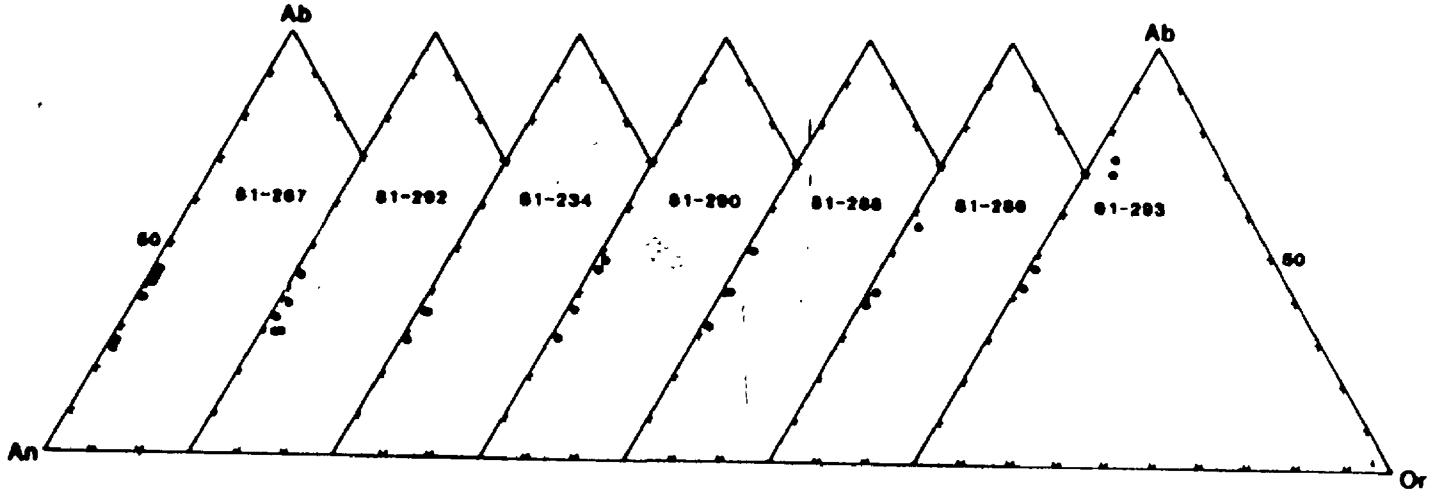

Orient Bay Section

5.6 Feldspar analyses in the Nipigon diabase.

An_{56-45}.

Drake (1976) has evaluated the equilibrium constant for the equilibrium of albite with melt. This allows the temperature of crystallization of a given plagioclase composition from a dry melt of known composition at low P to be calculated. Maximum anorthite contents of plagioclase phenocrysts in two chilled diabases in the D'Alton Lake section (80-1120 and 80-1121), yield temperatures of 1113°C and 1045°C respectively.

Tabular plagioclase from the medium grained diabase of the D'Alton Lake section show a compositional range of $An_{67-43}Ab_{32-55}Or_{01-02}$. Generally rims are more Na rich but weak oscillatory zoning is characteristic. There is a weak trend toward Na-enrichment toward the top of the sill. At the top of the sill granophyric intergrowth of potassium feldspar ($An_{01}Ab_{26}Or_{73}$) and quartz coexists with sodic oligoclase ($An_{23}Ab_{73}Or_{04}$) are present.

The Orient Bay section (Figure 5.6), shows a similar range in composition ($An_{74-41}Ab_{25-56}Or_{01-02}$) and also has a weak trend to Na-enrichment correlating with stratigraphic height. All samples of the section however have normal zoning with up to 20 mole % difference in core to rim variation. The most calcic plagioclase is from the core of plagioclase grains enclosed by augite oikocrysts. At the top of the section, oligoclase $An_{22}Ab_{73}Or_{05}$ occurs intergrown with quartz.

A pegmatite diabase (81-285) exhibits tabular plagioclase with normal zoning from $An_{45-31}Ab_{53-66}Or_{02-3}$. This sample has graphic intergrowths of albite ($An_{07}Ab_{88}Or_{05}$) and quartz.

5.8.4 Oxides

Oxides (Table 5.5) account for 2-7 % of the diabase. They occur as blocky, anhedral grains up to 4 mm diameter which are interstitial to plagioclase and olivine and locally enclose these silicates. Ilmenite occurs as discrete homogenous grains and as exsolution lamallae and rims with magnetite. Ilmenite appears less abundant than magnetite but relative proportions have not been determined. Magnetite usually exhibits varying amounts of coarse ilmenite exsolution, however some samples are homogenous in reflected light. Traces of fine chalcopyrite were also observed in most specimens of diabase.

Magnetite-ilmenite pairs plotted on a T-f(O_2) diagram (Figure 5.7) (Spencer and Lindsley, 1981) show varying degrees of re-equilibration to sub-solidus temperatures in the range 650 to 750°C. The highest temperatures were obtained from homogeneous grains, but even fine grained oxides in diabase chills yield sub-solidus temperatures. Most analyses fall near or within one log unit above the QFM buffer curve for 1 atm total pressure. A sub-solidus T-f(O_2) trajectory close to the QFM buffer is typical for other Keweenawan tholeiitic intrusive suites such as the Duluth complex (Pasteris, 1985).

5.8.5 Other Phases

Quartz is present as intergrowths with alkali feldspar in

Table 5.5: Representative oxide analyses

	Ilmenite Analyses					Magnetite Analyses			
	1	2	3	4		5	6	7	8
TiO_2	48.17	50.61	48.86	48.79		4.30	11.23	10.79	9.85
Al_2O_3	.35	.04	.08	.09		.69	2.64	2.43	1.01
Cr_2O_3	.00	.00	.00	.02		.07	.12	.13	.16
FeO^t	48.82	47.84	47.93	49.73		88.30	76.25	81.37	83.30
MnO	1.83	.61	.41	.85		.40	.62	.66	.37
MgO	.01	.42	1.68	.09		.11	.25	.16	.17
Total	99.18	99.52	98.86	99.57		93.87	91.25	95.54	94.86
Recalculated									
Fe_2O_3	7.91	4.07	8.16	7.55		59.68	72.55	45.25	48.45
FeO	41.69	44.17	40.58	42.92		34.53	10.89	40.61	39.65
Total	99.96	99.92	99.77	100.32		99.78	98.34	100.02	99.66
Mole% Ilmenite	91.91	96.07	92.17	92.66	Mole% ulvospinel	12.37	22.59	30.46	28.15

1	80-1116 (11)	Diabase chill, D'Alton Lake, fine ilmenite grain.
2	80-1120 (26)	Medium grained diabase, D'Alton Lake, ilmenite lamallae in magnetite.
3	81-293 (57)	Medium grained diabase with pegmatitic patches, Orient Bay, homogeneous ilmenite.
4	81-285 (1)	Pegmatitic diabase, Spruce Point, ilmenite rimming magnetite 81-285 (3).
5	80-1116 (9)	Diabase chill, D'Alton Lake, fine magnetite grain.
6	80-1120 (21)	Medium grained diabase, D'Alton Lake, magnetite with ilmenite exsolutions.
7	81-293 (59)	Medium grained diabase with pegmatitic patches, Orient Bay, homogeneous magnetite.
8	81-285 (3)	Pegmatitic diabase, Spruce Point, magnetite with ilmenite intergrowths.

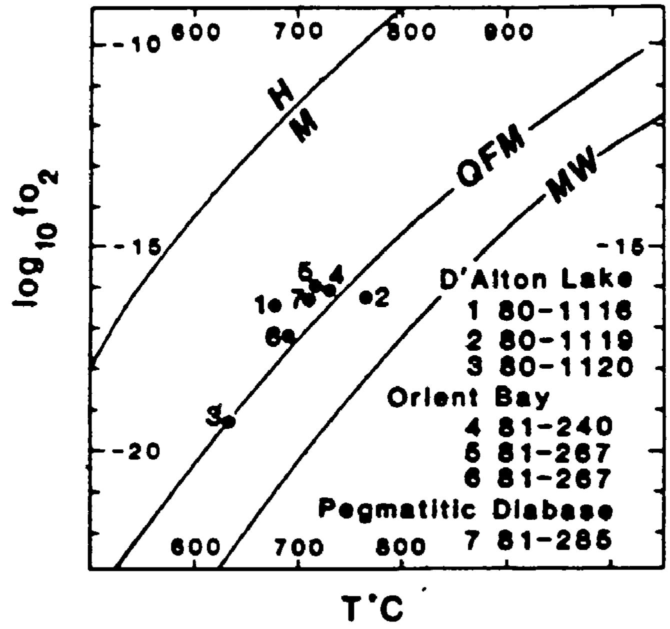

5.7 T-f(O_2) diagram for compositions of coexisting magnetite and ilmenite from Nipigon diabase. Based on model of Spencer and Lindsley (1981). Buffer curves at 1 atm plotted for reference. Points are based on average of 2 to 6 analyses of a single grain of each phase.

medium grained and pegmatitic diabase in the upper portions of the sills. Traces of amphibole and biotite locally rim pyroxenes and are interpreted to be a result of deuteric alteration. Amphibole is locally abundant in pegmatitic diabase. Accessory phases which are locally present, especially in pegmatitic diabases, are apatite, zircon and baddeleyite. Olivine is commonly altered to iddingsite.

5.9 Cooling

Heat flow calculations of Jaeger (1957) provide estimates of the time span of crystallization. Crystallization temperatures of plagioclase and pyroxenes indicate temperatures of 1113°C to approximately 1000°C. The temperature of final crystallization of graphic mesostasis is estimated at 800 C based on the hydrous granite melting curve at 0.4 kbar. The dat suggest an approximate melting range of 1100°C to 800°C for the Nipigon sills. Other assumptions for the heat flow calculation are: intrusion is instantaneous; initial wall rock temperature is 0°C; latent heat of crystallization is 100 cal/gm; the density of melt and country rock is 2.8 gm/cm^3; the specific heat of melt and country rock are 0.30 and 0.25 cal/gm-deg respectively and thermal conductivity of melt and country rock is 0.0005 (Jaeger, 1957; Kretz *et al.* 1984). Using these values the time for complete crystallization is 0.014 D^2 years. This suggests that the Nipigon sills which are 150 to 200 meters thick cooled in the order of 315 to 560 years.

Calculations by Jaeger (1957) also allow estimates of the temperature distribution within the country rocks. For a sill with a cooling range of 1100 to 800oC, given the above assumptions, the country rock at the contact should reach a temperature of 665oC. Metamorphic assemblages in the country rock suggest temperatures above 540oC were attained.

5.10 Olivine Compositions and Silica Activity

Olivines in the Nipigon sills range in composition from Fo_{72-09}. The most magnesian olivines (Fo_{72}) occur as phenocrysts in chilled phases of the D'Alton Lake sill and these would appear to be in equilibrium with liquids of Mg' equal to 0.44 based on the Mg-Fe exchange reaction equilibrium distribution coefficient of 0.30 (Roeder and Emslie, 1970). This is close to the Mg' of the chills.

Olivines from the medium grained diabase are considerably less Mg rich and in the range Fo_{56-32}. These olivines are interpreted to crystallize after liquidus plagioclase but prior to augite. Based on the Mg-Fe exchange reaction these olivines would be in equilibrium with liquids with Mg' <0.275. The olivines should not have crystallized from a liquid with Mg' of 0.44 to 0.54 corresponding to the Mg' of the diabase. The iron-rich nature of the olivines is probably related to sub-solidus reactions with late forming pyroxenes. In comparison to co-existing Ca-poor pyroxene and olivine in the Skaergaard Intrusion, Nipigon diabases exhibit similar compositions for coexisting olivine and late Ca-poor pyroxene.

The stability of Ca-poor pyroxene relative to olivine is dependent on the silica content of the magma (see Morse, 1980). In the absence of sufficient silica, the pyroxene reacts to olivine and a more silica rich liquid. Olivines and pigeonite in the D'Alton Lake and Orient Bay sections display different behaviour which can be related to silica activity $a(SiO_2)$ in the magma.

The D'Alton Lake sill contains olivine throughout the section but Ca-poor pyroxenes were not recognized in the uppermost part (Figure 5.3). The last sample in which pigeonite is recognized contains olivine of composition Fo_{40}. This is the same olivine composition for which Ca-poor pyroxene disappears in the Skaergaard sequence (Wager and Brown, 1968). In the Skaergaard, pigeonite coexisting with Fo_{40} is En_{49}. The corresponding D'Alton Lake pigeonite is En_{48}.

In contrast, no olivine was recognized in the upper part of the Orient Bay section but Ca-poor pyroxene persists throughout the sequence. This suggests a higher $a(SiO_2)$ than the D'Alton sequence. This is in agreement with the observation that augite and pigeonite probably co-precipitate in the Orient Bay sequence, but in the D'Alton section pigeonite is an interstitial, late crystallizing phase.

Analyses of co-existing pigeonite and olivine in both the D'Alton and Orient Bay sections allow estimates of $a(SiO_2)$ to be calculated based on the reaction

$$\underset{\text{in pyroxene}}{MgSiO_3} = \underset{\text{in olivine}}{MgSi_{1/2}O_2} + \underset{\text{in liquid}}{1/2SiO_2}. \quad (3)$$

A decrease in concentration of silica drives the reaction to the right and therefore Ca-poor pyroxene will tend to disappear in favour of olivine. For reaction (3), the equilibrium constant for a given temperature and pressure can be given as

$$K = \frac{a_{MgSi_{1/2}O_2} \cdot a^{1/2}_{SiO_2}}{a_{MgSiO_3}} \qquad (4)$$

Values of $a(MgSi_{1/2}O_2)$ and $a(MgSiO_3)$ can be estimated from the mole fractions of these components in olivine and pyroxene respectively using activity coefficients given by Williams (1971, 1972). The equilibrium constant for the endmember reaction (4) has been evaluated for cases in which olivine and pyroxene have intermediate values of Fe/Mg and is a function of T and P (Morse, 1980).

A temperature of 1000°C and pressure of 400 bars are assumed for the late crystallization of pigeonite. The equilibrium constant is relatively insensitive to changes in pressure within ~~the~~ range of conditions for the Nipigon sills. Olivine-pigeonite pairs from the sections indicate ranges of silica activity from 0.7 to 0.8 in the D'Alton section and 0.8 in the Orient Bay section. However, the estimates of silica activity are sensitive to the composition and therefore dependent on the interpretation of which phases actually coexist. The estimates, however, are in agreement with the interpretation of $a(SiO_2)$ based on pyroxene and olivine crystallization sequences, which is discussed in the next section. The $a(SiO_2)$ for the co-existing pigeonite

(En_{49}) and olivine (Fo_{40}) of the Skaegaard Intrusion is estimated at 0.9 by Morse (1980). The Nipigon diabases have slightly lower a(SiO_2) which is agreement with the persistence of olivine throughout most of the sequence. This has been noted in other Keweenawan tholeiites by Konda and Green (1974).

The presence of quartz in the late residuum of pegmatitic diabase indictes that a(SiO_2) rose to unity at the late stages of crystallization of the Nipigon diabases. The stable assemblage on these rocks is augite + fayalite + quartz.

5.11 Pyroxene Variation and Crystallization Sequences

Pyroxenes in the Nipigon sills exhibit different crystallization sequences and compositional trends. Diabases from the D'Alton Lake section have the crystallization sequence of olivine, augite and late pigeonite. This sequence is typical of oceanic tholeiites fractionating at low pressure (Longhi, 1981) and is the same as that determined by Konda and Green (1974) for the Keweenawan basalts. Diabases from the Orient Bay section have a similar sequence, except that augite and pigeonite appear to co-precipitate over a wider range of crystallization as indicated by the presence of sub-ophitic grains of both phases. A small group of Fe-rich diabases are characterized by the crystallization of pigeonite phenocrysts from the reaction of olivine and melt prior to the crystallization of augite. This sequence is characteristic of continental tholeiites, but the early crystallization of Ca-poor pyroxene is anomalous for mantle derived magmas

(Longhi, 1981; Campbell, 1985).

The difference between the two crystallization sequences is summarized using the system forsterite - diopside - silica (Figure 5.8) (Kushiro, 1972). In Figure 5.8, the typical pure fractionation sequence from a mantle derived melt will follow the path ABCD, and augite will crystallize before pigeonite. In the second sequence, the liquid will follow the path EFCD and Ca-poor pyroxene will crystallize first. Longhi (1981) and Campbell (1985) have suggested that the second sequence may result from the assimilation of silceous country rock by the primary melt before signficant fractionation, resulting in the path AEFCD. The Orient Bay section may represent an intermediate crystallization sequence where the fractionating melt reaches the olivine-pyroxene cotectic near C. Campbell (1985) has noted that this suggests most assimilation occurs at an early stage in the fractionation, ie before the magma enters an upper crustal chamber.

Chemical variation in Nipigon pyroxenes is variable on a scale of 1-2 mm ophitic to sub-ophitic grains. Within grain variation obscures systematic variation within sill sections. The two distinct trends of within grain variation are exhibited by the Orient Bay and D'Alton Lake sections (Figure 5.4). The trend of increasing Fe/Mg at relatively constant Ca/Ca+Fe+Mg exhibited by the D'Alton Lake section is similar to the intratelluric equilibrium trend of Muir and Tilley (1964) and similar but somewhat less calcic than that reported by Konda and Green (1974) in the Keweenawan lavas of

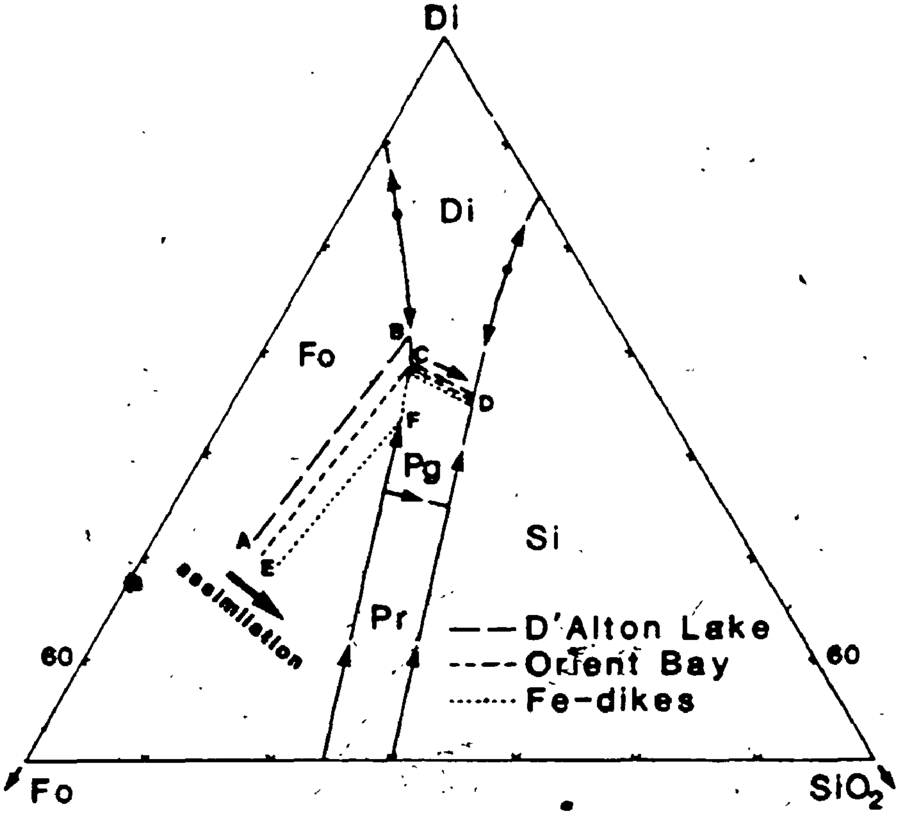
Di
Di
Fo
B
C
D
F
Pg
Si
A
E
assimilation
Pr
D'Alton Lake
Orient Bay
Fe-dikes
60
60
Fo
SiO_2

5.8 Part of the equilibrium phase diagram of the system forsterite-diopside-silica after Kushiro (1972) and Morse (1980). Mantle derived magmas at point A fractionate along path ABCD, magmas mixed with siliceous crust move to point E and fractionate along path EFCD (Longhi, 1980; Campbell, 1985). Different fractionation paths for rocks from Lake Nipigon are shown. Fo, forsterite; Pr, protoenstatite; Pg, pigeonite; Di, diopside; Si, silica.

Minnesota. The second trend in the Orient Bay section involves increasing Fe/Mg and variable Ca/Ca+Mg+Fe. This resembles the Ca-Fe substitution of the "quench trend" of Smith and Lindsley (1971).

The trends in pyroxene composition are systematic and therefore, they are not attributed to crystallization from a liquid with locally variable composition due to rapid crystal growth and slow diffusion gradients. Smith and Lindsley (1971) suggested this is a mechanism of producing scattered pyroxene compositions in a Hawaiian lava Lake.

Yamakawa (1971) has described two contrasting trends of pyroxene crystallization from a single tholeiitic diabase sill in Japan which resemble the Nipigon trends. The trend of increasing Fe/Mg at constant Ca is accounted for by cotectic crystallization of Ca-rich and Ca-poor pyroxene. The second trend of increasing Fe/Mg and decreasing Ca/Ca+Fe+Mg is explained as metastable crystallization resulting from undercooling of the liquid with respect to pigeonite. In the case of the D'Alton Lake section the former trend appears to be due to cotectic crystallization of augite and olivine, since the $a(SiO_2)$ in the liquid was too low to crystallize Ca-poor pyroxene until the final stages of solidification. In the case of the Orient Bay section, in which two pyroxene phases co-precipitate, the latter explanation appears to be appropriate. Any alternative explanation would involve varying intensive parameters such as P_{H_2O} to alter the configuration of the augite-pigeonite miscibility gap.

The variation in pyroxene chemistry on the scale [illegible] individual composite grains indicates that early formed pyroxene failed to react with remaining melt and that fractional crystallization took place on the scale of interstitial liquid cells.

5.12 Differentiation Processes

Systematic variation in mineral composition with stratigraphic height is evident in both olivine and plagioclase compositions. The presence of local accumulation of olivine at the base of the D'Alton sill suggests that crystal fractionation may have resulted in the evolution of liquid composition within the sills.

Crystal accumulation may have taken place by crystal settling or by flowage differentiation (Bhattacharji and Smith, 1964). Olivine is a possible mineral which may have accumulated by settling. Calculations using Stoke's law for magmas with a viscosity of approximately 790 poise, a crystal-liquid density contrast of 0.7 gm/cm^3 (olivine Fo_{70} = 3.35 gm/cm^3, melt = 2.65 gm/cm^3), and 1 mm diameter olivine crystals, indicate settling velocities on the order of 150 m/yr. Other factors, however, suggest settling would be less effective than Stokes Law suggests. These include: the magma has a yield strength such that it may not deform by flow under small stresses (McBirney and Noyes, 1979); petrographic evidence which indicates plagioclase crystallizes before olivine; and the possibility of convection stirring the magma more vigourously than crystals can settle.

The Rayleigh number, Ra_h for a horizontal layer of fluid is given by

$$Ra_h = \frac{L^4 \alpha_t g \beta}{\nu K} \qquad (5)$$

where L is the height of the layer, α_t is the thermal expansion coefficent, g is the gravitational constant (980 cm/sec), β is the vertical temperature gradient, ν is the kinematic viscosity (where $\nu = \eta / \rho$ and K is the kinematic viscosity. The variables are estimated as $L = 2X10^4$ cm, $\alpha_t =$ 5X10-5 deg-1 (Shaw, 1965), β = 10-3 deg-cm-1, η = 780 poise, ρ = 2.65 gm/cm^3 and K = 6 X10-3 cal/gm^oK (Jaeger, 1957). These values based on a low estimate of the vertical temperature gradient sugest a Ra of 5.6 X 10^3 for the Nipigon sills which is at the lower end of the range of convective behaviour (Cox et al. 1976).

These problems indicate settling is unlikely to be an effective mechanism of crystal accumulation, even for olivine. Plagioclase presents an even greater problem since plagioclase has neutral to positive buoyancy in iron-rich basaltic liquids (McBirney and Noyes, 1979). Given that multiple injections of magma have been emplaced, flowage differentiation is a more likely process of accumulating olivine near the base of injected units. This process would require laminar flow in the sills, a condition which is supported by estimates of Reynolds number.

The systematic variation of plagioclase and olivine indicates that the magma became more evolved upward. This process may have been achieved through a combination of flowage differentiation to accumulate suspended mienrals, and filter pressing of residual liquids enriched in H_2O, Na, Fe towards the late crystallizing portions at the top of the section. This mechanism is similar to that suggested by Jones (1984) as a process of differentiation in diabase sills in Cook County, Minnesota.

5.13 Summary

The study of the sills in the Lake Nipigon area has lead to the following conclusions.

1. One major sill is exposed over most of the Lake Nipigon area. The sill is 140 to 200 m thick and formed from several pulses of magma which cooled as a single unit. Discordant diabase sheets also show evidence of multiple magma pulses and may have locally fed the diabase sills.
2. Hydrostatic intrusion located the sills near the sediment/basement interface and controlled the thickness of the sills. The sills propagated as advancing fingers which subsequently coalesced to form a sill.
3. The sills probably took on the order of 300 to 600 years to solidify. Contact metamorphism suggests temperatures greater than 540°C were attained in the adjacent wall rocks, higher temperatures to 665°C are indicated by heat-flow models for a dry system.
4. Pyroxenes exhibit marked within sample chemical

variation. A trend of increasing Fe/Mg at constant Ca/Ca+Mg+Fe reflects an equilibrium trend. A second trend of increasing Fe/Mg with variable Ca/Ca+Mg+Fe reflects metastable crystallization.

5. Olivine compositions in most diabases reflects reaction with late forming pyroxenes and define a trend of Fe enrichment toward the top of the sills. Fayalite occurs in late Fe-rich pegmatitic diabase. Olivine phenocrysts in chills are in equilibrium with the liquid.

6. Plagioclase is the liquidus phase in the diabase. The maximum anorthite content of plagioclase in chilled margins (An_{71}) indicates liquidus temperatures of approximately 1110°C. Plagioclase exhibits a trend toward sodium enrichment toward the top of sill sections.

7. Oxides exhibit compositions consistent with equilibration to sub-solidus temperatures at an $f(O_2)$ close to the QFM buffer.

8. Crystallization sequences of the mafic minerals in the Nipigon diabase are sensitive indicators of silica activity. Differences in silica activity may relate to degree of contamination with crustal material.

CHAPTER 6

ASPECTS OF PRE-KEWEENAWAN MAGMATISM IN THE LAKE NIPIGON AREA

6.1 Camptonite Dikes and Associated Xenoliths: Implications for Bimodal Magmatism

Alkaline magmatism provides the main source of samples of lower continental crust and mantle. Although alkaline rocks occur throughout geologic history, there have been few studies of Precambrian lower crustal or mantle xenolith suites. This chapter summarizes data on a suite of possible deep crustal xenoliths from a middle Proterozoic camptonite dike in the Caribou Lake are, northwest of Lake Nipigon. The xenolith suite includes felsic garnet granulite, gabbro and websterite. Partial melting of garnet granulite xenoliths has occurred and the melt compositions have implications for the origin of Proterozoic granitoid magmatism in the area.

The Lake Nipigon area is dominated by late Precambrian igneous rocks related to the Keweenawan rift event at approximately 1110 ± 10 Ma (Silver and Green, 1972). U-Pb dating of rocks in the Nipigon area (Davis and Sutcliffe, 1985) has indicated that rift related magmatism may have occurred fof up to 500 Ma prior to Keweenawan rifting. The pre-Keweenawan igneous rocks are predominately granite and rhyolite but numerous minor dikes of camptonite, ultrabasic lamprophyre and trachyte are also present. In the Caribou

Lake area, 30 km northwest of Lake Nipigon, approximately 40 of these dikes ranging in width from a few centimeters to 3 m, have been observed during detailed mapping. All of the dikes are intrusive into Archean basement consisting of tonalitic granitoids and mafic metavolcanics. The dikes have not been dated but are considered to be pre-Keweenawan because they are not observed to cut 1108.8 + 4/-2 Ma Keweenawan diabase and there appears to be a bimodal relationship between the mafic alkaline dikes and anorogenic granitoids dated at 1536.7 + 10/-2.3 Ma (Davis and Sutcliffe, 1985) in the Nipigon area. In addition, alnoitic lamprophyres, in the Marathon area 160 km to the southeast, which are petrographically similar to the Caribou ultrabasic lamprophyres have been dated at 1653 ± 122 Ma (Platt and Mitchell, 1982).

This study is based on the examination of 5 xenoliths from one camptonite dike which occurs on the southwest end of Kellar Island, Caribou Lake (Figure 6.1). A xenolith was initially discovered while slabbing a hand specimen for a thin section. After re-sampling, additional xenoliths were found by repeated slabbing of approximately 50 kg of sample. Although the study is based on a small number of samples the results are significant because the samples provide direct evidence for the nature of and processes affecting the lower continental crust in this area.

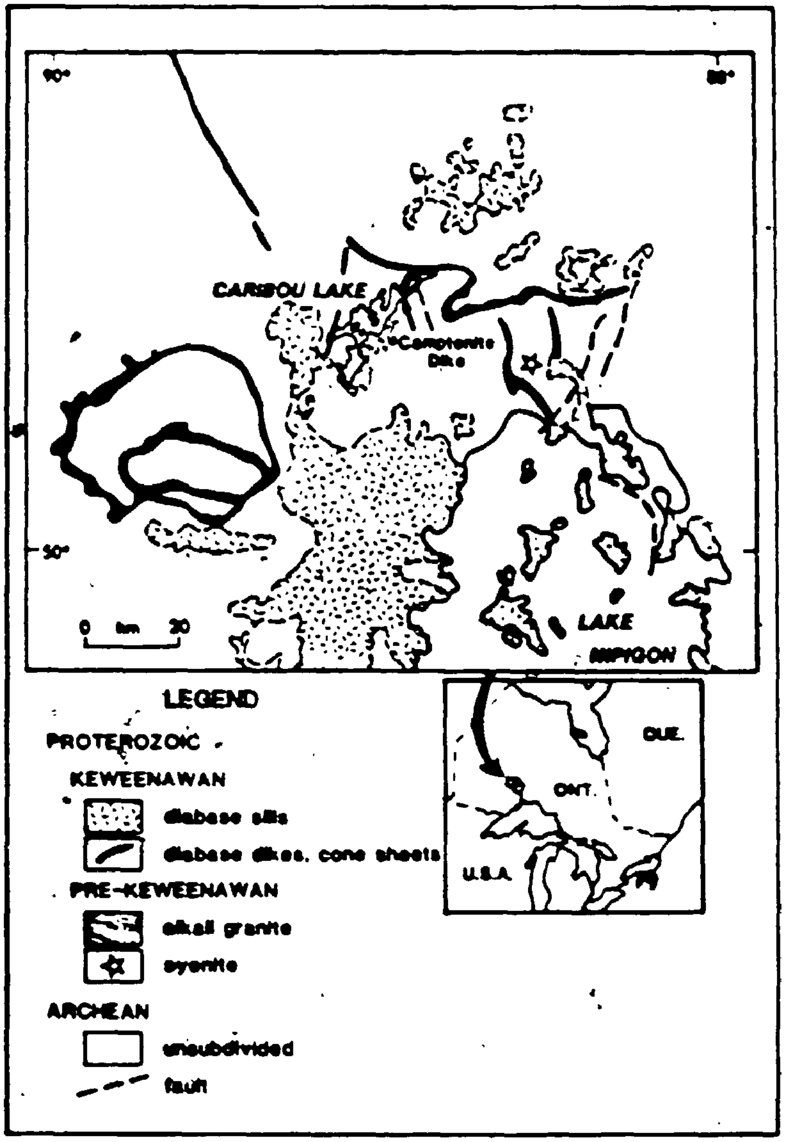
90°
88°
50°
CARIBOU LAKE
Camptonite Dike
LAKE NIPIGON
0 km 20
QUE.
ONT.
U.S.A.
LEGEND
PROTEROZOIC
KEWEENAWAN
diabase sills
diabase dikes, cone sheets
PRE-KEWEENAWAN
alkali granite
syenite
ARCHEAN
unsubdivided
fault

6.1 Generalized geological map of the northern Lake Nipigon area showing location of the sampled dike.

6.2.1 Petrography of the Xenoliths

The xenoliths examined are contained in a 1 m thick dike striking N25°E and dipping 45° east. The dike is porphyritic with an aphanitic matrix and contains 2 to 5 mm rounded miarolitic cavities filled with chlorite and carbonate. Phenocryst phases in the dike are 1 to 2 mm grains of clinopyroxene, 0.5 to 1.0 mm resorbed grains of olivine pseudomorphed by talc and carbonate, and 1 to 3 mm tabular plagioclase. Sparse megacrysts (to 1 cm) of partially resorbed clinopyroxene, ilmenite and anorthoclase are present. Some associated dikes contain kaersutite megacrysts. The matrix consists of tabular 0.1 to 0.2 mm grains of plagioclase, sparse orthoclase, 0.1 mm grains of clinopyroxene and fine 0.01 mm opaques. Carbonate and biotite, locally altered to chlorite, occur as interstitial phases in the matrix. Carbonate also occurs in fractures and as a local alteration of phenocrysts.

One specimen of a rounded green-black websterite xenolith 1.5 by 2.5 cm was examined. The xenolith has an anhedral, granular texture with an average grain size of 1.5 to 2 mm. The nodule consists of orthopyroxene (40%), clinopyroxene (35%), relict opaques largely altered to leucoxene (10%), plagioclase (5%), and talc and chlorite alteration of pyroxene (10%). Except for alteration along cracks and at grain margins, the pyroxenes are homogeneous.

Two rounded xenoliths of gabbro to 3 cm long were examined. These consist of clinopyroxene (30%) and plagioclase (70%). The gabbro xenoliths are moderately fresh, with an equigranular, polygonal, granoblastic texture and an average grain size of 1 mm. Carbonate occurs along fractures in plagioclase and clinopyroxene.

Two xenoliths of garnet granulite to 4 cm long have been partially melted and display more complex textures (Plate 8). These xenoliths consist of subequal proportions of quartz and plagioclase with an inequigranular, anhedral to interlobate, granoblastic texture. The grain size varies from 0.1 to 2 mm. Garnet (10%) occurs as equant 1 to 1.5 mm grains rimmed by 0.1 to 0.3 mm thick coronas of radially structured blue-green fibrous kelyphite. Fine grained orthopyroxene-plagioclase symplectite locally surrounds the kelyphite rims.

An interstitial, brown, partially devitrified glass phase (15%) occurs as 2 to 3 mm patches surrounding garnet and as veinlets between plagioclase and quartz. The glass contains abundant 0.1 mm skeletal to fibrous dendritic crystals of plagioclase and locally 0.1 mm dendritic crystals of an opaque phase. Rare 0.1 to 0.2 mm rounded grains of phlogopite were identified in one patch of glass. Plagioclase within 0.1 mm of the glass commonly has fine vermicular glass intergrowths which resemble graphic texture. Similar intergrowth textures are described by Jones et al. (1983) for partially melted xenoliths from Lashaine, Tanzania. The glass phase is locally devitrified to epidote and chlorite. The least altered areas of glass are almost isotropic and form 0.1

Plate 8

a) Photomicrograph of felsic garnet granulite xenolith showing fritted margins of plagioclase adjacent to melt. The melt contains skeletal plagioclase crystals. Labelled are garnet (gt), palgioclase (pl), quartz (qtz), melt phase (melt) and skeletal plagioclase (sk-p). Plane light.

b) Photomicrograph of same xenolith as a) showing distribution of melt which surrounds garnet (gt). Plane light.

Plate 8

mm domains of very weak birefringence. The analyses of glass were obtained from portions that were nearly isotropic. The glass is considered to have formed in situ by melting of the xenolith because of the textural association of glass surrounding garnet.

6.2.2 Chemistry

The host dike (Table 6.1) has many of the mineralogical and chemical characteristics typical of a camptonite (Rock, 1977). These include the volatile rich, nepheline normative basaltic composition, and distinctive mineralogy with aluminous titanium-rich augite phenocrysts and groundmass feldspars consisting predominately of labradorite with minor orthoclase.

Pyroxenes - Clinopyroxenes from the websterite and gabbro xenoliths and the cores of phenocrysts in the host dike are characterized by relatively high Na_2O (1.0-1.2%), Al_2O_3 (7.6-8.0%) and TiO_2 (0.73 to 1.7%) (Table 6.2). Sodium is apparently due to a high acmite component rather than jadeite. Despite high Al_2O_3 the pyroxenes are not fassaitic, since CaO is relatively normal (17 to 21%).. The clinopyroxenes show limited variation in CaO, MgO and FeO. The composition of the clinopyroxenes, particularly Na_2O, Al_2O_3, and TiO_2, is similar to other lower crustal xenolith suites in alkali basaltic magmas (eg. Kay and Kay, 1983). Ehrenberg and Griffin (1979) have also reported apparently low jadeite components in clinopyroxenes from deep crustal

Table 6.1 Whole Rock Compositions

	Camptonite Dike	Middle Proterozoic Granitoids	
		English Bay	Trachyte dike
	(80-396)	(avg. 2)	(80-391)
SiO_2	45.5	74.56	63.4
TiO_2	1.31	.20	.49
Al_2O_3	14.2	12.40	13.8
Fe_2O_3T	10.4	2.42	6.77
MnO	.17	.03	.07
MgO	6.74	.40	.72
CaO	10.6	.98	2.38
Na_2O	2.35	2.26	2.55
K_2O	1.74	5.80	5.49
P_2O_5	.39	.04	.06
LOI	5.6*	.9	3.3
Total	99.5	99.99	99.0

* Includes 3.46% CO_2.

3

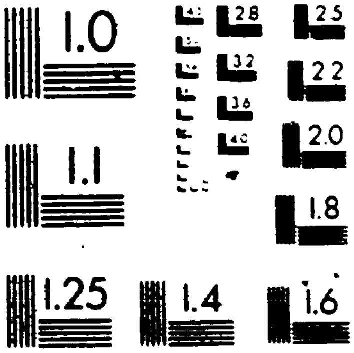
1.0
28
25
32
22
36
40
2.0
1.1
1.8
1.25
1.4
1.6

xenoliths from the Colorado Plateau. Fe/Mg partitioning between coexisting clinopyroxene and orthopyroxene in the pyroxenite xenolith indicates an equilibration temperature of 1009°C according to the geothermometer of Wells (1977) and 983°C using the geothermometer of Wood and Banno (1973).

Garnet - Garnets in garnet granulite xenoliths are homogeneous with significant pyrope component (45%) and low grossular component (4%) (Table 6.2). The garnets have comparable MgO contents to garnets from deep crustal granulite suites (eg. Queensland-Kay and Kay, 1983; Colorado-Ehrenberg and Griffin, 1979; Lashaine - Jones et al. 1983) and plot in the eclogite gneiss field of Coleman et al. (1965). Felsic garnetiferous granulites lacking additional mafic silicate phases have been reported in the charnockite series by Howie and Subramaniam (1958) although these garnets generally have lower pyrope components than observed here.

Melt Phase - Five analyses of uniform areas of dark brown glass from separate pods of melt gave variable results but consistently indicate a melt with high Al_2O_3, $Na_2O + K_2O$, and TiO_2. An average of the analyses is quartz normative, metaluminous (molecular $Al_2O_3/Na_2O + K_2O + CaO = 0.918$) with molecular $Na_2O/K_2O = 1.16$. The crystallization of quench skeletal plagioclase ($An_{41}Ab_{55}Or_4$) indicates that the original melt composition should be somewhat higher in Al, Na, and Ca and lower in Si, K, Mg, and Fe than the melt composition given in table 6.2.

Table 6.2 Representative Microprobe Analyses

	Camptonite Dike 80-396		Gabbro	Websterite		Garnet Granulite		
	Cpx (core)	Cpx (rim)	Cpx (avg. 3)	Cpx (avg. 4)	Opx (avg. 5)	Garnet (avg. 2)	Melt (avg. 5)	Range
SiO_2	48.86	51.46	48.26	47.54	50.45	39.[illegible]4	61.84	59.23-66.48
TiO_2	.87	1.03	.73	1.71	.38	.03	1.25	.90-1.67
Al_2O_3	7.62	3.08	7.61	8.00	5.89	22.64	18.11	14.50-20.19
Cr_2O_3	.16	.09	.19	0.00	0.00	0.02	-	-
FeO	12.58	9.21	10.72	10.63	19.36	24.39	2.59	1.63-4.44
MnO	.38	.27	.32	.02	.11	.35	0.05	.00-.14
MgO	11.66	13.43	12.43	12.27	22.91	12.06	1.07	.37-1.85
CaO	16.92	21.36	18.95	18.52	1.31	1.60	3.19	2.44-4.27
Na_2O	1.07	.20	.98	1.19	.14	-	4.54	3.94-5.60
K_2O	.01	.00	.01	0.00	0.00	-	5.97	4.28-7.72
Total	100.15	100.13	100.20	99.88	100.55	100.73	98.61	
Si	1.832	1.917	1.806	1.782	1.847	5.956		
Al IV	.168	.083	.194	.218	.153	.044		
Al VI	.168	.052	.142	.136	.102	3.962		
Ti	.025	.029	.021	.048	.011	.004		
Cr	.005	.003	.006	.000	.000	.002		
Fe3+	-	-	.126	.103	.109	-		
Fe2+	.394	.287	.214	.231	.484	3.064		
Mg	.651	.746	.694	.686	1.250	2.699		
Mn	.012	.009	.010	.001	.003	.044		
Ca	.679	.853	.760	.744	.051	.258		
Na	.078	.014	.071	.086	.010	-		
K	.000	.000	.000	.000	.000	-		
O	6.000	6.000	6.000	6.000	6.000	24.000		
Feldspar	$Or_4Ab_{37}An_{59}$ (avg.4) $Or_{55}Ab_{41}An_4$ (avg.2)		$Or_4Ab_{48}An_{47}$ (avg.6)	---------		$Or_8Ab_{63}An_{29}$ (avg.3)	$Or_4Ab_{55}An_{41}$ (skeletal, avg.4)	

6.3 Origin of the Xenoliths

Available data based on comparative mineral chemistry are broadly consistent with the xenoliths being derived from middle to lower crustal sources. The pyrope component of garnet is comparable to that from Lesotho mafic garnet granulites which crystallized at 5 to 10 kbar. (Griffin _et al_. 1979).

Studies of a pelitic composition with 5 wt% H_2O by Green (1976) have shown that quartz + plagioclase + garnet are residual phases in the presence of melt at 10 kbar and 980°C. At 10 kbar the melt and garnet compositions in these experiments are similar to compositions reported in Table 2. In general, garnet was found to be a residual phase coexisting with granitic liquid at pressures above 7 kbar (Green, 1976).

Ringwood (1975) has summarized studies of mineral stability fields at high pressure in intermediate to felsic compositions. These rocks display analogous behavior to basalts and pelites and with increasing pressure garnet appears at 8 kbar, 900°C in diorite and 12 kbar, 950°C in granite.

The similar composition of clinopyroxenes in gabbro and websterite xenoliths and phenocrysts in the camptonite dike suggests that they are comagmatic. Rock (1977) considers that camptonites are evolved from alkali basalt magmas, primarily through volatile enrichment. The xenoliths may have formed as cognate cumulates from an alkali basalt magma in a deep crustal magma chamber prior to a final stage of volatile rich dike emplacement.

The presence of aluminous orthopyroxene in the websterite xenolith is compatible with this model. Green and Ringwood (1967) have shown that aluminous hypersthene is a stable phase in alkali basalt magmas at pressures above 6 kbar at 1100°C.

The garnet granulite xenoliths must have been derived from a siliceous protolith such as a pelite or tonalite. A tonalite protolith is considered more likely because tonalite is a common lithology in the upper crust in the Lake Nipigon area and has been shown to be an important component of the Archean lower crust in the Superior province (Percival and Card, 1983). The garnet granulite xenoliths have a similar assemblage to felsic enderbites of the Pikwitonei subprovince (Bell, 1971) which are considered to be highly metamorphosed equivalents of typical Superior province tonalite gneiss terrains (Hubregtse, 1980).

Partial melting of the garnet granulite has produced a granitic, metaluminous, alkali rich melt. If the bulk composition of the melt was produced by closed system melting of garnet, plagioclase and quartz, the composition of the melt must lie within the compositional range of these minerals. Figure 6.2 shows that closed system melting of garnet, plagioclase and quartz reliably explains the major element composition of the glass for all elements except TiO_2 and K_2O. This suggests that phases containing K_2O and/or TiO_2 such as phlogopite, orthoclase, or rutile may have become dissolved in the melt. A similar relationship between primary

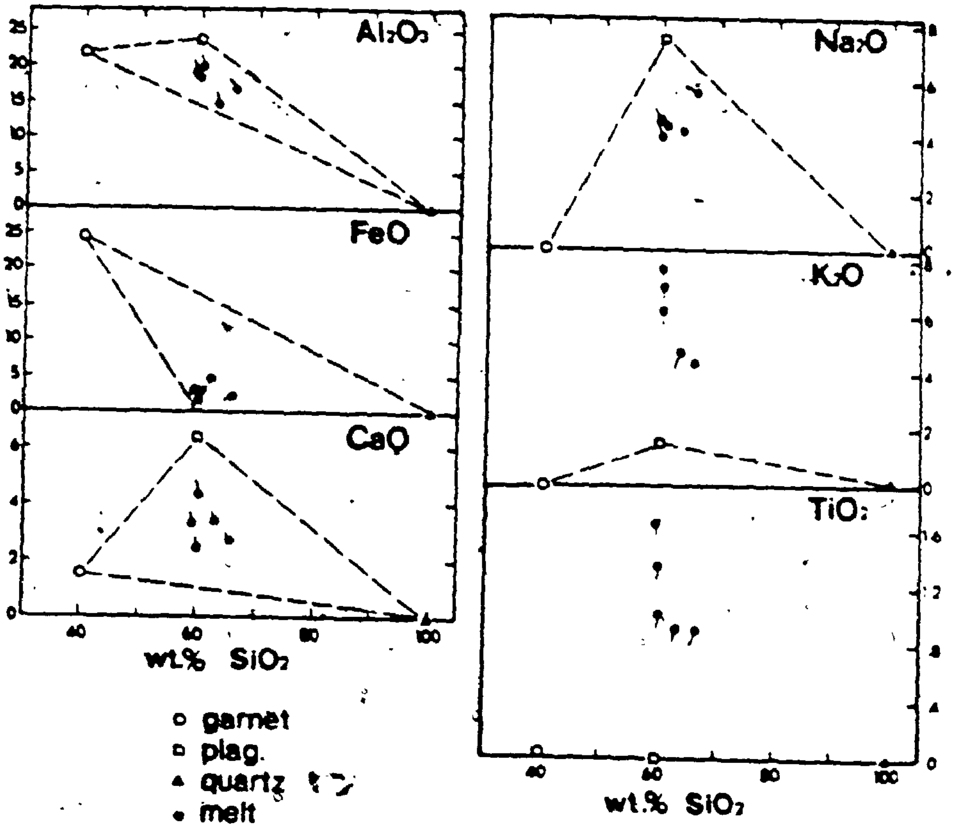

6.2 Chemical compositions of glasses and mineral phases in garnet granulite xenoliths. Ticks indicate direction in which melt should move if skeletal plagioclase crystals were re-dissolved.

glass composition and xenolith phases for TiO_2 and K_2O was observed by Jones et al. (1983), however, they explained the high K_2O as being a result of late ion-exchange of K with Na.

The quartz normative, alkali rich, and marginally metaluminas nature of the melt, suggests a similarity to middle Proterozoic anorogenic granitoids outcropping in the Lake Nipigon area (Table 6.1) and in Wisconsin area (Smith, 1983). In Wisconsin, these granitoids, which are also characterized by high abundances of incompatible elements and REE except Eu, have been modelled as being due to 10 to 20% partial melt of trondhjemite-granodiorite. This model, however, does not account for garnet as a residual phase.

Melting of the garnet granulite may have been caused by superheating by the host magma, decompression while the magma ascended, or by in situ melting of the crust. Within the limitations of the sample size, the results of this study suggest that the Proterozoic anorogenic granitoids may be produced by partial melting of lower crustal material. In situ crustal melting with the heat source associated with mafic alkaline magmatism is the process most likely to produce large amounts of granitic magma and is therefore favoured as a melt mechanism. Xenoliths of a cognate cumulate and the partially melted crust may have become entrained in the final stage of camptonite dike emplacement.

6.4 Summary

The results of this study suggest that partial melting of the lower crust may occur in regions associated with mafic alkaline magmatism. The assemblage garnet ($Py_{44}\ Alm_{51}Gr_{4}$) + plagioclase ($An_{29}Ab_{63}Or_{8}$) + quartz + melt in garnet granulite xenoliths probably formed at pressures in excess of 7 kbar from rocks of tonalitic composition. This evidence supports the results of studies on high-grade metamorphic terrains which indicate that rocks of tonalitic composition form a major component of the lower crust of the Superior province (Percival and Card, 1983; Hubregtse, 1980). The alkali rich, aluminous composition of the melt phase in the garnet granulite xenoliths is similar to the composition of Proterozoic anorogenic granitoids in the region. This indicates that these granitoids may have formed by melting of tonalitic lower crust in regions of high heat flow.

CHAPTER 7

CONCLUSIONS

The Nipigon plate hosted a failed arm during the Keweenawan rift event at 1110 Ma. During this period the Nipigon plate was the site of intrusion of picritic and diabasic magmas. The tectonic setting and lithologies within the Nipigon plate are similar to other late Proterozoic sequences which formed during a widespread global rifting event at 1000-1200 Ma. Rifting in the Nipigon area reactivated older, possibly rift related, structures which formed up to 400 Ma prior to Keweenawan rifting. The cause of Keweenawan rifting is not known, but evidence in the Nipigon area suggests an active mechanism of rifting related to mantle plumes.

Two major suites of igneous rocks were formed in the Nipigon area during the Keweenawan event. These are an early suite of picritic cumulates and a later suite of voluminous diabase with evolved compositions. The picritic suite crystallized from a magma controlled by olivine and minor clinopyroxene fractionation. The diabase crystallized from a magma controlled by cotectic crystallization of plagioclase, olivine and clinopyroxene. Differences between the suites are attributed to different parental magmas and the ability of the crust to filter the density of the magmas. Delamination of the crust mantle interface in response to an impinging mantle plume is suggested as a mechanism of establishing magma underplating and initiating the filtering process. As the igneous event progressed only fractionated low density diabase magmas were able to reach the upper crust.

A study of the emplacement and crystallization of diabase sills at Lake Nipigon indicates that sills formed from several pulses of magma which cooled as single units. Hydrostatic intrusion located the sills near the interface between Archean basement and Proterozoic sediments and also controlled the thickness of the sills. Crustal loading of the sedimentary sequence with sills probably enabled later magmas to erupt as basalts. The diabase appear to have been propogated as fingers which subsequently coalesced to form sills.

Chemical variation within the sills reflects the crystallization from multiple pulses of magma, minor crystal accumulation, and movement of volatiles to late crystallizing portions of sills. Variation in pyroxene crystallization sequences and the persistence of olivine with fractionation are a result of variation in $a(SiO_2)$ in the magma. This variation may be a sensitive indicator of the degree of contamination with siliceous crustal material.

Pre-Keweenawan, Proterozoic igneous rocks in the Nipigon area include anorogenic granitoids and lamprophyre dikes which are interpreted to be of similar age. Studies of xenoliths in a camptonite dike north of Lake Nipigon suggest that partial melting of lower crustal material during a mafic alkaline magmatic event is a possible mechanism of producing the anorogenic granites.

Proterozoic mafic rocks in the Nipigon area provide a geological record of the interaction of mantle derived magmas with the crust over a period of over 400 Ma. An investigation of the isotopic systematics of this interaction is suggested as a possible next phase of research in the Nipigon area.

APPENDIX 1

PUBLICATION

U-Pb ages from the Nipigon plate and northern Lake Superior

D. W. DAVIS Geology Department, University of Toronto, Toronto, Ontario M5S 1A1, Canada
R. H. SUTCLIFFE* Department of Geology, University of Western Ontario, London, Ontario N6A 5B7, Canada

ABSTRACT

U-Pb ages have been measured for six lithologies that are relevant to the Proterozoic igneous activity around Lake Nipigon and the northern part of Lake Superior. The data show the presence of previously unrecognized pre-Keweenawan felsic magmatic events and provide a framework for relating events in the Nipigon plate to the Keweenawan rift.

Tonalite gneiss from the Archean basement underlying the Nipigon plate has a minimum age of 2716 Ma. An anorogenic granite pluton at English Bay, Lake Nipigon, that is observed to grade into rhyolite is dated at $1536.7^{+10}_{-2.3}$ Ma. The rhyolites are intercalated with quartz arenites, and this may date the initiation of Sibley Group sedimentation. Samples (two) of the Logan diabase sills from different parts of Lake Nipigon have been dated using zircon and baddeleyite. The zircon fractions define an age of 1108.8^{+4}_{-2} Ma.

A rhyolite from the Osler volcanics at Agate Point on the north shore of Lake Superior gives an age of 1097.4 ± 3.7 Ma. This is from the magnetically reversed sequence and provides a maximum age for the magnetic reversal. The zircons show evidence of inheritance and define a mixing line with an upper intercept of 2635^{+143}_{-125} Ma. A porphyry, probably a flow, from the base of the Osler Group, dated at 1107.5^{+4}_{-2} Ma, is similar in age to the Logan sills. The presence of inherited zircons in the felsic rocks of the Osler Group indicates partial melting of Archean crust during emplacement of basaltic magma. A variety of zircon ages from a conglomerate containing felsic porphyry clasts at the base of the Osler Group suggests that pre-Keweenawan felsic magmatism took place at about 1730 Ma and 1600 Ma in the Black Bay Peninsula area.

INTRODUCTION

Evolution of the Lake Superior area culminated in the Keweenawan igneous event at about 1100 Ma, during which an arcuate rift structure was formed through Lake Superior and extending for at least 1,000 km to the southwest (King and Zietz, 1971; Chase and Gilmer, 1973). The Keweenawan rift aborted after a separation that has been estimated to be from 0 to 50 km (Klasner and others, 1982). Igneous rocks associated with the rift are primarily tholeiitic flood basalts and basic intrusions with lesser rhyolite and porphyry intrusions.

The Keweenawan rift is superimposed on a region that previously had undergone a prolonged geological history, and the shape of the rift is considered to be controlled by pre-existing structures (Klasner and others, 1982). Significant events in the evolution of the Lake Superior and mid-continent region that may have affected the style of Keweenawan activity are (1) formation of the Archean greenstone crust from 3500 to 2700 Ma, (2) Animikie Group basin sedimentation from 2100 to 1900 Ma, (3) remobilization of crust and widespread igneous activity during the Penokean orogeny at about 1850 Ma, (4) extensive epicontinental red-bed sedimentation between 1760 Ma and 1630 Ma in the mid-continent region, and (5) widespread anorogenic granitoid plutonism, largely in the period 1500 to 1400 Ma.

The results of previous geochronologic studies of Keweenawan rocks have been summarized by Van Schmus and others (1982). The most reliable estimate for the time of volcanic activity in the Keweenawan is a composite zircon age of 1,120 ± 10 m.y. (Van Schmus and others, 1982; Silver and Green, 1972) from a variety of volcanic units mainly in the upper Keweenawan sequence characterized by normal magnetic polarity.

The purpose of this paper is to present data relevant to the age evolution of rocks in the region of Lake Nipigon and the Black Bay Peninsula of Lake Superior (Fig. 1). The northern part of this area is referred to as the "Nipigon plate" (Stockwell and others, 1972), and the southern part is within the Keweenawan rift. This study provides U-Pb age data for rocks from the Nipigon plate and shows the relationship between the Nipigon plate and the Keweenawan rift. The data show a wider spectrum of pre-Keweenawan events, including several ages of felsic magmatism, than previously recognized.

GEOLOGY

The surface rocks of the Nipigon plate primarily consist of Helikian (late Proterozoic) Sibley Group sediments intruded by diabase sills known as the Logan sills. The sediments and diabase form a broad basinal structure that extends north from Lake Superior for 160 km. A stratigraphic section of the geology in the northern part of Lake Nipigon is shown in Figure 2.

Within the Nipigon plate, the Sibley Group of sediments rests unconformably on Archean basement. The Sibley Group was studied by Franklin and others (1980), who obtained a Rb-Sr age of 1,339 ± 33 m.y. for the sequence. The distribution of the Sibley Group led Franklin and others to suggest that the sediments are a red-bed sequence deposited in a down-faulted basin. The basin is postulated to have formed as a result of a failed third arm of the Keweenawan rift structure that passes north through Lake Nipigon. Green (1983), however, argued that the Sibley is older than the earliest Keweenawan rift-related igneous rocks and that therefore a "failed arm" model for Sibley sedimentation is unreasonable.

The Logan diabase sills form part of the lower Keweenawan igneous sequence and have a reversed magnetic polarity (DuBois, 1962). Previous dating attempts gave ages of 1,305 ± 65 m.y. by K-Ar (Hanson and Malhotra, 1971) and 1,170 m.y. by Ar/Ar (Hanson, 1975). The sills are weakly differentiated; however, the upper part of the sills contains highly differentiated pegmatitic patches consisting predominantly of albite + orthoclase, hedenbergite, fayalite, quartz, magnetite, and ilmenite. Felsic

---

*Present address: Ontario Geological Survey, 77 Grenville Street, Toronto, Ontario M5S 1B3.

Geological Society of America Bulletin, v. 96, p. 1572–1579, 8 figs., 2 tables, December 1985.

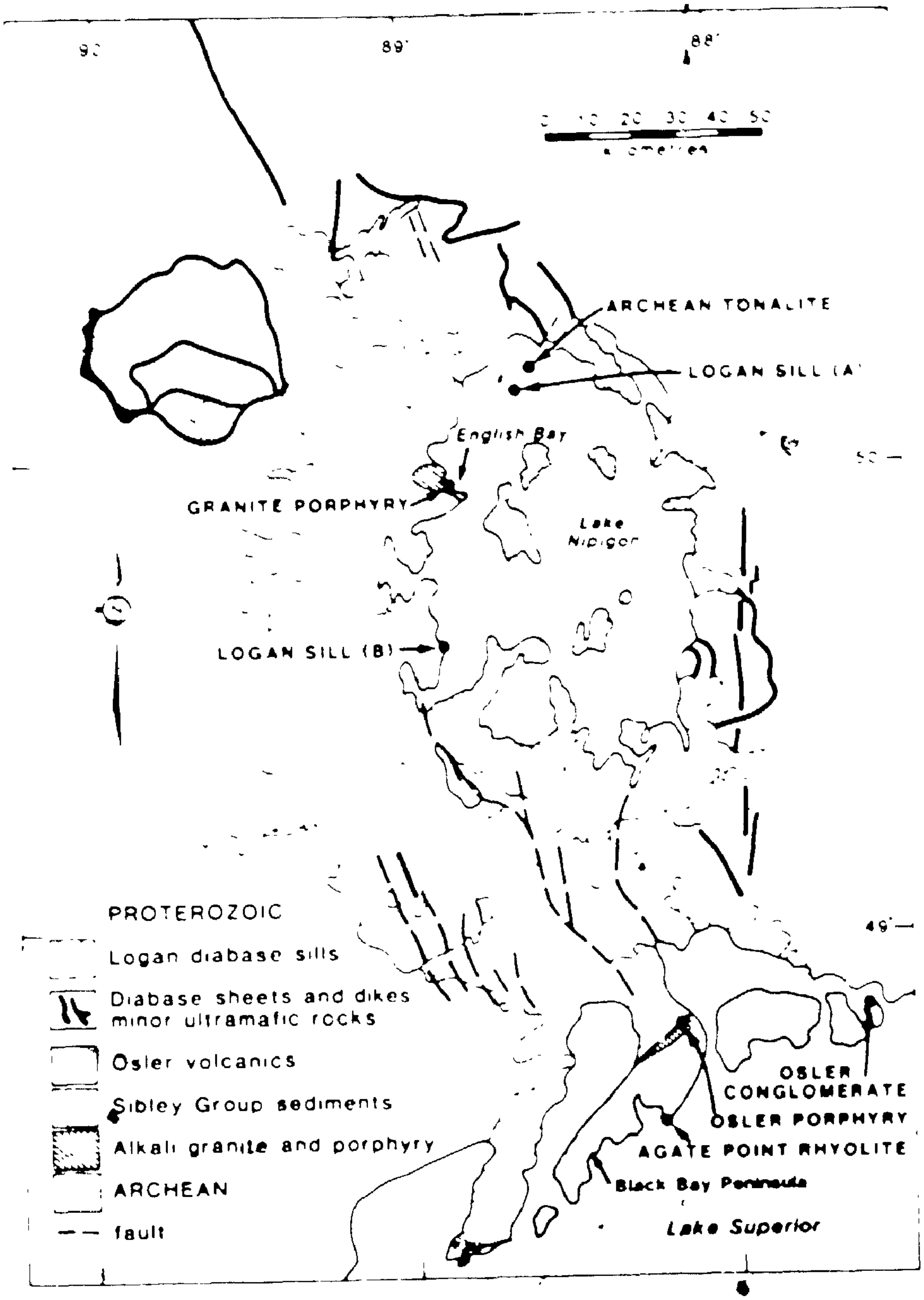
90°
89°
88°
50°
49°
0 10 20 30 40 50
kilometres
ARCHEAN TONALITE
LOGAN SILL (A)
English Bay
GRANITE PORPHYRY
Lake Nipigon
LOGAN SILL (B)
OSLER CONGLOMERATE
OSLER PORPHYRY
AGATE POINT RHYOLITE
Black Bay Peninsula
Lake Superior
PROTEROZOIC
Logan diabase sills
Diabase sheets and dikes minor ultramafic rocks
Osler volcanics
Sibley Group sediments
Alkali granite and porphyry
ARCHEAN
fault

Figure 1. Map of the Lake Nipigon and Black Bay Peninsula areas, showing sample locations.

granophyre dikes and segregations are also present at the top of the sills. Attempts by L. T. Silver and J. M. Franklin to date the sills using zircons obtained from the granophyres were frustrated due to the presence of Archean inheritance (Van Schmus and others, 1982).

Recent geological mapping (Sutcliffe and Greenwood, 1982) showed that a Proterozoic anorogenic magmatic event predates Sibley Group sedimentation in the northern part of Lake Nipigon. Rocks associated with this event that underlie the diabase sills include subvolcanic quartz-alkali feldspar porphyry, alkali granite, and fragmental dacite to rhyolite.

A stratigraphic section for the Black Bay Peninsula area is shown in

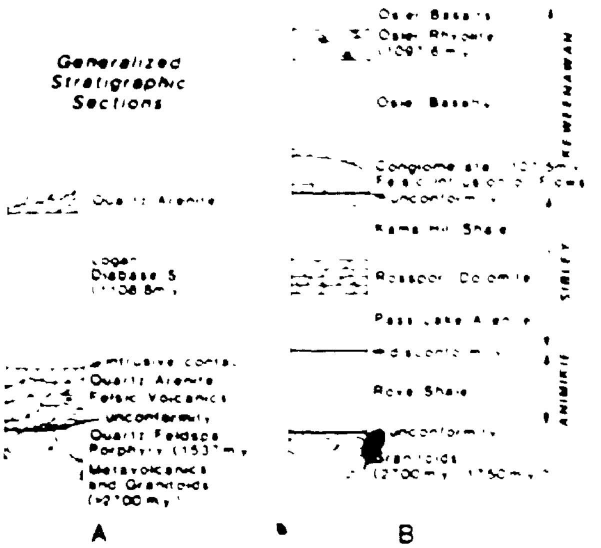
Generalized Stratigraphic Sections
Osler Basalts
Osler Rhyolite (1109.6 m.y.)
Osler Basalts
Conglomerate
Felsic intrusion or flows
unconformity
Kama Hill Shale
Rossport Dolomite
Pass Lake Arenite
disconformity
Rove Shale
unconformity
Granitoids (2700 m.y., 1750 m.y.)
KEWEENAWAN
SIBLEY
ANIMIKIE
Quartz Arenite
Logan Diabase S (1108.8 m.y.)
intrusive contact
Quartz Arenite
Felsic Volcanics
unconformity
Quartz Feldspar Porphyry (1537 m.y.)
Metavolcanics and Granitoids (>2700 m.y.)
A
B

Figure 2. Stratigraphic sections: A. Northern Lake Nipigon. B. Black Bay Peninsula. Quartz arenite in A may correlate with Pass Lake Arenite in B.

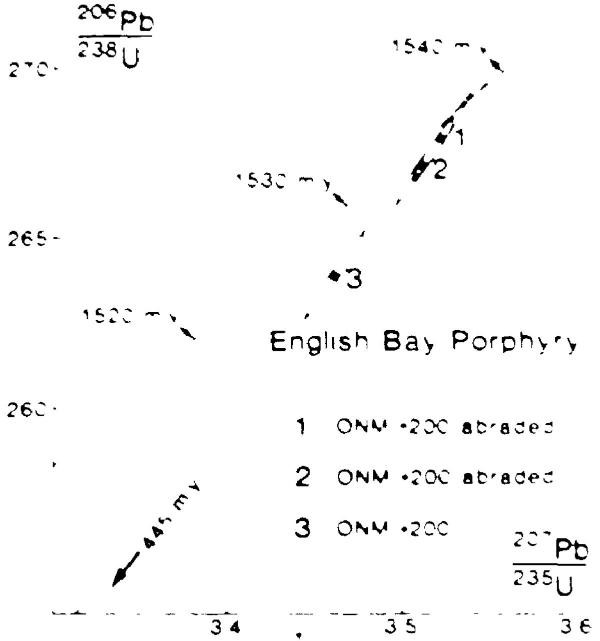

Figure 3. Concordia plot showing U-Pb analyses of zircons from the English Bay porphyry with the best-fit lead loss line.

Figure 2. The northern part of the Black Bay Peninsula and adjacent islands consist of Sibley sediments that unconformably overlie the Rove shale of the Animikie Group. To the south, the Sibley sediments are overlain by a quartz-feldspar porphyry that is probably a series of flows but may be a high-level intrusion into sediments (McIlwaine and Wallace, 1976). Conglomerate, locally containing abundant porphyry clasts, crops out sporadically along the north shore of the Black Bay Peninsula and the adjacent islands. The conglomerate, referred to here as the "Osler conglomerate," occurs above and below the quartz-feldspar porphyry and is overlain by Keweenawan basalts and interflow sediments of the Osler Group.

Most of the Black Bay Peninsula consists of Lower Keweenawan, magnetically reversed basalt flows, although a small amount of upper Keweenawan, magnetically normal flows is exposed near the top of the sequence (Halls, 1974). Quartz-feldspar-phyric rhyolite flows occur within the Osler Group near the top of the magnetically reversed sequence in the vicinity of Agate Point. The exposed thickness of the Osler Group in the Black Bay Peninsula area is 2,800 m.

The hypothesis that the Nipigon plate acted as a failed arm during the Keweenawan event (Franklin and others, 1980) has been supported by recent work on the Logan sills (Sutcliffe, 1984). Within this framework, the aim of the geochronology was to evaluate the timing of magmatism in the Nipigon plate and adjacent Osler sequence and to determine the extent of pre-Keweenawan magmatic and depositional events on which the Keweenawan rift is superimposed.

Sample locations are given in Figure 1. U-Pb ages have been determined for the following rocks: (1) a sample of the Archean gneissic basement in the northern part of Lake Nipigon, (2) an anorogenic granite porphyry that is intercalated with the base of a mudstone sequence at English Bay, Lake Nipigon, (3) two samples of Logan sills from different parts of the Lake Nipigon area, (4) a rhyolite flow from Agate Point near the top of the magnetically reversed part of the Osler volcanic group in the Black Bay Peninsula, (5) a rhyolite porphyry body, probably a flow, that underlies the Osler Group, and (6) granite porphyry clasts from the Osler conglomerate.

ANALYTICAL TECHNIQUES

U-Pb analyses of zircons were carried out using standard techniques of selection, abrasion, and dissolution (Krogh, 1973, 1982). Most samples contained abundant zircon, with the exception of the Logan sill samples that contained a small amount of zircon and a larger amount of baddeleyite (ZrO_2). Baddeleyite previously had been shown to be suitable for dating (Krogh and others, 1984). The crystals chiefly took the form of small, brown, very thin wafers. Their unequant shape made abrasion impractical. The clearest crystals obtainable were picked for each analysis.

Isotopic analyses of Pb and U were performed on both a Micromass 30 and a VG 354 mass spectrometer in single collector mode. Analytical results are given in Table 1 and shown in Figures 3-7. Error ellipses are given at the 2σ level. Analytical uncertainties in data points on a concordia diagram are usually estimated to be ±0.5% for U/Pb and ± 0.1% for $^{206}Pb/^{207}Pb$ at the 2σ level. In the case of very small samples that produced limited data, these estimates were increased. Data regression was carried out using a program described in Davis (1982). Errors for age results are quoted at the 95% confidence level.

Rare-earth analyses were performed on two of the samples by instrumental neutron activation using the SLOWPOKE reactor facility at the University of Toronto. Results are plotted in Figure 8.

RESULTS

A sample of Archean tonalite gneiss was collected from the northern part of Lake Nipigon in an area overlain by Logan sills. Analysis of a single

TABLE [illegible]. ISOTOPIC DATA FOR ROCKS FROM THE NIPIGON PLATE AND BLACK BAY PENINSULA

[illegible]

abraded zircon fraction that is almost concordant gives a $^{207}Pb/^{206}Pb$ age of 2,716 m.y.

The sample from English Bay is a red quartz-feldspar porphyry that yielded abundant zircon. The grains were mainly clear, broken fragments. The results of analyses on three fractions are given in Figure 3. They define a lead loss line within error and give an age of 1536.7 + 10/-2.3 Ma.

The two Logan sill samples were selected from large pegmatitic patches near the top of the sills. One sample, A, was analyzed using three zircon fractions and one baddeleyite fraction. The other sample, B, contained very little zircon and was analyzed using one baddeleyite and one small zircon fraction. The data are plotted in Figure 4. All of the zircon fractions define a line within error and give an age of 1108.8 +4/-2 Ma. The zircons were clear to turbid euhedral grains. The clearest possible grains were picked for abrasion. They have a remarkably high uranium content (3,000 ppm in sample A). It is therefore remarkable that the data points plot so close to concordia, because the grains are quite metamict.

The baddeleyite analyses plot somewhat to the right of the zircon fractions. They have $^{207}Pb/^{206}Pb$ ages slightly in excess of the best fi

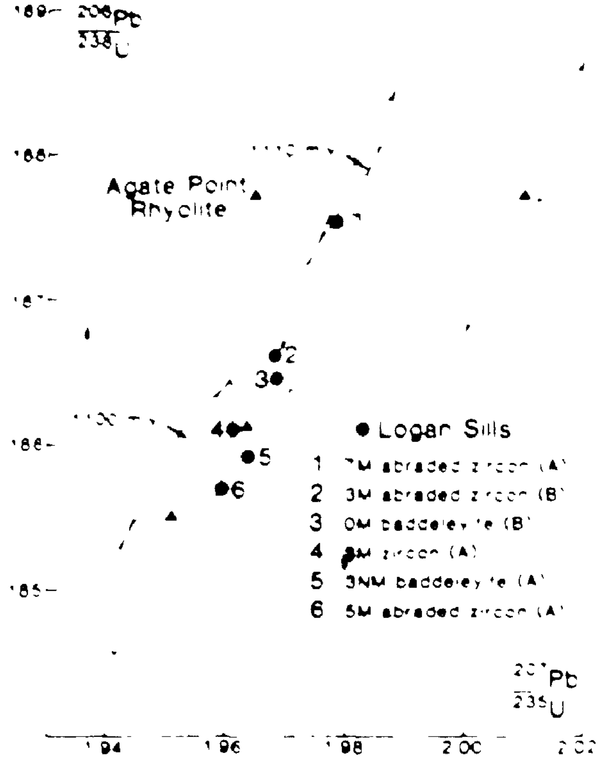

Figure 4. Concordia plot showing U-Pb analyses of zircon and baddeleyite fractions from two Logan sill samples, A and B, with the best fit lead loss line for the zircon. Also shown are three U-Pb zircon analyses from the Agate Point rhyolite, along with the best fit mixing line for this sample. Error ellipses at the 95% confidence level are drawn in for selected analyses.

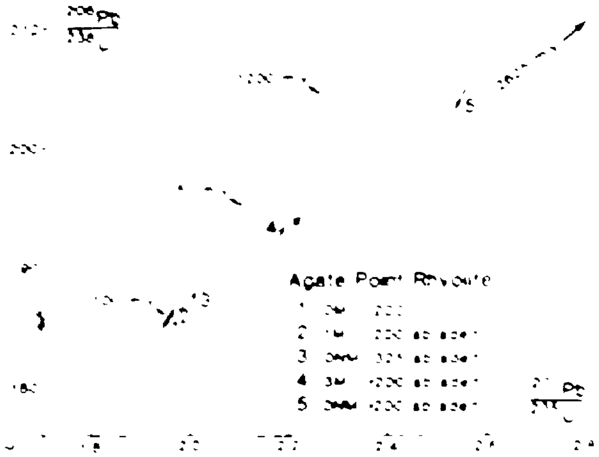

Figure 5. Concordia plot showing U-Pb analyses for all five zircon fractions from the Agate Point rhyolite sample, along with their best-fit mixing line. The filled square (■) symbol represents one analysis from a mixed zircon fraction of the Osler porphyry sample.

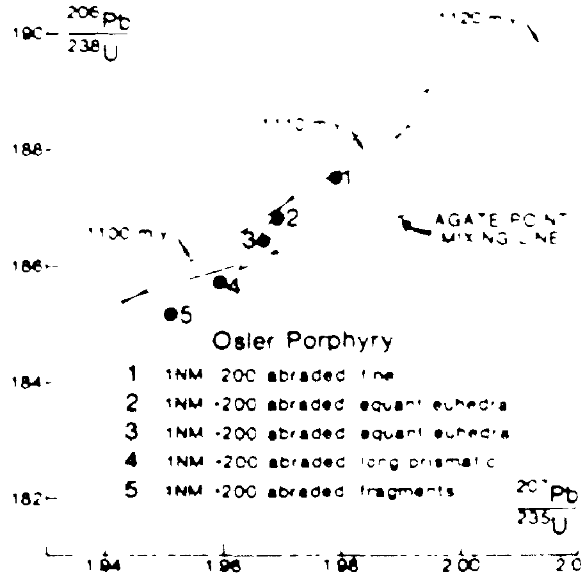

Figure 6. Concordia plot showing U-Pb analyses for five zircon fractions from the Osler porphyry sample. The 95% confidence error ellipse for fraction 1 is also shown along with the best-fit mixing line for the Agate Point rhyolite sample.

zircon age (Table 1) and may be on a line with a negative lower intercept. The baddeleyite crystals may not accumulate radiation damage like zircons and may not be subject to the same mechanisms of lead loss. The grains mainly had a high surface to volume ratio. Alpha recoil may therefore have been an important mechanism in producing the small amount of lead loss. This should produce a lead loss line with a lower intercept of zero. It is also possible that ^{222}Rn loss from the ^{238}U decay chain played some role. This would produce spuriously low ^{206}Pb/^{238}U ratios, causing the ^{207}Pb/^{206}Pb ages to be too high.

The zircons do not show inheritance relative to the baddeleyite, which must have crystallized as a result of differentiation in the sills. We therefore interpret the zircon age of 1,108.8 +4/-2 m.y. as the best estimate for the age of intrusion of the Logan sills.

The rhyolite sample from Agate Point near the top of the Osler Group is a quartz-feldspar porphyry with an aphanitic groundmass. Flow banding was evident in outcrop. The outcrop consisted of red and black colored flows with sharp boundaries and has been described by McIlwaine and Wallace (1976). The geochronology sample was taken from one of the red flows. The sample yielded abundant clear, broken grains with very low uranium contents (~30 ppm). There were no cores or zoning evident in the grains. The results of 5 analyses are plotted in Figure 5 and define a mixing line to well within error, with a lower intercept age of 1,097.6 ± 3.7 m.y. and an upper intercept age of 2,625 ± 120 m.y. The three lowest points are plotted in an expanded diagram in Figure 4. There does not appear to be any correlation between the degree of inheritance and size or magnetic properties of the grains.

We interpret the lower intercept age to be the age of volcanism.

whereas the upper age is the result of inheritance from an older crustal component. Definition of a mixing line requires the absence of all lead loss due to secondary recent processes. It is unlikely that these zircons would have undergone much secondary lead loss due to their low, uniform uranium content and consequent lack of radiation damage. Four of the fractions were also abraded, which normally removes most secondary loss. However, we can still not rule out the possibility that the lower intercept age is a few million years younger than the true age of crystallization because of slight loss of radiogenic lead over the past billion years.

The porphyry sample from the base of the Osler Group was taken from a unit described by McIlwaine and Wallace (1976). It contained quartz phenocrysts and large potassium feldspar phenocrysts as much as 1 cm. The sample also had abundant drusy gas cavities. Six fractions were picked for analysis from the various crystal types, described in Figure 6. The zircons in each fraction were selected to be clear and free of cracks. The results are plotted in Figure 6. One fraction containing fragments is plotted in Figure 5 and has inheritance, lying very close to the mixing line for the Agate Point rhyolite. The other five fractions are all close to concordia and have $^{207}\text{Pb}/^{206}\text{Pb}$ ages (1,106 to 1,109 m.y.) that are the same within experimental error. They have very low uranium content similar to that of the Agate Point zircons. In four cases, analyses had to be done on very small quantities of sample, hence the larger errors (Table 1). Assuming that any inherited component has been eliminated from the 3 youngest fractions, the age of this rock is 1,107.5 ± 4.2 m.y., determined by averaging the $^{207}\text{Pb}/^{206}\text{Pb}$ ages. The agreement among the $^{207}\text{Pb}/^{206}\text{Pb}$ ages for these fractions suggests that they have no inherited component, which may have been present entirely in some of the fragments.

The sample of conglomerate at the base of the Osler Group consisted of ~30 kg of red quartz-feldspar-phyric clasts, with an average diameter of ~10 cm. Most of the outcrop consisted of clasts of the same type, and the clasts were selected to be as similar to each other in composition as possible and therefore likely to be from the same source.

The zircons from the sample were all quite clear but showed a variety of grain morphologies from euhedral to anhedral. The population also contained a small fraction of rounded, frosted grains. Four fractions were analyzed: a euhedral, an anhedral, a rounded, and a fine (<200 mesh) fraction. The results are plotted in Figure 7 along with the results from the Keweenawan samples for comparison.

TABLE 3. CONCORDIA INTERCEPTS, ERRORS, AND FIT PROBABILITIES OF DISCORDIA LINES

Sample	Upper intercept (Ma)	Lower intercept (Ma)	Probability of fit (%)	No. of points
Tonalite gneiss	[illegible]			
English Bay Porphyry	[illegible]	[illegible]	[illegible]	
Logan sills	[illegible]	[illegible]	[illegible]	[illegible]
Agate Point Rhyolite	[illegible]	[illegible]	[illegible]	
Osler Porphyry	[illegible]	[illegible]	[illegible]	[illegible]

The analyses display a complex age pattern indicating a number of different sources for the zircons, all of which are pre-Keweenawan. The rounded zircons appear to have an Archean component, and these may be from a small amount of matrix material adhering to the clasts. Data for the anhedral and euhedral fractions plot close together, have $^{207}\text{Pb}/^{206}\text{Pb}$ ages of ~1,600 m.y., and are only several percent discordant. It is possible that the anhedral fraction may have been contaminated by a small amount of rounded zircon, as it was difficult to distinguish frosted rounded and anhedral grains. This would account for the fact that it is slightly older than the euhedral fraction, even though it is more discordant. The fine fraction is <1% discordant and has a $^{207}\text{Pb}/^{206}\text{Pb}$ age of 1,734 m.y. Frosted grains were picked out of this fraction, although no attempt was made to further discriminate between grain types. There may therefore be two sources for the clasts: one, a post-1600 Ma pluton with mostly coarse zircons and the other a pre-1734 Ma pluton with mostly fine zircons. Alternatively, the clasts may be from a pluton intruded shortly after 1600 Ma that was the result of remelting crust of pre-1,734 m.y. age. This is less likely because it is unusual for coarse grains to be more reset than fine grains.

DISCUSSION

The sample of Archean tonalite gneiss contains abundant relatively undeformed Archean mafic dikes, which suggested that it might precede the Kenoran event (Clark and others, 1981). The age of 2,716 m.y. obtained on 1 zircon fraction demonstrates, however, that intrusion of the tonalite occurred during the Kenoran period. No substantially older crust

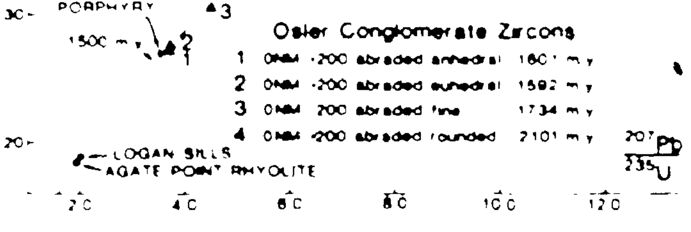

Figure 7. Concordia plot showing U-Pb analyses of four zircon fractions from the Osler conglomerate sample. The mixing line from the Agate Point rhyolite sample is shown. The line between the fine fraction (3) and the rounded fraction (4) demonstrates that the rounded fraction may contain an Archean component.

has thus far been reliably dated in the central Wabigoon subprovince, and it may be expected that most of the Archean basement underlying the Nipigon plate was formed during the Kenoran event.

The English Bay porphyry is an anorogenic granitic pluton close in age to, although slightly older than, a group of anorogenic plutons that were intruded in a wide belt from southern California to Labrador in the time interval from 1.4 to 1.5 Ga (Silver and others, 1977; Anderson, 1983). The porphyry is observed to grade into porphyritic fragmental rocks that are interbedded with quartz arenite. Outliers of quartz arenite in the area of Lake Nipigon have been interpreted as correlative with the lower formation of the Sibley Group (Franklin and others, 1980). If this is true, then the age of the English Bay porphyry gives the age of deposition of the base of the Sibley Group in the Lake Nipigon area. This age of 1,536.7 +10 -2.3 m.y. is considerably older than the age obtained by Franklin and others (1980) for the Sibley Group.

Extensive mid-Proterozoic red-bed sequences such as the Baraboo, Barron, and Sioux quartzites are common in the mid-continent region from Wisconsin to South Dakota. They are considered to be part of a period of epicontinental deposition known as the Baraboo interval, which probably occurred in the time between 1,760 Ma and 1,630 Ma (Greenberg and Brown, 1984; Van Schmus, 1978). There has been speculation as to whether the Sibley Group may be correlative with these sedimentary sequences. The present data for the base of the Sibley Group suggest that it is part of a younger sedimentary sequence not related to Baraboo sedimentation. The younger age limit for Baraboo sedimentation is circumstantial, however (Van Schmus, 1978), and therefore correlation of the Sibley and Baraboo sediments cannot be completely ruled out.

Rare-earth–element analyses performed on a whole-rock sample of the porphyry are shown in Figure 8. The REE pattern is similar in fractionation, although more enriched than those obtained for the more differentiated phases of the Wolf River Batholith, a slightly younger anorogenic granite in Wisconsin (Anderson and Cullers, 1978) and similar to a series of metaluminous rhyolites and granites ~1,760 m.y. old from Wisconsin (Smith, 1983). These rocks also show pronounced Eu anomalies and were modeled by Smith as being due to a 16% partial melt of a granitic source.

These anorogenic granites are similar to rocks found in modern extensional settings, as noted by Anderson and Cullers (1978). This would lend support to the failed-arm hypothesis of Franklin and others (1980) and would suggest that the Nipigon region acted periodically as an extensional regime for at least several hundred million years before the Keweenawan event.

The agreement of analyses from both Logan sill samples indicates that the sills were intruded very rapidly at 1108.8 +4/-2 Ma. Agreement between zircon and baddeleyite analyses demonstrates the usefulness of baddeleyite as a geochronometer, although more study is required of its lead loss characteristics. This mineral may occur in differentiated mafic rocks that have very little zircon. Baddeleyite previously has been shown not to be as susceptible to recent lead loss as zircon (Krogh and others, 1984). The small amount of lead loss that it does exhibit appears to be on a line with a lower intercept equal to or less than zero and may be due to surface-related mechanisms of lead loss.

Eruption of continental flood basalts should be aided by crustal loading due to intrusion of the diabase sills. The increase in crustal density makes it possible for basaltic magmas to reach the surface, and it can therefore be expected that flood basalt magmatism, such as that which makes up the bulk of the Osler Group, followed shortly upon intrusion of the sills. The Agate Point rhyolite sample, near the top of the Osler Group, would therefore be expected to be younger than the sills. This is confirmed by the age of 1,097.6 ± 3.7 m.y. for eruption of the rhyolite. This age should be very close to the upper magnetic reversal (Halls, 1974) and indicates a time gap of ~11.2 ± 4.2 m.y. between intrusion of the Logan sills and felsic volcanism at Agate Point.

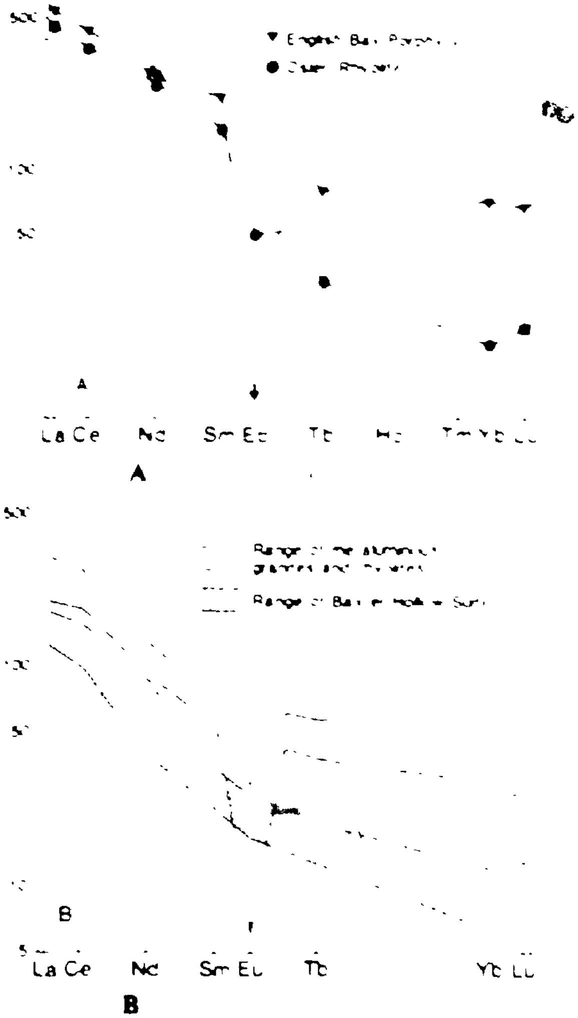

Figure 8. A. Chondrite normalized rare-earth element patterns for the English Bay porphyry sample and the Agate Point rhyolite sample. B. Range of chondrite normalized rare-earth element patterns for metaluminous granites and rhyolites from Wisconsin and for the Baxter Hollow granite in Wisconsin. Data from Smith (1983).

Assuming that the rhyolite is close in age to the top of the reversely magnetized Osler flows, a drift rate for the North American continent during the Keweenawan event can be calculated using these ages and the paleomagnetic pole positions of the Logan sills and the top of the normally magnetized Osler Group basalts (Halls and Pesonen, 1982). This gives a speed of ~19 cm/yr. Due to the closeness in age of these two units and uncertainties in paleomagnetic pole positions, this number is subject to large error, but the fact that this drift rate is comparable to Phanerozoic drift rates during times of active spreading (Patriat and Achache, 1984) suggests that high-precision dating of paleomagnetic pole positions in the Precambrian may potentially be useful for the study of tectonic processes.

The age of 1,107.5 +4/-2 m.y. for the porphyry at the base of the Osler Group shows that it is Keweenawan and therefore part of the Osler Group. The similarity between it and the Agate Point rhyolite in whole-rock mineralogy, the zircon uranium content, and the presence of inhertance suggests that they were generated by the same mechanism. This involved partial melting of an underlying Archean crust. The age of the basal porphyry agrees with the age of the Logan sills, indicating that basaltic magmatism, represented by the Logan sills and Osler flood basalts, probably provided the heat source to melt the crust. McIlwaine and Wallace (1976) were uncertain as to whether the basal porphyry was a high-level intrusion or a flow, but the evidence suggested it was a series of flows due to the presence of layers of sediment within the unit. In this case, eruption of rhyolite would have been the first igneous event in the development of the Osler Group. This was contemporaneous with intrusion of the Logan sills and was followed by eruption of the bulk of the Osler flood basalts, eruption of the Agate Point rhyolite, and continued eruption of basalts after the magnetic reversal. This sequence of events is well exhibited in the relative paleomagnetic pole positions of the Logan sills and samples throughout the Osler Group (Halls and Pesonen, 1982). Relating the above lithospheric drift rate to the paleomagnetic pole positions for the Osler Group rocks, we can calculate a time span for eruption of the Osler Group on the order of 20 Ma.

The rare-earth-element pattern for a whole-rock sample of the Agate Point rhyolite is shown in Figure 8. This pattern is similar in fractionation to that obtained from the 1,760-m.y.-old Baxter Hollow granite in Wisconsin, which was modeled as a 60% partial melt of quartz diorite (Smith, 1983). It is not surprising that such a large degree of partial melting of a rock that often contains abundant zircon would result in some inherited zircon component from the source. In contrast, the English Bay porphyry apparently resulted from a much smaller degree of melting of granite source rocks, which, in the present writers' experience with Archean rocks, typically contain less zircon. This may be the reason why the English Bay porphyry shows no evidence of inheritance.

The results of analyses of zircons from the Osler conglomerate indicates involvement of at least 3 age components: Archean, >1,730 m.y., and <1,600 m.y. There appears to be no involvement of a source of Keweenawan age. Deposition of the conglomerate apparently occurred during the Keweenawan event. This is suggested by soft-sediment deformation features in Osler sediments immediately underlying Keweenawan flows (Tanton, 1931). As previously mentioned, both 1760 Ma and ca. 1500 Ma magmatic events are well represented in the mid-continent region and must have been present at the surface near the north shore of Lake Superior at the time when Keweenawan magmatism occurred.

CONCLUSIONS

The basement to the Nipigon plate and Black Bay Peninsula area is late Archean crust.

The age of an anorogenic granite pluton in the northwest part of Lake Nipigon is 1,536.7 +10/−2.3 m.y. Rhyolites associated with this pluton are intercalated with the base of a sandstone sequence. Assuming this sequence to be correlative with the Sibley Group, this may date the initiation of Sibley sedimentation in the Lake Nipigon area.

The Logan sills were rapidly intruded at 1108.8 +4/−2 Ma. Rhyolitic magmatism occurred almost simultaneously, forming a porphyry body at the base of the Osler Group at 1107.5 +4/−2 Ma. Baddeleyite can be used to date mafic intrusions, but it probably has a lead-loss mechanism different from that of zircon.

Eruption of a rhyolite flow at Agate Point, near the top of the magnetically reversed part of the Osler Group, occurred at 1097.6 ±3.7 Ma, ~11 m.y. after intrusion of the Logan sills. Felsic magmas associated with bimodal volcanism during the Keweenawan event were formed at least to some degree by partial melting of Archean crust, the heat being supplied by basaltic magmatism.

A variety of zircon ages from a conglomerate containing granite porphyry clasts near the base of the Osler Group indicates that pre-Keweenawan intrusions of about 1730 Ma and 1600 Ma were present in the provenance of the Black Bay Peninsula area.

ACKNOWLEDGMENTS

Field assistance from W. McIlwaine and J. Scott is gratefully acknowledged. Laboratory assistance was ably rendered by R. Hollwell, B. Podraswsky, and J. Shaver. Discussions with T. Krogh were greatly appreciated.

The work was partly funded by a University Research Fellowship from the Natural Sciences and Engineering Research Council. Field support was given by the Ontario Geological Survey.

This paper is published with the permission of the Director of the Ontario Geological Survey.

REFERENCES CITED

[illegible]
[illegible]
[illegible]
[illegible]
[illegible]
[illegible]
[illegible]
[illegible]
[illegible]
[illegible]
[illegible]
[illegible]
[illegible]
[illegible]
[illegible]
[illegible]
[illegible]
[illegible]
[illegible]
[illegible]
[illegible]
[illegible]
[illegible]
[illegible]
[illegible]
[illegible]
[illegible]
[illegible]
[illegible]

[illegible]
[illegible]
[illegible]

Printed in U.S.A.

APPENDIX II

ANALYTICAL METHODS

II.1 Whole rock analysis

Samples weighing approximately 0.5 to 1 kg were stripped of weathered surfaces and split into small pieces in the field. Major elements including Na_2O were determined by XRF at the Geoscience Laboratories, Ontario Geological Survey, Toronto. The method uses disks produced by fusion with Li tetraborate and La oxide after Norrish and Hutton (1967). The precision of the method for major elements is given in table A1.

Loss on ignition (LOI) was done by gravimetric methods at the Ontario Geological Survey. Detection limits and precision at the 95% confidence limit are 0.4% and 0.4 respectively.

The trace elements Ba, Co, Cr, Cu, Ni, Pb, Zn were determined at the Ontario Geological Survey by atomic absorption. Detection limits, optimum ranges and precision are given in table A2.

The trace elements Ga, Nb, Rb, Sr, V, Y, Zr were determined at the University of Western Ontario by the author. Three grams of rock powder and 0.3 grams of Somar binding agent were mixed and compressed into a flat pellet with a boric acid base. The elements were determined on a Phillips P1450 XRF spectrometer. Detection limits and precision for these trace elements are given in table A3.

The rare earth elements were analyzed at the Ontario Geological Survey using ICP spectrometry. The rare earths La, Ce, Nd, Sm, Eu, Gd, Dy, Yb are pre-separated and pre-concentrated using ion-exchange chromatography. Detection limits and precision for the rare earths are given in table A4.

Chondrite values used for normalizing the data are those of the Leedly chondrite divided by 1.20 (cf. Taylor and Gorton, 1978) and are: La-0.315; Ce-0.813; Nd-0.597; Sm-0.192; Eu-0.722; Gd-0.259; Dy-0.325; Yb-0.208.

Table A1: Precision of major element analyses performed at the Geoscience Laboratories, Ontario Geological Survey

2

	Range	2σ precison at MRV
SiO_2	30-80	± 2.0
TiO_2	0-3	.16
Al_2O_3	0-20	.04
Fe_2O_3	0-15	.6
MnO	0-1	.015
MgO	0-20	.3
CaO	0-15	.15
Na_2O_3	0-10	.5
K_2O	0-10	.1
P_2O_5	0-1	.15

MRV - mid range value

Table A2: Detection limits, optimum ranges and precision of Ba, Co, Cr, Cu, Ni, Pb and Zn analyses using atomic absorption at the Ontario Geological Survey

Element	Detection Limit ppm	Optimum Range ppm	2σ Precision at 10Xdetection limit
Ba	10	10-1000	±16
Co	5	5- 200	5
Cr	10	10- 500	20
Cu	5	5- 200	4
Ni	5	5- 200	6
Pb	10	10- 200	8
Zn	10	10- 200	10

Table A3: Detection limits and precision of trace element analyses performed at the University of Western Ontario; from (Wu 1983).

Element	Detection Limit	Mean n=10	S.D.	Mean n=5	R.V.	S.D.
Nb	2.0	22.8	1.78	12.9	13	1.17
Zr	2.0	240.7	1.27	299.1	300	1.75
Y	1.5	27.1	.70	11.1	11	.21
Sr	3.0	210.7	3.00	478.7	480	1.33
Rb	3.0	198.0	1.50	170.7	170	2.42
Y	4.5	42.1	3.61	38.7	36	4.82
Ga	4.5	21.4	2.36	22.9	23	1.63

S.D. Standard Deviation
R.V. Recommended value from Abbey (1980).

Table A4: Detection limits, optimum ranges and precision of Rare Earth Element analyses at the Ontario Geological Survey

Element	Detection Limit ppm	Optimum Range ppm	2σ Precision at 10Xdetection limit
La	0.5	.5- 250	+ 1
Ce	5	5 - 400	10
Nd	3.5	3.5- 400	7
Sm	1.5	1.5- 100	3
Eu	0.1,	0.1- 10	0.2
Gd	1	1 - 150	2
Dy	0.5	0.5- 50	1
Yb	0.1	0.1- 15	0.2

II.2 Electron Microprobe Analyses of Minerals

The major element composition of silicate and oxide minerals was determined with a Materials Analysis Company (MAC) 400 Electron Microprobe fitted with three automated spectrometers using a Krisel Control Automation System. Analyses were performed by wave length dispersive analysis with operating conditions of 15 KV accelerating potential and a 250 or 500 micro-amp probe current. MAGIC correction procedures were used.

Minerals of known composition were periodically probed during the analytical session to ensure standardization. Tables A5 to A7 are compilations of analyses made on laboratory standards during routine operation of the instrument by the author. The detection limit is approximately 0.05 weight percent oxide.

Table A5: Major element analyses of olivine YS15 with a MAC 400 electron microprobe, University of Western Ontario

	1	2	3	4	5	6	X	S	P
SiO_2	35.23	35.62	36.52	36.68	35.61	35.08	35.79	±.66	35.40
TiO_2	.08	.07	.01	.00	.12	.05	.06	.04	-
Al_2O_3	.00	.00	.00	.00	.01	.04	.01	.02	-
Cr_2O_3	.01	.00	.00	.03	.28	.11	.07	.11	-
FeO	37.80	37.16	38.22	38.71	38.21	38.97	38.18	.65	38.30
NiO	.31	.08	.14	.10	.13	.11	.14	.08	.03
MnO	.48	.61	.48	.54	.64	.62	.56	.07	.50
MgO	24.84	25.61	25.66	24.53	25.57	25.27	25.08	.47	25.20
CaO	.15	.16	.10	.09	.06	.06	.10	.05	.10
Total	98.90	99.29	100.14	100.68	100.65	100.65	99.99	±.73	99.53

1-6 Analyses of YS15 standard
X Mean of analyses
S Standard deviation of analyses
P Preferred value

Total iron as FeO

Table A6: Major element analyses of Kaersutite standard with a MAC 400 electron microprobe, University of Western Ontario

	1	2	3	4	5	6	7	8	9	X	S	P
SiO_2	39.75	38.39	39.73	41.06	41.19	40.07	40.29	40.05	39.49	40.00	±.84	39.49
TiO_2	5.66	5.54	5.53	5.61	5.56	5.60	5.75	5.86	5.54	5.63	.11	5.66
Al_2O_3	14.05	13.84	13.99	14.60	14.19	13.97	13.93	14.08	14.19	14.09	.22	14.09
Cr_2O_3	.00	.00	.00	.03	.03	.04	.00	.03	.00	.01	.02	-
FeO	12.75	12.52	12.40	11.91	12.50	11.95	12.30	12.34	12.31	12.33	.27	12.01
MnO	.10	.01	.02	.03	.03	.02	.00	.07	.00	.03	.03	.12
MgO	11.51	11.57	11.61	11.12	11.26	10.87	11.40	10.96	11.26	11.28	.26	11.24
CaO	9.93	9.52	9.61	9.61	10.07	9.91	9.85	9.85	10.19	9.84	.22	9.88
Na_2O	3.15	3.04	3.15	2.89	3.13	3.22	3.25	2.98	3.05	3.10	.12	2.84
K_2O	1.67	1.60	1.54	1.63	1.61	1.62	1.70	1.60	1.54	1.61	.05	1.94
Total	98.57	96.02	97.58	98.87	99.54	97.27	98.48	97.82	97.57	97.97	1.03	97.27

1-9 Routine analyses of kaersutite standard
X Mean of analyses
S Standard deviation of analyses
P Preferred value

Total iron as FeO

36,

Table A7: Major element analyses of clinopyroxene BPX with MAC 400 electron microprobe, University of Western Ontario

	1	2	3	4	5	6	7	8	9	X	S	P
SiO_2	54.55	53.99	53.34	53.77	53.84	53.66	54.57	54.66	53.61	54.00	± .48	53.94
TiO_2	.14	.22	.20	.18	.20	.25	.17	.17	.21	.19	.03	.26
Al_2O_3	.34	.48	.48	.47	.50	.57	.57	.51	.52	.49	.07	.66
Cr_2O_3	.39	.31	.30	.36	.38	.37	.05	.32	.32	.31	.10	-
FeO	2.94	3.01	3.03	3.01	2.86	3.02	2.83	2.91	2.80	2.93	.09	2.92
MnO	.09	.10	.06	.09	.11	.05	.00	.00	.17	.07	.05	.06
MgO	17.09	17.18	16.90	17.20	16.93	17.00	16.68	15.59	16.78	16.82	.49	16.93
CaO	24.46	25.09	24.94	24.63	24.62	25.52	24.81	24.03	24.70	24.76	.42	24.54
Na_2O	.00	.07	.06	.13	.11	.04	.00	.16	.00	.06	.06	.24
Total	100.00	100.46	99.30	100.54	99.54	100.59	99.69	98.34	99.11	99.73	.75	99.55

1-9	Analyses of BPX standard
X	Mean of analyses
S	Standard deviation of analyses
P	Preferred value

Total iron as FeO

Table A8: Major element analyses of plagioclase standard An_{90} with a MAC 400 electron microprobe, University of Western Ontario

	1	2	3	4	5	6	7	8	9	X	S	P
SiO_2	45.23	44.88	44.74	45.26	45.49	46.71	45.53	46.88	45.33	45.56	±.75	48.35
Al_2O_3	33.80	35.16	35.53	34.76	35.48	34.25	34.88	33.79	33.91	34.62	.70	35.01
FeO	.12	.14	.13	.31	.30	.17	.18	.00	.19	.17	.09	.04
CaO	17.98	18.52	18.49	18.49	18.43	18.29	18.46	18.16	18.38	18.36	.18	18.19
Na_2O	1.19	1.08	1.02	.80	1.08	1.31	1.11	1.10	1.18	1.10	.14	1.05
K_2O	.02	.00	.00	.00	.03	.00	.00	.00	.01	.01	.01	-
Total	98.34	99.79	99.90	99.62	100.81	100.72	100.55	99.93	98.99	99.85	.81	99.64

1-9 Routine analyses of An90 standard
X Mean of analyses
S Standard deviation of analyses
P Preferred value

APPENDIX 3

SAMPLE LOCATIONS, DESCRIPTIONS, AND
SUMMARY OF ANALYTICAL WORK

SAMPLE NUMBER	LATITUDE	LONGITUDE	FIELD NAME AND COMMENTS	Majors	Traces	REE	Probe	Mode
79RHS-0018	50.54056	89.19889	Diabase, medium grained, Caribou Lake area	•	•			
79RHS-0044	50.60444	88.95278	Andesitic dike, porphyritic, Caribou Lake area	•	•		•	
80RHS-0322	50.54083	88.96722	Lamprophyre, phlogopite - olivine, Caribou Lake area	•	•		•	
80RHS-0337	50.52028	88.99889	Camptonite, dike, Caribou Lake area	•	•		•	
80RHS-0342	50.46333	88.93889	Trachyte dike, Caribou Lake area	•				
80RHS-0371	50.52778	88.92556	Camptonite, dike, Caribou Lake area	•			•	
80RHS-0391	50.52194	88.91667	Trachyte dike, Caribou Lake area	•	•			
80RHS-0396	50.52028	88.99889	Camptonite, dike, Caribou Lake area	•	•	•	•	
80RHS-0476	50.46694	88.90861	Trachyte dike, Caribou Lake area	•	•			
80RHS-1299	50.51528	88.98583	Lamprophyre, phlogopite - olivine, Caribou Lake area	•	•	•	•	
80RHS-1116	50.46056	88.90583	Diabase chill, lower contact, D'Alton Lake 0m	•				
80RHS-1117	50.46000	88.90583	Diabase, medium grained, D'Alton Lake, 4m	•				•
80RHS-1118	50.45917	88.90583	Diabase, medium grained, D'Alton Lake, 60m	•				•
80RHS-1119	50.45806	88.90583	Diabase, medium grained, pegmatitic patches, D'Alton Lake, 140m	•			•	•
80RHS-1120	50.46000	88.90600	Diabase, fine grained, D'Alton Lk, 0.5m	•	•		•	
80RHS-1121	50.46000	88.90600	Diabase, fine grained, internal contact, D'Alton Lk, 15m	•	•		•	•
80RHS-1122	50.46000	88.90600	Diabase, medium grained, D'Alton Lk, 62m	•	•		•	•
80RHS-1123	50.46000	88.90600	Diabase, medium grained, D'Alton Lk, 85m	•	•			
81RHS-0021	49.03056	88.95333	Anorthosite dike, medium grained, Leckie Lake area	•	•		•	
81RHS-0022	49.02833	88.96639	Peridotite, medium grained, Leckie Lake area	•	•		•	
81RHS-0051	49.11111	88.94389	Olivine gabbro, medium grained, Fox Mtn. area	•	•			
81RHS-0053	49.11889	88.98222	Peridotite, medium grained, Disraeli Lake area	•	•			
81RHS-0057	49.15444	88.96111	Diabase medium grained, Fox Mtn. dike	•	•			
81RHS-0058	49.14500	88.97028	Peridotite, medium grained Disraeli Lake area	•	•			
81RHS-0086	49.54083	88.96889	Diabase chill, Chief Bay area, sill	•	•			
81RHS-0104	49.57861	88.75000	Granophyre, Grand Bay area, dike in sill	•	•	•		
81RHS-0176	49.38111	88.32806	Diabase chill	•	•			
81RHS-0185	49.43500	88.45306	Diabase chill, South Bay, upper contact of lower s	•	•			
81RHS-0186	49.43500	88.45306	Diabase chill, South Bay, lower contact of upper s	•	•			
81RHS-0187	49.45194	88.44972	Diabase, medium grained, Otter Head, top of section	•	•			
81RHS-0188	49.45222	88.44778	Diabase, medium grained, Otter Head	•	•			
81RHS-0189	49.45278	88.44667	Diabase, medium grained, Otter Head	•	•			
81RHS-0190	49.45361	88.44500	Diabase, medium grained, Otter Head, base of section	•	•			
81RHS-0208	49.46778	88.26444	Diabase chill, Cooke Point, lower contact of upper s	•	•			
81RHS-0209	49.46778	88.26444	Diabase, fine grained, Cooke Point 60cm above 208	•	•			
81RHS-0210	49.46778	88.26444	Diabase, fine grained, Cooke Point, 2m above 208	•	•			
81RHS-0211	49.46778	88.26444	Diabase, medium grained, Cooke Point, 6m above 208	•	•			
81RHS-0216	49.30889	88.28833	Diabase, fine grained, South Bay, near upper contact	•	•			
81RHS-0234	49.39194	88.13028	Diabase, medium grained, ophitic, Pijitawabik Bay	•	•		•	•
81RHS-0267	49.33667	88.12639	Diabase, medium grained, Reflection Mtn.	•	•		•	•
81RHS-0273	49.59528	88.14611	Peridotite, medium grained, Intrusion in Eva-Kitto Twps.	•	•	•	•	•
81RHS-0275	49.58389	88.16083	Peridotite, medium grained, Intrusion in Eva-Kitto Twps	•	•			
81RHS-0276	49.57833	88.16639	Peridotite, medium grained, Intrusion in Eva-Kitto Twps	•	•	•	•	•
81RHS-0285	49.65722	88.90833	Diabase, Quartz - hornblende, coarse grained, Spruce Pt.	•	•	•	•	
81RHS-0286	49.31000	88.08333	Diabase, medium grained, Orient Bay Section, 125m	•	•	•	•	•
81RHS-0287	49.30944	88.08417	Diabase, medium grained, Orient Bay Section, 112m	•	•			
81RHS-0288	49.30889	88.08500	Diabase, medium grained, Orient Bay Section, 109m	•	•	•	•	•
81RHS-0289	49.30833	88.08583	Diabase, medium grained, Orient Bay Section, 93m	•	•			
81RHS-0290	49.30778	88.08722	Diabase, medium grained, Orient Bay Section, 77m	•	•	•	•	•
81RHS-0291	49.30722	88.08806	Diabase, medium grained, ophitic Orient Bay Section, 46m	•	•			
81RHS-0292	49.30667	88.08889	Diabase, medium grained, ophitic, Orient Bay Section, 14m	•	•	•	•	•
81RHS-0293	49.33583	88.09694	Diabase, pegmatitic patches, Orient Bay Section 140m	•	•	•	•	
82RHS-0001	49.53400	88.12900	Altered peridotite, Intrusion in Eva-Kitto Twps.	•	•			
82RHS-0004	49.57400	88.12200	Olivine leuco-gabbro, Intrusion in Eva-Kitto Twps.	•	•	•	•	•
82RHS-0016	49.12300	88.93800	Diabase, medium grained, Fox Mtn. dike	•	•			
82RHS-0034	49.93400	88.79700	Olivine gabbro, medium grained, Jackfish Island	•	•		•	
82RHS-0045	49.84500	88.71400	Diabase, medium grained, layered, Kelvin Island	•	•			

SAMPLE NUMBER	LATITUDE	LONGITUDE	FIELD NAME AND COMMENTS	Major	Traces	REE	Probe	Mode
82RHS-0043	49.8[illegible]00	88.6[illegible]00	Diabase chill, [illegible] Island	•	•			
82RHS-004[illegible]	49.85500	88.[illegible]400	Diabase chill, Dawson Island	•	•			
82RHS-0054	50.20500	88.56500	Biotite tonalite, Archean basement, Brittania Islands	•	•			
82RHS-0056	50.11500	88.44200	Anorthositic diabase, medium grained, Logan Island	•	•	•		•
82RHS-0061	50.08000	88.45500	Diabase, medium grained, Logan Island	•	•			
82RHS-0065	49.92700	88.[illegible]500	Carbonate breccia, Rabbit Islands	•	•			
82RHS-0069	50.29400	88.83500	Basaltic clast in debris flow, Castle Bay area	•	•	•		
82RHS-0071	50.12600	89.44500	Diabase chill, Kopka cone sheet, Kenakskaniss Lake	•	•	•		•
82RHS-0074	50.12600	89.44500	Diabase, medium grained, Kopka cone sheet, Kenakskaniss Lake	•	•	•	•	•
82RHS-0075	50.12600	89.44500	Diabase, medium grained, Kopka cone sheet, Kenakskaniss Lake	•	•	•	•	•
82RHS-0076	50.4[illegible]200	88.60000	Andesite dike, plagioclase phyric, Pikitigushi Road	•	•			
82RHS-0077	50.12400	89.70000	Diabase chill, lower contact of sill, Sandison Lake	•	•			
82RHS-0078	50.13500	89.69800	Diabase chill, Kopka cone sheet, Sandison Lake	•	•			
82RHS-0079	50.13500	89.69800	Diabase, medium grained, Kopka cone sheet, Sandison Lake	•	•			
82RHS-0080	50.13600	89.70000	Diabase, medium grained, Kopka cone sheet, Sandison Lake	•	•			
82RHS-008[illegible]	50.[illegible]8500	89.79000	Diabase, medium grained, Otter Bluff Lake	•	•			
82RHS-008[illegible]	50.37800	89.79500	Diabase, fine grained, Beiest Lake	•	•			
82RHS-0084	50.[illegible]0000	89.81800	Diabase chill, Kopka cone sheet, Aldridge Lake	•	•			
82RHS-0085	[illegible]	89.8[illegible]700	Diabase, medium grained, Kopka cone sheet, Aldridge Lake	•	•			
82RHS-0086	50.[illegible]3500	89.95600	Diabase, medium grained Wapikaimaski Lake	•	•			
82RHS-0087	50.13600	89.82800	Diabase, medium grained, Aldridge Lake area	•	•			
82RHS-0091	50.[illegible]1400	88.19700	Diabase, medium grained, ophitic, South Peninsula	•	•			
82RHS-0[illegible]	49.93500	88.13100	Altered peridotite, medium grained, Eva-Kitto Traps	•	•			
82RHS-0116	49.98900	88.12200	Peridotite, medium grained, Eva-Kitto Traps Intrusion	•	•	•		•
82RHS-0121	49.15000	88.95800	Diabase, medium grained, Disraeli Lake	•	•			
82RHS-0127	49.14500	88.96200	Peridotite, medium grained, Disraeli Lake Intrusion	•	•			
82RHS-0130	49.13800	88.95500	Olivine gabbro, medium grained, Disraeli Lake Intrusion	•	•			
82RHS-0132	49.12700	88.96900	Peridotite, medium grained, Disraeli Lake Intrusion	•	•			
82RHS-013[illegible]	49.12600	88.95000	Diabase, medium grained, Disraeli Lake	•	•			
82RHS-0136	49.13000	88.95600	Peridotite medium grained, Disraeli Lake Intrusion	•	•			
82RHS-0[illegible]	49.99400	88.90600	Diabase chill, upper contact, Undercliff Island area	•	•			
82RHS-0138	49.92200	88.86400	Diabase, medium grained, Undercliff Island area	•	•			
82RHS-0142	49.93500	88.83600	Alkali-feldspar granite, Proterozoic, Nipigon House area	•	•	•		
82RHS-0143	49.93700	88.8[illegible]700	Alkali-feldspar granite, Proterozoic, Redstone Point	•	•	•		
82RHS-0144	49.93800	88.83800	Olivine gabbro medium grained dike, English Bay	•	•	•		•
82RHS-0145	49.98200	88.89700	Quartz - feldspar porphyry, Proterozoic, English Bay	•	•			
82RHS-0150	49.76000	88.90900	Diabase, coarse grained, sill, Champlain Point	•	•			
82RHS-0151	49.83200	88.92600	Diabase, medium grained, West Bay area	•	•			
82RHS-0154	50.10400	88.65600	Diabase, anorthositic, Hunt Island	•	•			
82RHS-0156	50.10500	88.69100	Diabase, anorthositic, Cat Tal[illegible]slands	•	•			
82RHS-0157	50.13600	88.61400	Diabase, anorthositic, Murray Island	•	•			
82RHS-0160	50.05800	88.51800	Diabase, anorthositic, Whiteaves Island	•	•			
82RHS-0161	50.10000	88.56500	Diabase, medium grained, Barlow Island	•	•			
82RHS-0163	50.35400	88.66400	Diabase medium grained, ophitic, Pikitigushi Road	•	•			
82RHS-0168	50.26300	89.43500	Diabase, fine grained, Kopka cone sheet, Collins Lake	•	•			
82RHS-0169	50.26300	89.43500	Diabase, medium grained, Kopka cone sheet, Collins Lake	•	•			
82RHS-0171	50.26700	89.43800	Diabase, medium grained, Kopka cone sheet, Collins Lake	•	•			
82RHS-0172	50.38800	89.61400	Diabase, chill, Berry Lake	•	•			
82RHS-0173	50.40000	89.61700	Diabase, chill, Berry Lake	•	•			
82RHS-0175	50.06900	89.58200	Diabase, chill, North Whalen Lake	•	•			
82RHS-0178	50.02400	88.15600	Diabase, medium grained, South Peninsula	•	•			
82RHS-0186	50.22400	88.52400	Diabase, chill, sill, North Bay	•	•			
82RHS-0187	50.14600	88.37800	Diabase, medium grained, North Peninsula	•	•			
82RHS-0188	49.91300	88.33900	Diabase, coarse grained, Selwyn Island	•	•			
82RHS-0189	50.12200	88.35700	Diabase, coarse grained, North Peninsula	•	•			
82RHS-0190	50.12900	88.31800	Diabase, medium grained, North Peninsula	•	•			
82RHS-0194	50.03000	88.20100	Diabase, chill, South Peninsula	•	•			

SAMPLE NUMBER	LATITUDE	LONGITUDE	FIELD NAME AND COMMENTS	Majors	Traces	REE	Probe	Mode
82RHS-0200	50.02200	88.40300	Diabase, medium grained, Murchison Island	•	•			
82RHS-0201	49.82800	88.07800	Diabase, chill, dike, Flint Bay	•	•	•	•	•
82RHS-0202	49.82800	88.07800	Diabase, medium grained, dike, Flint Bay	•	•	•	•	•
82RHS-0204	49.55300	88.33800	Diabase, medium grained, ophitic, Gillespie Island	•	•			
82RHS-020[illegible]	49.86000	88.34100	Diabase, chill, dike, Gillespie Island	•	•			
82RHS-0207	49.93400	88.02900	Tonalite, Archean basement, Humboldt Bay	•	•			
82RHS-0210	49.91800	88.10900	Altered felsic volcanic, Proterozoic, Livingstone Point	•	•			
82RHS-0214	50.30400	88.57200	Diabase, medium grained, dike, Haystack Mtn.	•	•			
82RHS-0216	50.30000	88.57300	Diabase, chill, dike, Haystack Mtn	•	•			
82RHS-0218	50.01800	88.79000	Diabase, medium grained, Barn Island Section, 0m	•	•			•
82RHS-0219	50.01800	88.79000	Diabase, medium grained, Barn Island Section, 20m	•	•			•
82RHS-0220	50.01700	88.78900	Diabase, medium grained, Barn Island Section 40m	•	•			•
82RHS-0221	50.01700	88.78900	Diabase, medium grained, Barn Island Section, 60m	•	•			•
82RHS-0222	50.01600	88.78800	Diabase, medium grained, Barn Island Section, 80m	•	•			•
82RHS-0223	50.01600	88.78800	Diabase, medium grained, Barn Island Section 100m	•	•			•
82RHS-0224	50.01500	88.78700	Diabase, medium grained, Barn Island Section, 120m	•	•			•
82RHS-0225	50.01500	88.78700	Diabase, medium grained, Barn Island Section, 140m	•	•			•
82RHS-0226	49.98400	88.72200	Welded tuff, Proterozoic, Mountain Island, float	•	•			
82RHS-0228	49.91800	88.10900	Diabase, lower chill, Livingstone Point Section, 0m	•	•			
82RHS-0229	49.91800	88.10900	Diabase, fined grained, Livingstone Point Section, 1m	•	•	•		•
82RHS-0230	49.91800	88.10900	Diabase, medium grained, Livingstone Point Section, 10m	•	•			
82RHS-0231	49.92100	88.11800	Diabase, medium grained, ophitic, Livingstone Point Section 14m	•	•			•
82RHS-0232	49.92800	88.12800	Diabase, medium grained, ophitic, Livingstone Point Section 20m	•	•	•		•
82RHS-0233	49.91700	88.13300	Diabase, medium grained, Livingstone Point Section, 40m	•	•			•
82RHS-0234	49.91600	88.14700	Diabase, medium grained, Livingstone Point Section, 60m	•	•	•		•
82RHS-0235	49.91200	88.15800	Diabase, medium grained, Livingstone Point Section, 70m	•	•	•		•
82RHS-0236	49.91000	88.16600	Diabase, medium grained, pegmatitic patches, Livingstone Point Section, 80m	•	•			•
82RHS-0237	49.90800	88.17600	Diabase, medium grained, Livingstone Point Section, 90m	•	•	•		•
82RHS-0238	49.90600	88.18000	Diabase, upper fine grained, Livingstone Point Section 120m	•	•			•
82RHS-0302	49.97600	88.39000	Diabase, medium grained, Murchison Island	•	•			
82RHS-0306	49.85300	88.07000	Diabase, dike, Stone Bay	•	•			
82RHS-0307	49.99900	88.08200	Diabase, medium grained, Humboldt Bay	•	•			
82RHS-0317	50.02200	88.89300	Diabase, medium grained, Inner Barn Island	•	•			
82RHS-0318	50.02200	88.89300	Diabase, medium grained, Inner Barn Island	•	•			
82RHS-0319	50.02200	88.89300	Diabase, medium grained, Inner Barn Island	•	•			
82RHS-0320	50.02200	88.89300	Diabase, medium grained, Inner Barn Island	•	•			
82RHS-0322	50.09000	89.88900	Diabase, chill, Lookout Lake	•	•			
83RHS-0003	50.38900	88.66500	Aegirine augite garnet syenite, Pikitigushi River	•	•			
83RHS-0004	50.38900	88.66500	Aegirine augite garnet syenite, Pikitigushi River	•	•			
83RHS-0251	49.93700	88.83700	Picrite dike, porphyritic chill, English Bay	•	•			
83RHS-0253	49.93700	88.83700	Olivine gabbro, dike, medium grained, English Bay	•	•			
83RHS-0260	49.93700	88.83700	Olivine gabbro, dike, medium grained, English Bay	•	•			
83RHS-0341	48.80000	88.58300	Rhyolite clast, Proterozoic, St. Ignace Islands	•	•			
83RHS-0342	48.80000	88.58300	Rhyolite clast, Proterozoic, St. Ignace Islands	•	•			

NIPIGON SAMPLES - UTM Coordinates Zone 16

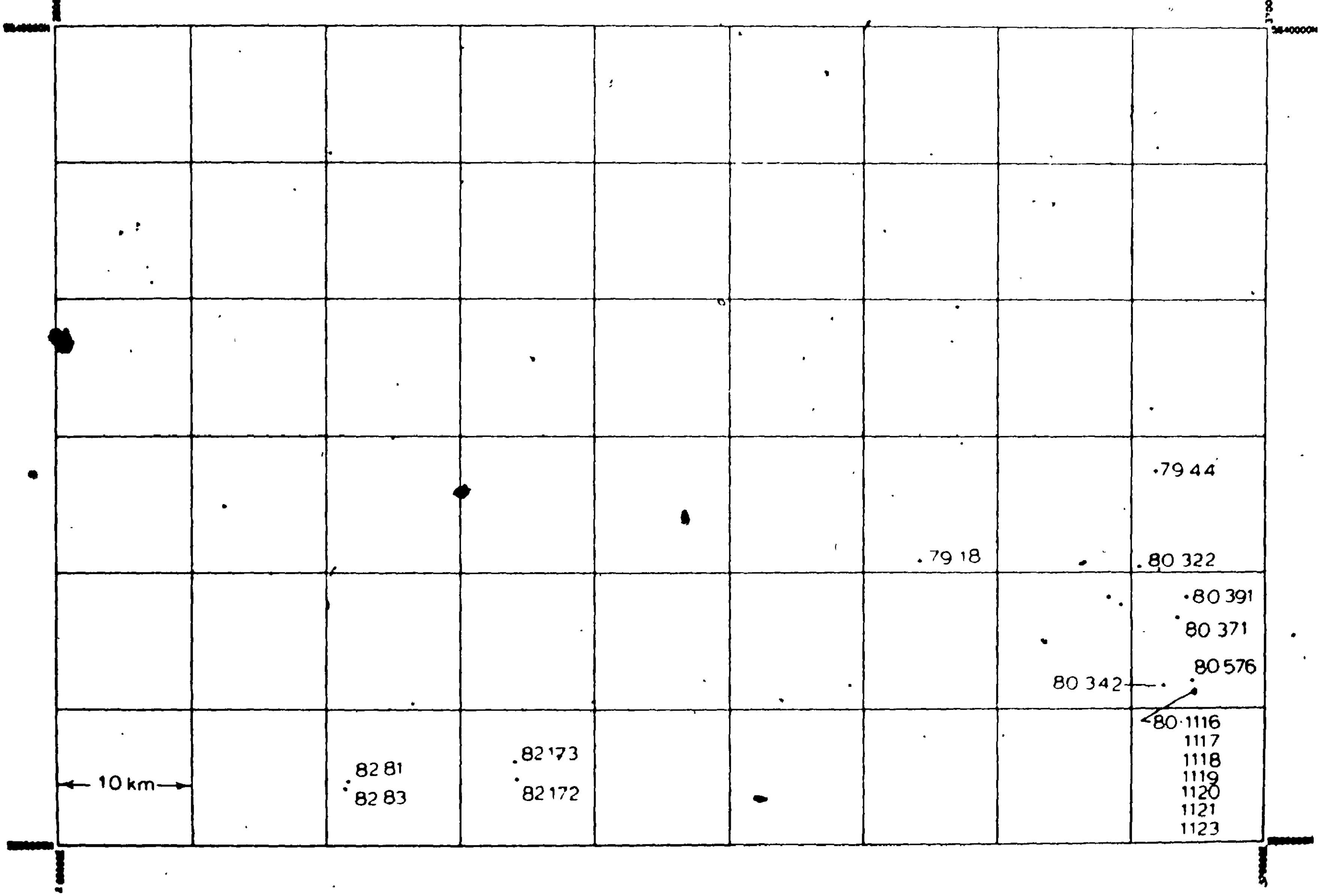
79 44
79 18
80 322
80 391
80 371
80 576
80 342
80 1116
1117
1118
1119
1120
1121
1123
82 173
82 172
82 81
82 83
10 km

NIPIGON SAMPLES - UTM Coordinates Zone 16

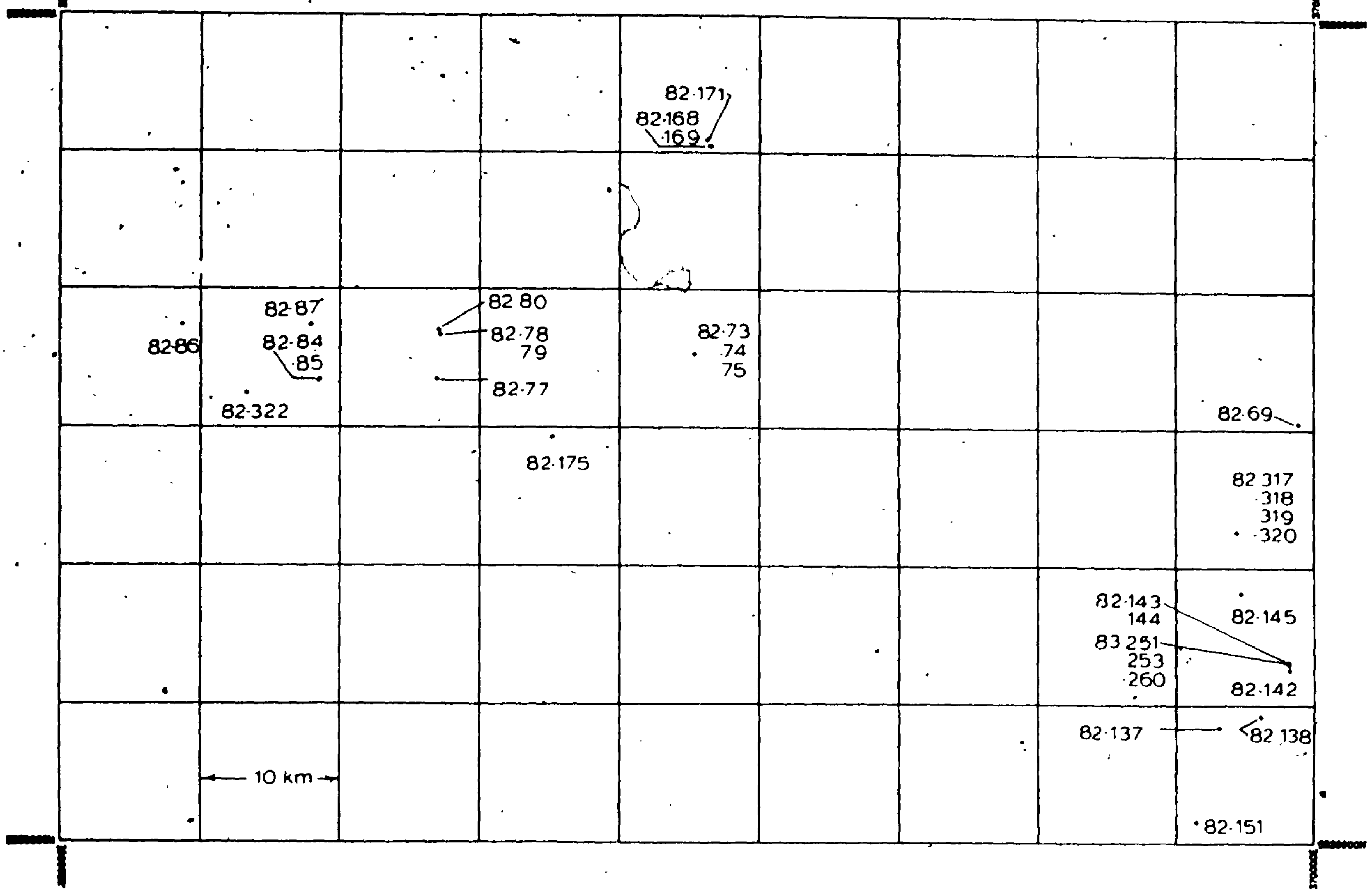
82·171
82·168
·169
82·87
82·86
82·84
·85
82·322
82 80
82·78
79
82·77
82·73
·74
75
82·175
82·69
82 317
·318
319
·320
82·143
144
83 251
253
·260
82·145
82·142
82·137
82 138
82·151
10 km

NIPIGON SAMPLES - UTM Coordinates, Zone 16

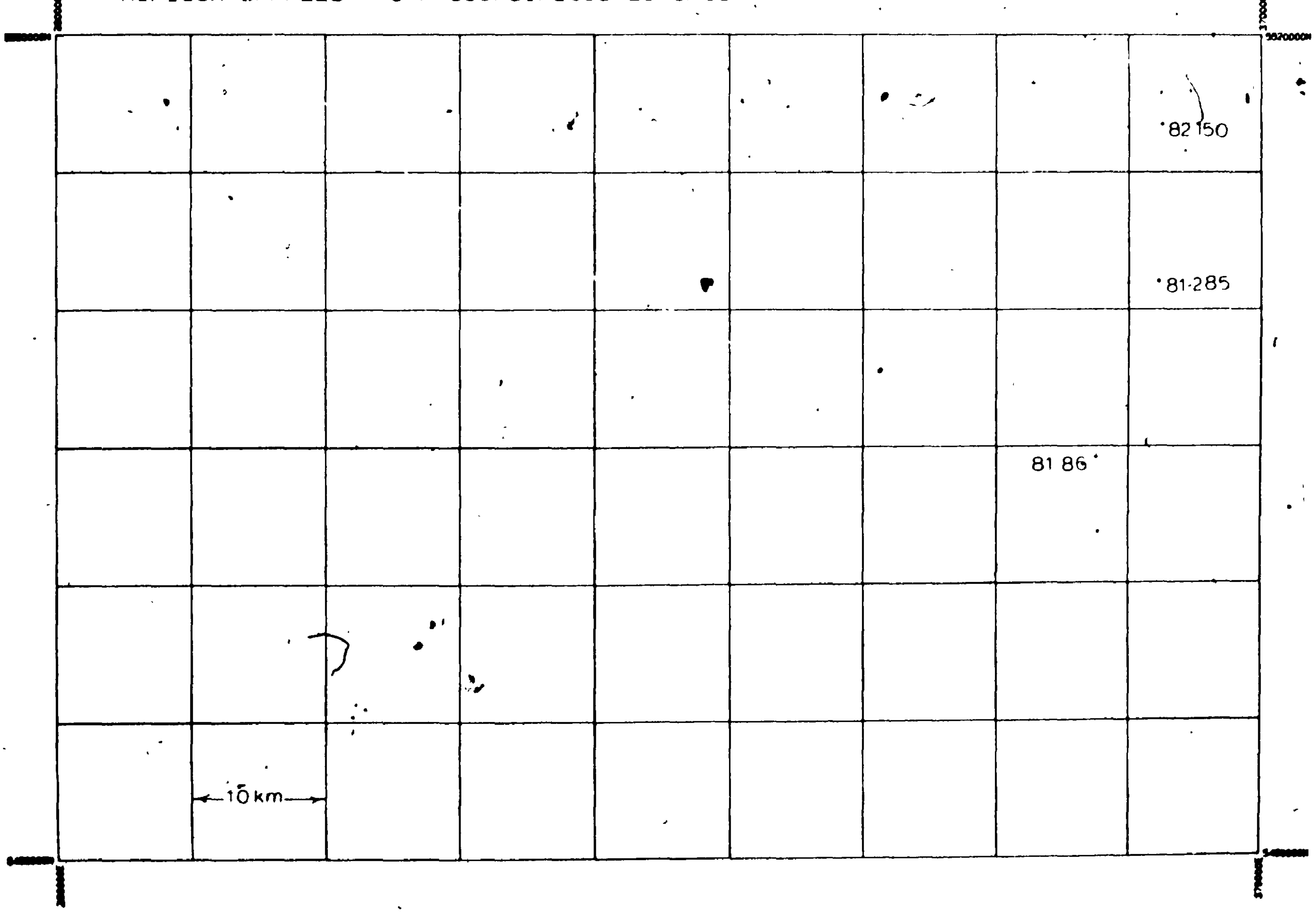
82 150
81-285
81 86
10 km
370000E
5620000N

NIPIGON SAMPLES - UTM Coordinates Zone 16

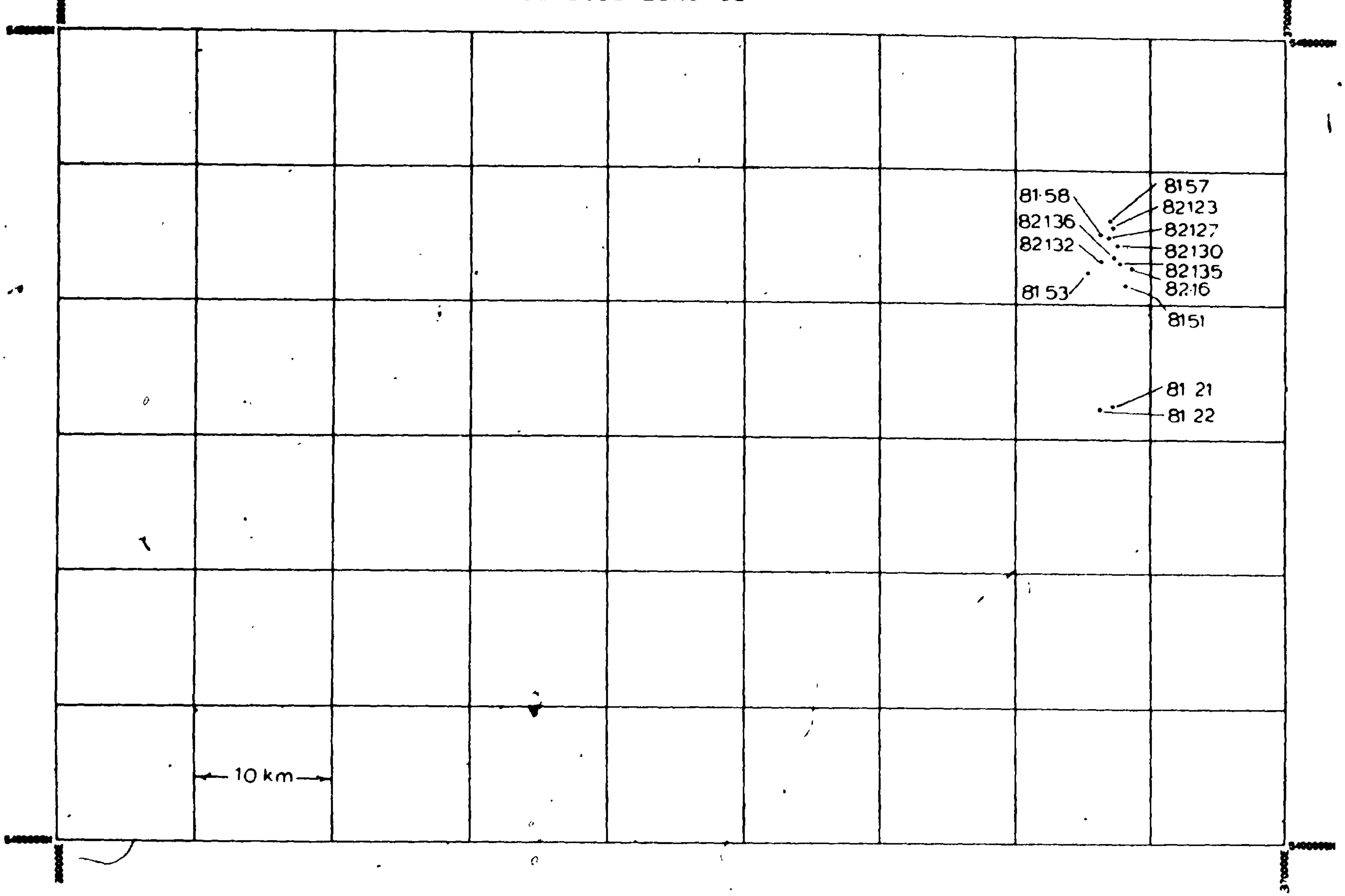
81·58
82136
82132
81 53
8157
82123
82127
82130
82135
82·16
8151
81 21
81 22
10 km

NIPIGON SAMPLES -- UTM Coordinates Zone 16

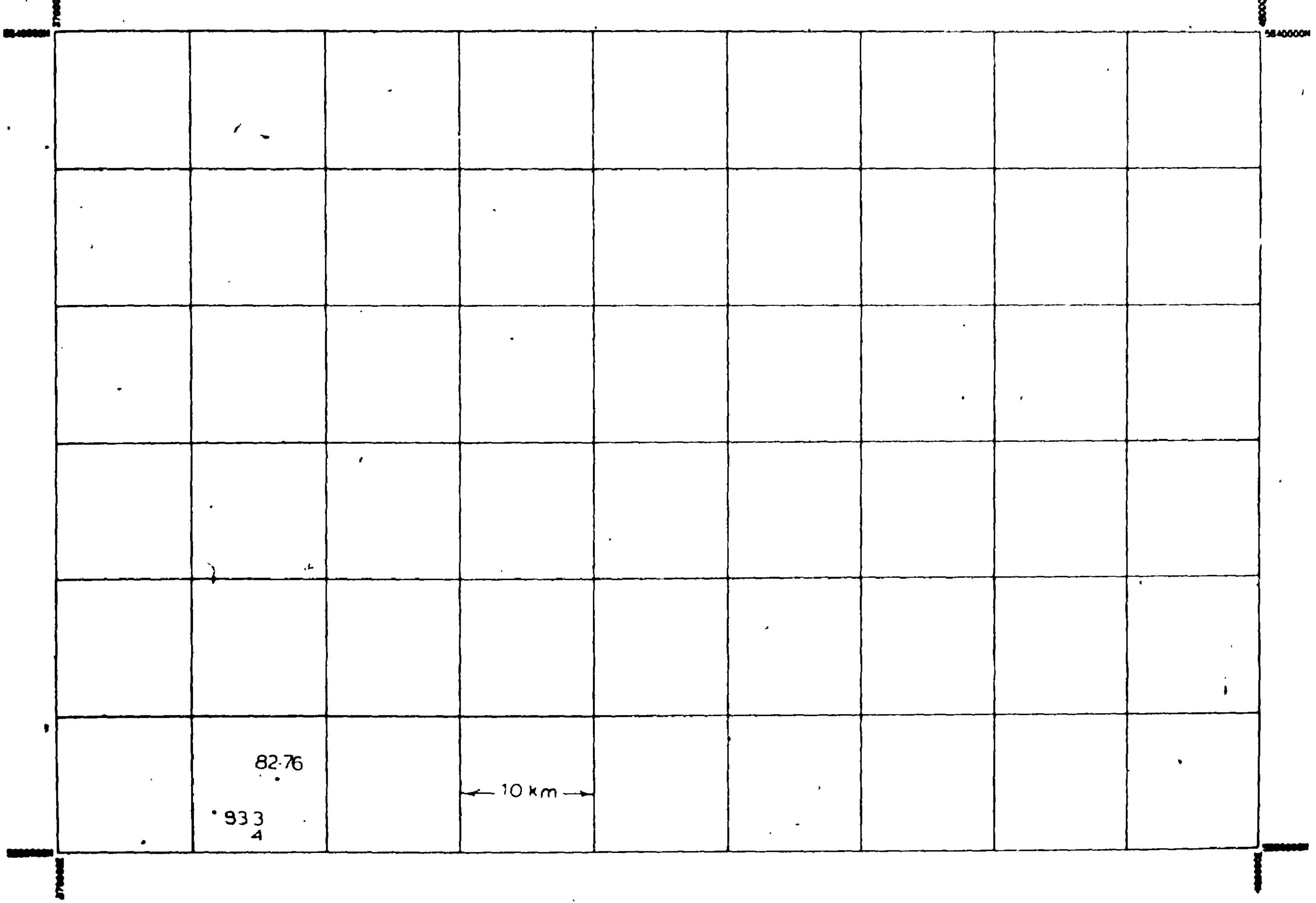
5840000N
82·76
933
4
10 km

NIPIGON SAMPLES - UTM Coordinates, Zone 16

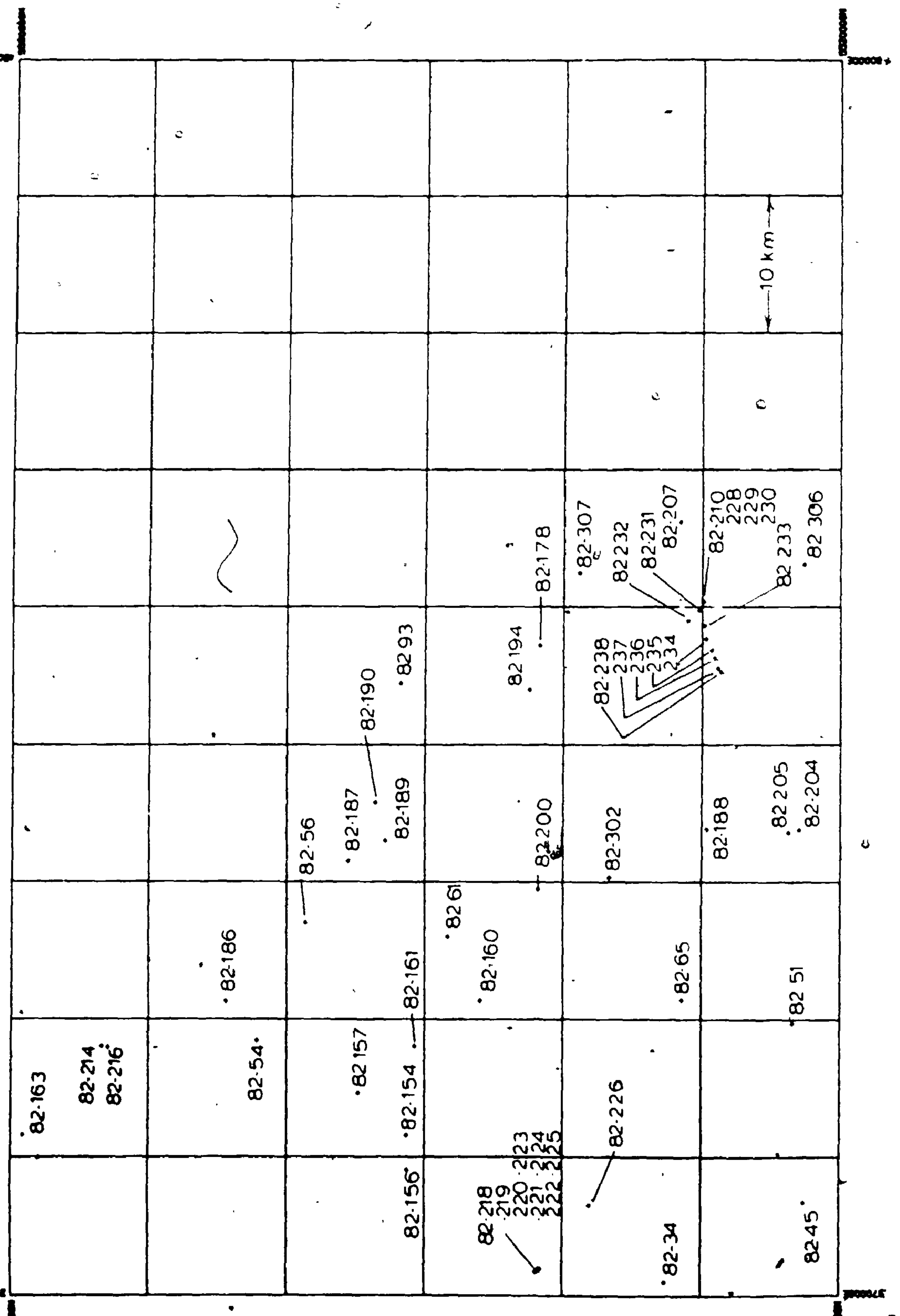
10 km
82·163
82·214
82·216
82·54
82·157
82·154
82·156
82·186
82·161
82·56
82·187
82·189
82·190
82 93
82·61
82·160
82·218
219
220
221
222
223
224
225
82·200
82·194
82·178
82·226
82·302
82·65
82·34
82·307
82 232
82·231
82·207
82·238
237
236
235
234
82·210
228
229
230
82 233
82 306
82·188
82 205
82·204
82 51
82·45

NIPIGON SAMPLES - UTM Zone 16

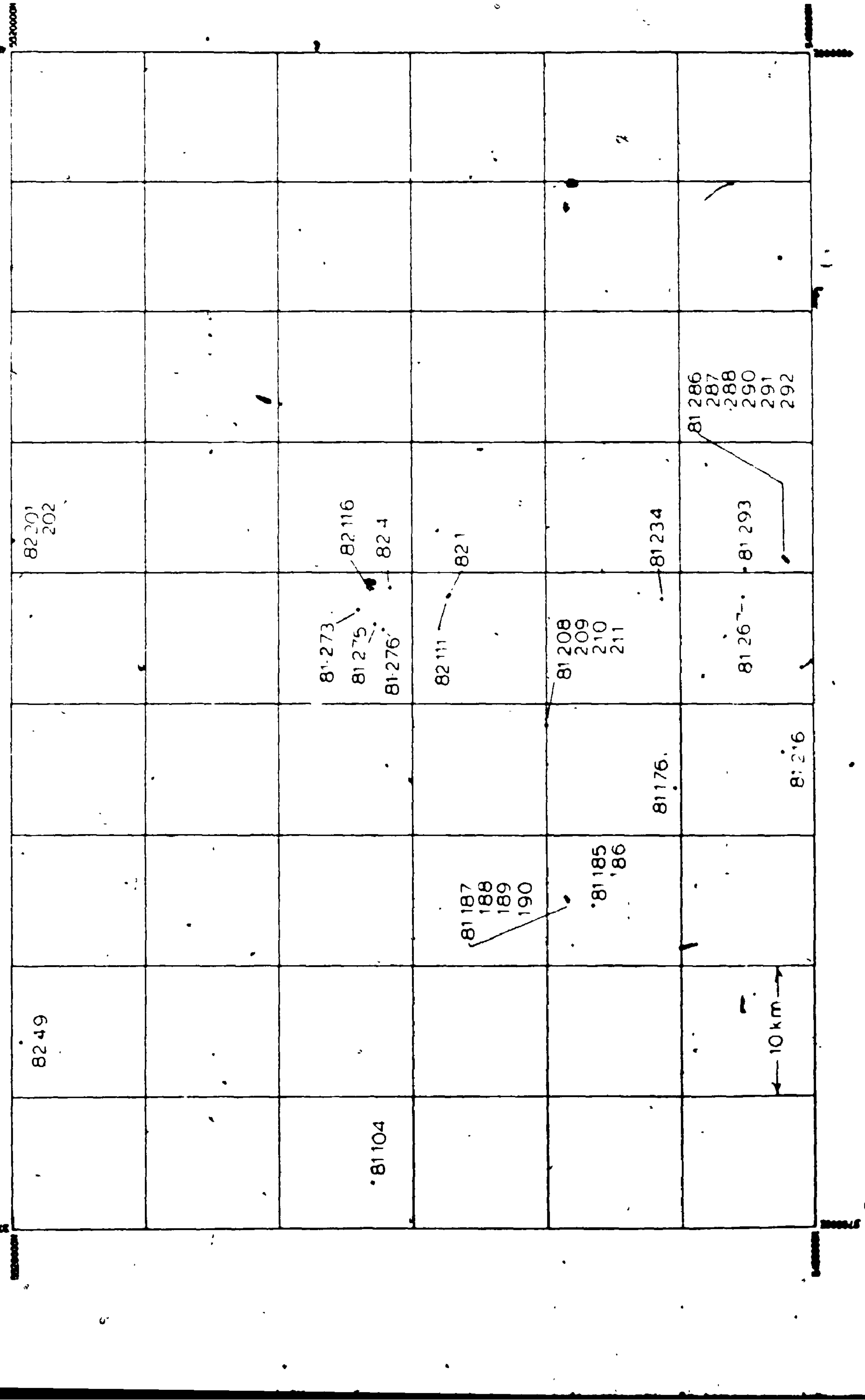
82201
202
82116
824
821
81234
81293
81286
287
288
290
291
292
81273
81275
81276
82111
81208
209
210
211
81267
81176
81216
81185
186
81187
188
189
190
8249
81104
10 km

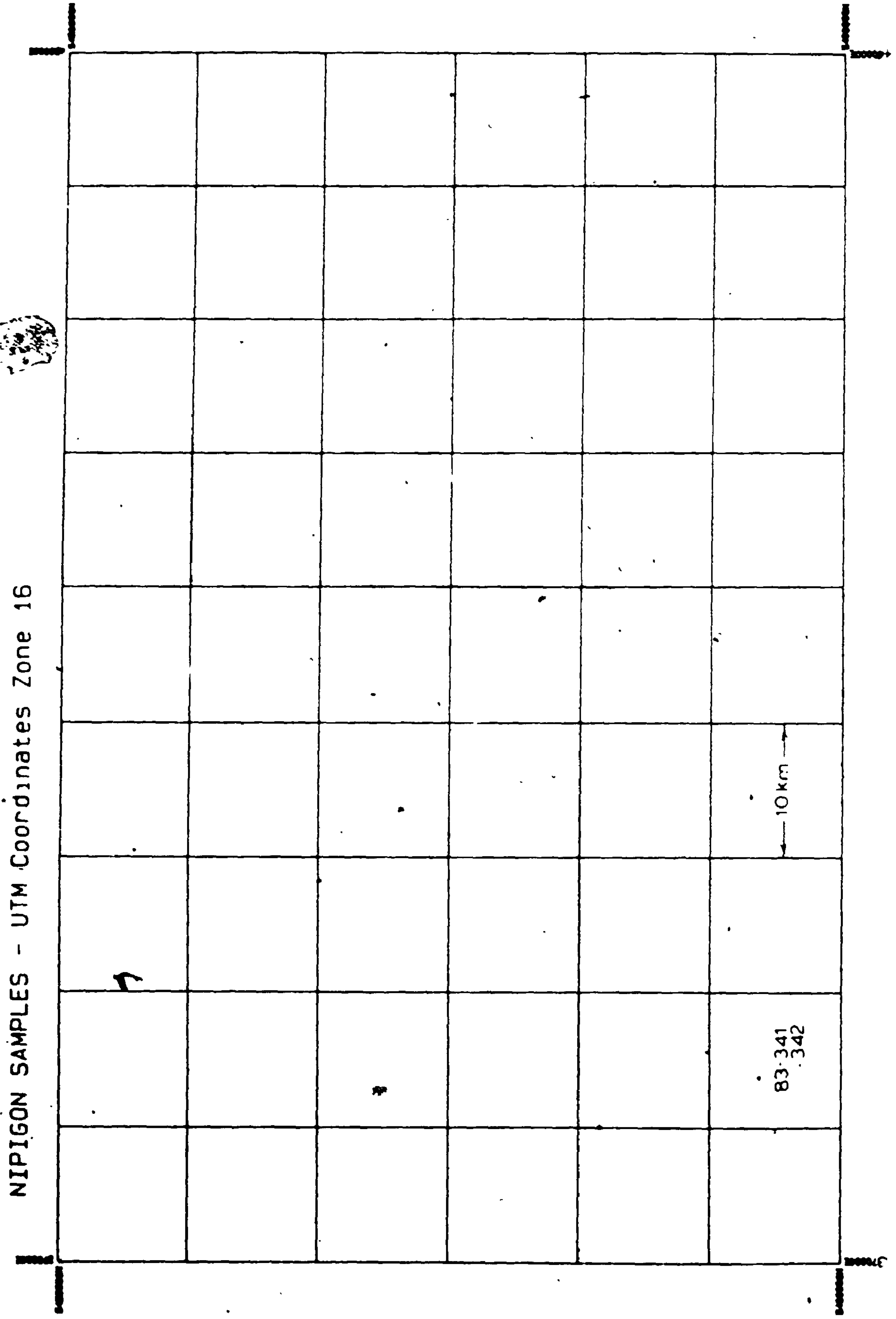

NIPIGON SAMPLES - UTM Coordinates Zone 16

10 km
83-341
.342

APPENDIX 4

MODAL ANALYSES

Appendix 4: Modal analyses of selected samples

	80-1117	80-1118	80-1119	80-1121	80-1122	80-1123	80-234
Olivine	18	6	-	15	11	3	2
Iddingsite	2	1	1	2	1	2	1
Clinopyroxene	23	36	40	24	37	37	34
Orthopyroxene	-	-	-	-	-	-	-
Plagioclase	52	47	40	51	45	50	57
Glass	-	-	-	-	-	-	-
Micrographophyre	-	-	3	-	-	-	-
Opaques	6	8	13	6	6	7	3
Biotite	1	1	2	1	TR	-	3
Hornblende	-	1	TR	TR	TR	1	-

	81-267	81-273	81-276	81-286	81-288	81-290	81-292
Olivine	2	62	31	-	1	2	1
Iddingsite	1	2	-	-	1	1	4
Clinopyroxene	27	14	50	46	35	38	33
Orthopyroxene	-	6	9	-	-	-	-
Plagioclase	60	11	9	51	58	55	55
Glass	-	-	-	-	-	-	-
Micrographophyre	-	-	-	-	-	-	-
Opaques	2	1	1	2	2	3	4
Biotite	1	3	1	1	2	1	2
Hornblende	-	-	-	-	TR	TR	TR

	82-4	82-56	82-73	82-74	82-75	82-116	82-144
Olivine	2	1	2	4	1	10	18
Iddingsite	8	1	1	1	1	6	-
Clinopyroxene	27	33	16	32	34	33	24
Orthopyroxene	14	-	-	-	-	27	4
Plagioclase	39	61	45	58	56	11	43
Glass	-	-	-	-	-	-	-
Microgranophyre	-	-	-	-	-	-	-
Opaques	3	2	14	3	4	3	6
Biotite	4	-	1	2	4	8	4
Hornblende	TR	-	21	1	-	TR	1

	82-201	82-202	82-218	82-219	82-220	82-221	82-222
Olivine	TR	-	10	10	11	13	8
Iddingsite	-	-	2	TR	1	-	2
Clinopyroxene	2	32	26	29	32	32	36
Orthopyroxene	-	-	-	-	-	-	-
Plagioclase	16	53	57	56	53	50	51
Glass	82	-	-	-	-	-	-
Microgranophyre	-	-	-	-	-	-	-
Opaques	-	4	3	4	3	4	4
Biotite	-	12	2	1	1	1	1
Hornblende	-	6	1	TR	-	TR	TR

	82-223	82-224	82-225	82-229	82-231	82-232	82-233
Olivine	8	4	11	-	-	3	TR
Iddingsite	TR	1	-	-	3	1	TR
Clinopyroxene	36	34	26	2	44	36	36
Orthopyroxene	-	--	-	-	-	-	-
Plagioclase	50	54	61	42	47	55	53
Glass	-	-	-	-	-	-	-
Micrographophyre	-	-	-	-	-	-	-
Opaques	5	7	1	4	4	3	4
Biotite	1	TR	1	2	1	1	1
Hornblende	TR	-	-	49	TR	1	5

	82-234	82-235	82-236	82-237	82-238
Olivine	16	1	2	4	0
Iddingsite	TR	1	TR	1	-
Clinopyroxene	35	38	34	34	10
Orthopyroxene	-	-	-	-	-
Plagioclase	46,	57	56	55	42
Glass	-	-	-	-	-
Micrographophyre	-	-	TR	-	-
Opaques	2	2	3	4	8
Biotite	1	-	TR	TR	TR
Hornblende	1	2	4	2	40

Samples 80-1117 to 80-1123 from Kavanagh (1981)
Analyses based on 700 to 1000 points
TR - trace (1%)

APPENDIX 5

WHOLE ROCK MAJOR AND TRACE ELEMENT ANALYSES

NIPIGON WHOLE ROCK CHEMISTRY

MAJOR OXIDE LISTING

	79RHS-0018	79RHS-0044	80RHS-0322	80RHS-0337	80RHS-0342	80RHS-0371
SIO2	47.90	57.50	36.60	46.40	67.90	46.50
TIO2	1.86	1.23	2.02	1.31	0.44	1.63
AL2O3	17.80	15.00	3.93	14.70	16.40	14.70
FE2O3	13.00	8.53	7.76	10.10	3.83	10.40
MNO	0.17	0.12	0.33	0.17	0.04	0.13
MGO	5.91	3.05	7.63	6.41	0.80	6.77
CAO	8.68	3.15	18.30	10.60	1.33	7.31
NA2O	2.96	3.65	0.40	2.72	3.44	2.77
K2O	0.79	3.95	1.01	1.82	4.19	3.70
P2O5	0.21	0.31	0.34	0.41	0.06	0.59
CO2	0.13	0.30	18.30	2.90	0.17	1.38
S	0.14	0.12	0.27	0.10	0.01	0.06
LOI	0.10	2.30	19.80	4.70	1.00	4.40
TOTAL	99.40	98.80	98.10	99.50	99.40	98.90

TRACE ELEMENT LISTING

	79RHS-0018	79RHS-0044	80RHS-0322	80RHS-0337	80RHS-0342	80RHS-037[illegible]
CR	127.00	32.00	1036.00	256.00		
V		119.00	93.00	177.00		
NI	59.00	23.00	944.00	110.00		
CO	43.00	35.00	88.00	45.00		
CU	41.00	40.00	74.00	58.00		
ZN	117.00	72.00	93.00	101.00		
LI	6.00					
GA		21.00	10.00	15.00		
PB	11.00	10.00	13.00	13.00		
BA	350.00	1642.00	721.00	1021.00		
SR		498.00	258.00	952.00		
RB		74.00	44.00	59.00		
ZR		382.00	106.00	160.00		
NB		41.00	75.00	51.00		
Y		30.00	26.00	26.00		

MAJOR OXIDE LISTING

	80RHS-0391	80RHS-0396	80RHS-0576	80RHS-1099	80RHS-1116	80RHS-1117
SIO2	63.40	45.50	66.70	31.40	48.50	48.80
TIO2	0.49	1.31	0.40	1.87	1.50	1.46
AL2O3	13.80	14.20	14.20	3.70	15.50	14.80
FE2O3	6.77	10.90	3.70	13.10	13.40	15.30
MNO	0.07	0.17	0.03	0.21	0.15	0.22
MGO	0.72	6.74	0.81	17.20	5.61	6.42
CAO	2.38	10.60	1.04	10.90	10.80	10.00
NA2O	2.55	2.35	0.05	0.21	3.30	2.37
K2O	5.49	1.74	9.38	1.96	0.22	0.40
P2O5	0.[illegible]6	0.39	0.03	0.51	0.14	0.15
CO2	1.52	3.46	1.22	15.90	0.23	0.08
S	0.02	0.09	0.01	0.16	0.02	0.02
LOI	3.30	5.60	2.40	17.50	0.70	0.20
TOTAL	99.00	99.50	98.80	98.60	99.80	99.70

TRACE ELEMENT LISTING

	80RHS-0391	80RHS-0396	80RHS-0576	80RHS-1099	80RHS-1116	80RHS-1117
CR	23.00	267.00	19.00	793.00		
V	N.D.	197.00	N.D.	209.00		
NI	13.00	100.00	9.00	810.00		
CO	18.00	55.00	14.00	80.00		
CU	34.00	56.00	61.00	60.00		
ZN	83.00	97.00	27.00	104.00		
GA	26.00	16.00	23.00	10.00		
PB	18.00	8.00	14.00	11.00		
BA	939.00	952.00	176.00	1406.00		
SR	96.00	860.00	39.00	1073.00		
RB	123.00	46.00	183.00	67.00		
ZR	686.00	166.00	1446.00	188.00		
NB	112.00	48.00	209.00	89.00		
Y	62.00	21.00	62.00	22.00		

MAJOR OXIDE LISTING

	80RHS-1118	80RHS-1119	80RHS-1120	80RHS-1121	80RHS-1122	80RHS-1123
SIO2	47.90	47.90	48.70	48.90	48.40	48.40
TIO2	1.32	1.79	1.52	1.56	1.40	1.44
AL2O3	15.90	15.50	13.50	13.40	13.80	13.90
FE2O3	14.40	15.90	14.50	15.80	15.20	15.50
MNO	0.20	0.22	0.20	0.22	0.21	0.22
MGO	6.91	5.97	6.04	5.91	7.06	6.30
CAO	9.87	9.77	10.90	10.30	10.30	10.40
NA2O	2.27	2.26	2.61	2.10	2.06	2.00
K2O	0.32	0.40	0.37	0.39	0.33	0.29
P2O5	0.14	0.15	0.14	0.15	0.13	0.12
CO2	0.11	0.10	0.12	0.11	0.11	0.18
S	0.01	0.01	0.02	0.02	0.01	0.01
LOI	0.10	0.20	0.40	N.D.	N.D.	N.D.
TOTAL	99.10	99.60	98.90	98.50	98.70	98.50

TRACE ELEMENT LISTING

	80RHS-1118	80RHS-1119	80RHS-1120	80RHS-1121	80RHS-1122	80RHS-1123
CR			112.00	108.00	123.00	153.00
NI			71.00	73.00	107.00	86.00
CO			41.00	46.00	51.00	50.00
CU			143.00	215.00	184.00	202.00
ZN			170.00	180.00	150.00	145.00
LI			12.00	6.00	6.00	6.00
PB			19.00	12.00	15.00	14.00
BA			160.00	140.00	130.00	130.00

MAJOR OXIDE LISTING

	81RHS-0021	81RHS-0022	81RHS-0051	81RHS-0053	81RHS-0057	81RHS-0058
SIO2	46.50	47.80	47.30	44.90	49.30	43.90
TIO2	1.90	0.64	1.63	1.01	1.21	1.01
AL2O3	14.70	2.53	6.83	4.30	14.70	4.04
FE2O3	4.36	11.00	15.80	14.90	13.60	15.70
MNO	0.10	0.19	0.23	0.22	0.19	0.27
MGO	3.60	21.50	15.20	21.70	5.48	23.70
CAO	17.80	14.70	9.31	10.30	10.10	8.27
NA2O	2.28	0.29	1.53	0.52	2.76	0.70
K2O	3.38	0.24	1.00	0.71	0.83	0.54
P2O5	0.52	0.02	0.14	0.07	0.10	0.09
CO2	0.52	0.07	0.21	0.08	0.17	0.32
S	0.02	0.03	0.04	0.04	0.03	0.05
LOI	3.90	1.00	0.90	1.40	0.80	1.60
TOTAL	99.00	100.00	99.90	100.00	99.30	99.80

TRACE ELEMENT LISTING

	81RHS-0021	81RHS-0022	81RHS-0051	81RHS-0053	81RHS-0057	81RHS-0058
CR	58.00	2020.00	1249.00	2293.00	89.00	2479.00
V			174.00	122.00	395.00	120.00
NI	74.00	560.00	384.00	664.00	77.00	779.00
CO	18.00	97.00	85.00	83.00	42.00	100.00
CU	12.00	30.00	23.00	12.00	108.00	19.00
ZN	43.00	79.00	147.00	90.00	103.00	195.00
LI	30.00	6.00				
GA			6.00	5.00	19.00	4.00
PB	N.D.	N.D.	32.00	23.00	13.00	51.00
BA	810.00	100.00	32.00	16.00	180.00	31.00
SR			25.00	12.00	191.00	18.00
RB			N.D.	N.D.	14.00	N.D.
ZR			242.00	124.00	92.00	136.00
NB			N.D.	N.D.	6.00	N.D.
Y			44.00	52.00	22.00	51.00

MAJOR OXIDE LISTING

	81RHS-0086	81RHS-0104	81RHS-0176	81RHS-0185	81RHS-0186	81RHS-0187
SIO2	48.80	77.10	49.50	48.50	48.90	48.90
TIO2	1.44	0.09	1.24	1.38	1.42	1.17
AL2O3	13.50	12.60	14.40	13.40	13.60	15.20
FE2O3	15.50	1.20	12.60	13.70	13.70	13.10
MNO	0.21	0.01	0.16	0.18	0.17	0.17
MGO	6.45	0.14	6.75	7.19	7.13	5.83
CAO	10.20	0.62	10.20	9.21	8.37	10.80
NA2O	2.89	6.65	2.83	3.76	3.82	2.69
K2O	0.50	0.79	1.25	0.58	0.92	0.52
P2O5	0.12	00.00	0.10	0.10	0.12	0.10
CO2	0.12	0.31	0.09	0.11	0.10	0.19
S	0.02	0.01	0.02	0.05	0.04	0.02
LOI	0.60	0.40	1.00	1.70	1.80	0.10
TOTAL	99.00	99.60	100.10	99.80	100.00	98.60

TRACE ELEMENT LISTING

	81RHS-0086	81RHS-0104	81RHS-0176	81RHS-0185	81RHS-0186	81RHS-0187
CR	130.00	13.00	148.00	115.00	139.00	111.00
V	424.00	12.00			422.00	344.00
NI	115.00	9.00	117.00	110.00	119.00	88.00
CO	51.00	12.00	44.00	48.00	51.00	38.00
CU	122.00	37.00	118.00	65.00	53.00	106.00
ZN	117.00	11.00	84.00	67.00	52.00	92.00
LI			27.00	26.00		
GA	17.00	16.00			21.00	18.00
PB	9.00	12.00	N.D.	N.D.	8.00	9.00
BA	173.00	130.00	390.00	170.00	258.00	164.00
SR	170.00	41.00			181.00	194.00
RB	12.00	16.00			10.00	21.00
ZR	119.00	246.00			122.00	110.00
NB	14.00	4.00			10.00	14.00
Y	31.00	22.00			27.00	30.00

MAJOR OXIDE LISTING

	81RHS-0188	81RHS-0189	81RHS-0190	81RHS-0208	81RHS-0209	81RHS-0210
SIO2	48.80	47.40	48.20	48.30	49.10	49.50
TIO2	1.04	1.07	1.36	1.45	1.45	1.49
AL2O3	15.00	15.30	14.10	13.50	13.80	13.90
FE2O3	13.60	13.70	14.60	14.90	15.10	15.00
MNO	0.18	0.18	0.20	0.19	0.20	0.19
MGO	7.18	8.11	6.59	6.19	6.11	5.91
CAO	10.70	10.20	9.98	10.30	9.81	9.86
NA2O	2.33	2.25	2.48	3.08	2.64	2.52
K2O	0.43	0.44	0.46	0.76	0.78	0.79
P2O5	0.08	0.09	0.11	0.13	0.13	0.12
CO2	0.25	0.42	0.27	0.09	0.15	0.08
S	0.01	0.03	0.05	0.02	0.02	0.02
LOI	0.30	00.00	0.60	0.60	0.40	0.50
TOTAL	99.00	98.80	98.70	99.40	99.50	99.90

TRACE ELEMENT LISTING

	81RHS-0188	81RHS-0189	81RHS-0190	81RHS-0208	81RHS-0209	81RHS-0210
CR	176.00	149.00	126.00	105.00	115.00	110.00
V	291.00	328.00	369.00			
NI	147.00	193.00	143.00	88.00	99.00	105.00
CO	46.00	55.00	53.00	50.00	53.00	54.00
CU	104.00	101.00	105.00	72.00	190.00	230.00
ZN.	97.00	95.00	91.00	115.00	124.00	144.00
LI				28.00	14.00	12.00
GA	20.00	20.00	19.00			
PB	14.00	8.00	8.00	N.D.	11.00	N.D.
BA	162.00	164.00	190.00	290.00	200.00	200.00
SR	200.00	181.00	177.00			
RB	37.00	12.00	16.00			
ZR	113.00	100.00	126.00			
NB	22.00	12.00	15.00			
Y	38.00	27.00	34.00			

MAJOR OXIDE LISTING

	81RHS-0211	81RHS-0216	81RHS-0234	81RHS-0267	81RHS-0273	81RHS-0275
SIO2	48.70	49.00	48.50	48.60	41.00	44.50
TIO2	1.39	1.23	0.96	1.01	0.71	0.75
AL2O3	14.00	14.20	15.70	14.80	2.88	3.29
FE2O3	14.80	13.20	12.80	13.80	17.50	15.50
MNO	0.21	0.18	0.17	0.19	0.23	0.21
MGO	6.53	7.23	8.15	8.59	30.20	26.10
CAO	9.78	9.54	10.30	10.30	4.05	8.41
NA2O	2.45	2.43	2.34	2.05	0.20	0.48
K2O	0.69	0.99	0.47	0.35	0.43	0.31
P2O5	0.12	0.08	0.07	0.08	0.06	0.06
CO2	0.11	0.14	0.11	0.05	0.19	0.17
S	0.05	0.07	0.03	0.02	0.06	0.05
LOI	0.40	0.90	00.00	0.10	2.30	0.10
TOTAL	99.10	99.00	99.60	99.80	99.50	99.50

TRACE ELEMENT LISTING

	81RHS-0211	81RHS-0216	81RHS-0234	81RHS-0267	81RHS-0273	81RHS-0275
CR	113.00	148.00	128.00	200.00	2549.00	2150.00
V			311.00	298.00	103.00	
NI	145.00	103.00	165.00	187.00	871.00	870.00
CO	56.00	48.00	55.00	50.00	104.00	127.00
CU	205.00	186.00	94.00	102.00	12.00	36.00
ZN	146.00	145.00	81.00	86.00	87.00	100.00
LI	12.00	28.00				6.00
GA			6.00	16.00	6.00	
PB	N.D.	44.00	2.00	7.00	26.00	N.D.
BA	230.00	210.00	104.00	130.00	12.00	120.00
SR			177.00	154.00	9.00	
RB			5.00	N.D.	N.D.	
ZR			86.00	68.00	134.00	
NB			19.00	2.00	N.D.	
Y			28.00	13.00	74.00	

MAJOR OXIDE LISTING

	81RHS-0276	81RHS-0285	81RHS-0286	81RHS-0287	81RHS-0288	81RHS-0289
SIO2	45.50	48.60	50.10	49.80	49.00	48.90
TIO2	0.74	2.89	1.10	0.92	0.91	0.88
AL2O3	3.61	10.20	13.50	14.80	15.30	14.70
FE2O3	15.50	20.70	12.70	12.10	12.10	12.90
MNO	0.21	0.24	0.19	0.17	0.17	0.18
MGO	24.70	3.99	7.96	7.41	7.58	8.75
CAO	8.87	8.36	12.00	11.70	11.70	10.80
NA2O	0.53	2.72	2.26	2.29	2.27	1.92
K2O	0.28	0.80	0.32	0.32	0.36	0.61
P2O5	0.06	0.20	0.09	0.06	0.07	0.06
CO2	0.18	0.07	0.07	0.06	0.09	0.06
S	0.02	0.04	0.03	0.02	0.02	0.02
LOI	0.10	0.20	00.00	0.10	00.00	00.00
TOTAL	99.90	98.60	100.20	99.40	99.40	99.80

TRACE ELEMENT LISTING

	81RHS-0276	81RHS-0285	81RHS-0286	81RHS-0287	81RHS-0288	81RHS-0289
CR	2458.00	78.00	167.00	173.00	243.00	285.00
V	118.00	579.00	381.00	331.00	327.00	300.00
NI	795.00	57.00	106.00	112.00	115.00	162.00
CO	96.00	47.00	38.00	45.00	40.00	47.00
CU	13.00	214.00	101.00	92.00	87.00	90.00
ZN	89.00	132.00	80.00	75.00	80.00	83.00
GA	4.00	21.00	18.00	4.00	19.00	16.00
PB	27.00	12.00	10.00	N.D.	10.00	9.00
BA	12.00	267.00	133.00	112.00	110.00	132.00
SR	9.00	154.00	160.00	178.00	193.00	176.00
RB	N.D.	19.00	14.00	N.D.	9.00	15.00
ZR	105.00	184.00	97.00	70.00	79.00	69.00
NB	N.D.	19.00	14.00	10.00	11.00	8.00
Y	49.00	44.00	30.00	17.00	26.00	21.00

MAJOR OXIDE LISTING

	81RHS-0290	81RHS-0291	81RHS-0292	81RHS-0293	82RHS-0001	82RHS-0004
SIO2	48.60	48.30	49.10	51.20	39.90	48.40
TIO2	0.88	0.97	1.27	1.05	0.87	1.88
AL2O3	15.40	15.50	14.60	13.20	3.15	10.10
FE2O3	12.70	13.20	13.50	13.90	17.50	15.60
MNO	0.18	0.18	0.19	0.23	0.22	0.22
MGO	8.66	8.51	7.50	7.14	31.00	10.90
CAO	10.80	10.20	10.30	10.60	3.29	8.66
NA2O	2.11	2.10	2.34	2.16	0.43	1.40
K2O	0.52	0.42	0.42	0.33	0.20	0.74
P2O5	0.06	0.07	0.09	0.06	00.00	0.05
CO2	0.04	0.07	0.09	0.10	0.16	0.14
S	0.02	0.03	0.03	0.02	0.05	0.06
LOI	0.10	00.00	0.40	0.10	3.70	0.70
TOTAL	99.90	99.50	99.80	99.80	100.30	98.60

TRACE ELEMENT LISTING

	81RHS-0290	81RHS-0291	81RHS-0292	81RHS-0293	82RHS-0001	82RHS-0004
CR	240.00	130.00	149.00	61.00	2840.00	519.00
V	251.00	266.00	338.00	357.00		343.00
NI	157.00	183.00	154.00	69.00	1280.00	318.00
CO	42.00	54.00	57.00	43.00	145.00	65.00
CU	88.00	93.00	108.00	106.00	21.00	140.00
ZN	76.00	86.00	101.00	100.00	130.00	207.00
LI					10.00	
GA	19.00	20.00	19.00	20.00		20.00
PB	10.00	8.00	9.00	8.00	148.00	62.00
BA	116.00	137.00	170.00	135.00	120.00	363.00
SR	185.00	176.00	195.00	152.00		473.00
RB	22.00	11.00	25.00	N.D.		26.00
ZR	81.00	70.00	99.00	68.00		127.00
NB	12.00	8.00	17.00	2.00		14.00
Y	26.00	21.00	33.00	17.00		25.00

MAJOR OXIDE LISTING

	82RHS-0016	80RHS-0034	82RHS-0045	82RHS-0049	82RHS-0051	82RHS-0054
SIO2	47.30	41.90	48.60	48.60	49.20	60.40
TIO2	1.54	1.51	1.10	1.75	1.50	1.09
AL2O3	8.97	6.06	14.10	14.50	14.10	16.90
FE2O3	12.90	19.10	14.70	12.50	6.57	8.02
MNO	0.17	0.23	0.19	0.19	0.08	0.10
MGO	13.60	23.50	9.03	6.69	8.24	1.71
CAO	11.90	5.32	10.80	10.10	15.90	4.87
NA2O	1.04	1.05	1.23	2.16	1.35	4.23
K2O	0.58	0.29	0.36	0.72	0.70	1.41
P2O5	0.04	0.12	0.01	0.06	0.05	0.15
CO2	0.28	0.25	0.19	0.14	0.22	0.10
S	0.06	0.02	0.03	0.04	0.02	0.01
LOI	0.80	N.D.	N.D.	1.80	1.60	0.50
TOTAL	98.80	98.30	100.00	99.10	99.20	99.40

TRACE ELEMENT LISTING

	82RHS-0016	80RHS-0034	82RHS-0045	82RHS-0049	82RHS-0051	82RHS-0054
CR	995.00	1460.00	296.00	147.00	127.00	14.00
V	226.00			440.00	325.00	
NI	338.00	1310.00	170.00	114.00	74.00	8.00
CO	80.00	120.00	60.00	57.00	25.00	15.00
CU	102.00	65.00	123.00	123.00	60.00	6.00
ZN	71.00	160.00	102.00	142.00	38.00	124.00
LI		6.00	6.00			16.00
GA	N.D.			27.00	10.00	
PB	50.00	N.D.	50.00	322.00	176.00	16.00
BA	237.00	130.00	110.00	198.00	540.00	410.00
SR	547.00			202.00	275.00	
RB	N.D.			32.00	14.00	
ZR	115.00			141.00	130.00	
NB	12.00			16.00	8.00	
Y	14.00			38.00	40.00	

MAJOR OXIDE LISTING

	82RHS-0056	82RHS-0061	82RHS-0065	82RHS-0069	82RHS-0073	82RHS-0074
SIO2	50.80	50.10	19.70	53.30	48.80	49.20
TIO2	0.95	1.40	0.21	1.48	1.64	1.69
AL2O3	17.70	15.70	4.32	14.90	13.50	14.00
FE2O3	10.90	13.60	3.84	8.35	16.80	15.80
MNO	0.14	0.19	0.11	0.06	0.22	0.20
MGO	6.16	5.13	13.90	7.52	6.47	6.32
CAO	11.40	10.10	20.70	5.47	10.20	10.10
NA2O	1.89	2.13	1.69	2.43	1.91	2.06
K2O	0.36	0.65	1.36	2.12	0.39	0.43
P2O5	00.00	0.04	00.00	0.05	0.01	0.05
CO2	0.06	0.07	35.10	1.22	0.12	0.06
S	0.03	0.04	0.08	0.02	0.02	0.01
LOI	N.D.	N.D.	33.30	3.80	N.D.	N.D.
TOTAL	100.10	98.80	99.10	99.40	99.70	99.60

TRACE ELEMENT LISTING

	82RHS-0056	82RHS-0061	82RHS-0065	82RHS-0069	82RHS-0073	82RHS-0074
CR	118.00	49.00	21.00	136.00	137.00	119.00
V	237.00			310.00	464.00	328.00
NI	118.00	55.00	N.D.	67.00	115.00	120.00
CO	46.00	42.00	6.00	52.00	49.00	43.00
CU	46.00	144.00	6.00	50.00	140.00	155.00
ZN	66.00	106.00	11.00	40.00	124.00	103.00
LI		9.00	4.00			
GA	3.00			N.D.	28.00	26.00
PB	38.00	182.00	70.00	44.00	331.00	32.00
BA	140.00	240.00	60.00	397.00	141.00	152.00
SR	231.00			224.00	167.00	165.00
RB	N.D.			39.00	18.00	N.D.
ZR	62.00			184.00	118.00	122.00
NB	15.00			22.00	19.00	15.00
Y	21.00			30.00	42.00	32.00

MAJOR OXIDE LISTING

	82RHS-0075	82RHS-0076	82RHS-0077	82RHS-0078	82RHS-0079	82RHS-0080
SIO2	50.10	58.80	48.70	49.80	48.90	50.20
TIO2	1.44	1.48	1.63	1.60	1.66	1.69
AL2O3	14.40	18.50	13.70	12.30	14.60	13.40
FE2O3	14.80	5.95	16.40	16.40	15.90	15.70
MNO	0.20	0.02	0.22	0.24	0.20	0.22
MGO	5.91	3.20	6.33	6.23	5.84	6.21
CAO	9.80	4.19	10.10	10.50	10.10	10.10
NA2O	2.25	3.50	2.11	1.76	2.15	2.01
K2O	0.69	2.64	0.49	0.40	0.44	0.49
P2O5	0.06	0.30	0.05	0.03	0.05	0.05
CO2	0.12	0.08	0.06	0.05	0.11	0.11
S	0.03	0.01	0.01	0.01	0.01	0.05
LOI	N.D.	1.10	N.D.	0.10	N.D.	N.D.
TOTAL	99.20	99.70	99.60	99.30	99.80	99.60

TRACE ELEMENT LISTING

	82RHS-0075	82RHS-0076	82RHS-0077	82RHS-0078	82RHS-0079	82RHS-0080
CR	120.00	24.00	122.00	56.00	98.00	138.00
V	358.00	47.00	393.00	233.00	385.00	428.00
NI	128.00	22.00	115.00	85.00	102.00	115.00
CO	59.00	29.00	43.00	20.00	40.00	55.00
CU	103.00	30.00	154.00	119.00	153.00	119.00
ZN	131.00	11.00	112.00	114.00	104.00	121.00
GA	8.00	N.D.	14.00	29.00	4.00	10.00
PB	132.00	4.00	71.00	4.00	4.00	85.00
BA	342.00	637.00	158.00	362.00	148.00	180.00
SR	199.00	464.00	156.00	220.00	164.00	139.00
RB	8.00	94.00	N.D.	20.00	N.D.	N.D.
ZR	132.00	382.00	118.00	186.00	123.00	105.00
NB	17.00	31.00	17.00	24.00	16.00	5.00
Y	30.00	41.00	28.00	40.00	28.00	23.00

MAJOR OXIDE LISTING

	82RHS-0081	82RHS-0083	82RHS-0084	82RHS-0085	82RHS-0086	82RHS-0087
SIO2	48.70	48.60	48.40	47.80	48.20	49.20
TIO2	1.34	1.63	1.63	1.65	1.44	1.39
AL2O3	14.20	13.70	13.70	13.50	14.30	14.50
FE2O3	15.50	16.10	16.70	16.40	16.10	15.20
MNO	0.20	0.22	0.22	0.21	0.21	0.19
MGO	7.53	6.31	6.70	7.03	7.01	7.50
CAO	10.50	10.10	10.50	9.84	10.20	10.00
NA2O	1.73	1.98	1.90	1.76	2.00	1.82
K2O	0.37	0.45	0.32	0.50	0.39	0.46
P2O5	00.00	0.05	0.03	0.03	0.04	0.02
CO2	0.07	0.09	0.07	0.08	0.08	0.09
S	0.01	0.03	0.01	0.01	0.01	0.03
LOI	N.D.	N.D.	N.D.	0.30	N.D.	N.D.
TOTAL	100.00	98.90	99.90	99.10	99.70	100.00

TRACE ELEMENT LISTING

	82RHS-0081	82RHS-0083	82RHS-0084	82RHS-0085	82RHS-0086	82RHS-0087
CR	215.00	124.00	136.00	139.00	148.00	157.00
V			488.00	437.00		
NI	120.00	89.00	128.00	141.00	112.00	141.00
CO	55.00	53.00	44.00	52.00	56.00	59.00
CU	166.00	205.00	111.00	131.00	184.00	164.00
ZN	120.00	150.00	114.00	107.00	119.00	122.00
LI	8.00	8.00			7.00	8.00
GA			20.00	6.00		
PB	N.D.	210.00	90.00	7.00	16.00	620.00
BA	130.00	150.00	124.00	161.00	120.00	150.00
SR			163.00	151.00		
RB			N.D.	8.00		
ZR			76.00	99.00		
NB			13.00	13.00		
Y			26.00	27.00		

MAJOR OXIDE LISTING

	82RHS-0093	82RHS-0111	82RHS-0116	82RHS-0123	82RHS-0127	82RHS-0130
SIO2	48.10	37.40	46.40	47.50	44.90	47.30
TIO2	1.28	0.54	1.26	1.22	1.12	1.41
AL2O3	15.10	2.92	6.19	15.10	4.05	5.40
FE2O3	15.30	14.80	15.40	12.80	13.40	13.90
MNO	0.19	0.14	0.24	0.15	0.19	0.21
MGO	7.48	30.40	19.30	7.71	20.80	16.20
CAO	10.30	3.65	8.53	8.03	11.60	12.40
NA2O	1.63	0.30	0.70	2.74	0.95	1.02
K2O	0.36	0.64	0.52	1.06	0.39	0.55
P2O5	0.03	0.06	0.02	0.18	0.04	0.11
CO2	0.09	0.53	0.19	0.10	0.26	0.19
S	0.02	0.05	0.05	0.04	0.04	0.03
LOI	N.D.	9.00	0.50	2.20	1.70	0.80
TOTAL	99.40	100.00	99.10	98.70	99.20	99.40

TRACE ELEMENT LISTING

	82RHS-0093	82RHS-0111	82RHS-0116	82RHS-0123	82RHS-0127	82RHS-0130
CR	118.00	3060.00	1305.00	125.00	2000.00	1180.00
V			200.00			
NI	138.00	1140.00	367.00	152.00	520.00	300.00
CO	58.00	121.00	97.00	50.00	88.00	78.00
CU	158.00	11.00	63.00	110.00	30.00	44.00
ZN	110.00	62.00	188.00	102.00	88.00	92.00
LI	8.00	8.00		26.00	20.00	10.00
GA			15.00			
PB	175.00	N.D.	14.00	N.D.	N.D.	N.D.
BA	120.00	60.00	396.00	140.00	110.00	160.00
SR			345.00			
RB			13.00			
ZR			104.00			
NB			29.00			
Y			22.00			

MAJOR OXIDE LISTING

	82RHS-0132	82RHS-0135	82RHS-0136	82RHS-0137	82RHS-0138	82RHS-0142
SIO2	46.20	47.80	45.30	46.60	49.20	74.50
TIO2	1.95	1.20	1.57	2.73	1.60	0.19
AL203	6.84	14.30	6.79	11.60	12.40	12.20
FE203	15.50	~~14.10~~	~~16.00~~	15.80	16.50	2.47
MNO	0.22	0.19	0.22	0.22	0.24	0.03
MGO	16.00	8.32	16.20	8.13	5.75	0.46
CAO	9.51	9.76	9.63	8.68	9.80	0.94
NA20	1.39	1.90	0.95	2.41	2.12	2.58
K20	0.71	0.84	0.93	1.02	0.59	5.16
P205	0.10	0.10	0.12	0.17	0.14	0.04
CO2	0.24	0.29	0.25	0.11	0.06	0.12
S	0.05	0.04	0.06	0.04	0.02	0.01
LOI	0.30	0.80	1.20	0.80	0.20	1.10
TOTAL	98.80	99.40	99.00	89.20	98.30	99.70

TRACE ELEMENT LISTING

	82RHS-0132	82RHS-0135	82RHS-0136	82RHS-0137	82RHS-0138	82RHS-0142
CR	1110.00	163.00	1180.00	335.00	133.00	16.00
V						5.00
NI	360.00	174.00	360.00	240.00	51.00	12.00
CO	82.00	55.00	87.00	56.00	43.00	13.00
CU	120.00	156.00	124.00	90.00	240.00	30.00
ZN	150.00	108.00	118.00	230.00	150.00	64.00
LI	14.00	12.00	28.00	30.00	12.00	
GA						26.00
PB	N.D.	N.D.	N.D.	158.00	N.D.	13.00
BA	200.00	190.00	250.00	220.00	190.00	122.00
SR						43.00
RB						254.00
ZR						497.00
NB						127.00
Y						108.00

MAJOR OXIDE LISTING

	82RHS-0143	82RHS-0144	82RHS-0145	82RHS-0150	82RHS-0151	82RHS-0154
SIO2	74.10	44.90	73.80	47.70	48.20	48.70
TIO2	0.20	2.03	0.20	2.74	2.90	0.89
AL2O3	12.50	9.26	12.80	11.40	12.90	15.60
FE2O3	2.36	17.00	1.46	20.30	16.10	12.40
MNO	0.03	0.19	0.02	0.25	0.18	0.18
MGO	0.35	13.90	1.90	4.03	5.26	7.26
CAO	1.03	8.65	1.81	8.77	9.03	10.90
NA2O	1.93	1.69	1.14	2.32	2.72	2.22
K2O	6.43	0.53	2.95	0.83	0.84	0.48
P2O5	0.04	0.09	0.02	0.14	0.17	0.09
CO2	0.28	0.12	1.22	0.19	0.14	0.08
S	0.01	0.03	0.01	0.06	0.05	0.03
LOI	0.70	0.20	3.40	0.20	0.20	0.40
TOTAL	99.70	98.20	99.50	98.50	98.30	98.40

TRACE ELEMENT LISTING

	82RHS-0143	82RHS-0144	82RHS-0145	82RHS-0150	82RHS-0151	82RHS-0154
CR	14.00	662.00	17.00	N.D.	86.00	156.00
V	10.00	272.00	5.00			
NI	14.00	405.00	16.00	27.00	87.00	118.00
CO	11.00	71.00	14.00	50.00	55.00	52.00
CU	29.00	68.00	28.00	290.00	68.00	100.00
ZN	60.00	127.00	28.00	160.00	143.00	90.00
LI				12.00	18.00	8.00
GA	27.00	18.00	28.00			
PB	15.00	21.00	14.00	N.D.	N.D.	N.D.
BA	233.00	174.00	51.00	240.00	270.00	200.00
SR	51.00	308.00	49.00			
RB	250.00	N.D.	203.00			
ZR	525.00	127.00	542.00			
NB	113.00	25.00	132.00			
Y	82.00	13.00	79.00			

MAJOR OXIDE LISTING

	82RHS-0156	82RHS-0157	82RHS-0160	82RHS-0161	82RHS-0163	82RHS-0168
SIO2	49.50	48.70	50.00	49.40	50.00	48.90
TIO2	1.04	1.19	1.23	0.89	1.30	1.48
AL2O3	16.70	14.20	16.10	15.50	14.00	13.70
FE2O3	11.60	14.90	12.40	12.80	14.50	15.50
MNO	0.16	0.19	0.17	0.16	0.19	0.21
MGO	6.01	5.96	4.75	7.08	6.07	6.28
CAO	10.90	10.10	10.20	10.70	9.85	10.00
NA2O	2.33	2.36	2.39	2.18	2.50	2.36
K2O	0.60	0.65	0.67	0.50	0.71	0.61
P2O5	0.05	0.05	0.06	0.10	0.15	0.14
CO2	0.14	0.15	0.09	0.09	0.08	0.06
S	0.02	0.04	0.04	0.03	0.04	0.01
LOI	00.00	0.10	0.30	00.00	0.40	0.10
TOTAL	99.00	98.30	99.10	99.40	98.90	99.20

TRACE ELEMENT LISTING

	82RHS-0156	82RHS-0157	82RHS-0160	82RHS-0161	82RHS-0163	82RHS-0168
CR	124.00	96.00	38.00	137.00	101.00	122.00
V				180.00		277.00
NI	84.00	85.00	51.00	146.00	92.00	124.00
CO	45.00	54.00	38.00	39.00	49.00	33.00
CU	109.00	150.00	131.00	68.00	158.00	92.00
ZN	86.00	112.00	99.00	79.00	106.00	113.00
LI	8.00	10.00	10.00		10.00	
GA				18.00		23.00
PB	N.D.	N.D.	N.D.	9.00	N.D.	10.00
BA	230.00	240.00	240.00	202.00	220.00	185.00
SR				232.00		169.00
RB				16.00		4.00
ZR				104.00		119.00
NB				29.00		26.00
Y				24.00		24.00

MAJOR OXIDE LISTING

	82RHS-0169	82RHS-0171	82RHS-0172	82RHS-0173	82RHS-0175	82RHS-0178
SIO2	49.10	50.10	49.40	48.50	50.50	48.40
TIO2	1.94	1.50	1.51	1.48	1.29	1.34
AL203	12.10	13.00	14.00	13.60	14.10	14.50
FE203	18.20	15.20	15.10	15.80	14.10	15.00
MNO	0.25	0.25	0.21	0.22	0.19	0.20
MGO	5.41	5.32	6.39	6.47	6.24	7.01
CAO	9.48	10.30	9.70	10.10	9.90	9.98
NA20	2.32	2.30	2.36	2.20	2.33	2.29
K20	0.50	0.61	0.57	0.50	0.70	0.44
P205	0.16	0.15	0.10	0.14	0.08	0.14
CO2	0.06	0.06	0.07	0.09	0.06	0.11
S	0.02	0.01	0.01	0.02	0.04	0.02
LOI	0.10	0.20	0.20	0.30	0.20	0.10
TOTAL	99.40	99.00	99.60	98.80	99.20	99.20

TRACE ELEMENT LISTING

	82RHS-0169	82RHS-0171	82RHS-0172	82RHS-0173	82RHS-0175	82RHS-0178
CR	62.00	58.00	111.00	118.00	111.00	101.00
V	342.00	288.00			244.00	243.00
NI	108.00	104.00	93.00	82.00	129.00	144.00
CO	28.00	34.00	48.00	49.00	46.00	37.00
CU	98.00	88.00	192.00	200.00	74.00	83.00
ZN	133.00	96.00	116.00	133.00	109.00	102.00
LI			12.00	10.00		
GA	22.00	19.00			26.00	22.00
PB	23.00	12.00	N.D.	N.D.	14.00	17.00
BA	160.00	194.00	200.00	180.00	240.00	149.00
SR	181.00	153.00			218.00	199.00
RB	17.00	N.D.			26.00	19.00
ZR	153.00	121.00			143.00	137.00
NB	38.00	20.00			37.00	36.00
Y	37.00	20.00			34.00	35.00

MAJOR OXIDE LISTING

	82RHS-0186	82RHS-0187	82RHS-0188	82RHS-0189	82RHS-0190	82RHS-0194
SIO2	48.50	49.00	49.90	48.90	48.70	49.60
TIO2	1.53	1.43	1.57	1.63	1.86	1.54
AL2O3	14.00	14.40	12.50	12.90	13.90	13.50
FE2O3	13.50	14.60	16.80	17.50	16.60	16.10
MNO	0.17	0.19	0.23	0.24	0.22	0.21
MGO	6.59	6.29	6.11	5.62	4.49	6.21
CAO	10.10	10.20	9.46	10.30	9.82	10.20
NA2O	2.79	2.85	2.14	2.17	2.55	2.09
K2O	0.62	0.42	0.54	0.40	0.57	0.46
P2O5	0.08	0.13	0.13	0.09	0.15	0.14
CO2	0.17	0.07	0.16	0.07	0.06	0.05
S	0.02	0.02	0.03	0.02	0.02	0.02
LOI	0.70	0.30	0.20	0.60	0.30	0.40
TOTAL	98.60	99.30	99.20	99.20	98.50	99.70

TRACE ELEMENT LISTING

	82RHS-0186	82RHS-0187	82RHS-0188	82RHS-0189	82RHS-0190	82RHS-0194
CR	116.00	95.00	12.00	50.00	28.00	116.00
V						302.00
NI	85.00	82.00	34.00	49.00	31.00	130.00
CO	46.00	49.00	36.00	52.00	46.00	40.00
CU	151.00	80.00	200.00	210.00	240.00	87.00
ZN	84.00	111.00	90.00	146.00	144.00	124.00
LI	20.00	8.00	5.00	10.00	10.00	
GA						21.00
PB	N.D.	N.D.	N.D.	N.D.	N.D.	13.00
BA	190.00	180.00	30.00	160.00	140.00	156.00
SR						170.00
RB						6.00
ZR						130.00
NB						29.00
Y						26.00

MAJOR OXIDE LISTING

	82RHS-0200	82RHS-0201	82RHS-0202	82RHS-0204	82RHS-0205	82RHS-0207
SIO2	49.60	49.20	49.60	50.00	47.90	70.50
TIO2	2.61	1.69	1.89	1.49	1.62	0.33
AL2O3	11.60	14.00	13.70	14.40	13.40	17.10
FE2O3	19.60	15.70	15.50	15.10	16.70	1.40
MNO	0.23	0.21	0.20	0.19	0.25	0.02
MGO	3.50	6.20	5.38	5.90	6.37	0.57
CAO	8.09	9.69	9.49	9.84	9.96	2.92
NA2O	2.57	1.96	1.92	2.15	2.01	5.28
K2O	1.12	0.78	0.90	0.66	0.38	1.00
P2O5	0.12	0.06	0.06	0.06	0.05	00.00
CO2	0.29	0.18	0.15	0.15	0.16	0.07
S	0.06	0.14	0.14	0.04	0.03	0.01
LOI	0.20	0.30	0.70	N.D.	0.30	0.40
TOTAL	99.30	99.70	99.40	99.70	99.00	99.50

TRACE ELEMENT LISTING

	82RHS-0200	82RHS-0201	82RHS-0202	82RHS-0204	82RHS-0205	82RHS-0207
CR	N.D.	158.00	129.00	104.00	122.00	8.00
V		313.00	351.00			
NI	31.00	129.00	95.00	83.00	84.00	5.00
CO	50.00	60.00	50.00	51.00	52.00	5.00
CU	230.00	82.00	83.00	132.00	152.00	7.00
ZN	140.00	128.00	120.00	105.00	86.00	150.00
LI	13.00			10.00	10.00	10.00
GA		9.00	10.00			
PB	N.D.	19.00	28.00	11.00	290.00	56.00
BA	360.00	265.00	129.00	280.00	140.00	330.00
SR		189.00	207.00			
RB		10.00	7.00			
ZR		155.00	153.00			
NB		22.00	18.00			
Y		29.00	27.00			

MAJOR OXIDE LISTING

	82RHS-0210	82RHS-0214	82RHS-0216	82RHS-0218	82RHS-0219	82RHS-0220
SIO2	34.30	49.30	48.40	48.10	47.80	48.30
TIO2	0.31	1.28	1.57	1.27	1.08	1.11
AL2O3	7.03	15.50	13.70	15.50	15.70	14.60
FE2O3	5.68	13.90	15.60	14.20	14.60	14.80
MNO	00.00	0.20	0.20	0.18	0.17	0.19
MGO	10.20	5.62	6.47	7.63	8.35	8.63
CAO	15.10	10.40	10.20	10.00	9.99	10.20
NA2O	00.00	2.46	2.69	1.78	1.55	1.73
K2O	1.79	0.38	0.47	0.45	0.41	0.39
P2O5	0.01	0.02	0.05	0.02	0.01	00.00
CO2	24.20	0.07	0.13	0.13	0.15	0.15
S	0.01	0.01	0.01	0.03	0.03	0.03
LOI	25.40	N.D.	0.20	00.00	00.00	N.D.
TOTAL	99.80	98.90	99.50	99.20	99.70	99.70

TRACE ELEMENT LISTING

	82RHS-0210	82RHS-0214	82RHS-0216	82RHS-0218	82RHS-0219	82RHS-0220
CR	56.00	60.00	118.00	111.00	99.00	173.00
V				247.00	232.00	269.00
NI	20.00	48.00	83.00	186.00	207.00	208.00
CO	8.00	42.00	47.00	43.00	46.00	67.00
CU	8.00	153.00	120.00	113.00	105.00	102.00
ZN	118.00	140.00	130.00	88.00	93.00	90.00
LI	12.00	7.00	10.00			
GA				8.00	25.00	9.00
PB	N.D.	N.D.	114.00	12.00	19.00	10.00
BA	60.00	130.00	140.00	139.00	144.00	136.00
SR				182.00	196.00	168.00
RB				2.00	15.00	N.D.
ZR				98.00	99.00	90.00
NB				11.00	17.00	10.00
Y				24.00	31.00	21.00

MAJOR OXIDE LISTING

	82RHS-0221	82RHS-0222	82RHS-0223	82RHS-0224	82RHS-0225	82RHS-0226
SIO2	48.50	48.40	46.80	48.00	47.20	75.60
TIO2	1.19	1.17	1.13	1.14	0.96	0.88
AL2O3	15.10	16.10	13.70	14.20	14.70	11.80
FE2O3	14.50	13.00	15.00	13.90	14.20	5.11
MNO	0.18	0.17	0.19	0.19	0.18	0.02
MGO	8.18	7.31	9.04	7.48	9.41	2.02
CAO	10.40	10.80	10.90	10.40	10.80	1.19
NA2O	1.65	1.77	2.07	2.46	1.80	0.40
K2O	0.41	0.42	0.34	0.54	0.34	0.91
P2O5	0.02	0.01	0.01	0.08	00.00	0.05
CO2	0.11	0.08	0.08	0.07	0.11	0.09
S	0.03	0.02	0.02	0.03	0.02	0.01
LOI	N.D.	N.D.	N.D.	0.20	N.D.	2.60
TOTAL	99.70	98.90	99.00	98.50	99.20	100.60

TRACE ELEMENT LISTING

	82RHS-0221	82RHS-0222	82RHS-0223	82RHS-0224	82RHS-0225	82RHS-0226
CR	188.00	179.00	257.00	148.00	245.00	20.00
V	284.00	254.00	323.00	270.00	265.00	N.D.
NI	185.00	153.00	196.00	152.00	215.00	11.00
CO	43.00	43.00	50.00	40.00	59.00	14.00
CU	103.00	98.00	95.00	96.00	90.00	31.00
ZN	91.00	81.00	92.00	87.00	84.00	24.00
GA	24.00	15.00	10.00	68.00	7.00	17.00
PB	17.00	10.00	11.00	10.00	7.00	12.00
BA	134.00	127.00	115.00	211.00	120.00	113.00
SR	194.00	188.00	170.00	203.00	175.00	215.00
RB	18.00	9.00	5.00	10.00	8.00	29.00
ZR	101.00	91.00	84.00	98.00	86.00	616.00
NB	17.00	9.00	13.00	12.00	20.00	51.00
Y	33.00	26.00	26.00	29.00	28.00	31.00

MAJOR OXIDE LISTING

	82RHS-0228	82RHS-0229	82RHS-0230	82RHS-0231	82RHS-0232	82RHS-0233
SIO2	48.60	47.90	46.70	49.80	46.30	49.60
TIO2	1.46	1.58	1.54	1.52	1.24	1.40
AL2O3	14.00	13.70	13.50	14.20	14.60	15.00
FE2O3	14.20	12.70	12.70	13.80	15.90	13.60
MNO	0.20	0.16	0.14	0.18	0.20	0.18
MGO	5.93	5.33	5.47	6.09	7.95	6.29
CAO	9.67	9.53	10.00	9.70	9.97	10.10
NA2O	2.87	2.34	2.87	2.56	2.22	2.50
K2O	0.50	0.67	0.49	0.62	0.38	0.65
P2O5	0.06	0.05	0.06	0.05	0.02	0.04
CO2	1.76	3.72	5.76	0.14	0.10	0.07
S	0.04	0.02	0.04	0.05	0.03	0.05
LOI	1.50	4.30	5.90	0.20	00.00	00.00
TOTAL	99.00	98.30	99.40	98.70	98.70	99.30

TRACE ELEMENT LISTING

	82RHS-0228	82RHS-0229	82RHS-0230	82RHS-0231	82RHS-0232	82RHS-0233
CR	117.00	113.00	126.00	110.00	115.00	117.00
V	334.00	292.00	276.00	318.00	277.00	234.00
NI	119.00	113.00	110.00	117.00	191.00	129.00
CO	50.00	57.00	46.00	45.00	47.00	48.00
CU	64.00	76.00	88.00	96.00	118.00	103.00
ZN	104.00	52.00	41.00	103.00	98.00	85.00
GA	9.00	N.D.	2.00	27.00	5.00	9.00
PB	2.00	N.D.	4.00	8.00	1.00	
BA	257.00	234.00	199.00	286.00	122.00	252.00
SR	197.00	183.00	212.00	216.00	164.00	202.00
RB	N.D.	N.D.	4.00	36.00	N.D.	N.D.
ZR	122.00	113.00	122.00	132.00	88.00	102.00
NB	12.00	9.00	13.00	22.00	12.00	12.00
Y	26.00	22.00	28.00	38.00	22.00	21.00

MAJOR OXIDE LISTING

	82RHS-0234	82RHS-0235	82RHS-0236	82RHS-0237	82RHS-0238	82RHS-0302
SIO2	47.20	52.30	49.80	49.50	49.90	50.70
TIO2	1.00	1.44	1.44	1.74	1.48	1.32
AL2O3	14.70	14.00	13.80	13.60	14.10	14.10
FE2O3	13.50	14.00	15.20	14.80	14.40	13.70
MNO	0.18	0.19	0.20	0.19	0.18	0.19
MGO	9.17	4.76	5.84	5.41	5.94	6.23
CAO	10.70	9.33	9.84	9.12	9.74	10.60
NA2O	1.83	2.66	2.34	2.98	2.45	2.66
K2O	0.37	0.94	0.60	0.70	0.66	0.65
P2O5	0.01	0.11	0.05	0.07	0.06	0.12
CO2	0.08	0.08	0.07	0.09	0.08	0.09
S	0.03	0.05	0.07	0.06	0.05	0.06
LOI	00.00	N.D.	0.20	00.00	00.00	0.30
TOTAL	98.60	99.70	99.40	98.20	98.90	100.00

TRACE ELEMENT LISTING

	82RHS-0234	82RHS-0235	82RHS-0236	82RHS-0237	82RHS-0238	82RHS-0302
CR	252.00	58.00	104.00	76.00	109.00	74.00
V	253.00	274.00	337.00	311.00	320.00	
NI	123.00	79.00	108.00	96.00	116.00	68.00
CO	62.00	42.00	42.00	44.00	42.00	38.00
CU	89.00	112.00	113.00	97.00	97.00	117.00
ZN	123.00	103.00	110.00	106.00	95.00	82.00
LI						16.00
GA	N.D.	10.00	18.00	21.00	11.00	
PB	4.00		11.00	14.00	8.00	N.D.
BA	117.00	363.00	300.00	291.00	285.00	160.00
SR	172.00	191.00	222.00	213.00	208.00	
RB	N.D.	1.00	25.00	26.00	11.00	
ZR	75.00	168.00	108.00	133.00	122.00	
NB	8.00	14.00	12.00	11.00	11.00	
Y	17.00	32.00	30.00	33.00	30.00	

MAJOR OXIDE LISTING

	82RHS-0306	82RHS-0307	82RHS-0317	82RHS-0318	82RHS-0319	82RHS-0320
SIO2	48.70	49.80	48.20	48.60	47.70	49.00
TIO2	1.85	1.32	0.90	0.91	1.08	1.37
AL2O3	13.10	14.20	14.80	15.20	14.90	14.30
FE2O3	16.00	13.70	13.00	12.80	14.70	14.20
MNO	0.20	0.18	0.18	0.17	0.19	0.18
MGO	5.89	6.32	9.01	8.46	8.31	7.03
CAO	9.06	9.54	11.10	11.20	10.30	10.40
NA2O	2.28	2.75	1.85	1.98	2.06	2.41
K2O	1.08	0.76	0.35	0.36	0.42	0.53
P2O5	0.14	0.14	0.09	0.11	0.10	0.11
CO2	0.17	0.17	0.15	0.17	0.19	0.09
S	0.16	0.04	0.02	0.02	0.03	0.02
LOI	0.80	0.50	00.00	0.20	0.40	0.30
TOTAL	99.10	99.30	99.60	99.70	99.30	99.90

TRACE ELEMENT LISTING

	82RHS-0306	82RHS-0307	82RHS-0317	82RHS-0318	82RHS-0319	82RHS-0320
CR	121.00	96.00	233.00	240.00	172.00	123.00
V			193.00	192.00	214.00	255.00
NI	72.00	87.00	163.00	159.00	171.00	143.00
CO	57.00	53.00	50.00	52.00	48.00	41.00
CU	90.00	126.00	69.00	70.00	77.00	79.00
ZN	115.00	100.00	81.00	84.00	104.00	99.00
LI	14.00	18.00				
GA			16.00	20.00	21.00	19.00
PB	N.D.	21.00	3.00	12.00	17.00	14.00
BA	260.00	240.00	114.00	127.00	135.00	162.00
SR			174.00	196.00	194.00	214.00
RB			7.00	17.00	16.00	24.00
ZR			90.00	106.00	116.00	147.00
NB			24.00	32.00	33.00	37.00
Y			21.00	27.00	26.00	35.00

MAJOR OXIDE LISTING

	82RHS-0322	83RHS-0003	83RHS-0004	83RHS-0251	83RHS-0253	83RHS-0260
SIO2	48.70	46.40	58.00	47.10	45.50	44.60
TIO2	1.55	1.64	0.60	2.68	80.23	1.88
AL2O3	13.60	8.08	14.70	11.50	97.41	7.72
FE2O3	15.60	14.60	4.87	15.30	66.00	17.30
MNO	0.21	0.27	0.10	0.21	9.02	0.21
MGO	6.50	1.64	0.90	8.82	1.36	17.10
CAO	10.10	18.50	7.00	9.32	0.80	7.98
NA2O	2.18	0.97	2.35	2.53	90.18	1.32
K2O	0.47	3.58	7.30	0.66	50.05	0.41
P2O5	0.13	0.40	0.20	0.20	2.01	0.14
CO2	0.10	0.20	0.43	0.21	0.03	0.19
S	0.02	0.02	0.01	0.04	80.00	0.02
H2O+	00.00	00.00	00.00	00.00	30.00	00.00
LOI	0.30	0.70	0.90	-0.10	0.10	0.20
TOTAL	98.80	96.80	96.90	98.40	98.80	98.90

TRACE ELEMENT LISTING

	82RHS-0322	83RHS-0003	83RHS-0004	83RHS-0251	83RHS-0253	83RHS-0260
CR	108.00	6.00	N.D.	430.00	705.00	1000.00
NI	87.00	N.D.	N.D.	305.00	605.00	755.00
CO	50.00	9.00	5.00	57.00	75.00	91.00
CU	200.00	8.00	8.00	96.00	108.00	82.00
ZN	143.00	90.00	42.00	250.00	155.00	150.00
LI	9.00	9.00	6.00	38.00	10.00	10.00
PB	N.D.	N.D.	15.00	62.00	N.D.	N.D.
BA	130.00	1500.00	3680.00	270.00	240.00	140.00

MAJOR OXIDE LISTING

	83RHS-0341	83RHS-0342
SIO2	72.70	73.30
TIO2	0.33	0.22
AL2O3	13.10	12.20
FE2O3	3.60	2.97
MNO	0.03	0.03
MGO	1.03	0.68
CAO	0.14	0.10
NA2O	00.00	00.00
K2O	7.57	8.51
P2O5	0.08	0.06
CO2	0.11	0.09
S	00.00	00.00
H2O+	00.00	00.00
LOI	1.70	1.40
TOTAL	100.20	99.50

TRACE ELEMENT LISTING

	83RHS-0341	83RHS-0342
CR	20.00	19.00
NI	6.00	N.D.
CO	6.00	N.D.
CU	8.00	10.00
ZN	73.00	85.00
LI	30.00	53.00
PB	40.00	33.00
BA	1020.00	800.00

APPENDIX 6

RARE EARTH ELEMENT ANALYSES

Appendix 6· Rare earth element analyses

	80-396	80-1099	81-104	81-273	81-276	81-285	81-286	81-288	81-290	81-292	81-293	82-4	82-56	82-69	82-73
La	52	150	23	8	7	18	7	5	6	6	8	14	5	21	7
Ce	105	310	50	15	15	40	14	11	11	15	30	30	10	45	17
Nd	40	115	20	8	9	23	8	6	7	8	18	15	4	18	10
Sm	8	21	5	ND	ND	7	3	3	3	3	9	4	2	5	3
Eu	21	50	3	8	8	19	10	9	9	10	14	14	9	12	12
Gd	6	14	4	3	4	8	3	3	3	3	6	4	2	4	4
Dy	4.0	7.0	4.1	1.5	1.8	8.0	3.5	2.9	2.7	3.5	5.0	3.0	1.9	4.4	4.5
Yb	1.5	1.4	2.3	0.5	0.7	4.2	1.7	1.5	1.4	1.8	1.8	1.1	0.9	2.2	2.3

	82-74	82-75	82-116	82-142	82-143	82-144	82-201	82-202	82-229	82-232	82-234	82-235	82-237
La	8	12	9	140	180	16	17	20	10	7	10	20	14
Ce	17	26	22	310	345	31	35	22	20	15	11	40	30
Nd	10	12	11	100	120	15	17	6	11	7	6	18	14
Sm	4	4	ND	26	31	7	5	6	5	3	4	6	5
Eu	12	12	15	9	11	19	13	17	13	10	12	16	14
Gd	4	4	2	22	19	8	4	5	4	3	4	6	4
Dy	4.3	4.1	2.8	23.0	20.0	4.5	4.3	5.2	4.1	3.1	30	6.0	4.8
Yb	2.2	2.1	0.9	13.0	10.0	1.4	2.2	2.6	2.0	1.5	1.3	3.0	2.4

ND- not detected

APPENDIX 7

MINERAL ANALYSES

```
                         PYROXENE ANALYSES

          1             2             3             4             5             6             7             8
SIO2    47.93         51.68         50.59         52.70         51.46         52.57         49.34         49.72
TIO2     1.05           .87          1.15           .30          1.33           .43           .00           .77
AL2O3    6.25          7.62          7.37          6.57          3.03          6.18          6.77          7.42
CR2O3     .10           .16           .31           .02           .03           .34           .14           .31
FEO     12.17         12.58          9.35          5.56          9.21          5.48         12.46          8.96
MNO       .31           .30           .24           .16           .27           .12           .31           .23
MGO     11.70         11.66         13.01         15.63         13.43         15.00         11.31         14.17
CAO     17.73         16.72         19.18         20.38         21.36         20.78         17.97         19.86
NA2O     1.10          1.07           .52           .42           .20           .33           .36           .52
K2O       .01           .01          0.00           .01          0.00          0.00           .02           .01
SUM    100.35        100.15         99.64        100.03        100.13        100.49        100.43         99.98

SI      1.793         1.932         1.834         1.842         1.917         1.873         1.845         1.933
AL       .207  2.000   .168  2.000   .166  2.000   .158  2.000   .083  2.000   .127  2.000   .154  2.000   .172  2.000
AL       .154          .163          .136          .123          .052          .139          .143          .152
TI       .034          .025          .032          .017          .029          .012          .023          .020
CR       .003          .005          .009          .023          .001          .027          .004          .014
FE       .382          .396          .292          .169          .287          .167          .390          .214
MG       .654          .651          .724          .840          .740          .813          .063          .777
MN       .010          .012          .006          .005          .009          .007          .010          .007
CA       .712          .679          .768          .797          .853          .794          .705          .787
NA       .080          .078          .036          .030          .014          .023          .377          .037
K        .000  2.032   .000  2.012  0.000  2.007   .000  2.007  0.000  1.992  0.000  1.990   .001  2.114   .048  2.302
O       6.000         6.000         6.000         6.000         6.000         6.000         6.000         6.000
   WO          40.75         39.79         43.03         43.96         45.22         44.77         40.17         44.11
   EN          41.83         22.46         16.37          9.34         15.22          9.40         22.11         12.07
   FS          17.41         37.76         40.60         46.90         39.56         45.84         37.73         43.82

   F/M          .599          .624          .414          .205          .396          .213          .601          .235
   F/FM         .374          .384          .293          .170          .284          .175          .375          .222

 1 80-337 ZONED CPX  PHENO 1A CORE                 5 80-337 CPX 23 RIM
 2 80-337 CPX PHENO 1A CORE                        6 80-337 CPX 2A CORE
 3 80-337 CPX PHENO 1B                             7 80-337 CPX PHENO 3A CORE
 4 80-337 CPX 2A CORE                              8 80-337 CPX PHENO 3B CORE
```

```
SUM [illegible] CAL                   [illegible]
       57            58            59            60            61            62            63            64
SIO2   [illegible]   [illegible]   [illegible]   [illegible]   52.39         52.[illegible]6  52.74      54.35
TIO2   .4[illegible] .[illegible]  .[illegible]  .1[illegible] .42           1.16          .1[illegible]  .27
AL2O3  1.41          .7[illegible] 1.[illegible]1  1.[illegible]3  1.42      2.43          1.89          .65
CR2O3  [illegible]   .1[illegible] .[illegible]  .[illegible]7 .53           .45           .43           .19
FEO    [illegible]7  [illegible]   [illegible]2  7.17          6.30          [illegible].76  5.82        5.41
MNO    [illegible]   .0[illegible] [illegible]   .11           .01           .05           .02           .04
MGO    1[illegible]  [illegible]6  1[illegible]  16.[illegible]  1[illegible].20  16.39    16.29         16.56
CAO    20.[illegible] [illegible]  20.19         19.[illegible]  1[illegible].40  19.63    22.52         21.42
NA2O   .[illegible]4 .[illegible]  .41           .42           .28           .30           .45           .62
K2O    0.10          [illegible]0  0.[illegible]0  0.[illegible]0  0.00      0.10          0.00          0.00
SUM    10[illegible]7 [illegible]  [illegible]   [illegible]21 [illegible].10 [illegible].63  101.69      99.49

SI     [illegible]   1.[illegible]  1.[illegible]  1.941        1.957         1.923         1.926         1.990
AL     .0[illegible] 2.000  .111 2.000  .1[illegible] 2.000  .0[illegible] 2.000  .047 2.000  .077 2.000  .076 2.000  .002 2.000
AL     .10[illegible] .[illegible]  .0[illegible]  .021        .015          .02[illegible]  .005        .026
TI     .[illegible]  .10[illegible] .01[illegible]  .0[illegible]2  .012     .024          .026          .007
CR     .01[illegible] .[illegible]  .001          .006          .017          .025          .012          .006
FE     .21[illegible] .1[illegible] .203          .21[illegible]  .194      .204          .179          .166
MG     .[illegible]  .[illegible]   .[illegible]7  .917         .903          .902          .886          .906
MN     .002          .002          .003          .003          .000          .002          .001          .001
CA     .[illegible]7 .[illegible]   .81[illegible]  .776        .767          .777          .880          .844
NA     .[illegible]6 .0[illegible]  .020          .030          .020          .021          .032          .044
K      0.00[illegible] 2.0[illegible]  0.0[illegible] 1.004  [illegible] 2.0[illegible]2  0.000 2.0[illegible]5  0.000 2.005  0.000 1.9[illegible]3  0.000 2.019  0.000 2.000
O      6.000         6.000         6.000         6.000         6.000         6.000         6.000         6.000
  MG          41.[illegible]1   44.[illegible]   42.[illegible]   40.64   38.46   41.15   45.29   44.03
  FE          10.[illegible]    [illegible]      10.37            11.45   10.01   11.06   9.14    8.68
  CA          47.[illegible]    4[illegible].74  47.10            47.90   51.53   47.79   45.57   47.29

  F/[illegible]   .[illegible]   .[illegible]   .[illegible]   .[illegible]3   .195   .233   .201   .165
  F/FM            .19[illegible]  .17[illegible]  .14[illegible]  .19[illegible]  .163   .181   .167   .156

57 41-276 CPX [illegible]                           61 41-273 CPX 1A CORE
58 41-276 [illegible]                               62 41-273 CPX 1B RIM
59 41-276 [illegible]                               63 41-273 CPX 2
60 41-276 [illegible]                               64 41-273 CPX 3A CORE
```

202

```
SUPRA [illegible]                [illegible]PTION PYX- [illegible]
          17            18            19            20            21            22            23            24
SIO2     51.46         4[illegible]   43.45         4[illegible].7 47.34        47.[illegible]8 4[illegible].34  44.60
TIO2       [illegible]   .[illegible]   .[illegible]4  .[illegible]1   .41          .77          1.04           .75
AL2O3     [illegible]    5.6[illegible] 7.[illegible]  [illegible].1[illegible] 4.13     4.21         3.14          7.61
CR2O3      [illegible]   .36            .37            .11            .10          .14           .19           .18
FEO       4.4[illegible] [illegible].21 13.[illegible]4 [illegible].7[illegible] 10.03  10.[illegible]1  4.25   10.77
MNO        .11           .1[illegible]  .[illegible]7  .11            .27          .33           .10           .30
MGO      1[illegible].[illegible]7 16.70 1[illegible].[illegible] 13.3[illegible] 13.41  13.06        14.05         12.52
CAO      22.49         1[illegible].[illegible] 21.34  14.46          17.8[illegible] 17.78      21.62         18.98
NA2O       .43           .2[illegible]  .[illegible]7  .[illegible]1  .84          .74           .16          1.01
K2O       [illegible].10 [illegible].[illegible]0 0.00 [illegible].0[illegible] .02    .01           .01          0.00
SUM      10[illegible].[illegible] 10[illegible].4[illegible] 10[illegible].[illegible]5 9[illegible].75 9[illegible].7[illegible] 100.45 94.15 100.72

 SI     1.[illegible]   .      1.[illegible]  .      1.667    .      1.744    .      1.765    .      1.773    .      1.[illegible]71 .    1.609    .
 AL      .115  2.0[illegible]0 .2[illegible] 2.00[illegible] .[illegible]14 1.9[illegible] .[illegible]1[illegible] 2.000 .232 2.000 .227 2.000 .124 2.000 .191 2.000
 AL      .[illegible]7  .      .1[illegible]  .      0.000    .       .192    .       .159    .       .174    .       .011    .       .142    .
 TI      .[illegible]1[illegible] . .[illegible] .        .024    .       .117    .       .123    .       .021    .       .030    .       .021    .
 CR      .[illegible]17 .      .[illegible]2[illegible] . .011   .       .[illegible]0[illegible] . .003 .       .004    .       .00[illegible] . .005 .
 FE      .134   .      .[illegible]6[illegible] . .434    .       .272    .       .311    .       .309    .       .293    .       .335    .
 MG      .[illegible]  .      .[illegible]    .       .743    .       .741    .       .746    .       .752    .       .793    .       .694    .
 MN      .[illegible]0[illegible] . .[illegible]0[illegible] . .007 . .[illegible]10 .     .009    .       .010    .       .010    .       .009    .
 CA      .[illegible]7[illegible] . .77[illegible] . .477  .       .[illegible]34 .        .713    .       .704    .       .[illegible]74 .    .757    .
 NA      .033   .      .[illegible]     .       .020    .       .050    .       .061    .       .05[illegible] . .[illegible]12 .     .073    .
 K       .[illegible]0[illegible] 2.011 [illegible].00[illegible] 2.053 0.000 2.167 .00[illegible] 2.018 .001 2.038 .001 2.030 .[illegible]00 2.032 0.000 2.037
 O      [illegible].000 .      [illegible].[illegible]0[illegible] . 6.000 .     6.000    .      6.000    .      6.000    .      6.000    .      6.000    .
      MG        41.9[illegible]   3[illegible].74   41.6[illegible]  42.01    40.24    39.87    44.64    42.36
      FE         7.[illegible]    17.03    20.55    15.6[illegible]  17.67    17.52    14.92    18.76
      CA        45.97    47.23    37.67    42.31    42.10    42.61    40.40    38.87

      F/M        .15[illegible]   .2[illegible]   .[illegible]54   .381     .431     .425     .382     .496
      F/FM       .13[illegible]   .220     .354     .276     .301     .294     .276     .332

17 80-271  PX PHENO 1F CORE                  21 80-336 CPX PHENO 1B
18 80-337 CPX 4A CORE                        22 80-336 CPX PHENO 1C RIM
19 80-337  PX 4B RIM                         23 80-336 CPX 2
20 80-196  PX PHENO 1A COR                   24 80-337 GAM INCL CPX 1
```

257

```
[illegible] CAL          [illegible]

         25          26          27          28          29          30          31          32
SIO2     [illegible] [illegible] 47.[illegible] 4[illegible].21 50.38  50.53      50.52      49.62
TIO2     .27         [illegible] 1.23        1.[illegible]  .40         .36         .33         .38
AL2O3    7.70        7.[illegible] 7.36      7.[illegible]0 5.73        6.02        5.74        5.93
CR2O3    [illegible] [illegible] 0.30        0.00        0.00        0.00        0.00        0.00
FEO      [illegible] 10.[illegible] 16.25    10.[illegible]3 19.45      18.91       19.26       19.64
MNO      [illegible] [illegible] 0.00        .35         .14         .16         .13         .03
MGO      [illegible] 12.[illegible] 12.70    12.[illegible]4 22.21      23.16       23.27       22.89
CAO      [illegible] 14.30       1[illegible].66 1[illegible].45 1.25   1.39        1.33        1.31
NA2O     [illegible] [illegible] 1.19        1.0[illegible] .04         .10         .24         .18
K2O      [illegible] [illegible] 0.00        0.00        0.00        0.00        0.00        0.00
SUM      [illegible] 10[illegible] 111.11    [illegible] 100.26      100.63      100.82      99.98

 SI   1.[illegible]        1.[illegible]        1.7[illegible]       1.80[illegible]      1.869        1.848        1.846        1.833
 AL    .21[illegible] 2.000 [illegible] 2.00[illegible] .241  2.100  .196   2.000  .131   2.000  .152   2.010  .154   2.000  .167   2.000
 AL    .177                [illegible]          .107                 .155                 .117         .107         .093         .091
 TI    .022                [illegible]          .[illegible]         .034                 .013         .010         [illegible]  .011
 CR    .00[illegible]      [illegible]          0.009                0.000                0.000        0.000        0.000        0.000
 FE    .34[illegible]      [illegible]          .317                 .3[illegible]0       .596         .577         .588         .607
 MG    .6[illegible]       [illegible]          .678                 .[illegible]46       1.214        1.260        1.267        1.260
 MN    .012                [illegible]          0.000                .002                 .004         .005         .004         .001
 CA    .771                [illegible]          .746                 .741                 .049         .056         .052         .052
 NA    .071                [illegible]          .085                 .17[illegible]       .003         .007         .117         .013
 K     .00[illegible] 2.050 [illegible] 2.0[illegible] 0.000 2.019 0.00[illegible] 2.024 0.000 1.996 0.000 2.016 0.000 2.030 0.000 2.034
 O     [illegible]         [illegible]          6.000                6.000                6.000        6.000        6.000        6.000
    WO        42.72        [illegible]          42.66                42.2[illegible]      2.64         2.67         2.73         2.70
    FS        [illegible]  1[illegible].6[illegible] 1[illegible]   1[illegible].91      32.08        30.59        30.85        31.62
    EN        [illegible].47 [illegible].96     39.17                [illegible]          65.28        66.75        66.42        65.68

    F/M       .50[illegible] [illegible]        .45[illegible]       [illegible]          .495         .462         .468         .492
    F/FM      [illegible]  [illegible]          .319                 [illegible]          .331         .316         .319         .325

25 40-337 CA INCL CPX 3                               29 40-337 UM 100 OPX 1A CORE
26 40-337 CA INCL CPX 4                               30 40-337 UM 100 OPX 1B EDGE
27 40-337 UM 100 CPX 1                                31 40-337 UM 100 OPX 1C MIDDLE
28 40-337 UM 100 CPX 2                                32 40-337 UM 100 OPX 2A CORE
```

```
SUM[illegible]                          [illegible]
         35              36              37             [illegible]      47              48              33              40
SIO2   [illegible]     [illegible]     [illegible]     [illegible]     44.51           48.[illegible]9  49.51           51.27
TIO2   [illegible]      1.[illegible]6   1.16            .76            .44            .[illegible]2    .65             .51
AL2O3   1.[illegible]  .7[illegible]   [illegible].17  [illegible]     5.02           [illegible]     6.12            3.06
CR2O3  [illegible]     [illegible]     [illegible]      0.00           0.00           0.[illegible]0  0.00             .27
FEO    [illegible]     [illegible]     10.7[illegible] 13.64           13.15          1[illegible].61 13.00            8.75
MNO    [illegible]      1.11             .07           [illegible]      0.00            .06           0.00             .02
MGO    [illegible]     [illegible]     12.[illegible]  11.[illegible]  11.13          10.82           11.08           16.11
CAO     1.[illegible]7 [illegible]     1[illegible].49 1[illegible].02 19.65          19.69           19.21           19.42
NA2O    .[illegible]    1.[illegible]   1.[illegible]3  1.0[illegible]  1.04           1.01            1.13            0.00
K2O    [illegible]      0.00            0.00            0.00            0.00           0.00             .02            0.00
SUM    101.[illegible]7 [illegible].17 [illegible]     100.44          94.31          100.08          100.25           99.41

SI      1.941     .    1.78[illegible]  .    1.777     .    1.837     .    1.877     .    1.840     .    1.937     .    1.908     .
AL      .17[illegible] 2.0[illegible]0  .211 2.000   .223 2.000   .163 2.000   .123 2.000   .160 2.000   .163 2.000   .092 2.000
AL      .1[illegible]   .    .141      .    .143      .    .130      .    .101      .    .105      .    .118      .    .043      .
TI      .011      .    .13[illegible]   .    .[illegible]33  .    .021      .    .013      .    .018      .    .025      .    .014      .
CR     [illegible]   .    0.[illegible]   .    0.10[illegible] .    0.000     .    0.000     .    0.000     .    0.000     .    .008      .
FE      .5[illegible]  .    .[illegible]66  .    .[illegible]41  .    .471      .    .417      .    .437      .    .411      .    .272      .
MG     [illegible]   .    .[illegible]00  .    .[illegible]4[illegible] .    .620      .    .632      .    .513      .    .624      .    .894      .
MN      .[illegible]07  .    0.000     .    .001      .    0.000     .    0.000     .    .001      .    0.000     .    .001      .
CA      .[illegible]56  .    .[illegible]44  .    .[illegible]52  .    .770      .    .788      .    .802      .    .774      .    .774      .
NA      .[illegible]1   .    .101      .    .091      .    .079      .    .076      .    .074      .    .083      .    0.000     .
K      [illegible].901 2.02[illegible] 0.000 2.046  0.000 2.052  0.000 2.040  0.000 2.037  0.000 2.047   .001 2.039  0.000 2.006
O       6.000     .    6.000     .    6.000     .    6.000     .    6.000     .    6.000     .    6.000     .    6.000     .
   MG          2.42            41.79           42.1[illegible]   42.27           43.22           41.40           42.91           39.31
   FE         [illegible].37   13.47           13.3[illegible]   23.66           22.57           23.42           22.66           14.04
   CA         [illegible].31   18.73           18.76             34.07           34.21           33.19           34.43           46.06

   F/M         .[illegible]73   .[illegible]01   .436           .[illegible]34   .660            .708            .658            .305
   F/FM        .324            .[illegible]4    .[illegible]3[illegible] .410      .398            .414            .397            .234

35 80-337 JM [illegible] CPX 2[illegible] RIM              47 90-337 GAR NOD CPX 2A CORE
36 80-337 JM [illegible] CPX 3A RIM                        48 90-337 GAR NOD CPX 2B RIM
37 80-337 JM [illegible] CPX 3[illegible] CORE             54 30-337 GAR NOD CPX 3 CORE
38 80-337 [illegible] CPX 1                                40 41-292 CPX 1A CORE
```

```
SUPER ACCOL                    [illegible] BY [illegible]
 #          41             42             43             44             45             46             47             48
SIO2    [illegible]    [illegible]    [illegible]    [illegible]        55.31          55.16          54.51          54.43
TIO2    [illegible]        .46            .53            .48            1.12           .58            .55            .51
A2O3    [illegible]    [illegible]    [illegible]    [illegible]        1.04           1.19           .93            .92
C2O3        .13        [illegible]        0.00           .02            .43            .47            .10            .06
FEO     [illegible]    [illegible]    [illegible]        12.01          12.15          12.15          12.16          12.22
MNO         .10            .15            .21            .27            .03            .04            .11            .13
MGO     [illegible]        17.17      [illegible]    [illegible]        28.48          29.19          28.69          28.37
CAO     [illegible]        17.43          17.26          1.34           1.74           1.57           1.67           1.70
NA2O    [illegible]        1.90           0.00           .04            .04            0.00           0.00           .15
K2O     [illegible]    [illegible]        0.00           0.00           0.00           0.00           0.00           0.00
SUM     [illegible]    [illegible]    [illegible]        100.08         100.44         100.40         98.72          98.49

 SI    [illegible]  .     [illegible]  .     [illegible]  .     [illegible]  .     1.950   .      1.955   .      1.965   .      1.968   .
 AL    [illegible] 2.000  [illegible] 2.000  [illegible] 2.000  [illegible] [illegible]  .040 2.000  .045 2.000  .035 2.000  .032 2.000
 AL    [illegible]  .     [illegible]  .      .020  .     [illegible]  .      .005   .       .005   .       .005   .       .008   .
 TI    [illegible]  .     [illegible]  .     [illegible]  .      .013  .      .030   .       .015   .       .015   .       .014   .
 CR    [illegible]  .     [illegible]  .     [illegible]  .      .001  .      .012   .       .013   .       .003   .       .002   .
 FE    [illegible]  .     [illegible]  .      .416  .     [illegible]  .      .360   .       .360   .       .367   .       .370   .
 MG    [illegible]  .     [illegible]  .     [illegible]  .     [illegible]  .     1.504   .      1.542   .      1.542   .      1.529   .
 MN    [illegible]  .     [illegible]  .      .007  .     [illegible]  .      .003   .       .003   .       .003   .       .004   .
 CA    [illegible]  .     [illegible]  .     [illegible]  .      .051  .      .066   .       .060   .       .065   .       .066   .
 NA    [illegible]  .     [illegible]  .     [illegible]  .     [illegible]  .      .003   .      0.000   .      0.000   .       .011   .
 K     [illegible] [illegible]  [illegible] [illegible]  [illegible] [illegible]  [illegible] 2.011  0.000 1.981  0.000 1.938  0.000 1.999  0.000 2.002
 O     [illegible]  .     [illegible]  .     [illegible]  .      6.000  .     6.000   .      6.000   .      6.000   .      6.000   .
      WO    [illegible]      [illegible]      [illegible]        2.56           3.42           3.04           3.27           3.35
      FS    [illegible]        15.51            21.22            17.88          18.65          18.35          18.58          18.41
      EN    [illegible]      [illegible]      [illegible]        79.50          77.91          78.60          78.15          77.84

      [illegible]  [illegible]  [illegible]  [illegible]  [illegible]  .241  .235  .240  .244
      [illegible]  [illegible]  [illegible]  [illegible]  [illegible]  .194  .191  .194  .196

41 81-282  PX 1[illegible]                         45 81-273 OPX 1A CORE
42 81-282  PX 1[illegible]                         46 81-273 OPX 1C RIM
43 81-2[illegible]  [illegible]                    47 81-273 OPX 1D RIM
44 81-273  PX 14                                   48 81-273 OPX 2 CORE
```

```
                                                                    53        54        55        56
[illegible]                                                      51.6?     5?.?0     52.15     56.05
                                                                   .56       .61       .43       .04
                                                                  2.7?      1.55      2.07       .1?
                                                                   .5?       .57       .33   [illegible]
                                                                  7.65      1.08      6.97      0.1?
                                                                   .01       .10      0.06     14.?0
                                                                 15.47     17.05     16.11     28.?7
                                                                 20.11     14.69     20.47      1.07
                                                                   .11       .02       .44       .02
                                        0.30                      0.00      0.00      0.00      0.00
                                      101.64                     99.70     99.17     99.66    100.71

          2.010           2.000           2.100    1.917            1.912    1.947      1.918      1.992
                                                    .10?     1.946   .105     .057 2.010 .070 2.000 .007 1.999
                                           .016    0.020             .021     .019      .110      0.000
                                           .009     .014             .023     .017      .026      .001
                                           .007                      .112     .017      .010      0.000
                                                    .204             .737     .215      .211      .422
                                          1.40?                      .165     .936      .909      1.535
                                                   0.000             .901     .003      0.000     .006
                                                    .921             .480     .777      .825      .021
                                                    .015             .029     .012      .034      .001
               2.077          1.945        1.?49   0.000    2.043    0.000 2.021 0.000 2.010 0.000 2.013 0.000 2.006
                                                   6.000             6.000    6.000     6.000     6.000
                                                            41.51         41.14     40.39     42.80      2.0?
               18.?5          20.25        19.61            10.44         12.22     11.15     10.96     21.13
               75.77          7?.67        7?.03            4?.1?         46.60     48.55     46.1?     76.83

               .27?            .270         .?92             .2?1          .263      .231      .230      .279
               .21?            .211         .21?             .171          .204      .191      .192      .218

49 41-276 CPX 1A RIM                       53 41-276 CPX 1B RIM
50 41-276 OPX 1A CORE                      54 41-276 CPX 1C RIM
51 41-276 PX 1C CORE                       55 41-276 CPX 2
52 41-276 CPX 1A CORE                      56 41-275 OPX 2 OVERGROWTH
```

```
SUM [illegible] CAL                    [illegible] PYROXENES
            57          58          59          60          61          62          63          64
SIO2   [illegible]  [illegible]  [illegible].43  [illegible]  5[illegible].18  5[illegible].6  52.74       54.35
TIO2       .40         .36     [illegible]   [illegible]   .42        1.16       .1[illegible]    .27
AL2O3     1.41         .7[illegible]   1.[illegible]1  1.[illegible]3  1.42  2.43   1.49         .65
CR2O3  [illegible]     .[illegible]4   .0[illegible]   .[illegible]7   .53    .45    .43          .19
FEO    [illegible]7   [illegible]    6.[illegible]2  7.17       6.30       [illegible].76  5.82    5.41
MNO    [illegible]     .0[illegible]   .[illegible]5   .11        .01        .05        .02          .04
MGO      17.1[illegible]  16.16   1[illegible]   16.[illegible]  15.20   16.19      16.29       16.56
CAO      20.[illegible]  [illegible]  20.19   1[illegible].[illegible]6  1[illegible].10  19.63  22.52  21.42
NA2O       .44         .[illegible]9   .41        .[illegible]2   .[illegible]8  .30        .45          .62
K2O       0.00        [illegible].00   0.00       0.00       0.00       0.00       0.00         0.00
SUM     10[illegible].[illegible]7  [illegible].1[illegible]  [illegible]  [illegible].21  [illegible].10  9[illegible].63  101.69  99.49

SI    [illegible]    .   1.[illegible]    .    1.[illegible]16   .    1.[illegible]41   .    1.[illegible]5[illegible]   .    1.923    .    1.924    .    1.990    .
AL     .0[illegible]  2.0[illegible]0  .111  2.000  .[illegible]4[illegible]  2.000  .[illegible]5[illegible]  2.000  .147  2.000  .077  2.000  .076  2.000  .007  2.000
AL     .10[illegible]  .   .[illegible]   .   .[illegible]20   .   .[illegible]21   .   .015   .   .026   .   .005   .   .026   .
TI     .[illegible]   .   .1[illegible]   .   .[illegible]1[illegible]   .   .[illegible]27   .   .012   .   .029   .   .026   .   .007   .
CR     .[illegible]   .   .[illegible]   .   .001   .   .[illegible]0[illegible]   .   .117   .   .025   .   .012   .   .106   .
FE     .21[illegible]   .   .1[illegible]   .   .203   .   .21[illegible]   .   .196   .   .204   .   .179   .   .166   .
MG     .[illegible]   .   .[illegible]   .   .[illegible]07   .   .[illegible]1[illegible]   .   [illegible]   .   .902   .   .946   .   .906   .
MN     .102   .   .002   .   .003   .   .[illegible]03   .   .300   .   .002   .   .001   .   .001   .
CA     .[illegible]17   .   .[illegible]   .   .[illegible]1[illegible]   .   .77[illegible]   .   .747   .   .777   .   .860   .   .844   .
NA     .[illegible]26   .   .[illegible]   .   .029   .   .[illegible]30   .   .020   .   .021   .   .032   .   .344   .
K     [illegible]  2.0[illegible]0  [illegible]  2.004  [illegible]  2.0[illegible]2  0.000  2.003  [illegible].000  2.005  0.000  1.9[illegible]3  0.000  2.019  0.000  2.000
O     6.000    .   6.000    .   6.000    .   6.000    .   6.000    .   6.000    .   6.000    .   6.000    .
   MG     41.61       44.35       42.33       40.64       38.46       41.15       45.29       44.03
   FE     10.[illegible]  [illegible].31  10.57   11.45       10.01       11.06       9.14        8.60
   CA     47.54       45.74       47.10       47.90       51.53       47.71       45.57       47.29

   F/[illegible]   .2[illegible]   .20[illegible]   .22[illegible]   .[illegible]43   .195   .231   .201   .185
   F/FM    .19[illegible]   .173   .14[illegible]   .19[illegible]   .163   .1[illegible]1   .167   .156

57 91-276 [illegible]
58 91-276 [illegible]
59 91-276 [illegible]
60 91-276 [illegible]
                                        61 91-273 CPX 1A CORE
                                        62 91-273 CPX 1B RIM
                                        63 91-273 CPX 2
                                        64 91-273 CPX 3A CORE
```

```
SUPER FOCAL                   [illegible] PYROXENES
            65          66          67          68          69          70          71          72
SIO2   [illegible] [illegible] [illegible]   5?.45       51.71       5?.?2       53.61       53.59
TIO2   [illegible] [illegible] [illegible]     .?         .59         .?6         .5?         .46
AL2O3  [illegible] [illegible]    1.71         .30        1.22        1.?0        1.65        1.39
CR2O3      .1?         .65         .?4         .?6         .34         .66         .74         .07
FEO       ?.?6         .?4        ?.?0       11.27        5.91        6.?1        6.24        5.89
MNO        .11         .15         .11         .14         .11         .01         .26         .20
MGO       1?.??      1?.?6       1?.?6       2?.74       16.75       16.?5       1?.35       18.40
CAO       2?.73      2?.?1       2?.?6         .?4       21.11       20.62       18.65       19.71
NA2O       .67         .?4         .1?         .05         .25         .44         .42         .54
K2O        .0?         .1?        ?.?0        0.00        0.00        0.00         .01         .01
SUM       ??.??      ??.?1      100.1?      101.00       99.47      100.07      100.46      101.01

 SI    [illegible]  •  1.??  •     1.??  •     1.?96  •    1.9?3  •    1.9?1  •    1.943  •    1.944  •
 AL    [illegible] 2.??? .0?? 1.??? .0?2 2.0?0 .01? 2.000 .?31 2.000 .0?9 2.010 .057 2.000 .056 2.000
 AL      .0??  •     1.??  •     .012  •     .002  •     .022  •     .019  •     .014  •     .001  •
 TI      .00?  •     .1??  •     .0??  •     .004  •     .016  •     .024  •     .016  •     .013  •
 CR      .0??  •     .01?  •     .0??  •     .00?  •     .010  •     .013  •     .021  •     .025  •
 FE      .1?   •     .2?1  •     .191  •     .?01  •     .17?  •     .200  •     .191  •     .179  •
 MG      .?01  •     .??   •     .9??  •    1.562  •     .915  •     .901  •     .?12  •     .995  •
 MN     ?.?0?  •     .00?  •     .?0?  •     .004  •     .003  •     .006  •     .008  •     .006  •
 CA      .?50  •     .?0?  •     .?2?  •     .032  •     .829  •     .81?  •     .724  •     .766  •
 NA      .0??  •     .0??  •     .024  •     .00?  •     .01?  •     .031  •     .159  •     .038  •
 K      0.00?  1.9?3  0.00?  ?.??8  0.000  2.?0?  0.000  2.0?1  0.000  1.992  0.00?  2.0?6  .000  2.024  .000  2.022
 O      6.00?  •     6.00?  •     6.000  •     6.000  •     6.000  •     6.000  •     6.000  •     6.000  •
     WO        4?.??       41.9?       42.74        1.60       41.13       42.32       37.49       39.50
     FS         7.1?       11.??        ?.4?       19.70        9.27       10.43       10.00        9.21
     EN        47.7?       47.??       47.??       70.70       47.61       47.25       52.02       51.29

     F/M        .15?        .251        .21?        .?5?        .194        .221        .200        .186
     F/FM       .13?        .200        .17?        .?02        .166        .181        .167        .157

 65 91-27? CPX ?? ?TM                         69 11-22 CPX 2A CORE
 66 91-32 CPX 16 ?-1                          70 11-22 CPX 2B RIM
 67 91-22 CPX 1?-1?                           71 11-271 CPX 4
 68 91-22 CPX INTERSTITIAL                    72 11-271 CPX 5
```

```
SUPERFICIAL     [illegible] PYROXENES
          73          74          75          76          77          78          79          80
SIO2   51.72       [illegible].41 4[illegible].3[illegible] 50.[illegible]5  50.77  50.73  49.65  55.13
TIO2     .56         .38        1.12         .62         .64     .[illegible]6    .71     .42
AL2O3  [illegible]  1.31        4.35        1.1[illegible] 1.41  1.74   1.71    .89
CR2O3    .6[illegible] .20       .1[illegible]  .12        .01    0.00    .05    .27
FEO    [illegible]  [illegible].55  12.36   20.1[illegible] 16.[illegible]7  19.18  [illegible]7.56  12.01
MNO      .[illegible]2  .24       .3[illegible]   .45        .47    .[illegible]0   .49    .23
MGO    1[illegible].[illegible]7  1[illegible].46  14.14  11.01  11.23  11.63  13.37  29.42
CAO    1[illegible].[illegible]  1[illegible].45  17.01  15.[illegible]1  14.42  14.24  15.54  1.55
NA2O     .4[illegible]  .52        .56         .44        .44     .46    .49    .30
K2O      .61         .02         .02        0.00        .02     .12    .01    0.00
SUM   101.[illegible]6  [illegible].2[illegible]  [illegible].[illegible]1  [illegible].77  100.32  100.56  99.58  100.22

 ST  [illegible].91[illegible]   .    1.[illegible]71   .    1.[illegible]55   .    1.94[illegible]   .    1.962   .    1.936   .    1.814   .    1.959   .
 AL   .08[illegible] 2.019   .0[illegible]  2.000   .145 2.016   .052 2.000   .038 2.000   .061 2.010   .178 1.992   .037 1.997
 AL   .03[illegible]   .    .0[illegible]   .    .[illegible]44   .    .002   .    .026   .    .013   .    0.000   .    0.000   .
 TI   .01[illegible]   .    .111    .    .0[illegible]2   .    .11[illegible]   .    .018   .    .019   .    .021   .    .011   .
 CR   .01[illegible]   .    .[illegible]0[illegible]   .    .00[illegible]   .    .001   .    .000   .    0.000   .    .002   .    .008   .
 FE   .[illegible]8[illegible]   .    .[illegible]6[illegible]   .    .404   .    .657   .    .604   .    .586   .    .565   .    .357   .
 MG   .[illegible]87   .    .[illegible]6[illegible]   .    .7[illegible]   .    .633   .    .754   .    .775   .    .768   .    1.558   .
 MN   .007   .    .[illegible]0[illegible]   .    .011   .    .015   .    .015   .    .016   .    .016   .    .007   .
 CA   .72[illegible]   .    .[illegible]0[illegible]   .    .5[illegible]   .    .651   .    .591   .    .582   .    .642   .    .059   .
 NA   .0[illegible]   .    .[illegible]   .    .141   .    .03[illegible]   .    .33[illegible]   .    .034   .    .037   .    .021   .
 K    .[illegible]0  2.0[illegible]2   .0[illegible]1 1.[illegible]11   .001 2.0[illegible]   0.000 2.0[illegible]3   .001 2.026   .001 2.025   .000 2.052   0.000 2.021
 O   6.00[illegible]   .    6.000   .    6.000   .    6.000   .    6.000   .    6.000   .    6.000   .    6.000
     WO     37.9[illegible]   37.62   36.31   33.71   30.32   29.95   32.48    2.99
     FS     15.91   16.07   21.5[illegible]   33.60   30.97   30.17   28.65   18.88
     EN     46.24   46.31   42.11   32.67   38.70   39.89   38.87   78.33

     F/M     .15[illegible]    .[illegible]57    .526   1.052    .420    .777    .758    .233
     F/FM    .253    .[illegible]61    .345    .511    .451    .437    .431    .189

73 AU-[illegible]CEX PHENO 1A CORE                     77 41-245 CPX 1B CORE
74 AU-[illegible]CEX PHENO 1B RIM                      78 41-245 CPX 2A CORE
75 BP-[illegible]CEX [illegible] MATRIX                79 41-245 CPX 2B CORE
76 A1-[illegible]45 CPX 1A RIM                         80 A6-273 OPX 3A CORE
```

```
SUPER-CAL        [illegible]
             #1            #2            #3            #4            #5            #6            #7            #8
SIO2     [illegible]   [illegible]      53.1[illegible]  51.[illegible]4  51.53      53.11         53.24         53.27
TIO2     [illegible]     .15         [illegible]     .[illegible]1     .28          .20           .14           .34
AL2O3    [illegible]    3.91          1.[illegible]1    .56          .4[illegible]   .[illegible]3   2.10         1.95
CR2O3      .1[illegible]  .11         0.00           0.00           .11          .06           .21           .18
FEO       11.57         13.1[illegible]  12.52       24.[illegible]4   21.75       21.29          8.46         10.02
MNO      [illegible]     .30           .2[illegible]   .41          .36          .29           .09           .17
MGO      [illegible]    13.75         14.[illegible]1  20.16        20.03       20.[illegible]1  15.77       16.66
CAO       1.[illegible]  [illegible]  17.6[illegible]  1.71          5.[illegible]5   4.[illegible]1  19.55     17.01
NA2O      .[illegible]1   .[illegible]9   .21           .27         0.00          .04           .35           .12
K2O        .00          0.00           .02          0.00           .06         0.00           .03          0.00
SUM      [illegible]   [illegible]    99.3[illegible]  99.61      101.00      101.04        100.12         99.72

 SI    1.9[illegible]      1.826          1.93[illegible]     1.971          1.934          1.96[illegible]    1.961          1.968
 AL     .0[illegible]  1.9[illegible]6   .174  2.0[illegible]   .062  2.000   .025  1.9[illegible]6   .039  1.973   .032  2.000   .039  2.000   .032  2.000
 AL    0.001            .01[illegible]    .023           0.000          0.000           .006           .152           .053
 TI     .012            .027           .01[illegible]     .009           .00[illegible]    .006           .009           .009
 CR     .00[illegible]    .003          0.000          0.000           .003           .002           .006           .005
 FE     .351            .42[illegible]    .390           .76[illegible]    .682           .660           .260           .310
 MG    1.577            .7[illegible]1    .841          1.140          1.119          1.155           .866           .917
 MN     .007            .010           .009           .01[illegible]    .011           .009           .003           .005
 CA     .051            .795           .717           .070           .234           .171           .772           .673
 NA     .01[illegible]    .015           .01[illegible]    .020          0.000           .003           .025           .009
 K     0.00[illegible]  2.022  0.000  2.007   .001  2.012  0.000  2.022   .003  2.065  0.000  2.039   .001  1.944  0.000  1.987
 O     6.000           6.000          6.000          6.000          6.000          6.000          6.000          6.000
     WO        2.57         [illegible].47      36.[illegible]0      3.51          11.71          8.62          40.66          35.43
     FS       17.7[illegible]  21.6[illegible]  20.[illegible]    [illegible]8.47    33.43         33.22          13.70          16.29
     EN       74.71         40.3[illegible]  [illegible]3.1[illegible]  57.62      54.85         58.16          45.6[illegible]  48.28

     F/M       .227          .[illegible]90       .474          .[illegible]87       .619          .57[illegible]      .304           .343
     F/FM      .18[illegible]    .[illegible]55      .322          .40[illegible]      .382          .367           .23[illegible]      .256

 #1 A1-273 CPX 3B RIM                                  #5 A1-210 CPX 2B CORE
 #2 A1-290 CPX 1A RIM                                  #6 A1-210 CPX 3 CORE
 #3 A1-290 CPX 1B CORE                                 #7 A1-210 CPX 4A CORE
 #4 A1-290 CPX 2A RIM                                  #8 A1-210 CPX 4B
```

```
SUPER CAL[illegible]                    [illegible]CTION BY CYCLES
          [illegible]      [illegible]      91       92       93       94       95       96
SIO2      [illegible]      [illegible]      [illegible]  52.08  [illegible]  52.32  50.66  50.71
TIO2      .40      .41      .25      .43      .31      .23      .45      .38
AL2O3     1.[illegible]  .55      1.73     .43      .40      .17      1.83     1.66
CR2O3     .02      [illegible]  .02      .03      0.00     0.00     .09      .09
FEO       [illegible]  [illegible]  14.32    11.92    28.01    26.86    16.60    16.12
MNO       .1[illegible]  [illegible]  .18      .20      .51      .42      .49      .48
MGO       1[illegible]  1[illegible]  13.78    12.53    17.95    18.66    12.09    12.10
CAO       1[illegible]  4.7[illegible]  17.35    19.27    2.24     1.70     17.31    18.14
NA2O      .[illegible]2  .0[illegible]  .29      .26      0.00     0.00     .54      .47
K2O       [illegible].10  .05      .[illegible]  0.00     0.00     0.00     0.00     0.00
SUM       100.[illegible]  110.16   [illegible].47  [illegible]  100.67   100.76   100.76   100.23

SI        1.[illegible]  .      1.[illegible]  .      1.961  .      1.976  .      1.995  .      1.994  .      1.931  .      1.938  .
AL        .02[illegible]  2.0[illegible]  .00[illegible]  2.00[illegible]  .05[illegible]  2.[illegible]  .024  2.000  .005  2.000  .006  2.010  .069  2.000  .062  2.000
AL        .0[illegible]  .      .01[illegible]  .      .021  .      .011  .      .013  .      .020  .      .013  .      .013  .
TI        .011  .      .012  .      .021  .      .012  .      .009  .      .007  .      .013  .      .011  .
CR        .001  .      .0[illegible]2  .      .001  .      .001  .      0.000  .      0.000  .      .003  .      .003  .
FE        .[illegible]  .      .[illegible]  .      .458  .      .342  .      .884  .      .848  .      .531  .      .515  .
MG        .[illegible]  .      .[illegible]  .      .781  .      .726  .      1.014  .      1.056  .      .687  .      .694  .
MN        .00[illegible]  .      .01[illegible]  .      .006  .      .008  .      .016  .      .013  .      .016  .      .016  .
CA        .[illegible]  .      .17[illegible]  .      .702  .      .783  .      .091  .      .069  .      .732  .      .743  .
NA        .01[illegible]  .      .0[illegible]2  .      .021  .      .018  .      0.000  .      0.000  .      .040  .      .035  .
K         0.00[illegible]  1.[illegible]  .0[illegible]2  1.[illegible]  .007  2.011  0.000  2.031  0.000  1.987  0.000  1.986  0.000  2.034  0.000  2.029
O         6.00[illegible]  .      [illegible].0[illegible]  .      6.000  .      6.000  .      6.000  .      6.000  .      6.000  .      6.000  .
     [illegible]   [illegible]     [illegible]     36.34    40.16    4.67     2.61     37.55    38.06
     FS   1[illegible]     41.1[illegible]  23.48   22.64    43.31    43.57    27.23    26.40
     EN   44.[illegible]   49.7[illegible]  40.28   37.21    52.03    53.94    35.22    35.55

     F/M   .185    .[illegible]     .510     .[illegible]    .349     .829     .796     .765
     F/FM  .27[illegible]  .[illegible]  .371  .[illegible]  .453     .451     .443     .433

89 81-299  PX  4C RIM                       93 81-286  OPX  1B CORE
90 81-286  CPX 1A C[illegible]              94 81-286  OPX  6 RIM
91 81-286  [illegible]PX 2 CO[illegible]    95 73-44   CPX  1
92 81-286  [illegible]PX 1A C[illegible]    96 74-44   CPX  1B
```

```
SUPER [illegible]                  [illegible] PROGRAM [illegible]
            97                 98                 99                100                101                102                103                104
SIO2    [illegible]        [illegible].61     [illegible]1.1[illegible]  52.[illegible]5   51.78              51.[illegible]4    50.86              50.77
TIO2    [illegible]        .[illegible]       .46                .50                .50                .[illegible]7      .64                .61
AL2O3   1.[illegible]      .[illegible]       .[illegible]       .[illegible]6      1.11               1.75               1.91               1.35
CR2O3   .[illegible]7      .01                .1[illegible]      .0[illegible]      .11                .17                .12                .03
FEO     1[illegible].[illegible]1  [illegible].51  23.6[illegible]  24.55          11.42              1[illegible].59    14.24              11.66
MNO     .[illegible]       .41                .41                .[illegible]       .34                .13                .33                .28
MGO     1[illegible]       1[illegible].95    17.31              1[illegible].47    15.06              15.[illegible]6    14.34              10.95
CAO     17.02              [illegible].46     [illegible].03     2.[illegible]5     17.60              15.18              17.16              21.28
NA2O    .10                1.00               .04                0.00               .16                .16                .09                .25
K2O     0.00               0.00               0.00               0.00               0.00               .01                0.00               0.00
SUM     9[illegible]       100.1[illegible]   100.07             100.37             [illegible]9.45    99.96              99.69              99.18

 SI   1.97[illegible]  .      1.[illegible]  .       1.956   .        1.972   .        1.942   .        1.951   .        1.[illegible]24  .       1.[illegible]54  .
 AL    .0[illegible]  2.010    .01[illegible] 2.000   .042  1.[illegible]  .028  2.000    .058  2.000     .049  2.000     .072  2.000       .046  2.000
 AL    .10[illegible]  .       .0[illegible]  .       0.0[illegible]0  .   .001   .        .026   .        .024   .        .014   .          .015   .
 TI    .01[illegible]  .       .011   .               .013   .          .009   .        .014   .        .011   .        .018   .          .018   .
 CR    .10[illegible]  .       .00[illegible]  .      .002   .          .002   .        .003   .        .005   .        .004   .          .001   .
 FE    .4[illegible]   .       .[illegible]   .       .7[illegible]  .   .7[illegible]  .  .358   .      .424   .        .452   .          .440   .
 MG    .7[illegible]   .       1.0[illegible]  .      .9[illegible]  .   1.045   .        .975   .        .[illegible]91  .  .910   .          .628   .
 MN    .011   .                .014   .               .013   .          .014   .        .011   .        .011   .        .011   .          .009   .
 CA    .64[illegible]  .       .16[illegible]  .      .247   .          .115   .        .707   .        .614   .        .697   .          .877   .
 NA    .007   .                0.0[illegible]  .      .003   .          0.000   .       .012   .        .012   .        .007   .          .019   .
 K    0.10[illegible] 2.015    0.000  1.[illegible]   0.000  2.018      0.000  2.004    0.000  2.006     .000  2.003     0.000  2.017      0.000  2.007
 O    6.000   .                6.000   .              6.000   .          6.000   .       6.000   .        6.000   .        6.000   .          6.000   .
      WO      4[illegible]            7.20                 12.41               5.8[illegible]      36.44             31.7[illegible]     35.58              45.11
      FS      24.47                [illegible].29           38.02               38.83              19.46             22.17               23.05              22.60
      EN      [illegible]            54.51                 49.57               55.34              45.11             46.11               41.37              32.29

      F/M     .61[illegible]          .711                  .740                .716               .[illegible]21     .491                .570               .716
      F/FM    .[illegible]91          .41[illegible]        .418                .417               .[illegible]97     .33[illegible]      .[illegible]63     .417

  97 [illegible]1-291 PX 1 [illegible]                              101 A1-24[illegible] CPX 1D
  98 A1-2[illegible] CPX 1A                                          102 A1-24[illegible] CPX 2A CORE
  99 A1-2[illegible] CPX 11                                          103 A1-24[illegible] CPX 2B [illegible]
 100 A1-2[illegible] CPX 1C                                          104 A1-243 CPX 2
```

```
SUPER [illegible]                     [illegible] PYROXENES
          105         106          107          108          109          110          111          112
SIO2   [illegible]  [illegible]  [illegible]   52.22        52.21        54.17        53.06        54.13
TIO2   [illegible]  [illegible]  [illegible]  [illegible]    .46          .74          .65          .57
AL2O3  [illegible]  [illegible]  [illegible]  [illegible]   1.73         1.86         2.36         1.20
CR2O3  [illegible]    .30        [illegible]    .34          .13          .20          .09          .20
FEO    [illegible]  [illegible]   11.7[illegible] 20.33     11.64        11.[illegible] 10.13      17.53
MNO    [illegible]    .17          .12          .40          .25          .30          .25          .15
MGO    [illegible]  [illegible]  [illegible]   20.12        17.45        15.07        14.65        24.38
CAO    [illegible]  [illegible]   14.07        [illegible]  15.68        14.20        19.20         1.35
NA2O     0.10       [illegible]  [illegible]   0.00          .05          .06          .07         0.00
K2O    [illegible]    0.00         0.00         0.10         0.00         0.00         0.00         0.00
SUM    [illegible]  [illegible]   99.61        99.13        99.63       100.72       100.46        99.51

 SI    1.97[illegible] .   [illegible] .   1.956   .    1.966   .    1.944   .    1.976   .    1.959   .    1.980   .
 AL     .024  2.000   .041  2.000   .044  2.000   .[illegible]  2.000   .056  2.000   .024  2.000   .041  2.000   .020  2.000
 AL    [illegible] .   [illegible] .    .044   .     .011   .     .020   .    [illegible] .    1061   .     .031   .
 TI    [illegible] .    .021   .     .020   .     .011   .     .013   .     .009   .     .018   .     .016   .
 CR     .001   .   [illegible] .     .003   .     .001   .     .004   .     .006   .     .003   .     .006   .
 FE    [illegible] .   [illegible] .   [illegible] .  .641   .     .364   .    [illegible] .    .315   .     .536   .
 MG    1.0[illegible] . [illegible] .  [illegible] .  1.142   .    [illegible] .   [illegible] .   .806   .    1.329   .
 MN     .015   .   [illegible] .     .010   .     .013   .     .008   .     .009   .     .008   .     .005   .
 CA    [illegible] .   [illegible] .   [illegible] .  .181   .     .626   .     .555   .     .753   .     .053   .
 NA    [illegible] .   [illegible] .   [illegible] . 0.000   .     .004   .     .004   .     .005   .    0.000   .
 K      .000  2.001   [illegible] [illegible]  0.000  [illegible]  0.000  1.999  0.000  2.005  0.000  1.974  0.000  1.973  0.000  1.976
 O     6.000   .    6.000   .    6.000   .    6.000   .    6.000   .    6.000   .    6.000   .    6.000   .
    WO     11.11       [illegible]     40.42       [illegible]     31.95        29.34        40.43         2.76
    FS    [illegible]     20.09        19.44       [illegible]     18.58        18.61        16.65        27.95
    EN     52.23        42.67        40.13       [illegible]     49.47        52.01        42.92        69.29

    F/M    [illegible]  [illegible]  [illegible]  [illegible]  [illegible]    .367         .399         .407
    F/FM    .417        [illegible]    .332         .364         .277         .261         .285         .289

105 A1-[illegible] CPX [illegible]                           109 A1-236 CPX 2
106 A1-236 CPX 1A [illegible]                                110 A1-236 CPX 3 OIKOCRYST
107 A1-236 CPX 1B                                            111 A1-236 CPX 10
108 A1-236 CPX 1C                                            112 A2-4 OPX 1A CORE
```

```
SUP.B [illegible]               TYPICAL PYROXENES
              113                 114                 115                 116                 117                 118                 119                 120
SIO2         53.02               52.72               51.47               51.76               52.01               51.16               52.63               52.50
TIO2           .63                 .51                 .42                 .30                 .69                 .53                1.02                 .36
AL2O3         1.18                 .47                2.01                1.59                1.90                2.28                1.68                2.70
CR2O3          .04                 .17                 .77                 .19                 .21                 .67                 .21                 .19
FEO          17.13               15.86                8.45                5.19               10.27                7.24                8.79               13.65
MNO            .18                 .27                 .11                 .13                 .14                 .12                 .11                 .18
MGO          24.33               25.61               15.12               15.46               16.05               15.47               16.13               21.13
CAO           2.66                3.12               21.11               19.23               18.00               20.82               19.63                9.05
NA2O          0.00                0.00                 .32                 .25                 .21                 .30                 .43                 .09
K2O           0.00                0.00                0.00                0.00                0.00                0.00                0.00                0.00
SUM          99.12              100.17              100.54              100.08               99.59               99.76              100.63               99.91

 SI    1.953    .     1.974    .     1.925    .     1.926    .     1.919    .     1.925    .     1.938    .     1.929    .
 AL     .041  2.000    .026  2.000    .075  2.000    .074  2.000    .051  2.000    .075  2.000    .052  2.000    .071  2.000
 AL     .011    .      .011    .      .012    .      .009    .      .026    .      .023    .      .011    .      .046    .
 TI     .019    .      .016    .      .023    .      .022    .      .019    .      .015    .      .028    .      .009    .
 CR     .001    .      .001    .      .008    .      .005    .      .007    .      .020    .      .006    .      .006    .
 FE     .551    .      .565    .      .276    .      .311    .      .320    .      .224    .      .271    .      .419    .
 MG    1.323    .     1.267    .      .835    .      .860    .      .882    .      .862    .      .885    .     1.156    .
 MN     .006    .      .008    .      .003    .      .004    .      .004    .      .001    .      .003    .      .006    .
 CA     .105    .      .087    .      .836    .      .767    .      .714    .      .828    .      .774    .      .356    .
 NA    0.000    .     0.000    .      .023    .      .018    .      .015    .      .022    .      .031    .      .006    .
 K     0.000  1.996   0.000  1.996   0.000  2.016   0.000  2.016   0.000  2.003   0.000  2.012   0.000  2.010   0.000  2.083
 O     6.000    .     6.000    .     6.000    .     6.000    .     6.000    .     6.000    .     6.000    .     6.000    .
     WO          4.70           4.25          43.04          39.18          37.22          42.76          40.12          18.43
     FS          8.11          20.43          14.08          15.87          16.58          11.61          14.02          21.70
     EN         87.59          65.92          42.88          44.95          46.20          45.69          45.86          59.87

     F/M          .471           .451           .331           .361           .364           .255           .310           .367
     A/FM         .294           .315           .250           .263           .267           .201           .236           .269

113 A2-4 CPX 1C RIM                              117 A2-4 CPX 1C RIM
114 A2-4 CPX 1C                                  118 A2-34 CPX 1A CORE
115 A2-4 CPX 1A                                  119 A2-34 CPX 1B RIM
116 A2-4 CPX 1B RIM                              120 A2-201 CPX 1 OVERGROWING OL
```

209

```
SUPER [illegible]                    [illegible]
        121            122            123            124            125            126            127            128
SIO2    [illegible]    [illegible]    [illegible]    [illegible]    51.56          50.46          51.61          51.78
TIO2    [illegible]    [illegible]    [illegible]    .76            .30            [illegible]    .25            .38
AL2O3   [illegible]    [illegible]    [illegible]    2.32           1.14           [illegible]    [illegible]    1.32
CR2O3   [illegible]    .00            [illegible]    .04            .02            .18            .05            .04
FEO     [illegible]    14.64          [illegible]    [illegible]    21.27          17.57          20.05          19.86
MNO     [illegible]    [illegible]    [illegible]    [illegible]    .31            .23            .24            .27
MGO     [illegible]    [illegible]    [illegible]    [illegible]    19.43          [illegible]    19.73          19.69
CAO     [illegible]    15.64          9.74           [illegible]    5.71           13.68          5.80           6.22
NA2O    [illegible]    [illegible]    .02            .14            0.00           .36            0.00           0.00
K2O     [illegible]    0.00           0.00           0.00           0.00           0.00           0.00           0.00
SUM     [illegible]    [illegible]    [illegible]    [illegible]    99.74          100.57         98.66          99.56

 SI   [illegible]   .     [illegible]   .     1.901   .      [illegible]   .      [illegible]   .      [illegible]   .      1.962   .      1.950   .
 AL   [illegible] [illegible]  [illegible] [illegible]  .099 2.000  [illegible] 2.000  [illegible] 2.000  .080 [illegible]  .038 2.000  .050 2.000
 AL.  [illegible]   .     [illegible]   .     .014    .      [illegible]   .      0.000   .      0.000   .      .001    .      .008    .
 TI   [illegible]   .     [illegible]   .     .009    .      .021    .      .009    .      .015    .      .007    .      .011    .
 CR   [illegible]   .     [illegible]   .     [illegible]   .      .001    .      .001    .      .005    .      .002    .      .001    .
 FE   [illegible]   .     [illegible]   .     [illegible]   .      [illegible]   .      .572    .      .551    .      .637    .      .625    .
 MG   [illegible]   .     [illegible]   .     1.176   .      [illegible]   .      1.095   .      [illegible]   .      1.118   .      1.105   .
 MN   .006    .     [illegible]   .     [illegible]   .      .009    .      .010    .      .007    .      .009    .      .009    .
 CA   .727    .     [illegible]   .     [illegible]   .      [illegible]   .      [illegible]   .      [illegible]   .      .236    .      .251    .
 NA   [illegible]   .     [illegible]   .     .001    .      .010    .      0.000   .      .004    .      0.000   .      0.000   .
 K    [illegible] [illegible]  [illegible] [illegible]  0.000 [illegible]  0.000 2.023  0.000 2.017  0.000 2.037  0.000 2.011  0.000 2.010
 O    6.000   .     6.000   .     6.000   .      6.000   .      6.000   .      6.000   .      6.000   .      6.000   .
      WO      [illegible]    14.04          [illegible]    [illegible]    11.57          27.64          11.85          12.66
      FS      [illegible]    [illegible]    21.77          [illegible]    33.65          27.71          32.01          31.56
      EN      [illegible]    42.9[illegible] [illegible]   40.7[illegible] 54.78         44.65          56.13          55.77

      F/M     .41[illegible] [illegible]    .377           [illegible]    .523           [illegible]    .573           .574
      F/FM    [illegible]    [illegible]    .274           [illegible]    [illegible]    .386           .366           .365

121 82-76 CPX CTK 1[illegible]                 125 82-202 HOU-GLASS CPX 1[illegible]
122 82-76 CPX [illegible] 1[illegible] [illegible]   126 82-202 HOU-GLASS CPX 1[illegible]
123 82-201 [illegible] 1                     127 82-202 HOU-GLASS CPX 1[illegible]
124 82-202 HOU[illegible] CPX 1[illegible]     128 82-202 HOU-GLASS CPX 1[illegible]
```

270

```
SUPER PICAL                    [illegible] PYROXENES
          129           130           131           132           133           134           135           136
SIO2      4[illegible]  51.71         52.64         51.21         49.33         51.76         51.75         51.59
TIO2      [illegible]   .46           .24           .57           .66           1.18          .24           .39
AL2O3     1.73          1.12          1.12          1.00          1.51          2.12          1.42          1.08
CR2O3     .17           .11           .08           .10           .05           .27           .27           .08
FEO       29.44         23.14         21.02         24.11         17.55         8.45          9.28          10.82
MNO       .79           .42           .37           .52           .31           .11           .21           .19
MGO       [illegible]   18.41         23.19         15.21         12.95         15.75         18.12         16.82
CAO       13.13         5.12          4.36          6.24          16.31         20.02         17.63         17.77
NA2O      .36           0.10          .02           0.00          .15           .45           .14           .09
K2O       0.00          0.00          .01           0.00          0.00          0.00          0.00          0.00
SUM       99.45         100.12        100.38        100.51        99.42         100.31        99.46         99.55

 SI   1.935    .     1.966    .     1.961    .     1.967    .     1.927    .     1.909    .     1.924    .     1.929    .
 AL    .065  1.951    .034  2.000    .039  2.000    .037  2.000    .054  1.996    .084  1.997    .076  2.000    .071  2.000
 AL   1.000    .      .016    .      .010    .      .104    .     0.000    .     0.020    .      .104    .      .009    .
 TI    .017    .      .010    .      .004    .      .015    .      .014    .      .033    .      .007    .      .011    .
 CR    .002    .      .003    .      .002    .      .001    .      .002    .      .006    .      .039    .      .002    .
 FE    .961    .      .701    .      .653    .      .405    .      .567    .      .279    .      .284    .      .338    .
 MG    .561    .     1.051    .     1.126    .      .869    .      .745    .      .874    .     1.004    .      .936    .
 MN    .013    .      .017    .      .010    .      .017    .      .010    .      .003    .      .007    .      .006    .
 CA    .515    .      .215    .      .197    .      .291    .      .675    .      .799    .      .702    .      .712    .
 NA    .007    .     0.007    .      .001    .     0.000    .      .011    .      .032    .      .010    .      .007    .
 K    0.000  2.046   0.101  2.007    .000  2.006   0.000  1.998   0.000  2.028   0.000  2.029   0.000  2.010   0.000  2.022
 O    6.000    .     6.000    .     6.000    .     6.000    .     6.000    .     6.000    .     6.000    .     6.000    .
    WO       9.62           10.90          9.34          14.37          33.96          40.95          35.20          35.82
    FS      42.27           35.49         33.07          41.19          28.52          14.29          14.46          17.02
    EN      48.11           51.61         56.38          44.45          37.51          44.71          50.33          47.16

    F/M      1.523           .675          .532           .466           .776           .323           .294           .367
    F/FM      .594           .403          .371           .446           .436           .244           .227           .269

129 82-282 [illegible] CPX 1F                    133 82-75 CPX OIK 4 ENCLOSING OL
130 82-75 CPX OIK 1                              134 82-34 CPX 1 ENCLOSING OL
131 82-75 CPX OIK 2                              135 81-234 CPX 1A CORE
132 82-75 CPX OIK 3                              136 81-234 CPX 1B RIM
```

```
SUPER [illegible]            [illegible] PY-CPX [illegible]
        137         13[illegible]       13[illegible]       14[illegible]       141         142         143         144
SIO2    [illegible] [illegible] [illegible] [illegible] 50.54       50.15       50.56       52.19
TIO2    [illegible] [illegible] .7[illegible] [illegible] .24       .30         .79         .33
A2O3    1.[illegible] 1.[illegible] 1.[illegible] 1.72   1.93        2.01        2.02        .51
C2O3    .1[illegible] .1[illegible] .1[illegible] .1[illegible] .11  .07         .11         .16
FEO     1[illegible] 1[illegible] 14.[illegible] 1[illegible] 14.15    11.60       13.68       25.34
MNO     [illegible] [illegible] .27     .27         .24         .14         .23         .43
MGO     1[illegible] 1[illegible] 1[illegible] 14.35     14.73       14.32       14.30       19.21
CAO     15.11       1[illegible] 1[illegible] 17.[illegible] 15.19  13.46       13.23       1.89
NA2O    .1[illegible] [illegible] .07     .1[illegible] .14         .17         .16         0.00
K2O     0.[illegible] [illegible] 0.[illegible] 0.00     .01         0.00        0.00        0.00
SUM     [illegible] 1[illegible] 100.44  [illegible].31   99.78       100.16      101.76      100.06

SI      1.[illegible]           1.[illegible]           1.42[illegible]          1.[illegible]             1.915          1.914          1.877          1.980
AL      .[illegible] [illegible] .1[illegible] [illegible] .071 2.10[illegible] .176 2.000    .085 2.000     .085 2.000     .099 1.976     .020 2.000
AL      .[illegible]            .11[illegible]           .062                     .101                      .102           .012           0.036          .002
TI      .[illegible]            .11[illegible]           .021                     .0[illegible]              .024           .020           .022           .009
CR      .[illegible]            .[illegible]             .003                     .00[illegible]             .003           .002           .003           .005
FE      .41[illegible]          .[illegible]             .471                     .44[illegible]             .441           .364           .427           .804
MG      .[illegible]            .[illegible]             .[illegible]76           .[illegible]16             .832           .802           .833           1.086
MN      .[illegible]            .[illegible]             .009                     .00[illegible]             .009           .005           .007           .014
CA      .647                    .[illegible]             .632                     .797                      .619           .804           .763           .077
NA      .011                    .[illegible]             .00[illegible]           .00[illegible]             .013           .012           .012           0.000
K       .0[illegible] [illegible] 0.00[illegible] [illegible] 0.000 2.114   0.00[illegible] 2.015      .000 2.023     0.005 2.022    0.006 2.074    0.000 1.997
O       [illegible]             [illegible]              6.000                    6.000                     6.000          6.000          6.009          6.000
   WO         [illegible]           [illegible]          32.04                 [illegible].46            35.01          40.77          37.84          3.91
   EN         [illegible]           [illegible]          23.36                 22.61                     22.77          18.51          21.04          40.87
   FS         [illegible]           4[illegible]         44.[illegible]        41.43                     42.22          40.71          41.07          55.22

   F/M        .46[illegible]        .[illegible]         .551                  .[illegible]               .551           .467           .521           .753
   F/FM       .[illegible]          .[illegible]         .55[illegible]        .[illegible]               .35[illegible] .31[illegible] .34[illegible] .429

 137 41-23[illegible] PX 1[illegible] [illegible]              141 41-234 CPX 3B
 138 41-234 CPX 1D [illegible]                                142 41-234 CPX 3D
 139 41-234 CPX 2A [illegible]                                143 41-234 CPX 3E
 140 41-234 CPX 2A                                            144 41-234 PIGEONITE 1A OVERGROWTH
```

```
SHE[illegible] [illegible]                            [illegible] PY-[illegible]
          145             146              147              148              149              150              151              152
SIO2      51.51           [illegible]      [illegible].75   51.11            50.44            51.16            51.70            51.32
TIO2        .27             [illegible]      .36              .42              .83              .31              .36              .83
AL2O3      1.17            1.[illegible]     .[illegible]     .[illegible]     1.61              .47              .44             1.66
CR2O3       .[illegible]    .[illegible]     .14              .17              .14              .04              .20              .04
FEO       11.1[illegible] [illegible].27   24.61            23.46            14.13            27.30            26.54            14.37
MNO         .[illegible]    .22              .[illegible]     .49              .25              .53              .46              .31
MGO       1[illegible].[illegible]  1[illegible].[illegible]6  14.47   14.74    13.42            16.36            16.41            13.77
CAO       21.[illegible]  [illegible].[illegible]6  1.[illegible]1  [illegible].39  17.70            1.68             1.69            16.69
NA2O        .12             .16             0.00              0.30              .15             0.00             0.00              .09
K2O        0.00            0.00              .[illegible]     0.00              .02             0.00             0.00             0.00
SUM       10[illegible].[illegible]1  [illegible].66  100.56    99.16            99.16           100.65           100.42            99.08

SI        1.[illegible]   .    1.[illegible]   .    1.980   .    1.973   .    1.861   .    1.977   .    1.967   .    1.953   .
AL         .066  2.110     .0[illegible]  2.000  .0[illegible]  2.000  .027  2.000  .139  2.000  .021  1.998  .020  1.986  .047  2.000
AL         .00[illegible] .    .11[illegible] .   .[illegible]  .   .010   .    .013   .    0.000   .    0.000   .    .028   .
TI         .01[illegible] .    .075[illegible] .  .011   .    .012   .    .126   .    .009   .    .025   .    .024   .
CR         .001   .    .0[illegible]  .    .004   .    .005   .    .004   .    .001   .    .006   .    .001   .
FE         .[illegible]   .    .41[illegible] .   .77[illegible] .  .746  .    .451   .    .861   .    .844   .    .457   .
MG         .747   .    .[illegible]   .    1.118   .    1.120  .    .763   .    1.041  .    1.044  .    .781   .
MN         .00[illegible] .    .00[illegible] .   .01[illegible] .  .01[illegible] .  .008  .  .017  .  .015  .  .010   .
CA         .8[illegible]  .    .7[illegible]  .    .1[illegible]  .   .1[illegible]  .  .724   .    .066   .    .069   .    .681   .
NA         .00[illegible] .    .01[illegible] .   0.00[illegible] .  0.009  .   .012   .    0.000  .    0.000  .    .007   .
K         0.00[illegible] 2.017  [illegible]  2.016  [illegible]  1.[illegible]  0.000  1.[illegible]6  .001  2.002  0.000  2.015  0.000  2.006  0.000  1.986
O         6.00[illegible] .    6.100   .    6.000   .    6.000   .    6.000   .    6.000   .    6.000   .    6.000   .
    WO           4[illegible].[illegible]7   37.50     [illegible].[illegible]1   4.[illegible]   37.34   3.46   3.57   35.46
    FS           17.77      21.31     3[illegible].[illegible]   3[illegible].[illegible]  23.27  43.91  43.14  23.83
    EN           17.57      41.12     [illegible]7.1[illegible]  57.41   39.39   52.63   53.34   40.70

    F/M          .44[illegible]   .[illegible]27   .70[illegible]   .[illegible]   .591   .851   .823   .598
    FE/FM        .[illegible]6    .[illegible]4[illegible]   .414   .40[illegible]   .376   .463   .451   .374

145 A1-236 CPY [illegible]                              149 A1-236 CPX 31
146 A1-236 CPX [illegible]                              150 A1-236 PIGEONITE 24
147 A1-236 PIGEONITE [illegible]                        151 A1-236 PIGEONITE 20
148 A1-236 CPX [illegible]                              152 A1-236 CPX 28
```

```
SU[illegible] [illegible](CA)[illegible]  [illegible]       [illegible]     1[illegible]6      1[illegible]7      1[illegible]8      159      160
SIO2   [illegible]   [illegible]   [illegible]   [illegible]   [illegible]   [illegible]   [illegible]   52.09
TIO2      .76   [illegible]   [illegible]      .79      .44      .38      .53      .55
AL2O3    1.79   [illegible]   [illegible]     1.[illegible]4     1.45     1.27     1.32     2.42
CR2O3  [illegible]   [illegible]   [illegible]   [illegible]      .35      .27      .24      .32
FEO    [illegible]   [illegible]   [illegible]     6.1[illegible]   1[illegible].04    12.38    13.60     9.93
MNO    [illegible]   [illegible]      .[illegible]6      .26      .11      .24      .19      .25
MGO    [illegible]   [illegible]   [illegible]    15.[illegible]1    27.96    28.03    27.63    15.65
CAO    [illegible]   [illegible]   [illegible]   [illegible]     1.96     1.76     1.43    18.66
NA2O   [illegible]   [illegible]   [illegible]      .1[illegible]     0.00     0.00     0.00      .09
K2O    [illegible]   [illegible]   [illegible]     0.00     0.00     0.00     0.00      .02
SUM    [illegible]   [illegible]   101.[illegible]1    [illegible]7.71   [illegible].41   99.11   [illegible]9.13   99.98

 SI  1.927   •    1.[illegible]   •    1.970   •    1.961   •    1.967   •    1.948   •    1.945   •    1.934   •
 AL   .073 2.000  [illegible] 2.000  .030 2.000  .0[illegible] 2.000  .033 2.000  .052 2.010  .055 2.006  .066 2.000
 AL   .[illegible]   •    .015  •    .[illegible]   •    .133  •    .003  •    .002  •    .001  •    .040  •
 TI   .021  •    .01[illegible]  •    .010  •    .020  •    .012  •    .013  •    .016  •    .015  •
 CR   .[illegible]   •    [illegible]   •    .0[illegible]   •    .014  •    .011  •    .008  •    .008  •    .009  •
 FE   .[illegible]   •    .[illegible]   •    .720  •    .1[illegible]   •    .343  •    .392  •    .412  •    .308  •
 MG   .7[illegible]   •    1.1[illegible]  •    1.[illegible]  •    .86[illegible]  •    1.501  •    1.516  •    1.492  •    .866  •
 MN   .[illegible]   •    .[illegible]   •    .014  •    .00[illegible]  •    .003  •    .007  •    .006  •    .008  •
 CA   .[illegible]   •    .1[illegible]   •    .13[illegible]  •    .[illegible]   •    .075  •    .076  •    .071  •    .742  •
 NA   .[illegible]   •    [illegible]   •    .0[illegible]   •    .011  •    0.000  •    0.000  •    0.000  •    .006  •
 K   0.00[illegible] 2.01[illegible]  0.[illegible] 1.9[illegible]  0.000 1.[illegible]  0.000 1.992  0.000 2.005  0.000 2.008  0.006 2.007  .001 1.997
 O   6.000  •    [illegible]   •    6.000  •    6.000  •    6.000  •    6.000  •    6.000  •    6.000  •
    W[illegible]   [illegible]     [illegible]     6.[illegible]0    43.97     3.84     3.84     3.60    38.73
    [illegible]   [illegible]     [illegible]    17.14    10.17    19.96    19.83    20.86    16.09
    [illegible]   [illegible]     [illegible]    [illegible]    45.86    76.20    76.33    75.54    45.19

    [illegible]   .16[illegible]    .171     .176     .[illegible]     .266     .265     .280     .365
    F/FM   .[illegible]    .[illegible]     .49[illegible]     .[illegible]     .209     .201     .213     .267

153 81-136 [illegible]                           157 81-275 OPX 1A CORE
154 81-136 [illegible]                           158 81-276 OPX 1B
155 81-[illegible]36 [illegible] 2F                       159 81-276 OPX 1C EDGE
156 81-[illegible] [illegible]                           160 80-183 [illegible]PX 1A CORE
```

```
[illegible]                               [illegible] OLIVINE
          41             42         43          44          45          46          47
MGO   [illegible]   [illegible] [illegible] [illegible] [illegible]    22.12       22.13
AL2O3 [illegible]        .10   [illegible]  [illegible]    0.00        0.00        0.00
SIO2  [illegible]   [illegible] [illegible] [illegible] [illegible]    35.41       35.48
CAO        .1[illegible] .05   [illegible]  [illegible]     .22         .12         .13
TIO2  [illegible]        .1[illegible] [illegible] [illegible] 0.90      .02         .02
CR2O3 [illegible]        .06   [illegible]  [illegible]     .04         .02         .05
MNO   [illegible]   [illegible]    .46      [illegible]     .50         .50         .52
FEO      41.[illegible] [illegible] [illegible] [illegible] [illegible] 40.30       41.03
NIO        .11  [illegible]        .14      [illegible]     .15         .14         .10
SUM   [illegible]   100.[illegible] 100.[illegible] [illegible] 99.81   99.13       99.54

SI    1.009  .        1.012  .        1.021  .        1.12[illegible] .  1.118  .        1.019  .        1.120  .
AL    [illegible] 1.[illegible] [illegible] 1.012 [illegible] 1.021 [illegible] 1.020  0.000  1.019    0.000  1.019    0.000  1.020
AL    [illegible]  .  [illegible]  .      0.000  .        [illegible] .  0.000  .        0.000  .        0.000  .
TI    [illegible]  .  [illegible]  .      [illegible] .   [illegible] .  0.000  .         .000  .         .000  .
CR    [illegible]  .   .111  .            0.000  .        [illegible] .   .001  .         .000  .         .101  .
FE    1.[illegible] .  [illegible] .       .844  .         .847  .        .865  .         .970  .         .847  .
NI    [illegible]  .   .006  .             .004  .         .005  .        .003  .         .003  .         .104  .
MG    [illegible]  .   .844  .            1.010  .        1.071  .       1.074  .         .971  .         .949  .
MN    [illegible]  .   .016  .             .011  .         .016  .        .012  .         .012  .         .013  .
CA    [illegible] 1.9[illegible] .102 1.971 [illegible] 1.9[illegible] .10[illegible] 1.959 .107 1.963 .004 1.961 .004 1.958
O     4.000  .        4.000  .        4.000  .        4.000  .       4.000  .        4.000  .        4.000  .
    FA      [illegible]       50.61           [illegible]     44.7[illegible]    44.65         49.99         50.99
    FO      [illegible]       49.31           [illegible]     55.2[illegible]    55.35         50.01         49.01

    F/M     1.[illegible]     1.347            .734            .81[illegible]    .806         1.012         1.154
    F/FM     .514              .513            .440            .45[illegible]    .450          .503          .513

41 81-290 OLIVINE 23 CORE                  45 41-292 OLIVINE 2 CORE
42 81-290 OLIVINE [illegible] RIM          46 41-234 OLIVINE 1[illegible] RIM
43 81-292 OLIVINE 11 CORE                  47 41-234 OLIVINE 2[illegible] CORE
44 81-292 OLIVINE 11 RIM
```

```
SUPER FICAL [illegible]
         161        162        163        164        165        166        167        168
SIO2   [illegible] [illegible] [illegible] [illegible] [illegible] [illegible] [illegible]  50.29
TIO2     .51        .76        .56        .47        .41        [illegible] .46         .70
AL2O3  [illegible] 1.61       .77        1.15       1.36       1.35       1.75        1.93
CR2O3  [illegible] .35        .17        .03        .11        .10        .27         .23
FEO    [illegible] [illegible] 22.56     24.[illegible] 24.14   20.[illegible] 10.14   18.94
MNO    [illegible] .60        [illegible] .47       [illegible] .48       .29         .38
MGO    [illegible] [illegible] [illegible] [illegible] 15.66   11.10      16.65       12.21
CAO    [illegible] [illegible] 5.37      [illegible] 6.37     [illegible] 17.45      14.95
NA2O     .13        .11       [illegible] [illegible] 0.00     .08        .14         .13
K2O    [illegible] .11        .11        [illegible] .02       0.10       0.00        0.00
SUM    [illegible] [illegible] [illegible] [illegible] 100.37  [illegible] 99.69      99.76

 SI    [illegible]         [illegible]         [illegible]          [illegible]          [illegible]          [illegible]          1.951                1.936
 AL    [illegible] 2.000   [illegible] 2.000   [illegible] [illegible] [illegible] 2.000  .142  2.000        [illegible] 2.010    .049  2.000          .064  2.000
 AL      .036              [illegible]           .010                .116                 .106                 .009                 .028                 .024
 TI      .014              [illegible]           .010                .114                 .114                 .019                 .013                 .020
 CR    [illegible]         [illegible]           .004                [illegible]          .104                 .003                 .008                 .007
 FE    [illegible]         [illegible]           .700                .109                 .101                 [illegible]          .315                 .610
 MG    [illegible]         [illegible]           [illegible]         [illegible]          .135                 [illegible]          .922                 .701
 MN      .104                .013                .014                [illegible]          .019                 .018                 .009                 .012
 CA    [illegible]         [illegible]           .264                .146                 .263                 [illegible]          .694                 .617
 NA    [illegible]         [illegible]           .000                0.020                0.100                .001                 .010                 .010
 K     0.000 2.106         [illegible] 2.014     .001  2.115          0.000 1.991          .001  2.001          0.000 2.012          0.000 1.999          0.000 2.001
 O     6.000               6.000                 6.003                6.000                6.103                6.000                6.000                6.000
     MG      17.56      14.99      10.25      [illegible]  13.40      32.51      35.96      32.00
     FE      17.00      31.15      [illegible] 41.71      40.90      [illegible] 16.31     31.64
     CA      [illegible] [illegible] 56.41    [illegible]  45.70      [illegible] 47.73     36.36

     F/M     [illegible] [illegible] .451     [illegible]  .816       1.332      .352       .888
     F/FM    [illegible] .646      [illegible] .663      .478       [illegible] .263       .478

161 40-MICPX IN SECTOR CORE              165 40-MICPX IN RIM
162 40-MICPX IN RIM                      166 40-MICPX IN EXTREME SECTOR CORE
163 40-MICPX IN RIM                      167 40-MICPX IN SECTOR CORE
164 40-MICPX IN RIM                      168 40-MICPX IN RIM
```

```
SUM [illegible]
        169        170    [illegible]    171        172        173        174        175        176
SIO2   [illegible] [illegible]      [illegible]  52.?3      51.75      51.43      52.29      51.26
TIO2     .71        .?3              .1?       [illegible]   .15        .46        .44        .65
AL2O3   2.16       1.?6             1.??       1.?2        1.40       1.14       1.83       1.09
CR2O3    .26        .0?              .06        .09         .41        .19        .14        .06
FEO     1?.1?      [illegible]     27.?6      13.?1        4.06       9.26       8.21      10.77
MNO      .14        .4?              .?1        .31         .21        .27        .23        .28
MGO     1?.?6      11.?7            1?.?5      1?.29       17.76      16.40      14.89      14.65
CAO     1?.?7      15.61            5.56      15.74       17.12      18.41      21.14      20.40
NA2O     .1?        .14             0.09        .06         .16        .08        .21        .19
K2O     ?.16        .11              .11       0.00        0.00       0.70       0.00       0.00
SUM     9?.??     1??.6?            99.?6     100.??       99.66      98.88      99.58     100.07

 SI   1.??          1.??           1.91?          1.942          1.935          1.943          1.949          1.923
 AL    .??  2.0??    .??? 2.000     .07?  1.9??    .054  2.000    .065  2.000    .057  2.000    .051  2.000    .077  2.000
 AL    .?2           .00?          0.000           .022           .015           .029           .023           .006
 TI    .021          .1??           .011           .015           .010           .012           .012           .018
 CR    .01?          .00?           .00?           .003           .012           .004           .004           .002
 FE    .?3?          .015           .7??           .420           .243           .290           .256           .338
 MG    .74?          .?6?          1.044           .?02           .991           .915           .827           .819
 MN    .011          .?3?           .?37           .010           .007           .009           .007           .006
 CA    .47?          .?7?           .22?           .627           .686           .738           .452           .820
 NA    .067          .333          1.00?           .00?           .012           .006           .015           .014
 K    ?.0??  2.0?5   .311  ?.0??    .30?  2.?1?   0.00?  2.005   0.000  2.015   0.000  2.002   0.000  2.004   0.000  2.023
 O    6.00?         6.000          6.000          6.000          6.000          6.000          6.000          6.000
     WO        ?6.7?         1?.6?          11.41          32.17          35.00          38.00          44.03          41.47
     FS        ?0.??         ?6.1?          ?6.51          21.55          14.43          14.97          13.22          17.09
     EN        ?.4?          ?1.2?          ?2.08          46.28          50.57          47.03          42.74          41.43

     F/M       .?11          1.??            .71?           .?76           .293           .325           .310           .420
     F/FM      .41?          .?13            .41?           .??1           .226           .240           .241           .296

169 A8-[illegible]CPX 1J SE[illegible] RIM                     173 41-267 CPX 1A CORE
170 A8-[illegible]CPX 1K [illegible] SECTOR RIM                 174 41-267 CPX 1B RIM
171 A8-[illegible]CPX 1L SECTOR RIM                             175 41-267 CPX 1C OVERGROWTH
172 A8-[illegible]CPX 1H SECTOR RIM                             176 41-267 CPX 1D OVERGROWTH
```

```
SUPFO [illegible] CAL        [illegible] PYX SERIES
          177          178          179          180          181          182          183          184
SIO2      [illegible]  [illegible]  [illegible]  52.64        52.62        51.?0        51.74        49.79
TIO2      .?1          .?3          .??          .64          .49          .79          .50          .68
AL2O3     [illegible]  ?.1?         1.?3         2.41         2.24         2.10         2.29         1.88
CR2O3     .?6          .3?          .??          .06          .32          .05          .27          0.00
FEO       11.??        ??.?6        10.?7        12.11        10.66        16.12        10.45        15.65
MNO       .?P          .??          .?6          .34          .23          .32          .39          .30
MGO       1?.?1        ??.1?        1?.73        15.41        16.47        13.77        16.59        13.65
CAO       20.??        ?.??         17.77        17.44        17.99        16.59        17.45        16.78
NA2O      .17          .1?          .09          .10          .11          .11          .06          0.00
K2O       0.?0         .1?          [illegible]  0.00         .04          .01          0.00         0.00
SUM       [illegible]  ??.4?        [illegible]  100.33       101.13       101.06       99.74        98.73

SI        1.9??        ?.??         1.91?        1.960        1.95?        1.926        1.926        1.920
AL        .0?? 2.01?   .0?? 2.000   .0?1 2.000   .040 2.000   .0?7 2.000   .074 2.000   .074 2.000   .080 2.000
AL        .12          .11?         .107         .028         .030         .019         .027         .005
TI        .0?1         .11?         .014         .115         .012         .022         .014         .020
CR        .001         .0??         .00?         .002         .004         .001         .008         0.000
FE        .?67         .5??         .???         .384         .128         .507         .325         .505
MG        .771         1.12?        .???         .857         .192         .772         .921         .785
MN        .??1         .31?         .???         .011         .007         .010         .012         .010
CA        .??0         .11?         .7??         .698         .706         .669         .696         .693
NA        .?1?         .11?         .0?7         .007         .008         .008         .004         0.000
K         ?.000 2.0??  ?.??1 ?.0?1  ?.01? 2.?23  0.000 2.003  .002 2.006   .000 2.019   0.000 2.008  0.000 2.018
O         6.000        6.000        6.000        6.000        6.000        6.000        6.000        6.000
   WO     42.??        ?.46         ?5.4?        [illegible]  36.55        34.31        35.84        34.97
   EN     1?.?5        ??.7?        17.1?        19.92        16.90        26.04        16.75        25.46
   FS     ??.47        ?7.?6        46.1?        44.23        46.55        39.66        47.40        39.57

   F/M    .474         .?37         .37?         .461         .371         .670         .367         .656
   F/FM   .?2?         .?74         .?72         .315         .271         .401         .26?         .396

177 MI-267 CPX 1F [illegible]                181 10-MM CPX 2A CORE
178 MI-267 CPX 1F [illegible]                182 10-MM CPX 2A RIM
179 AL-MA CPX 1F [illegible]                 183 10-MM CPX 3A CO-F
180 AU-MA CPX 1F [illegible]                 184 10-MM CPX 3A RIM
```

```
SUPER RECAL              [illegible] PY-[illegible]
         1-6             [illegible]       1-7              188          189          190          191          192
SIO2     51.6[illegible] [illegible]       51.55            50.[illegible]1  50.01    [illegible]  52.29        52.61
TIO2     .5[illegible]   [illegible]       .42              .4[illegible]    .60      .[illegible]2  .36        .36
A2O3     [illegible]     [illegible]       2.0[illegible]   1.[illegible]0   2.11     .49          2.12         1.93
C2O3     [illegible]     [illegible]       .16              0.00         0.00         0.00         0.00         .16
FEO      1[illegible]    1[illegible]      17.[illegible]   24.[illegible]1  16.77    23.70        10.37        10.50
MNO      [illegible]     .[illegible]4     .41              .4[illegible]    .35      .50          .21          .30
MGO      1[illegible]    1[illegible].16   1[illegible]     1[illegible].50  14.93    16.86        18.01        17.21
CAO      17.[illegible]7 1[illegible]      1[illegible].05  [illegible].[illegible]9  14.67  6.70  15.85      16.67
NA2O     [illegible]     .31               .02              [illegible]  .11          0.[illegible]0  0.00      .06
K2O      [illegible]     [illegible]       0.09             0.[illegible]0   0.00     0.00         0.00         0.00
SUM      10[illegible]   10[illegible]     9[illegible].46  100.67       99.55        100.73       99.21        99.76

 SI   1.9[illegible]          1.9[illegible]          1.9[illegible]          1.925         1.910         1.955         1.942         1.949
 AL   .0[illegible]  1.9[illegible]6  .0[illegible]  2.000  .0[illegible]1  2.000  .045  1.970  .090  2.000  .045  1.990  .058  2.000  .051  2.000
 AL   [illegible].10[illegible]       .0[illegible]           .031            0.000         .005          0.000         .035          .034
 TI   .01[illegible]          .01[illegible]          .012            .014          .017          .015          .009          .009
 CR   [illegible]             0.000           .00[illegible]          0.001         0.000         0.000         0.000         .005
 FE   .417                    .5[illegible]           .5[illegible]7  .781          .534          .758          .322          .329
 MG   .9[illegible]           .9[illegible]           .[illegible]71  1.0[illegible]  .[illegible]57  .961     .990          .951
 MN   [illegible]             .00[illegible]          .01[illegible]  .015          .011          .016          .007          .009
 CA   .70[illegible]          .6[illegible]           .60[illegible]  .[illegible]20  .600       .278          .631          .662
 NA   .0[illegible]1          .001                    .001            0.000         .008          0.000         0.000         .003
 K    0.[illegible]  2.0[illegible]2  0.00[illegible]  2.01[illegible]  0.[illegible]00  2.003  0.000  2.970  0.000  2.029  0.000  2.027  0.000  2.002  0.000  1.998
 O    6.00[illegible]         6.000                   6.000           6.000         6.000         6.000         6.000         6.000
        WO         [illegible].21    37.75        31.1[illegible]  10.74     30.21         13.91         32.33         34.15
        FS         [illegible].91    21.27        14.42        [illegible]       26.88         17.96         16.51         16.79
        EN         4[illegible].3[illegible]  4[illegible]  [illegible].40  50.94  42.91  48.13         51.16         49.05

        F/M        .441        .431         .421         .766          .640          .406          .329          .352
        F/FM       .[illegible]2[illegible]  .[illegible]25  .296  .434  .390          .446          .248          .260

185 AP-MICPY 1C                                         189 40-MICPX 1C PIM
186 AP-MICPY 3D                                         190 40-MICPX 1D PIM
187 AP-MICPY 1A G LF                                    191 40-MICPX 1A CORE
188 AP-MICPY 1F GIM                                     192 40-MICPX 1[illegible]
```

```
SUPER [illegible]              HIGH[illegible] PY[illegible]
            1[illegible]        196       165           19[illegible]        192          194
SIO2        4[illegible]   [illegible].56   4[illegible].22   5[illegible]   5[illegible].27     49.74
TIO2         .13          .1[illegible]      .14         .1[illegible]        .[illegible]6          .21
AL2O3        .[illegible]3          .[illegible]1      .[illegible]5         1.[illegible]0        1.4[illegible]          .22
CR2O3        .0[illegible]        [illegible].[illegible]0     0.00          .11          .09         0.00
FEO          [illegible].11        [illegible].36     [illegible].1[illegible]         10.70      12.4[illegible]        [illegible].18
MNO          .[illegible]0          .71      .[illegible]3          .36          .25          .67
MGO          [illegible]        [illegible]     [illegible]        17.11        1[illegible].02        10.06
CAO         1.41         [illegible].[illegible]4     1.[illegible]1         17.[illegible]1        1[illegible].[illegible]7        1.51
NA2O        0.[illegible]0        1.[illegible]     0.00          .11          .32         0.00
K2O         0.00        0.[illegible]0     0.00         0.00         0.00         0.00
SUM       10[illegible]       1[illegible].[illegible]5     [illegible].[illegible]0        [illegible]0.45       100.14       101.49

 SI    1.[illegible]          1.[illegible]6          1.[illegible]0          1.[illegible]2[illegible]          1.[illegible]41          1.984
 AL     .[illegible]6  1.[illegible]9    .0[illegible]  1.[illegible]    .[illegible]12  1.[illegible]9[illegible]   .0[illegible]  1.9[illegible]5   .0[illegible]9  2.000   .010  1.9[illegible]9
 AL    0.[illegible]0          0.[illegible]          0.[illegible]00          0.000          .0[illegible]          0.000
 TI     .0[illegible]           .015           .00[illegible]           .[illegible]10           .004           .00[illegible]
 CR    [illegible]          [illegible]          0.00[illegible]           .003           .003          0.000
 FE    [illegible]          1.[illegible]1          1.311           .[illegible]           .[illegible]7          1.[illegible]03
 MG     .[illegible]           .[illegible]43           .604           .[illegible]           .[illegible]           .[illegible]44
 MN     .[illegible]2[illegible]           .1[illegible]           .[illegible]26           .[illegible]11           .0[illegible]           .02[illegible]
 CA     .011           .10[illegible]           .[illegible]6           .[illegible]1[illegible]           .60[illegible]           .064
 NA    0.000          0.[illegible]0[illegible]          0.00[illegible]           .001           .001          0.000
 K     [illegible]  2.0[illegible]   [illegible]  [illegible]   0.0[illegible]0  2.017   0.[illegible]00  2.0[illegible]1   0.[illegible]00  2.017   0.000  2.001
 O     6.00[illegible]          6.[illegible]00          6.000          6.000          6.000          6.000
   [illegible]      3.0[illegible]         3.[illegible]        3.34        1[illegible].65        30.51        3.50
   [illegible]      [illegible]         [illegible]        55.1[illegible]        16.7[illegible]        19.41        56.10
   [illegible]      3[illegible].9[illegible]         [illegible]        [illegible]0.6[illegible]        [illegible]        50.08        [illegible]0.40

   F/[illegible]     [illegible]         2.[illegible]74        2.1[illegible]         .[illegible]          .196        2.212
   F/FM      .[illegible]         .[illegible]95         .1[illegible]         .266          .[illegible]83         .683

193 40-MM OPX [illegible]                             191 40-MM C[illegible]X 4[illegible]
196 40-MM OPX 21                             192 40-MM C[illegible]X 41
19[illegible] 40-MM OPX [illegible]                             19[illegible] 40-MM OPX 4[illegible]
```

```
[illegible]                    TYPICAL OLIVINES

           1          2          3          4          5          6          7          8
MGO   [illegible]  [illegible]  35.19  [illegible]  36.52      35.75      37.70      15.43
AL2O3 [illegible]   1.91       0.00       0.00       0.00       0.00       0.00       0.00
SIO2  [illegible]  [illegible] [illegible] [illegible] 39.70    38.37      38.81      33.55
CAO      .1?        .16        .20        .22        .15        .22        .44        .31
TIO2  [illegible]   .17        .0?       0.00        .01       0.00       0.00        .11
CR2O3 [illegible]  0.00       [illegible]  .02        .03        .05        .04        .01
MNO   [illegible]   .62        .64        .11        .56        .18        .27        .77
FEO   [illegible]  25.51      [illegible] [illegible] 24.01     23.15      21.50      56.82
NIO   [illegible]   .66        .46        .44        .60        .53        .39        .42
SUM   [illegible]  [illegible] 100.60    [illegible] 101.08     98.95      99.23     100.95

SI  1.0??         1.11?        1.09?        1.021        1.001        1.012        1.015        1.004
AL  [illegible] 1.0?1  0.1??  1.01?  0.000  1.0??  0.000  1.021  0.000  1.001  0.000  1.012  0.000  1.015  0.000  1.004
[illegible] [illegible]  1.000   0.000        0.100        0.000        0.000        0.000        0.000
TI  [illegible]   .10?         .001        0.000         .000        0.000        0.001         .002
CR  [illegible]  [illegible]  0.000         .100         .002         .001         .001         .000
FE  [illegible]   .517         .574         .477        [illegible]   .577         .472        1.259
MN  [illegible]   .010         .010         .010         .013         .011         .008         .011
MG  1.1?1         1.3?1        1.382        1.307        1.473        1.416        1.470         .600
NI  [illegible]   .012         .011         .007         .012         .004         .006         .020
CA  [illegible] 1.9??  .00?  1.974  .00?  1.943  .006  [illegible]  .004  1.997  .006  1.976  .012  1.959  .010  1.990
O   4.000         4.00?        4.000        4.000        4.000        4.000        4.000        4.000
    FA    [illegible]     29.10        28.95     [illegible]    27.60        27.32        24.31        64.66
    FO    [illegible]     70.40        71.05     [illegible]    72.40        72.65        75.69        35.34

    F/M     .43?         .61?         .423         .2??         .190         .187         .125        1.058
    -F/FM   .30?         .295         .297         .224         .280         .276         .245         .650

1 42-?6 OLIVINE PHENO 1? RIM                 5 42-34 OLIVINE PHENO 10 RIM
2 42-?6 OLIVINE PHENO 11 CORE                6 42-34 OLIVINE PHENO 1C
3 42-?6 PATCHY OLIVINE [illegible]           7 42-34 OLIVINE PHENO 30
4 42-?6 OLIVINE PHENO ?4 CORE                8 42-75 OLIVINE 1A CORE
```

```
ANAL [illegible]     9          10   [illegible] OLIVIN 11      12         13         14         15         16
MGO         14.[illegible]   [illegible]      17.[illegible]     11.76      10.44      22.14      21.57      19.78
AL2O3       [illegible]      .13        0.00       0.00       0.00       0.00       .04        .01
SIO2        [illegible].14   [illegible].15   [illegible]   33.14      32.13      35.55      35.06      34.65
CAO         .[illegible]     .[illegible]     .10        .19        .21        .16        .21        .19
TIO2        .[illegible]     .11        .16        .13        .16        .04        .06        .07
CR2O3       .[illegible]     .12        0.00       .04        .15        0.00       .14        0.00
MNO         .[illegible]     .[illegible]     .[illegible]6      .17        .49        .65        .73        .73
FEO         [illegible]1.[illegible]   [illegible]7.49   [illegible]   5[illegible].76   55.0[illegible]   40.75   42.18   43.56
NIO         .[illegible]7    .[illegible]     .36        .57        .43        .37        .28        .44
SUM         10[illegible].[illegible]6   10[illegible].1[illegible]   100.[illegible]2   9[illegible].[illegible]6   9[illegible].[illegible]2   99.46   100.27   99.43

 SI   1.002          1.011          1.015          1.020          1.003          1.020          1.004          1.015
 TI   [illegible] 1.002   .001 1.017   0.000 1.015   0.000 1.020   0.000 1.003   0.000 1.020   .001 1.011   .000 1.016
 AL   0.000          0.000          0.000          0.000          0.000          0.000          0.000          0.000
 TI   .[illegible]   .[illegible]   .004           .003           .001           .001           .001           .002
 CR   .001           .[illegible]   .006           .001           .004           0.000          .003           0.000
 FE   1.2[illegible] 1.1[illegible] 1.146          1.336          1.436          .962           1.016          1.267
 NI   .[illegible]   .011           .009           .009           .011           .009           .006           .010
 MG   .6[illegible]  .7[illegible]  .743           .574           .504           .967           .926           .864
 MN   .[illegible]   .02[illegible] .021           .025           .124           .016           .018           .018
 CA   .009  1.3[illegible]9   .012 1.96[illegible]   .009 1.961   .006 1.356   .007 1.989   .005 1.959   .006 1.976   .000 1.967
 O    4.00[illegible] 4.00[illegible]   4.000      4.000          4.000          4.000          4.000          4.000
      FA   [illegible]   62.17     [illegible]9.26   72.60      74.01      50.41      52.32      55.27
      FO   [illegible].54   37.[illegible]   41.72   27.40      25.99      49.07      47.68      44.73

      F/M  [illegible]   1.[illegible]   1.693    2.639      2.895      1.054      1.116      1.257
      F/FM .[illegible]  .[illegible]26   .637    .71[illegible]   .743   .513       .528       .557

  9 82-5 OLIVINE 1 [illegible]                13 82-74 OLIVINE 2
 10 82-5 OLIVINE 2A [illegible]               14 41-267 OLIVINE 1A CORE
 11 82-5 OLIVINE 2C [illegible]               15 41-267 OLIVINE 2
 12 82-76 OLIVINE 1                           16 41-267 OLIVINE 4
```

```
[illegible] [illegible]          [illegible] OLIVINES
          17            18            19            20            21            22            23            24
MGO    [illegible]     41.76      [illegible]     34.61      [illegible]     33.17        20.45         21.88
AL2O3  [illegible]      0.01      [illegible]      0.00          0.00         0.00         0.00           .03
SIO2   [illegible]  [illegible]  [illegible]  [illegible]  [illegible]  [illegible]      34.66         34.98
CAO          .12        .09          .07          .09           .23          .72          .18           .20
TIO2        0.1[illegible]  0.10        0.00         0.10           .25          .03          .13           .04
CR2O3   [illegible]      .08          .11          .07           .21          .17         0.00           .17
MNO          .23        .30          .45          .38           .50          .34          .65           .66
FEO        1[illegible].79  1[illegible].74  21.29   21.94         27.07        27.03        44.16         41.98
NIO          .37        .2[illegible]  .24        .14           .34          .25          .02          0.00
SUM    [illegible]     101.19       100.74       101.05         99.44        99.71    [illegible]       99.80

 SI  [illegible]  .   1.015  .       .999  .      1.004  .      1.008  .      1.016  .      1.002  .      1.009  .
 AL  [illegible] [illegible] 0.000 1.015  0.000 .993  0.000 1.004  0.000 1.008  0.000 1.016  0.000 1.002   .001 1.010
 AL  [illegible]  .   0.000  .      0.000  .      0.000  .      0.000  .      0.000  .      0.000  .      0.000  .
 TI  [illegible]  .   0.000  .      0.000  .      0.000  .       .005  .       .001  .       .003  .       .001  .
 CR    .001  .         .001  .       .002  .       .001  .       .004  .       .004  .      0.000  .       .004  .
 FE    .351  .         .403  .       .456  .       .446  .       .608  .       .605  .      1.067  .      1.012  .
 NI  [illegible]  .    .007  .       .005  .       .007  .       .007  .       .005  .       .000  .      0.000  .
 MG   1.57[illegible] . 1.55[illegible] . 1.525 .  1.504  .      1.335  .      1.322  .       .302  .       .839  .
 MN    .005  .         .006  .       .010  .       .008  .       .008  .       .006  .       .016  .       .015  .
 CA    .003 1.9[illegible]  .012 1.979   .002 2.000   .102 1.991   .008 1.976   .021 1.969   .006 1.994   .006 1.978
 O    4.000  .        4.000  .      4.000  .      4.000  .      4.000  .      4.000  .      4.000  .      4.000  .
     FO      [illegible]       20.57         23.32         23.55         31.24         31.34         54.18         51.86
     FA      [illegible]       79.43         76.38         76.45         68.77         68.62         45.82         48.16

     F/M      .256              .263          .306          .314          .461          .461         1.780         1.036
     F/FM     .286              .20[illegible]  .236        .234          .316          .316          .546          .523

 17 81-271 OLIVINE 1                                21 40-■■OLIVINE PHENO 1 CORE
 18 81-274 OLIVINE 2                                22 40-■■OLIVINE PHENO 2 CORE
 19 81-276 OLIVINE 1A                               23 40-■■OLIVINE 1A RIM
 20 81-276 OLIVINE 2A CORE                          24 40-■■OLIVINE 1A CORE
```

```
SUPER FLOAL 25          26      [illegible] OLIVINES 27      28             29             30             31             32
MGO       [illegible]   [illegible]      ?1.76       1?.?7          17.70           3.72           3.76           3.65
AL2O3     [illegible]   [illegible]        .14         .11            .03           0.00           0.00           0.00
SIO2      [illegible]   [illegible]      37.34       34.54          34.14          30.73          30.91          30.64
CAO       [illegible]        .1?           .15         .20            .14            .10            .15            .31
TIO2      [illegible]        .11           .34         .15            .01            .03            .02           0.00
CR2O3     [illegible]        .1?           .11         .17            .05           0.00            .05            .13
MNO             .6?          .2?           .24         .46            .46            .41            .91            .86
FEO       [illegible]      26.61         50.10       47.36          47.55          65.45          64.77          64.30
NIO       [illegible]        .6?           .59         .20            .02            .02            .11            .04
SUM       [illegible]     10?.?1        100.63      100.55         100.72          99.74         100.68          99.93

SI      1.02?    .     1.007    .     1.014    .     1.012    .     1.007    .     1.010    .     1.008    .     1.007    .
AL      0.000  1.021    .001  1.007    .004  1.011    .002  1.015    .001  1.009  0.000  1.010  0.000  1.008  0.000  1.007
AL      0.00?    .     0.0?     .     0.000    .     0.000    .     0.003    .     0.000    .     0.000    .     0.000    .
TI      ?.00?    .      .00?    .      .001    .      .003    .      .002    .      .001    .      .000    .      .003    .
CR      0.00?    .      .001    .      .002    .      .004    .      .001    .     0.000    .      .001    .     1.767    .
FE       .6??    .      .541    .      .672    .     1.141    .     1.174    .     1.757    .     1.766    .      .001    .
NI      1.00?    .      .017    .      .004    .      .005    .      .000    .      .001    .      .003    .      .179    .
MG      1.344    .     1.426    .     1.277    .      .746    .      .777    .      .18?    .      .143    .      .024    .
MN       .?0     .      .005    .      .072    .      .021    .      .021    .      .025    .      .025    .      .011    .
CA       .??   1.967    .005  1.996    .004  1.979    .004  1.967    .004  1.981    .013  1.990    .005  1.984    .011  1.985
O       4.061    .     4.00?    .     4.000    .     4.001    .     4.000    .     4.000    .     4.000    .     4.000    .
   FO         2?.56          27.51          34.73          61.30          60.17          10.61          90.62          90.81
   FA         69.44          72.49          65.27          38.70          39.83           9.39           9.38           9.19

   F/M         .??            .3??           .5??          1.53?          1.539          4.78?          9.403         10.010
   M/FM        .??            .277           .?91           .617           .606           .907           .907           .909

25 AR-MB OLIVINE [illegible] 1 CORE              29 40-MB OLIVINE 2
26 AR-MB OLIVINE [illegible] 2 CORE              30 41-245 OLIVINE 1A CORE
27 AR-MB OLIVINE [illegible] RIM                 31 41-245 OLIVINE 1B RIM
28 AR-MB OLIVINE 1                               32 41-245 OLIVINE 2 RIM
```

303

```
SUPPO TOTAL 33               81-103, OLIVINE
                             34              35              36              37              38              39              40
MGO      1[illegible]        1[illegible]    1[illegible]    20.25           19.16           21.13           21.31           21.93
AL2O3    [illegible]         .10             0.00            0.10            0.00            0.00            0.00            0.00
SIO2     35.33               3[illegible]    34.44           34.54           34.01           35.55           35.24           35.50
CAO      .15                 .20             [illegible]     .13             .16             .09             .21             .09
TIO2     0.16                0.00            0.00            .01             0.07            .01             .07             .04
CR2O3    [illegible]         0.00            0.30            0.00            .11             0.00            0.00            0.00
MNO      [illegible]         .54             .70             .57             .05             .64             .51             .56
FEO      52.[illegible]      41.60           44.10           44.75           44.22           43.57           47.21           41.20
NIO      0.66                .11             0.00            .14             .16             .08             .11             .18
SUM      10[illegible]       [illegible]     101.00          100.39          94.24           101.07          100.23          99.66

 SI      1.011   .           1.015   .       1.022   .       1.005   .       1.002   .       1.018   .       1.012   .       1.023   .
 AL      [illegible]  1.011  0.103   1.015   0.005   1.022   1.000   1.005   0.000   1.002   0.000   1.018   0.000   1.012   0.000   1.023
 AL      [illegible]  .      [illegible] .   0.000   .       0.000   .       0.000   .       0.000   .       0.000   .       0.000   .
 TI      [illegible]  .      [illegible] .   0.000   .       .000    .       0.000   .       .000    .       .003    .       .001    .
 CR      .001    .           [illegible] .   0.000   .       0.000   .       .003    .       0.000   .       0.000   .       0.000   .
 FE      1.127   .           1.271   .       1.240   .       1.199   .       1.140   .       1.063   .       1.114   .       .892    .
 NI      [illegible]  .      .303    .       0.000   .       .003    .       .004    .       .002    .       .003    .       .004    .
 MG      .827    .           .599    .       .45     .       .776    .       .777    .       .961    .       .934    .       .940    .
 MN      .11     .           .016    .       .01     .       .114    .       .116    .       .016    .       .012    .       .014    .
 CA      .11     1.374       .104    1.360   .003    1.376   .004    1.199   .005    1.996   .003    1.965   .006    1.975   .003    1.953
 O       4.00    .           4.009   .       4.000   .       4.100   .       4.000   .       4.000   .       4.000   .       4.000   .
     FA       [illegible]        64.45           64.30           55.36           55.42           53.64           51.92           51.37
     FO       [illegible]        35.55           35.70           44.64           44.58           46.36           48.08           48.63

     F/M      2.170              1.836           1.827           1.256           1.262           1.174           1.093           1.071
     F/FM     .686               .647            .646            .557            .559            .540            .522            .517

 33 80-80 OLIVINE 1A RIM                                  37 81-24P OLIVINE 1B CORE
 34 80-80 OLIVINE 1B CORE                                 38 81-24P OLIVINE 2
 35 80-80 OLIVINE 1C CORE                                 39 81-2 10 OLIVINE 1A CORE
 36-81-2A? OLIVINE 1A RIM                                 40 81-2 10 OLIVINE 1B RIM
```

304

```
SUPER [illegible] CAL        [illegible] OLIVINE
              41                 42                 43                 44                 45                 46                 47
MGO        [illegible]        22.[illegible]     21.64              25.[illegible]     25.6[illegible]    22.[illegible]2    22.13
AL2O3      [illegible]         0.00               0.10               0.10               0.00               0.00               0.00
SIO2       [illegible]        35.66              36.[illegible]     36.[illegible]     36.50              35.41              35.48
CAO           .11               .05                .22                .[illegible]1       .22                .12                .13
TIO2       [illegible]          .12               0.13               0.00               0.00                .02                .02
CR2O3      [illegible]          .06               0.10               0.00                .04                .02                .05
MNO        [illegible]          .59                .46                .41                .50                .50                .52
FEO        41.[illegible]     41.64              [illegible]        36.[illegible]5    36.42              40.30              41.03
NIO           .11               .16                .18                .[illegible]3       .15                .14                .18
SUM        [illegible]       100.31             100.16              9[illegible]        99.41              99.13              99.54

 SI     1.009             1.012             1.021             1.020             1.018             1.019             1.020
 AL     [illegible]  1.0[illegible]  0.000  1.012  0.000  1.021  0.000  1.020  0.000  1.018  0.000  1.019  0.060  1.020
 AL     [illegible]       0.000             0.000             0.000             0.000             0.000             0.000
 TI     [illegible]        .000             0.000             0.000             0.000              .000              .000
 CR     [illegible]        .001             0.000             0.000              .001              .000              .001
 FE     1.[illegible]      .991              .844              .867              .865              .970              .987
 NI     [illegible]        .006              .004              .005              .003              .003              .004
 MG     [illegible]        .944             1.090             1.071             1.074              .971              .949
 MN     [illegible]        .015              .011              .010              .012              .012              .013
 CA     [illegible] 1.9[illegible]  .002  1.976  .015  1.9[illegible]  .007  1.959  .007  1.963  .004  1.961  .004  1.958
 O      4.000             4.000             4.000             4.000             4.000             4.000             4.000
      FA      [illegible]1.91       50.6[illegible]       [illegible]       44.7[illegible]       44.65       49.99       50.99
      FO      48.[illegible]        49.31                 56.36             55.2[illegible]       55.35       50.01       49.01

      F/M     1.05[illegible]       1.347                 .7[illegible]     .8[illegible]         .818        1.012       1.054
      F/FM     .514                  .513                 .440              .459                  .450         .501        .513

41 81-290 OLIVINE 21 CORE                                    45 41-232 OLIVINE 2 CORE
42 81-290 OLIVINE [illegible]                                46 41-234 OLIVINE 14 RIM
43 81-292 OLIVINE 11 CORE                                    47 41-234 OLIVINE 2C CORE
44 81-292 OLIVINE 11 RIM
```

```
SUPER RECAL                          FELDSPAR ANALYSES
SUB GROUP SI   AL   /    AL   FE   CA   NA   K    /    O    /
SUB GROUP NA   /    CA   /    K    /
                1                  2                  3                  4                  5                  6                  7                  8
SIO2        62.66              66.70              56.25              54.90              59.52              60.37              59.92              56.40
A2O3        22.58              15.51              25.40              27.25              24.11              24.07              24.02              26.76
NA2O         7.38               2.32               6.49               5.74               7.49               7.72               7.36               6.36
CAO          3.58                .23               8.57              10.39               6.03               6.33               6.28               8.92
K2O          3.66              11.44                .62                .43               1.78               1.16               1.63               1.24
FEO           .21                .35                .36                .41                .04                .02               0.00                .72
SUM        100.07              96.57              98.09              99.12              98.97              99.67              99.21             100.30

SI      11.218      *     12.486      *     10.329      *     10.022      *     10.787      *     10.833      *     10.820      *     10.189      *
AL       4.763 15.981      3.426 15.911      5.582 15.910      5.862 15.884      5.149 15.937      5.090 15.923      5.111 15.931      5.697 15.886
AL       0.000      *      0.000      *      0.000      *      0.000      *      0.000      *      0.003      *      0.000      *      0.000      *
FE        .031      *       .055      *       .059      *       .063      *       .006      *       .003      *      0.000      *       .109      *
CA        .687      *       .046      *      1.686      *      2.032      *      1.171      *      1.217      *      1.215      *      1.707      *
NA       2.562      *       .842      *      2.318      *      2.032      *      2.632      *      2.686      *      2.577      *      2.228      *
K         .836  4.115      2.731  3.674       .145  4.197       .100  4.226       .411  4.220       .260  4.172       .375  4.167       .286  4.330
O       32.000      *     32.000      *     32.000      *     32.000      *     32.000      *     32.000      *     32.000      *     32.000      *
  AB           62.72             23.26             55.79             48.79             62.45             64.43             61.83             52.78
  AN           16.81              1.27             40.71             48.80             27.78             29.20             29.16             40.45
  OR           20.46             75.46              3.51              2.40              9.76              6.37              9.01              6.77

  1 80-331 ANORTHOCLASE CORE OF OCCELLI                           5 80-337 GRAN NOD PLAG 1
  2 80-331 KSPAR IN OCCELLI                                       6 80-337 GAN NOD PLAG 2
  3 80-337 GRAN NOD SKELETAL PLAG 1                               7 80-337 GRAN NOD PLAG 3
  4 80-337 GRAN NOD SKELETAL PLAG 2                               8 80-337 GRAN NOD SKELETAL PLAG 1

                9                 10                 11                 12                 13                 14                 15                 16
SIO2        59.89              55.68              55.02              55.35              54.93              65.43              51.76              58.50
A2O3        25.51              27.95              27.34              28.44              27.88              18.42              30.36              25.21
NA2O         7.65               5.96               5.84               5.77               5.45               6.54               4.21               6.60
CAO          7.28               9.59              10.02              10.47              10.06                .08              12.44               8.79
K2O           .85                .78                .71                .81                .77               7.87                .17                .43
FEO           .32                .18                .21                .20                .21                .09                .37                .32
SUM        101.42             100.14              99.14             101.04              99.30              98.43              99.31              99.85

SI      10.598      *     10.039      *     10.037      *      9.924      *      9.994      *     11.968      *      9.803      *     10.521      *
AL       5.320 15.918      5.938 15.977      5.877 15.915      6.009 15.932      5.977 15.971      3.970 15.938      6.094 15.896      5.343 15.863
AL       0.000      *      0.000      *      0.000      *      0.000      *      0.000      *      0.000      *      0.000      *      0.000      *
FE        .047      *       .027      *       .032      *       .030      *       .032      *       .014      *       .055      *       .048      *
CA       1.365      *      1.853      *      1.959      *      2.011      *      1.961      *       .016      *      2.430      *      1.694      *
NA       2.625      *      2.083      *      2.066      *      2.006      *      1.922      *      2.319      *      1.488      *      2.301      *
K         .192  4.229       .179  4.143       .165  4.221       .185  4.232       .179  4.094      1.836  4.185       .040  4.015       .099  4.142
O       32.000      *     32.000      *     32.000      *     32.000      *     32.000      *     32.000      *     32.000      *     32.000      *
  AB           62.77             50.63             49.31             47.73             47.33             55.60             37.60             56.22
  AN           32.65             45.02             46.75             47.86             48.28               .38             61.40             41.37
  OR            4.59              4.36              3.94              4.41              4.40             44.02              1.00              2.41

  9 80-337 GRAN NOD SKELETAL PLAG 2                              13 80-337 GAB INCL PLAG 2B RIM
 10 80-337 GAB INCL PLAG 1A                                      14 82-60 PHENO
 11 80-337 GAB INL PLAG 1B RIM                                   15 81-286 PLAG 1 CORE
 12 80-337 GAB INCL PLAG 2A                                      16 81-286 PLAG 2 EDGE
```

```
SUPER RECAL                                   FELDSPAR ANALYSES
              17               18               19               20               21               22               23               24
SIO2        51.09            53.68            55.36            51.77            51.34            53.54            51.09            52.52
A2O3        29.77            28.60            26.81            29.00            30.16            27.52            29.49            29.29
NA2O         3.67             4.64             5.68             3.82             3.43             5.07             3.42             4.31
CAO         14.00            12.34            10.21            13.92            14.36            11.98            14.24            13.16
K2O           .22              .26              .23              .14              .09              .17              .54              .12
FEO.          .55              .48              .71              .68              .82              .89             1.34              .65
SUM         99.30           100.00            99.00            99.33           100.20            99.17           100.08           100.05

 SI      9.397      .     9.748      .    10.105      .     9.516      .     9.363      .     9.827      .     9.371      .     9.564      .
 AL      6.452 15.858     6.120 15.868     5.767 15.872     6.281 15.797     6.482 15.845     5.952 15.779     6.381 15.754     6.285 15.849
 AL      0.000      .     0.000      .     0.000      .     0.000      .     0.000      .     0.000      .     0.000      .     0.000      .
 FE       .085      .      .073      .      .108      .      .105      .      .125      .      .137      .      .206      .      .099      .
 CA      2.759      .     2.401      .     1.997      .     2.741      .     2.806      .     2.356      .     2.801      .     2.568      .
 NA      1.309      .     1.634      .     2.010      .     1.361      .     1.213      .     1.804      .     1.217      .     1.522      .
 K        .052  4.204      .060  4.168      .054  4.169      .033  4.240      .021  4.165      .040  4.337      .126  4.351      .028  4.216
 O      32.000      .    32.000      .    32.000      .    32.000      .    32.000      .    32.000      .    32.000      .    32.000      .
     AB          31.77            39.90            49.[illegible]   32.92            30.02            42.96            29.37            36.96
     AN          66.98            58.[illegible]   49.18            66.29            69.46            56.09            67.58            62.36
     OR           1.25             1.47             1.32              .79              .52              .95             3.05              .68

 17 81-288 PLAG 1A CORE                                      21 81-292 PLAG 1B
 18 81-288 PLAG 1B                                           22 81-232 PLAG 1C RIM
 19 81-288 PLAG 1C RIM                                       23 81-292 PLAG 2A CORE
 20 81-292 PLAG 1A CORE                                      24 81-242 PLAG 2B RIM

              25               26               27               28               29               30               31               32
SIO2        52.36            54.13            63.68            63.23            53.00            54.34            55.52            52.90
A2O3        28.28            28.36            22.68            23.27            28.53            27.93            27.62            29.77
NA2O         4.28             4.69             8.21             7.84             4.49             4.85             5.34             4.07
CAO         12.98            12.27             4.57             4.98            12.45            11.80            10.70            12.89
K2O           .09              .29              .82             1.01              .13              .13              .25              .25
FEO           .63              .45              .30              .26              .57              .48              .81              .54
SUM         98.62           100.19           100.26           100.59            99.17            99.53           100.24           100.42

 SI      9.665      .     9.805      .    11.253      .    11.154      .     9.708      .     9.886      .    10.017      .     9.574      .
 AL      6.151 15.816     6.053 15.858     4.723 15.975     4.837 15.991     6.158 15.866     5.988 15.874     5.872 15.890     6.349 15.923
 AL      0.000      .     0.000      .     0.000      .     0.000      .     0.000      .     0.000      .     0.000      .     0.000      .
 FE       .097      .      .068      .      .044      .      .078      .      .087      .      .073      .      .122      .      .082      .
 CA      2.567      .     2.381      .      .865      .      .941      .     2.443      .     2.300      .     2.068      .     2.500      .
 NA      1.532      .     1.647      .     2.813      .     2.681      .     1.595      .     1.711      .     1.868      .     1.428      .
 K        .021  4.217      .067  4.164      .185  3.907      .227  3.888      .030  4.156      .030  4.114      .058  4.116      .058  4.067
 O      32.000      .    32.000      .    32.000      .    32.000      .    32.000      .    32.000      .    32.000      .    32.000      .
     AB          37.18            40.22            72.82            69.65            39.19            42.33            46.77            35.83
     AN          62.31            58.15            22.40            24.45            60.06            56.92            51.79            62.72
     OR            .51             1.64             4.78             5.90              .75              .75             1.44             1.45

 25 81-292 PLAG 3 IN CPX                                     29 81-293 PLAG3A CORE
 26 81-286 PLAG 2 CORE                                       30 81-293 PLAG 4A CORE
 27 81-293 PLAG 1 IN GRAPHIC INTERGROWTH                     31 81-293 PLAG 4B RIM
 28 81-233 PLAG 2 IN GRAPHIC INTERGROWTH                     32 81-290 PLAG 1A CORE
```

```
SUPER RECAL                       FELDSPAR ANALYSES
          33                  34               35               36               37               38               39               40
SIO2    55.49               50.71            55.29            51.77            51.89            53.36            50.57            54.36
A2O3    27.17               30.66            24.27            31.20            28.94            29.64            31.21            28.74
NA2O     5.19                3.37             5.20             2.49             6.60             4.17             2.96             4.73
CAO     10.52               14.49            11.06            14.57            12.01            12.99            15.00            11.41
K2O       .34                 .13              .27              .13              .20              .25              .14              .21
FEO       .36                 .46              .52              .41              .33              .68              .40              .41
SUM     99.22               99.82           100.41           100.49            99.97           100.69           100.18            99.86

 SI   10.000     .        9.274     .      9.916     .      9.300     .      9.760     .      9.626     .      9.216     .      9.836     .
 AL    5.923  15.909      6.611  15.849    5.987  15.923    6.661  15.961    6.176  15.937    6.301  15.927    6.702  15.918    6.130  15.966
 AL    0.000     .        0.000     .      0.000     .      0.000     .      0.000     .      0.000     .      0.000     .      0.000     .
 FE     .052     .         .070     .       .078     .       .062     .       .050     .       .103     .       .061     .       .062     .
 CA    2.050     .        2.841     .      2.130     .      2.821     .      2.331     .      2.513     .      2.929     .      2.213     .
 NA    1.900     .        1.195     .      1.812     .      1.015     .      1.615     .      1.458     .      1.011     .      1.660     .
 K      .079   4.001       .030   4.137     .062   4.001     .030   3.929     .046   4.042     .058   4.052     .033   4.033     .040   3.983
 O    32.000     .       32.000     .     32.000     .     32.000     .     32.000     .     32.000     .     32.000     .     32.000     .
    AB         47.17             29.50            45.26            26.26            40.46            36.93            25.44            42.11
    AN         50.87             69.85            53.20            72.96            58.38            61.61            73.74            56.63
    OR          1.96               .75             1.55              .78             1.16             1.46              .82             1.24

 33 81-238 PLAG 1B RIM                                        37 81-267 PLAG 2B RIM
 34 81-238 PLAG 2A CORE                                       38 81-267 PLAG 2 CORE
 35 81-238 PLAG 2B RIM                                        39 81-267 PLAG 3A CORE IN CPX OIK
 36 81-267 PLAG 1A CORE                                       40 81-267 PLAG 3B RIM IN CPX OIK

          41                  42               43               44               45               46               47               48
SIO2    54.84               55.74            52.50            55.71            55.94            56.29            55.40            53.41
A2O3    29.19               28.05            29.00            27.76            26.93            26.86            27.33            28.57
NA2O     4.91                5.34             4.01             5.10             5.09             5.54             5.44             4.23
CAO     11.57               10.04            12.92            10.04            10.11             9.61            10.30            12.81
K2O       .20                 .73              .45              .69              .66              .88              .80              .51
FEO       .27                 .17              .65              .25              .30              .21              .30              .70
SUM    100.30              100.07            99.43            99.55            99.83            99.39            99.65            99.43

 SI    9.739     .       10.042     .      9.615     .     10.080     .     10.175     .     10.207     .     10.067     .      9.754     .
 AL    6.242  15.981      5.955  15.997    6.258  15.873    5.919  15.999    5.772  15.947    5.739  15.946    5.844  15.911    6.148  15.903
 AL    0.000     .        0.000     .      0.000     .      0.000     .      0.000     .      0.000     .      0.003     .      0.000     .
 FE     .041     .         .026     .       .100     .       .038     .       .046     .       .032     .       .045     .       .107     .
 CA    2.234     .        1.938     .      2.516     .      1.946     .      1.970     .      1.867     .      2.002     .      2.150     .
 NA    1.716     .        1.865     .      1.424     .      1.799     .      1.795     .      1.949     .      1.916     .      1.498     .
 K      .046   4.036       .168   3.997     .105   4.144     .159   3.933     .153   3.964     .204   4.050     .185   4.147     .119   4.074
 O    32.000     .       32.000     .     32.000     .     32.000     .     32.000     .     32.000     .     32.000     .     32.000     .
    AB         42.94             46.97            35.20            45.94            45.81            48.47            46.66            37.76
    AN         55.91             48.80            62.20            49.97            50.28            46.46            48.82            59.25
    OR          1.15              4.22             2.60             4.09             3.91             5.07             4.51             2.99

 41 81-267 PLAG 4 CORE IN CPX OIK                             45 80-337 PLAG PHENO 1D
 42 80-337 PLAG PHENO 1A CORE                                 46 80-337 GAB INCL PLAG 3
 43 80-337 PLAG PHENO 1B RIM                                  47 80-337 GAB INCL PLAG 4
 44 80-337 PLAG PHENO 1C                                      48 80-337 MATRIX PLAG 2
```

```
SUPER RECAL                                  FELDSPAR ANALYSES
             49                      50               51                 52                53               54                55                56
SIO2       54.23                   59.58            58.18              59.16             65.07            65.64             65.85             64.52
A2O3       27.77                   25.71            25.46              24.86             17.71            18.73             13.56             21.83
NA2O        4.73                    6.44             6.49               6.82               .2[illegible]     .29              8.82              6.89
CAO        11.64                    7.13             7.16               6.83              0.00              .02               .65              2.60
K2O          .63                    1.58             1.18               1.48             15.[illegible]    15.80              4.31              4.60
FEO          .47                     .43              .22                .16              [illegible]       .13               .49               .09
SUM        99.47                  100.97            99.58              99.49             99.05            100.61             99.68            100.53

 SI        9.893      .           10.600    .      10.597     .       10.693    .       12.109    .       12.010    .       11.794    .       11.463    .
 AL        5.970   15.863          5.390 15.990     5.400  15.997      5.273 15.965      3.884 15.991      3.990 16.000      4.124 15.918      4.537 16.000
 AL        0.000      .            0.000    .       0.000     .        0.000    .        0.000    .         .040    .        0.000    .         .033    .
 FE         .072      .             .064    .        .033     .         .024    .         .033    .         .020    .         .071    .         .011    .
 CA        2.275      .            1.359    .       1.381     .        1.318    .        0.000    .         .004    .         .125    .         .495    .
 NA        1.673      .            2.221    .       2.261     .        2.342    .         .079    .         .103    .        3.069    .        2.373    .
 K          .147    4.166           .359  4.003      .317   3.992       .340  4.054      3.760  3.872      3.647  3.862       .983  4.250      1.042  3.957
 O        32.000      .           32.000    .      32.000     .       32.000    .       32.000    .       32.000    .       32.000    .       32.000    .
     AB           40.86                 56.39             57.12             58.96              2.07              2.71             73.33             60.69
     AN           55.56                 34.50             34.88             32.63              0.00               .10              2.99             12.66
     OR            3.58                  9.10              8.00              8.42             97.93             97.19             23.68             26.66

49 80-337 MATRIX PLAG 3                                      53 80-371 MATRIX KSPAR 1
50 80-371 MB-PLAG INCL PLAG 1                                54 80-371 MATRIX KSPAR 2
51 80-371 MB-PLAG INCL PLAG 2                                55 80-371 MATRIX KSPAR 3
52 80-371 MB PLAG INCL PLAG 3-                               56 80-396 FELD PHENO 1

             57                      58               59                 60                61               62                53                64
SIO2       64.35                   64.34            51.14              52.71             53.16            54.02             66.82             65.78
A2O3       20.95                   20.77            29.04              29.40             29.50            28.95             18.73             19.23
NA2O        6.79                    6.55             4.05               4.24              4.20             4.17              4.71              4.25
CAO         2.42                    2.30            12.30              10.66             12.34            11.94               .64               .87
K2O         5.02                    5.16              .41               1.35               .48               .44             9.15              8.94
FEO          .38                     .28              .78                .75               .69               .55               .20               .37
SUM        99.91                   99.40           100.34              99.21            100.37            100.07             99.25             99.36

 SI       11.540      .           11.583    .       9.588     .        9.642    .        9.624    .        9.777    .       11.920    .       11.914    .
 AL        4.427   15.967          4.406 15.990     6.302  15.889      6.358 16.000      6.297 15.926      6.174 15.951      4.059 15.978      4.086 16.000
 AL        0.000      .            0.000    .       0.000     .         .065    .        0.000    .        0.003    .        0.000    .         .023    .
 FE         .057      .             .042    .        .118     .         .115    .         .105    .         .083    .         .031    .         .056    .
 CA         .465      .             .444    .       2.494     .        2.089    .        2.395    .        2.315    .         .126    .         .169    .
 NA        2.361      .            2.286    .       1.417     .        1.504    .        1.479    .        1.463    .        1.679    .        1.494    .
 K         1.148    4.031          1.183  3.957      .099   4.127       .245  4.018       .111  4.085       .102  3.963      2.146  3.982      2.068  3.810
 O        32.000      .           32.000    .      32.000     .       32.000    .       32.000    .       32.000    .       32.000    .       32.000    .
     AB           59.41                 58.40             35.16             39.18             37.05             37.71             42.50             40.05
     AN           11.73                 11.33             62.28             54.44             60.16             59.67              3.19              4.53
     OR           28.89                 30.27              2.47              6.38              2.79              2.62             54.31             55.42

57 80-396 FELD PHENO 2                                       61 80-396 MATRIX PLAG 2
58 80-396 FELD PHENO 3                                       62 80-396 MATRIX PLAG 3
59 80-396 MATRIX PLAG 1A RIM                                 63 80-396 MATRIX KSPAR 1
60 80-396 MATRIX PLAG 1A CORE                                64 80-337 MATRIX KSPAR 1
```

```
SUPER RECAL                          FELDSPAR ANALYSES
              65                 66                 67                 68                 69                 70                 71                 72
SIO2        53.59              53.43              54.00              53.34              52.52              53.84              54.75              56.67
A2O3        29.14              29.70              29.24              29.85              30.19              28.29              29.53              27.57
NA2O         4.96               4.93               4.33               4.68               4.34               4.67               4.56               5.83
CAO         11.32              11.38              11.75              11.59              11.62              11.08              11.41               9.11
K2O           .14                .17                .16                .21                .10                .17                .21                .38
FEO           .52                .42                .55                .54                .59                .50                .50                .76
SUM         99.67             100.03              99.33             100.21              99.56              99.55             100.56             100.32

 SI       9.736     *        9.678     *        9.769     *        9.643     *        9.557     *        9.860     *        9.765     *       10.166     *
 AL       6.237  15.972      6.330  16.000      6.271  16.008      6.157  16.000      6.443  16.000      6.109  15.975      6.235  16.000      5.828  15.994
 AL       0.000     *         .004     *         .004     *         .003     *         .031     *        0.000     *         .015     *        0.000     *
 FE        .079     *         .064     *         .083     *         .082     *         .090     *         .077     *         .073     *         .114     *
 CA       2.203     *        2.207     *        2.142     *        2.245     *        2.305     *        2.175     *        2.196     *        1.751     *
 NA       1.747     *        1.730     *        1.729     *        1.640     *        1.541     *        1.654     *        1.599     *        2.028     *
 K         .032   4.061       .039   4.044       .037   3.994       .048   4.018       .023   3.980       .040   3.951       .048   3.924       .087   3.980
 O       32.000     *       32.000     *       32.000     *       32.000     *       32.000     *       32.000     *       32.000     *       32.000     *
     AB          43.86              43.51              44.25              41.70              39.68              42.83              41.44              52.45
     AN          55.32              55.50              54.81              57.07              59.72              56.15              57.30              45.30
     OR            .81                .99                .94               1.23                .60               1.03               1.26               2.25

 65 81-273 PLAG 1A                                          69 81-273 PLAG 3B RIM
 66 81-273 PLAG 1B                                          70 81-276 PLAG 1A
 67 81-273 PLAG 2                                           71 81-276 PLAG 1B
 68 81-273 PLAG 3A CORE                                     72 81-276 PLAG 2A RIM

              73                 74                 75                 76                 77                 78                 79                 80
SIO2        54.95              53.63              52.48              51.99              51.90              51.07              53.11              50.75
A2O3        28.26              31.09              30.51              30.59              30.73              30.47              30.29              29.[illegible]
NA2O         5.50               3.18               4.06               4.05               3.41               3.45               3.52               4.06
CAO         10.20              14.70              13.49              13.50              14.43              14.46              13.95              13.80
K2O           .25                .05                .05                .08                .09                .13                .09                .13
FEO           .85                .32                .52                .67                .69                .66                .67                .73
SUM        100.01             100.05             101.07             100.88             101.25             100.24             101.63              99.87

 SI       9.935     *        9.234     *        9.449     *        9.396     *        9.355     *        9.317     *        9.508     *        9.376     *
 AL       6.021  15.955      6.682  15.916      6.477  15.923      6.514  15.910      6.527  15.882      6.547  15.860      6.390  15.897      6.431  15.806
 AL       0.000     *        0.000     *        0.000     *        0.000     *        0.000     *        0.000     *        0.000     *        0.000     *
 FE        .129     *         .049     *         .078     *         .101     *         .104     *         .101     *         .101     *         .113     *
 CA       1.976     *        2.888     *        2.595     *        2.614     *        2.787     *        2.825     *        2.675     *        2.767     *
 NA       1.928     *        1.125     *        1.417     *        1.419     *        1.192     *        1.220     *        1.222     *        1.467     *
 K         .058   4.090       .012   4.073       .011   4.102       .018   4.153       .021   4.103       .030   4.176       .021   4.018       .031   4.330
 O       32.000     *       32.000     *       32.000     *       32.000     *       32.000     *       32.000     *       32.000     *       32.000     *
     AB          48.67              27.94              35.23              35.03              29.80              29.93              31.18              34.25
     AN          49.86              71.77              64.49              64.52              69.68              69.33              68.29              65.03
     OR           1.46                .29                .29                .46                .52                .74                .52                .73

 73 81-276 PLAG 2B CORE                                     77 80-46 PLAG PHENO 1A CORE
 74 81-234 PLAG 1A IN CPX OIK                               78 80-46 PLAG PHEN 1B
 75 81-234 PLAG 1B RIM IN CPX OIK                           79 80-46 PLAG PHENO 1C
 76 81-234 PLAG 2 IN CPX OIK                                80 80-46 PLAG PHENO 2A CORE
```

```
SUPER RECAL                      FELDSPAR ANALYSES
            81            82            83            84            85            86            87            88
SIO2     51.67         49.53         53.20         51.31         51.91         54.52         55.88         56.51
A203     29.33         31.35         30.14         29.80         29.22         28.00         27.05         26.67
NA20      3.76          3.23          3.43          3.46          3.64          5.06          6.11          6.44
CAO      13.72         14.91         14.12         13.88         13.44         11.71         10.67         10.03
K20        .12           .15           .13           .12           .11           .18           .32           .34
FEO        .80           .66           .10           .88           .80          1.25          1.30          1.22
SUM      99.40         99.83        101.06         99.45         99.12        100.72        101.33        101.21

 SI    9.407   .     9.096   .     9.420   .     9.417   .     9.538   .     9.848   .    10.033   .    10.136   .
 AL    6.346 15.832  6.784 15.880  6.460 15.880  6.445 15.862  6.327 15.865  5.960 15.807  5.723 15.755  5.637 15.773
 AL    0.000   .     0.000   .     0.000   .     0.000   .     0.000   .     0.001   .     0.003   .     0.000   .
 FE     .123   .      .101   .      .121   .      .135   .      .123   .      .189   .      .195   .      .183   .
 CA    2.699   .     2.934   .     2.730   .     2.729   .     2.646   .     2.266   .     2.052   .     1.928   .
 NA    1.338   .     1.150   .     1.203   .     1.231   .     1.297   .     1.772   .     2.127   .     2.240   .
 K      .028  4.188   .035  4.220   .030  4.081   .028  4.124   .026  4.091   .041  4.269   .073  4.448   .078  4.428
 O    32.000   .    32.000   .    32.000   .    32.000   .    32.000   .    32.000   .    32.000   .    32.000   .
     AB       32.92        27.92        30.30        30.87        32.68        43.44        50.01        52.76
     AN       66.39        71.23        68.94        68.41        66.67        55.55        48.26        45.41
     OR         .69          .85          .76          .70          .65         1.02         1.72         1.83

81 80-[illegible] PLAG PHENO 2B EDGE                 85 80-[illegible] PLAG PHENO 3C RIM
82 80-[illegible] PLAG PHENO 2C                      86 80-[illegible] PLAG MATRIX 4
83 80-[illegible] PLAG PHENO 3A CORE                 87 80-[illegible] MATRIX PLAG 5
84 80-[illegible] PLAG PHENO 3B                      88 80-[illegible] MATRIX PLAG 6
            89            90            91            92            93            94            95            96
SIO2     51.80         51.57         53.35         51.34         52.68         54.40         65.89         56.95
A203     30.06         29.77         29.47         30.75         29.98         29.57         20.77         26.42
NA20      3.74          4.50          4.71          3.72          4.30          4.83         11.04          6.41
CAO      13.01         13.04         12.74         13.48         12.90         12.00          1.48          9.12
K20        .11           .16           .20           .14           .19           .32           .95           .41
FEO        .58           .48           .39           .55           .47           .52           .21           .50
SUM      99.30         99.52        101.06        100.48        100.51        101.64        100.34         99.81

 SI    9.378   .     9.451   .     9.610   .     9.325   .     9.531   .     9.808   .    11.612   .    10.280   .
 AL    6.504 15.882  6.428 15.879  6.255 15.866  6.581 15.906  6.392 15.923  6.070 15.877  4.313 15.926  5.620 15.899
 AL    0.000   .     0.000   .     0.000   .     0.000   .     0.000   .     0.000   .     0.000   .     0.000   .
 FE     .089   .      .074   .      .089   .      .084   .      .071   .      .078   .      .031   .      .079   .
 CA    2.717   .     2.560   .     2.459   .     2.720   .     2.501   .     2.314   .      .279   .     1.764   .
 NA    1.331   .     1.594   .     1.645   .     1.310   .     1.508   .     1.688   .     3.772   .     2.243   .
 K      .026  4.163   .037  4.270   .046  4.239   .032  4.146   .042  4.122   .074  4.158   .214  4.296   .075  4.177
 O    32.000   .    32.000   .    32.000   .    32.000   .    32.000   .    32.000   .    32.000   .    32.000   .
     AB       32.68        38.10        39.64        32.24        37.24        41.38        88.44        54.69
     AN       66.69        61.01        59.25        66.96        61.74        56.81         6.55        43.00
     OR         .63          .89         1.11          .80         1.03         1.81         5.01         2.30

89 80-[illegible] PLAG 1A CORE                       93 80-[illegible] PLAG 2C
90 80-[illegible] PLAG 1B RIM                        94 80-[illegible] PLAG 2D RIM
91 80-[illegible] PLAG 2A CORE                       95 81-285 PLAG 1 IN INTERGROWTH
92 80-[illegible] PLAG 2B                            96 81-285 PLAG 2A CORE
```

```
SUPER REJAL                     FELDSPAR ANALYSES
             97                     98              99                   100                  101                  102                  103                  104
SIO2      60.27                  58.27           56.77                59.61                51.00                51.80                53.78                52.93
A2O3      24.77                  29.46           27.20                25.19                30.14                29.35                29.03                29.45
NA2O       7.93                   6.79            6.23                 7.87                 3.92                 4.34                 4.31                 4.18
CAO        6.00                   8.23            9.52                 7.55                13.86                13.17                12.91                13.13
K2O         .51                    .51             .43                  .57                  .14                  .16                  .14                  .16
FEO         .52                    .64             .71                  .68                  .65                  .59                  .64                  .66
SUM      100.00                  99.90          100.96               101.49               100.31               100.61               100.73               100.69

 SI      10.710      .        10.486      .    10.163      .       10.574      .        9.394      .        9.592      .        9.689      .        9.575      .
 AL       5.187  15.897.       5.394  15.885    5.738  15.302       5.264  15.838       6.666  15.860       6.259  15.852       6.172  15.860       6.278  15.853
 AL       0.000      .         0.000      .     0.000      .        0.000      .        0.000      .        0.000      .        0.000      .        0.000      .
 FE        .077      .          .096      .      .106      .         .101      .         .099      .         .089      .         .097      .         .108      .
 CA       1.295      .         1.587      .     1.826      .        1.434      .        2.703      .        2.454      .        2.496      .        2.565      .
 NA       2.732      .         2.369      .     2.162      .        2.706      .        1.384      .   [illegible]     .        1.500      .        1.536      .
 K         .116   4.220         .117   4.169     .098   4.193        .129   4.370        .033   4.218        .037   4.203        .032   4.132        .032   4.213
 O       32.000      .        32.000      .    32.000      .       32.000      .       32.000      .       32.000      .       32.000      .       32.000      .
      AB         65.96                58.17            32.31                63.38                33.59                37.82                37.16                37.15
      AN         31.25                38.96            64.68                33.60                65.62          [illegible]                61.84                61.57
      OR          2.79                 2.87             2.40                 3.02                  .79                  .90                  .80                  .79

 97 81-285 PLAG 2B RIM                                           101 80-MW PLAG PHENO 1A
 98 81-285 PLAG 2C                                               102 80-MW PLAG PHENO 1B
 99 81-285 PLAG 3A CORE                                          103 80-MW PLAG PHENO 1C
100 81-285 PLAG 3B RIM                                           104 80-MW PLAG PHENO 1D

            105                    106             107                  108                  109                  110                  111                  112
SIO2      56.68                  55.11           53.70                52.31                51.88          [illegible]                52.58                51.57
A2O3      26.61                  27.96           28.19                29.26                29.57                27.54                29.46                30.31
NA2O       6.14                   5.54            5.36                 4.68                 4.64                 6.83                 4.72                 4.67
CAO        9.11                  10.90           10.94                12.08                12.45                 9.00                12.57                12.71
K2O         .43                    .34             .32                  .25                  .22          [illegible]                  .25                  .21
FEO         .72                   1.02             .67                  .73                  .45                  .73                  .63                  .80
SUM       99.69                 100.87           99.58                99.31                99.21               101.20               100.21               100.27

 SI      10.247      .         9.920      .     9.802      .        9.587      .        9.919      .       10.023      .        9.561      .        9.393      .
 AL       5.669  15.916        5.931  15.850    6.064  15.866       6.319  15.906       6.394  15.913       5.818  15.841       6.313  15.874       6.506  15.899
 AL       0.000      .         0.000      .     0.000      .        0.000      .        0.000      .        0.000      .        0.000      .        0.000      .
 FE        .109      .          .154      .      .102      .         .112      .         .069      .         .109      .         .093      .         .122      .
 CA       1.765      .         2.102      .     2.120      .        2.372      .        2.448      .        1.882      .        2.449      .        2.480      .
 NA       2.152      .         1.933      .     2.076      .        1.663      .        1.651      .        2.374      .        1.666      .        1.649      .
 K         .099   4.125         .074   4.247     .075   4.271        .058   4.205        .051   4.219        .089   4.455        .059   4.267        .049   4.300
 O       32.000      .        32.000      .    32.000      .       32.000      .       32.000      .       32.000      .       32.000      .       32.000      .
      AB         51.59.               47.00            48.59                40.62                39.78                54.63                39.90                39.47
      AN         43.94                51.10            49.67                57.95                58.98                43.32                58.71                59.36
      OR          2.47                 1.90             1.75                 1.43                 1.24                 2.05                 1.39                 1.17

105 80-MWMATRIX PLAG 2                                           109 80-MSPLAG 1C RIM
106 80-MWMATRIX PLAG 3 CORE                                      110 80-MSPLAG 2A CORE
107 80-MWPLAG 1A CORE                                            111 80-MSPLAG 2B
108 80-MWPLAG 1B                                                 112 80-MSPLAG 2C
```

```
SUPER RECAL                          FELDSPAR ANALYSES
          113              114              115              116              117              118              119              120
SIO2     51.54            63.54            64.36            61.37            52.10            51.83            51.43            54.41
A2O3     29.19            18.85            18.72            23.71            29.41            29.70            29.59            27.42
NA2O      4.36             3.18             2.55             9.02             4.34             4.27             4.21             6.06
CAO      12.71              .23              .23             5.12            12.96            12.97            12.79            10.21
K2O        .26            11.99            12.66              .73              .23              .21              .48              .34
FEO        .63              .20              .48              .64              .50              .54              .69              .44
SUM      98.69            97.99            99.00           100.59            99.54            99.52            99.19            98.88

 SI    9.581     *    11.852     *    11.903     *    10.917     *     9.540     *     9.489     *     9.467     *     9.966     *
 AL    6.354 15.875    4.143 15.995    4.080 15.983    4.970 15.897    6.324 15.864    6.407 15.896    6.410 15.885    5.918 15.885
 AL    0.000     *     0.000     *     0.000     *     0.000     *     0.000     *     0.000     *     0.000     *     0.004     *
 FE     .097     *      .031     *      .074     *      .095     *      .092     *      .083     *      .106     *      .067     *
 CA    2.516     *      .046     *      .046     *      .976     *     2.542     *     2.544     *     2.522     *     2.004     *
 NA    1.562     *     1.150     *      .914     *     3.111     *     1.541     *     1.516     *     1.502     *     2.152     *
 K      .061  4.236    2.853  4.080    2.986  4.021     .166  4.347     .054  4.229     .049  4.191     .113  4.244     .079  4.303
 O    32.000     *    32.000     *    32.000     *    32.000     *    32.000     *    32.000     *    32.000     *    32.000     *
      AB     37.73            28.41            23.17            73.16            37.24            36.89            36.31            50.81
      AN     60.79             1.14             1.15            22.95            61.46            61.92            60.96            47.31
      OR      1.48            70.46            75.68             3.90             1.30             1.19             2.72             1.88

113 80-MMPLAG 2D RIM                                         117 A0-MMPLAG 2A CORE
114 80-MMKSPAK 1 IN INTERGPOWTH                              118 A0-MMPLAG 2A RIM
115 80-MMKSPAR b IN INTERGFOWTH                              119 A0-MMPLAG 3A CORE
116 80-MMPLAG 1 ADJACENT TO INTERGROWTH                      120 A0-MMPLAG 3A RIM
```

```
LAKE NIPIGON [illegible]

              1          2          3          4          5          6          7          8          9         10
SIO2  [illegible] [illegible] [illegible] [illegible]    0.00       0.10       1.00       0.00       0.10      0.00
TIO2  [illegible] [illegible] [illegible] [illegible]   11.74 [illegible]     49.76      10.63       4.10      7.29
AL2O3 [illegible] [illegible]     1.11   [illegible]     .75        .10        .06        .71        .69      1.26
V2O3  [illegible]     0.10       0.10       0.00       0.16       0.00       0.00       0.00       0.00      0.00
CR2O3 [illegible]      .16        .16        .16        .13        .14        .03        .20        .07       .05
FEO   [illegible] [illegible] [illegible] [illegible]   84.79 [illegible]     41.36      87.45      88.30     81.17
MNO        .45        .36        .17        .18        .22        .14        .43        .22        .40       .28
MGO        .09        .16        .17 [illegible]        .16        .18        .08        .08        .11       .70
SUM   [illegible]   100.61 [illegible] [illegible]    97.18     100.01     101.17      95.69      93.97     92.75
RECALCULATED ANALYSIS - MAGNETITE-ULVOSPINEL BASIS
FE2O3 [illegible]   -27.94 [illegible]     40.30      47.59 [illegible]    -21.97      47.73      59.69     43.79
FEO       74.44 [illegible] [illegible] [illegible]     41.13 [illegible]     75.46      46.85      34.58     36.32
TOTL  [illegible] [illegible] [illegible] [illegible]  101.40 [illegible]     97.30     100.48      99.74     97.68
USP   [illegible] [illegible] [illegible] [illegible]   31.46     160.40     143.43      30.20      12.37     20.94
RECALCULATED ANALYSIS - ILMENITE-HEMATITE BASIS
FE2O3 [illegible] [illegible] [illegible] [illegible]   82.59       6.47       6.21      82.21      93.41     91.99
FEO   [illegible] [illegible] [illegible]     10.10      10.39      41.66      41.77       9.79       9.74      7.36
TOTL  [illegible] [illegible] [illegible]    105.36     105.16     100.75     102.74     103.46     103.17    100.67
ILMN  [illegible] [illegible] [illegible] [illegible]   21.10 [illegible]     34.01      20.26       8.33     14.32

             11         12         13         14         15         16         17         18         19         20
SIO2  [illegible] [illegible]     0.00 [illegible]      0.00       0.10       1.00       0.00       0.00      0.00
TIO2      64.17 [illegible] [illegible]      7.75      16.85 [illegible]      6.66       6.63      48.19     18.32
AL2O3 [illegible]     1.72       2.46       2.61       2.59        .12       2.29       3.28        .13      1.44
V2O3  [illegible]     0.00 [illegible] [illegible]     0.00       0.00       0.00       0.00       0.00      0.00
CR2O3 [illegible]      .37 [illegible]     17.14      16.36       1.11 [illegible]     20.16       1.14       .09
FEO   [illegible] [illegible] [illegible] [illegible] [illegible] [illegible] [illegible]   65.09      44.54     78.37
MNO   [illegible]      .23 [illegible] [illegible]     .66        .46        .75        .64        .42       .29
MGO   [illegible]      .12 [illegible] [illegible]     2.06 [illegible]      1.29       2.48       5.27       .06
SUM   [illegible] [illegible] [illegible] [illegible] [illegible] [illegible] [illegible]   99.78      99.65     98.37
RECALCULATED ANALYSIS - MAGNETITE-ULVOSPINEL BASIS
FE2O3 [illegible] [illegible] [illegible] [illegible] [illegible]   -24.00 [illegible]     34.13     -24.15     32.99
FEO   [illegible] [illegible] [illegible]     35.41 [illegible] [illegible]     36.06      34.16      66.40     48.46
TOTL  [illegible] [illegible] [illegible] [illegible] [illegible] [illegible] [illegible]  101.60      97.26    101.64
USP   [illegible]     14.61 [illegible]     21.74 [illegible]    131.73 [illegible]     17.12     131.45     50.87
RECALCULATED ANALYSIS - ILMENITE-HEMATITE BASIS
FE2O3 [illegible] [illegible] [illegible] [illegible]   65.32      11.54 [illegible] [illegible]     11.57     67.79
FEO   [illegible] [illegible] [illegible] [illegible] [illegible]    34.53      14.96      12.73      34.12     17.13
TOTL  [illegible] [illegible] [illegible] [illegible] [illegible] [illegible] [illegible]  104.04     100.90    105.08
ILMN  [illegible] [illegible] [illegible] [illegible]   13.56 [illegible]     13.57      13.56      88.17     34.28
```

```
LAKE ST. JOHN [illegible]
            21          22          23          24          25          26          27          28          29          30
SIO2      0.10        0.00        0.10        0.11        0.10        0.10        0.00        0.10        0.32        0.00
TIO2    [illegible] [illegible]  11.38       11.47        9.51        9.70        9.31        4.46        5.90        5.68
AL2O3   [illegible] [illegible]    .71        2.16         .67         .77         .79        7.48        8.32        9.03
V2O3      0.00        0.00        0.00        0.00        0.00        0.00        0.00        0.00        0.00        0.00
CR2O3   [illegible] [illegible]   1.14        0.30        4.95        1.17        0.00       34.17       34.72       34.45
  FEO   [illegible]  67.74       76.17       79.77       70.10       70.59       73.00       44.34       41.48       43.93
  MNO     1.10         .28         .35         .05         .20         .19         .03        1.49        1.37        1.79
  MGO   [illegible]    .56         .73         .07         .27         .26        2.78        2.12        5.34        3.32
  SUM   [illegible] [illegible]  90.60       90.62       89.40       90.57       83.71       95.16       95.33       97.70
RECALCULATED ANALYSIS  -  MAGNETITE-ULVOSPINEL BASIS
F2O3     17.41       33.06       40.71       74.15       36.34       36.45       44.36       14.54       15.23       14.26
  FEO    33.28       37.37       39.59       39.79       37.60       37.48       21.43       30.44       27.76       31.09
TOTL    [illegible] [illegible]  96.61       96.38       93.48       94.22       86.50       96.00       97.44       99.11
  USP   [illegible] [illegible]  35.64       26.66       29.15       27.70       21.76       13.40       13.37       15.15
RECALCULATED ANALYSIS  -  ILMENITE-HEMATITE BASIS
F2O3    [illegible] [illegible]  73.03       71.45       63.71       64.45       73.44       26.66       27.44       27.05
  FEO    21.46       14.26       10.57       11.04       12.74       12.61        1.43       20.03       16.40       14.56
TOTL     96.11       96.10       97.41       97.74       96.21       95.00       11.58       97.40       98.60      100.38
ROMH    [illegible]  21.09       23.47       24.11       20.53       19.10       14.60       11.48       11.44       12.94

            31
SIO2       .60
TIO2       .44
AL2O3     7.38
V2O3      0.00
CR2O3   [illegible]
  FEO    45.17
  MNO     1.32
  MGO     2.66
  SUM    95.10
RECALCULATED ANALYSIS  -  MAGNETITE-ULVOSPINEL BASIS
F2O3     14.40
  FEO    31.30
TOTL     97.37
  USP   [illegible]
RECALCULATED ANALYSIS  -  ILMENITE-HEMATITE BASIS
F2O3    [illegible]
  FEO    13.55
TOTL    [illegible]
ROMH     14.13
```

```
LAKE [illegible] OXIDES

          41          42          43          44          45          46          47          48          49          50
SIO2  [illegible]     0.00        0.10        0.00    [illegible]     0.00        0.00        0.00        0.00        0.00
TIO2  [illegible] [illegible]     50.1[illegible] [illegible] [illegible] 10.1[illegible] [illegible] 44.29  10.03       10.46
A2O3      .13         .11     [illegible]     .08    [illegible] [illegible]     .11         .07        1.25        2.34
V2O3      0.10    [illegible]     0.00        0.00        0.00        0.03        0.00        0.00        0.00        0.09
C2O3  [illegible] [illegible]     .02         0.00         .07         .05        0.00        0.00         .10         .09
 FEO  [illegible] [illegible] [illegible] [illegible]     81.50   [illegible] [illegible] [illegible]    80.75       80.64
 MNO  [illegible]     .49         .52         .49         .59     [illegible]     .56         .56         .61         .50
 MGO  [illegible]    1.16     [illegible] [illegible]     .22         .31         .74         .77         .06         .26
 SUM  [illegible] [illegible] [illegible] [illegible] [illegible] [illegible] [illegible] [illegible]    92.46       94.29
RECALCULATED ANALYSIS  -  MAGNETITE-ULVOSPINEL BASIS
F2O3  [illegible] [illegible] [illegible]    -28.06       46.74       44.16   [illegible] [illegible]    46.10       45.22
 FEO  [illegible] [illegible] [illegible]     74.37   [illegible] [illegible]    75.52    [illegible]    39.15       39.90
TOTL  [illegible] [illegible] [illegible]     97.40   [illegible]     97.14   [illegible] [illegible]    97.44   [illegible]
 USP  [illegible] [illegible] [illegible]    139.34       20.54   [illegible] [illegible] [illegible]    29.46   [illegible]
RECALCULATED ANALYSIS  -  ILMENITE-HEMATITE BASIS
F2O3  [illegible] [illegible] [illegible]      7.34       80.06       71.40        7.22   [illegible]    79.34       78.27
 FEO  [illegible] [illegible] [illegible]     42.46   [illegible]     10.44       41.30       42.43        9.29       10.13
TOTL  [illegible] [illegible]    101.24      100.11      102.22      101.13      102.05       94.18      100.72      102.05
[illegible] [illegible] [illegible] [illegible] 92.15 [illegible]     19.75   [illegible]     94.10       19.84       20.29

          51          52          53          54          55          56          57          58          59          60
SIO2  [illegible] [illegible]     0.10        0.00        0.00        0.00        0.00        0.00        0.00        0.00
TIO2  [illegible]    50.15    [illegible] [illegible] [illegible] [illegible] [illegible] [illegible]    10.79       11.00
A2O3  [illegible]     .11         .12     [illegible]     .08     [illegible]     .08     [illegible]    2.43        1.62
V2O3  [illegible]     0.00        0.00    [illegible]     0.00        0.00        0.00        0.00        0.00        0.00
C2O3  [illegible] [illegible] [illegible]     .15         0.00        0.10        0.00        0.00         .13         .13
 FEO  [illegible] [illegible] [illegible]    83.17        47.21   [illegible]    47.93       47.26       81.37       79.11
 MNO  [illegible]     .54         .52         .64     [illegible]     .50         .41     [illegible]     .66        1.68
 MGO  [illegible]    1.35     [illegible]     .09        1.12        1.73        1.68        1.40         .16         .11
 SUM  [illegible]   101.17    [illegible]    94.79    [illegible] [illegible] [illegible]    94.58       95.54       93.65
RECALCULATED ANALYSIS  -  MAGNETITE-ULVOSPINEL BASIS
F2O3  [illegible] [illegible] [illegible]    49.50    [illegible] [illegible]   -27.08    [illegible]    45.25       44.42
 FEO  [illegible] [illegible] [illegible] [illegible]    75.17    [illegible] [illegible] [illegible]    40.61       39.10
 TOT  [illegible] [illegible] [illegible] [illegible] [illegible] [illegible] [illegible]    96.74      100.02       98.05
 USP  [illegible]   141.74    [illegible]    24.57    [illegible]   137.57    [illegible]   140.22       30.46       31.80
RECALCULATED ANALYSIS  -  ILMENITE-HEMATITE BASIS
F2O3  [illegible] [illegible]     7.49    [illegible] [illegible] [illegible] [illegible]     6.76       78.64       77.60
 FEO      7.71    [illegible] [illegible] [illegible]    41.64        40.00   [illegible]    41.17       10.52        9.20
TOTL  [illegible] [illegible] [illegible]   103.00    [illegible] [illegible] [illegible]   100.25      103.33      101.34
[illegible] [illegible] [illegible] [illegible] [illegible] [illegible] [illegible] [illegible] 93.54 20.69     21.48
```

```
LAKE [illegible]

MOL PERCENT  [illegible]  [illegible]  [illegible]
  1     [illegible]   1.0          7.36         A1-285 ILM 1
  2     [illegible]   1.30         [illegible]  A1-285 ILM 2
  3     14.17         [illegible]  [illegible]  A1-285 MGT 3
  4     13.42         [illegible]  35.1[illegible]  A1-285 MGT 4
  5     15.73         [illegible]  34.27        A1-285 MGT 5
  6     [illegible]   1.30         [illegible]  A1-285 ILM 6
  7     [illegible]   1.0          5.1[illegible]   A1-285 ILM 7
  8     15.11         [illegible]  34.[illegible]   A1-285 MGT 8
  9     [illegible]   [illegible]  45.[illegible]   A0-[illegible] MGT
 10     10.47         [illegible]  34.5         A0-[illegible] MGT
 11     31.[illegible]  [illegible]  3.0[illegible]  A0-[illegible] ILM
 12     7.[illegible]   [illegible]  42.6[illegible]  A0-[illegible] MGT
 13     10.61         [illegible]  33.3[illegible]  A1-276 CH 1
 14     10.35         [illegible]  [illegible]  A1-276 CH 2
 15     3.1[illegible]  [illegible]  4[illegible].82  A1-276 CH 3
 16     [illegible]   0.00         11.65        A1-276 ILM 4
 17     9.04          [illegible]  40.46        A1-276 CH 6
 18     4.96          [illegible]  41.04        A1-276 CH 7
 19     [illegible]   [illegible]  11.[illegible]   A1-276 [illegible]
 20     [illegible]   [illegible]  24.57        A0-[illegible] MGT 1
 21     16.50         [illegible]  33.41        A0-[illegible] MGT 6
 22     [illegible].27  1.13       3.7          A0-[illegible] ILM 7
 23     14.59         [illegible]  11.41        A0-[illegible] MGT [illegible]
 24     17.17         [illegible]  32.0         A0-[illegible] MGT 10
 25     13.13         [illegible]  33.67        A0-[illegible] MGT 11
 26     [illegible]6.07  0.01      [illegible]  A0-[illegible] ILM 13
 27     16.1[illegible]  0.0[illegible]  1.82   A0-[illegible] ILM 14
 28     13.50         [illegible]  35.51        A0-[illegible] MGT 15
 29     35.93         0.00         4.07         A0-[illegible] ILM 16
 30     10.61         [illegible]  33.3[illegible]  A1-273 CH 1
 31     9.[illegible]0  [illegible]  40.1[illegible]  A1-273 CH 2
 32     [illegible]6.97  0.0[illegible]  1.0[illegible]  A1-273 ILM 4
 33     [illegible]7.47  0.00      2.5[illegible]   A1-273 ILM [illegible]
 34     [illegible]   1.07         5.20         A1-257 ILM 1
 35     [illegible]3.74  0.0[illegible]  5.26   A1-267 ILM 2
 36     13.46         53.0         [illegible]  A1-267 MGT 4
 37     13.44         0.00         6.0[illegible]   A1-267 ILM 5
 38     [illegible].57  0.30       [illegible]  A1-267 ILM 6
 39     [illegible].57  0.0[illegible]  [illegible]  A1-267 ILM 7
 40     14.72         [illegible]  3[illegible].7[illegible]  A1-267 MGT 8
 41     31.9[illegible]  0.0[illegible]  4.16   A1-290 ILM 1
 42     [illegible]0.7[illegible]  1.00  4.3[illegible]  A1-290 ILM 2
 43     14.42         0.01         [illegible]  A1-290 ILM 3
 44     12.9[illegible]  1.00      7.05         A1-290 ILM 4
 45     14.27         [illegible]  35.7[illegible]  A1-290 MGT 5
 46     14.5[illegible]  [illegible]  [illegible].41  A1-290 MGT 6
 47     33.13         0.0          6.87         A1-290 ILM 7
 48     36.10         0.00         5.9[illegible]   A1-290 ILM 8
 49     14.73         [illegible]  35.27        A1-290 MGT 9
 50     14.35         [illegible]  35.0[illegible]  A1-2[illegible] MGT 1
 51     11.15         [illegible]  [illegible]  A1-2[illegible] MGT [illegible]
 52     13.40         0.00         6.1[illegible]   A1-243 ILM 2
 53     12.74         [illegible]  7.26         A1-243 ILM 3
 54     17.26         [illegible]  37.71        A1-243 MGT 4
 55     16.60         1.0[illegible]  6.0[illegible]  A1-243 ILM 5
 56     11.76         0.0[illegible]  4.22      A1-243 ILM 6
 57     12.17         [illegible]  7.[illegible]    A1-243 ILM 7
 58     [illegible]   [illegible]  [illegible]  A1-243 ILM [illegible]
 59     15.[illegible]  [illegible]  34.77      A1-243 MGT 9
 60     15.[illegible]0  [illegible]  14.31     A1-2[illegible] MGT 1
```

```
                         G
LAKE MICHIGAN  [illegible]
             1          2          3          4          5          6          7          8          9         10
SIO2      0.00       0.00       0.00       0.17       0.00       0.00       1.00       0.10       0.30       0.00
TIO2  [illegible]   49.09  [illegible] [illegible] [illegible]  19.17      11.46      44.91      50.24      50.76
AL2O3     1.50        .04  [illegible] [illegible]  2.[illegible] 2.13       2.07        .95        .06        .11
V2O3      0.00       0.00       0.00       0.10       0.00       0.10       0.00       0.00       0.00       0.00
CR2O3      .17       0.00        .24        .05        .17        .16        .06       0.00        .07       0.00
FEO  [illegible]    47.61      74.62  [illegible]  76.05      73.43      74.64      47.72      46.65      47.54
MNO  [illegible]      .66        .42        .50  [illegible]    .48        .35        .48        .57        .53
MGO        .11       1.14        .66        .38        .37        .48        .82       1.12       1.33        .96
SUM  [illegible] [illegible] [illegible] [illegible]  97.35      96.45      37.40      96.78      98.16      99.90
RECALCULATED ANALYSIS  -  MAGNETITE-ULVOSPINEL BASI
F2O3 [illegible]   -27.50  [illegible]    29.74      31.56      29.17      21.58     -29.67     -30.14     -30.77
FEO  [illegible] [illegible] [illegible]  49.14      67.62  [illegible]  47.19      73.95      73.80      75.26
TOTL [illegible]    96.17  [illegible]   101.68     100.44  [illegible]  100.33      95.44      95.74      96.95
USP  [illegible] [illegible] [illegible] [illegible] [illegible]  55.69      54.16     142.25     142.61     143.25
RECALCULATED ANALYSIS  -  ILMENITE-HEMATITE BASIS
F2O3 [illegible]     7.76      67.01      66.44      65.72      62.18      64.79       5.31       4.94       5.51
FEO  [illegible]    49.65      17.56      17.41  [illegible]  17.70      17.17      42.43      42.20      43.47
TOTL    101.76  [illegible] [illegible] [illegible] [illegible] 103.10     101.72  [illegible]   99.67     100.35
POMP [illegible] [illegible] [illegible] [illegible] [illegible]  37.73      36.67  [illegible]   95.15      95.58

            11         12         13         14         15         16         17         18         19         20
SIO2      0.00       0.00       0.00       0.00       0.00       0.00       0.00       0.00       0.00       0.00
TIO2      5.10      10.41  [illegible]     9.44      10.50      10.69      11.65       3.15       8.14       3.85
AL2O3     4.47  [illegible]     1.19       1.53       2.14       2.72       1.25  [illegible]     4.10       5.32
V2O3      0.00       0.00       0.00       0.10       0.00       0.00       0.00       0.00       0.00       0.00
CR2O3 [illegible]   11.13       0.30  [illegible]     8.27  [illegible]     0.00      28.72      17.31      16.35
FEO      45.19  [illegible] [illegible]   71.50      69.71      66.14      74.08      44.79      66.37      60.01
MNO       1.43        .17       0.90        .50        .15        .34        .01       1.02        .40        .39
MGO        .25        .29  [illegible]     .42        .36        .40        .43       2.07        .25       1.12
SUM  [illegible] [illegible] [illegible]   92.41  [illegible]   89.77      87.92      87.78      92.17      89.04
RECALCULATED ANALYSIS  -  MAGNETITE-ULVOSPINEL BASIS
F2O3 [illegible]    30.62      -4.90      36.98      34.46      30.65      34.90      16.11      32.26      32.45
FEO  [illegible] [illegible]   57.13  [illegible]    38.57      38.52      34.14      26.48      37.31      31.57
TOTL [illegible] [illegible] [illegible]   96.27      94.34      92.41      91.87      89.77      95.17      93.06
USP  [illegible] [illegible]  103.14      27.75      30.67      32.13      35.72  [illegible]    23.73      11.35
RECALLULATE  ANALYSIS  -  ILMENITE-HEMATITE BASIS
F2O3 [illegible]    56.12  [illegible] [illegible]   61.47      56.65      71.47      26.51      56.51      52.52
FEO  [illegible] [illegible]   27.14      13.01  [illegible]   15.10  [illegible]    17.49      15.46      13.49
TOTL [illegible] [illegible] [illegible]   94.04      97.07      95.38  [illegible]    96.18      97.77      95.04
ROMP     12.65      21.70      64.59  [illegible]    21.75      23.12      24.05       7.90      17.53       8.76
```

```
LAKE MICHIGAN [illegible]

          21          22          23          24          25          26          27          28          29          30
SIO2  [illegible]     0.06        0.10        0.11        0.10        0.00        0.00  [illegible]      0.13        0.00
TIO2  [illegible] [illegible]    1?.14       11.17  [illegible] [illegible] [illegible]      4.46        5.00        5.68
AL2O3 [illegible] [illegible]      .71        2.16         .07         .07         .79        7.48        8.32        8.03
V2O3      0.00        0.00        0.00        0.00        0.00        0.00        0.00        0.00        0.00        0.00
CR2O3 [illegible] [illegible]     1.14        0.10        4.05  [illegible]      0.00       34.17       34.72       34.45
FEO   [illegible]    67.74  [illegible]   [illegible]     70.10  [illegible]     73.00       44.14       41.48       43.91
MNO   [illegible] [illegible]      .15         .05         .20         .19         .03        1.49        1.17        1.79
MGO   [illegible]      .56         .23         .07         .27         .26  [illegible]      2.32        5.04        3.32
SUM   [illegible] [illegible] [illegible]  [illegible]     89.40  [illegible]     83.71  [illegible]     95.33       97.70
RECALCULATED ANALYSIS  -  MAGNETITE-ULVOSPINEL BASIS
FE2O3 [illegible]    71.06       40.71  [illegible] [illegible]     36.45       64.36  [illegible]     15.23       14.26
FEO   [illegible] [illegible] [illegible]  [illegible]     37.60       37.48       21.43       30.94       27.76       31.09
TOTL  [illegible] [illegible] [illegible]  [illegible]     93.48  [illegible] [illegible] [illegible]     97.44       99.11
USP   [illegible] [illegible] [illegible]  [illegible]     29.15       27.70       21.76       13.40       13.37       15.15
RECALCULATED ANALYSIS  -  ILMENITE-HEMATITE BASIS
FE2O3 [illegible] [illegible] [illegible]     71.45       63.71       64.45       71.44  [illegible]     27.44       27.05
FEO       21.41  [illegible]      10.37       11.04       12.74       12.61        1.43  [illegible]     16.40       14.56
TOTL  [illegible] [illegible] [illegible]  [illegible] [illegible] [illegible]     11.58  [illegible] [illegible]    100.38
ROMH  [illegible]    21.09       23.47       24.11       20.53  [illegible]     14.60       11.48       11.44       12.94

          31
SIO2  [illegible]
TIO2  [illegible]
AL2O3 [illegible]
V2O3      0.00
CR2O3 [illegible]
FEO   [illegible]
MNO   [illegible]
MGO   [illegible]
SUM   [illegible]
RECALCULATED ANALYSIS  -  MAGNETITE-ULVOSPINEL BASIS
FE2O3 [illegible]
FEO   [illegible]
TOTL  [illegible]
USP   [illegible]
RECALCULATED ANALYSIS  -  ILMENITE-HEMATITE BASIS
FE2O3 [illegible]
FEO   [illegible]
TOTL  [illegible]
ROMH  [illegible]
```

LAKE HE[illegible] [illegible]

M[illegible]L [illegible]	[illegible]	[illegible]	[illegible]	
1	15.[illegible]	[illegible].00	36.[illegible]	[illegible]1-2[illegible] MGT 1
2	62.67	0.00	7.63	[illegible]1-2[illegible] ILM 1
3	27.71	[illegible].00	22.25	R0-MM MGT 1
4	27.15	[illegible].00	22.65	R0-MM MGT [illegible]
5	25.72	50.00	24.2[illegible]	R0-MM MGT [illegible]
6	27.66	50.0[illegible]	22.16	R0-MM MGT 4
7	27.0[illegible]	50.00	[illegible]	R0-MM MGT 5
8	16.27	0.00	5.13	R0-MM ILM 6
9	45.1[illegible]	0.00	4.4[illegible]	R0-MM ILM 7
10	35.5[illegible]	0.00	4.42	R0-MM ILM [illegible]
11	7.2[illegible]	50.0[illegible]	42.77	R0-1099 [illegible]IRO
12	15.0[illegible]	50.00	36.[illegible]	R0-1049 CHRO
13	61.3[illegible]	0.00	11.61	R0-1049 I[illegible]M[illegible]
14	13.[illegible]	50.00	35.1[illegible]	R0-1099 ATOL
15	15.[illegible]	50.00	34.67	R0-1099 ATOL
16	16.0[illegible]	50.00	33.[illegible]	R0-1049 ATOL
17	17.[illegible]	50.00	32.14	R0-1099 MAGN
18	4.0[illegible]	50.00	45.34	R0-1099 CHRO
19	11.[illegible]7	50.00	34.1[illegible]	R0-1099 CHRO
20	5.67	50.06	44.3[illegible]	R0-1099 CHRO
21	[illegible].1[illegible]	50.00	46.1[illegible]	R0-1049 CHRO
22	14.70	50.00	35.[illegible]	R0-1049 CHRO
23	17.77	50.00	32.7[illegible]	R0-1099 MAGN
24	17.7[illegible]	50.00	32.27	R0-1019 MAGN
25	14.55	50.00	35.42	R0-1099 ATOL
26	13.[illegible]	50.00	36.1[illegible]	R0-1019 ATOL
27	10.[illegible]	50.00	39.1[illegible]	R0-1099 ATOL
28	6.70	51.00	41.30	R0-122 CH[illegible]OM
29	6.6[illegible]	50.00	43.3	R0-122 CH[illegible]OM
30	7.58	50.00	42.42	R0-322 CH[illegible]OM
31	4.11	50.0[illegible]	41.65	R0-122 CH[illegible]OM

```
SUB [illegible]                    GARNET ANALYSES
SUB GROUP [illegible]  FE  /  AL  [illegible]  /  MG  /  FE  /  O  /
SUB GROUP FE  /  MN  /  [illegible]  /  MG  /
            1              2              3              4              5              6              7              8
MGO       [illegible]     .04            .67            .02          12.03          12.18          12.38            .04
AL2O3     [illegible]    [illegible]     .41            .10          22.55          22.72          22.75           5.72
SIO2      [illegible]    [illegible]    35.19          35.45          39.53          39.70          39.95          35.92
CAO       [illegible]    [illegible]    32.64          32.35           1.67           1.64           1.64          31.96
TIO2       1.14           1.10            .99           1.07            .04            .02            .04           1.00
CR2O3      0.00           0.00            .12            .02            .04           0.00            .02           0.00
MNO         .14            .60            .37            .35            .34            .16            .33            .37
FEO       22.[illegible] 22.36          24.26          24.28          24.34          24.44          24.56          23.33
SUM       [illegible]    96.70          97.24          96.77         100.50         100.96         101.67          96.34

 SI     6.40[illegible]   *     6.27[illegible]   *     6.430     *     6.440     *     5.160     *     5.956     *     5.946     *     6.431     *
 AL     [illegible]  6.4[illegible]  0.0[illegible]  6.278  0.000  6.430  0.000  6.440   .840  6.000   .044  6.000   .054  6.000  0.000  6.431
 AL      .26[illegible]   *     [illegible]       *      .611     *      .535     *     3.161     *     3.904     *     3.117     *      .785     *
 TI      .154     *      .155     *      .131     *      .145     *      .106     *      .002     *      .034     *      .135     *
 CR     0.000     *     0.000     *      .003     *      .003     *      .005     *     0.000     *      .002     *     0.000     *
 MG      .01[illegible]   *      .011     *      .029     *      .005     *     2.694     *     2.641     *     2.747     *      .011     *
 CA     6.2[illegible]    *     6.2[illegible]    *     6.250     *     6.232     *      .253     *      .263     *      .262     *     6.131     *
 MN      .0[illegible]    *      .002     *      .056     *      .053     *      .165     *      .046     *      .042     *      .056     *
 FE     3.[illegible]47  10.6[illegible]3  3.525  10.471  3.626  10.699  3.667  10.678  3.064  10.031  3.064  10.018  3.057  10.051  3.493  10.610
 O     24.000     *    24.000     *    24.000     *    24.000     *    24.000     *    24.000     *    24.000     *    24.000     *
   GROS         64.5[illegible]       63.2[illegible]        62.81          62.71           4.18           4.34           4.28          63.26
   SPES           .53            .9[illegible]          .56            .54            .72            .75            .64            .58
   ALM          34.91          35.6[illegible]        36.44          36.70          50.56          50.46          50.06          36.05
   PYRP           .14            .11            .19            .05          44.54          44.45          44.97            .11

   F/M     25[illegible].13[illegible]   336.192        137.456        631.090          1.151          1.152          1.128        332.503
   F/FM           .99[illegible]          .997           .995           .998           .536           .535           .530           .997

 1 82-166 GARNET 1 CORE                           5 40-337 GARNET 1 CORE
 2 82-166 GARNET 2 RIM                            6 40-337 GARNET 2 CORE
 3 82-166 GARNET 2 CORE                           7 40-337 GARNET 3
 4 82-166 GARNET 4 CORE                           8 82-166 GARNET 4A RIM
```

nature and development of the middle Proterozoic (Keweenawan) Midcontinent Rift of North America, in Processes of continental rifting: Morgan P., and Baker, B.H., (eds.), Tectonophysics, v. 94, pp. 413-437.

Green, T.H. 1976. Experimental generation of cordierite - or garnet-bea[illegible]ng granitic liquids from a pelitic composition. Geology, v. 4, pp. 85-88.

Green, D.H., and Ringwood, A.E. 1967. An experimental investigation of the gabbro to eclogite transformation and its petrological applications. Geochimica et Cosmochimica Acta, v. 31, pp.767-833.

Greenburg, J.K. and Brown, B.A. 1984. Cratonic sedimentation during the Proterozoic: An anorogenic connection in Wisconsin and the upper Midwest. Jounal of Geology, v. 92, pp. 159-171.

Griffin, W.L., Carswell, D.A., and Nixon, P.H. 1979. Lower crustal granulites and eclogites from Lesotho, southern Africa. In The Mantle Sample: Inclusions in Kimberlites and other Volcanics. Edited by F.R. Boyd and H.O.A. Meyer, American Geophysical Union, 2nd Kimberlite Conference Proceedings, pp. 59-86.

Hall, R.P., Hughes, D.J., and Friend, C.R.L. 1985. Geochemical evolution and unusual pyroxene chemistry of the MD tholeiite dyke swarm from the Archean craton of southern west Greenland. Journal of Petrology, v. 26, pp. 253-282.

Halls, H.C. 1978. The late Precambrian central North American rift system - A survey of recent geological and geophysical

REFERENCES

Abbey, S. 1978. Calibration standards. X-ray Spectrometry, v. 7, pp. 99-121.

Anderson, E.M. 1937. The dynamics of formation of cone-sheets, ring-dikes and cauldron subsidences, Proceedings Royal Society of Edinburgh, v. 56, pp. 128-157.

Anderson, J.L. 1983. Proterozoic anorogenic granite plutonism of North America. Geological Society of America Memoir 161, pp. 133-154.

Anderson, S.L., and Burke, Kevin. 1983. A Wilson Cycle approach to some Proterozoic problems in Eastern NorthAmerica. Geological Society of America Memoir 161, pp. 75-93.

Basaltic Volcanism Study Project. 1981. Basaltic Volcanism on the Terrestrial Planets. Pergamon Press, Inc., New York, 1286p.

Bell, K.C. 1971. Boundary geology, upper Nelson River area, Manitoba and Northwestern Ontario. In Geoscience Studies in Manitoba. Edited by A.C. Turnock, Geological Association of Canada,'Special Paper 9, pp. 11-40.

Bhattacharji, S. and Koide, H. 1975a. Mechanistic interpretation of rift valley formation. Science, v. 189, pp. 791-793.

Bhattacharji, S. and Koide, H. 1975b. Mechanistic model for triple junction fracture geometry. Nature, v.255, pp. 21-24.

Bhattacharji, S. and Smith, C.H. 1964. Flowage differentiation. Science, v. 145, pp. 150-153.

Bird, P. 1979. Continental delamination and the Colorado Plateau. Journal of Geophysical Research, v. 84, pp.

7561-7571.

Blackadar, R.G. 1956. Differentiation and assimilation in the Logan sills, Lake Superior district, Ontario. American Journal of Science, v. 254, pp. 623-645.

Books, K.G. 1972. Paleomagnetism of some Lake Superior Keweenawan rocks. U.S. Geological Survey Professional Paper 760, 42 p.

Bottinga, Y., Weill, D.F., and Richet, P. 1982. Density calculations for silicate liquids. I. Revised method for aluminosilicate compositions. Geochimica et Cosmochimica Acta, v. 46, pp. 909-919.

Bowen, N.L. 1928. The Evolution of the Igneous Rocks. Princeton University Press, 332p.

Breaks, F.W. 1980. Lithophile Minerlization in Northwestern Ontario, Rare Element Granitoid Pegmatites; p. 5-9 In Summary of Field Work, 1980, by the Ontario Geological Survey, V.G. Milne, O.L. White, R.B. Barlow, J.A. Robertson, and A.C. Colvine (editors), Ontario Geological Survey, Miscellaneous Paper 96, 201 p.

Bradley, J. 1965. Intrusion of major dolerite sills. Transactions of the Royal Society of New Zealand, v. 3, pp. 27-55.

Burke, K.C. 1978. Evolution of continental rift systems in the light of plate tectonics. In Ramberg, I.B., and Neumann, E-R, (eds), Tectonics and Geophysics of Continental Rifts: NATO Advanced Study Institute Series C, D. Reidel, Boston, p. 1-9.

Burke, K.C.A. and Dewey, J.F. 1973. Plume-generated triple junctions: Key indicators in applying plate tectonics to old rocks. Jour. Geology, v.81, pp.406-433.

Campbell, I.H. 1985. The difference between oceanic and continental tholeiites: a fluid dynamic explanation, Contributions to Mineralogy and Petrology, v. 91, pp. 37-43.

Card, K.D., Church, W.R., Franklin, J.M., Frarey, M.I., Robertson, J.A., West, G.F., and Young, G.M. 1972. The Southern Province, in R.A. Price and R.J.W. Douglas, (eds.), Variations in tectonic styles in Canada: Geological Assoc. of Canada, Special Paper 11, 688 p.

Carey, S.W. 1958a. The isostrat, A new technique for the analysis of the structure of Tasmanian dolerite. University of Tasmania, Geology Department, Dolerite Symposium, pp. 130-164.

Carey, S. W. 1958b. Relation of basic intrusions to thickness of sediments. University of Tasmania, Geology Department, Dolerite Symposium, pp. 165-169.

Carmichael, I.S.E., Turner, F.J., and Verhoogen, J. 1974. Igneous Petrology, McGraw Hill, 739p.

Carter, J.L. 1970. Mineralogy and chemistry of the Earth's upper mantle based on the partial fusion - partial crystallization model. Bulletin of the Geological Societyof America, v. 81, pp. 2021-34.

Chandler, V.W., Bowman, P.L., Hinze, W.J., and O'Hara, N.W. 1982. Long wavelength gravity and magnetic anomalies of the Lake Superior region, in Wold, R.J., and Hinze, W.J., eds., Geology and Tectonics of the Lake Superior Basin: Geological

Society of America, Memoir 156, pp. 223-237.

Chase, C.G., and Gilmer, T.H. 1973. Precambrian plate tectonics: The Midcontinent Gravity High. Earth and Planetary Science Letters, v. 21, pp. 70-78.

Cheadle, B. A. 1986. Alluvial-playa sedimentation in the lower Keweenawan Sibley Group, Thunder Bay District, Ontario. Canadian Journal of Earth Sciences, v. 23, pp. 527-542.

Clarke, D.B. 1970. Tertiary basalts of Baffin Bay: Possible primary magma from the mantle. Contributions to Mineralogy and Petrology, v. 25, pp. 203-224.

Coates, M.E. 1972. Geology of the Black Sturgeon River Area, District of Thunder Bay. Ontario Department of Mines and Northern Affairs, GR 98, 41 p.

Coleman, R.G., Lee, D.E., Beatty, L.B. and Brannock, W.W. 1965. Eclogites and eclogites: Their differences and similarities. Geological Society of America Bulletin, v. 76, pp.483-508.

Cox, K.G. 1978. Komatiites and other high-magnesia lavas: Some problems. Philosophical Transactions of the Royal Society of London, v. A288, pp. 599-609.

Cox, K.G. 1980. A model for flood basalt volcanism. Journal Petrology, v. 21, pp. 629-650.

Cox, K.G., Bell, J.D. and Pankhurst, R.J. 1979. The interpretation of igneous rocks. George Allen and Unwin Ltd., London, 450 p.

Cox, K.G., Johnson, R.L., Monkman, L.J., Stillman, C.J., Vail, J.R., and Wood, D.N. 1965. The geology of the Nuanetsi igneous province. Philosophical Transactions of the Royal Society of London, v. A257, pp. 71-218.

Davis, D.W., and Sutcliffe, R.H. 1985. U-Pb ages from the Nipigon plate and northern Lake Superior. Bulletin of the Geological Society of America, v. 96, pp. 1572-1579.

Deer, W.A., Howie, R.A., and Zussman, J. 1978. Rock Forming Minerals. Volume 2A: Single-chain Silicates. Longman Group Ltd., London, 668 p.

Donaldson, J.A. and Irving, E. 1972. Grenville Front and rifting of the Canadian Shield. Nature Phys. Sci., v. 237, pp. 139-140.

Drake, M.J. 1976. Plagioclase-melt equilibria. Geochimica et Cosmochimica Acta, v. 40, pp. 457-465.

Ehrenberg, S.N., and Griffin, W.L. 1979. Garnet granulite and associated xenoliths in minette and serpentinite diatremes of the Colorado plateau. Geology, v. 7, pp. 483-487.

Fodor, R.V., Keil, K. and Bunch, T.E. 1975. Contributions to the mineral chemistry of Hawaiian rocks. IV. Pyroxenes from Hakeakala and West Maui volcanoes, Maui, Hawaii. Contributions to Mineralogy and Petrology, v. 50, pp. 173-195.

Francis, D., Ludden, J., and Hynes, A. 1983. Magma evolution a Proterozoic rifting environment. Journal of Petrology, v. 24, pp. 556-582.

Francis, E.H. 1982. Magma and sediment: Emplacement mechanism of late Carboniferous tholeiitic sills in northern Britain. Journal of Geological Society of London, v. 139, pp. 1-20.

Franklin, J.M. 1970. Metallogeny of the Proterozoic Rocks of Thunder Bay District; Ph.D. Thesis, University of Western Ontario, London, Ontario, 317 p.

Franklin, J.M., McIlwaine, W.H., Poulsen, K.H., and Wanless, R.K. 1980. Stratigraphy and depositional setting of the Sibley Group, Thunder Bay District, Ontario, Canada. Canadian Journal of Earth Sciences, v. 17, pp. 633-651.

Fyfe, W.S. 1978. Evolution of the earth's crust. Chemical Geology, v. 23, pp. 89-114.

Geul, J.J.C. 1980. Geology of Devon and Pardee Townships and the Stuart Location. Ontario Department of Mines, Geological Report 87, 52p.

Ghose, M.C. 1976. Composition and origin of the Deccan basalts. Lithos, v. 9, pp. 65-73.

Grapes, R.H., Reid, D.L., and McPherson, J.G. 1972. Shallow dolerite intrusion and phreatic eruption in the Allan hills region, Antarctica. New Zealand Journal of Geology and Geophysics, v. 17, pp. 563-577.

Green, J.C. 1979. High-Al olivine tholeiite - A Keweenawan speciality - and the variability of plateau magmatism (abs.) Geological Society of America, Abstracts with Programs, v. 11,No.5, pp. 231.

Green, J.C. 1982. Geology of Keweenawan extrusive rocks. *in* Wold, R.J., and Hinze, W.J. eds., Geology and Tectonics of the Lake Superior Basin: Geological Society of America Memoir 156, pp. 47-55.

Green, J.C. 1983. Geologic and geochemical evidence for the nature and development of the middle Proterozoic (Keweenawan) Midcontinent Rift of North America, in Processes of continental rifting: Morgan P., and Baker, B.H., (eds.), Tectonophysics, v. 94, pp. 413-437.

Green, T.H. 1976. Experimental generation of cordierite - or garnet-bearing granitic liquids from a pelitic composition. Geology, v. 4, pp. 85-88.

Green, D.H., and Ringwood, A.E. 1967. An experimental investigation of the gabbro to eclogite transformation and its petrological applications. Geochimica et Cosmochimica Acta, v. 31, pp.767-833.

Greenburg, J.K. and Brown, B.A. 1984. Cratonic sedimentation during the Proterozoic: An anorogenic connection in Wisconsin and the upper Midwest. Jounal of Geology, v. 92, pp. 159-171.

Griffin, W.L., Carswell, D.A., and Nixon, P.H. 1979. Lower crustal granulites and eclogites from Lesotho, southern Africa. In The Mantle Sample: Inclusions in Kimberlites and other Volcanics. Edited by F.R. Boyd and H.O.A. Meyer, American Geophysical Union, 2nd Kimberlite Conference Proceedings, pp. 59-86.

Hall, R.P., Hughes, D.J., and Friend, C.R.L. 1985. Geochemical evolution and unusual pyroxene chemistry of the MD tholeiite dyke swarm from the Archean craton of southern west Greenland. Journal of Petrology, v. 26, pp. 253-282.

Halls, H.C. 1978. The late Precambrian central North American rift system - A survey of recent geological and geophysical investigations, in Neumann, E-R., and Ramberg, I.B., eds., Tectonics and Geophysics of Continental Rifts: NATO Advanced Study Institute, Series C., v. 37, D. Reidel, Boston, pp.111-123.

Halls H.C., and Pesonen, L.T. 1982. Paleomagnetism of Keeweenawan rocks. Geological Society of America Memoir 156, pp. 173-201.

Hanson, G.N. 1975. $^{40}Ar/^{39}Ar$ spectrum ages on Logan intrusions, a lower Keweenawan flow and mafic dikes in northeastern Minnesota-northwestern Ontario. Canadian Journal of Earth Sciences, v. 12, pp. 821-835.

Hanson, G.N., and Langmuir, C.H. 1978. Modelling of major elements in mantle-melt systems using trace element approaches. Geochimica et Cosmochimica Acta, v. 42, pp. 725-742.

Hanson, G.N., and Malhotra, R. 1971 K-Ar ages of mafic dikes and evidence for low grade metamorphism in northeastern Minnesota. Geological Society of America Bulletin, v. 82, p. 1107-1114.

Herzberg, C.T., Fyfe, W.S., and Carr, M.J. 1983. Density constraints on the formation of the continental moho and crust. Contributions to Mineralogy and Petrology, v. 84, pp. 1-5.

Howie, R.A., and Subramaniam, A.M. 1958. The paragenesis of garnet in charnockite, enderbite and related granulites. Mineralogical Magazine, v. 31, pp.565-585.

Hubregtse, J.J.M.W. 1980. The Archean Pikwitonei granulite domain and its position at the margin of the northwestern Superior Province (central Manitoba). Manitoba Department of Energy and Mines, Geological Paper GP80-3.

Irvine, T.N. 1979. Rocks whose composition is determined by crystal accumulation and sorting. *In* Yoder, H.S. (editor), The Evolution of the Igneous Rocks. Fiftieth Anniversary Perspectives, Princeton University Press, pp. 245-306.

Irvine, T.N., and Smith, C.H. 1967. The ultramafic rocks of the Muskox Intrusion, Northwest Territories, Canada *in* Wyllie, P.J., (ed.), Ultramafic and related rocks: J. Wiley, New York, pp. 38-49.

Jaeger, J.C. 1957. The temperature in the neighbourhood of a cooling intrusive sheet. American Journal of Science, v. 255, pp. 306-318.

Jones, A.P., Smith, J.V., Dawson, J.B., Hansen, E.C. 1983. Metamorphism partial melting, and K-metasomatism of garnet-scapolite-kyanite granulite xenoliths from Lashaine, Tanzania. Journal of Geology, v. 91, pp.143-165.

Jones, N.W. 1984. Petrology of some Logan diabase sills, Cook County, Minnesota. Minnesota Geological Survey, Report of Investigations 29, 40 p.

Kavanagh, G.W.L. 1981. Differentiation of a Keweenawan diabase sill at D'Alton Lake, Ontario. Unpublished B.Sc. Thesis, University of Western Ontario, London, Ontario, 52p.

Kay, S.M. and Kay, R.W. 1983. Thermal history of the deep crust inferred from granulite xenoliths, Queensland, Australia, American Journal of Science, v. 283-A, pp.486-513.

Kaye, L. 1969. Geology of the Eayrs Lake-Starnes Lake Area, District of Thunder Bay; Ontario Department of Mines, Geological Report 77, 29 p. Accompanied by Map 2172, scale 1 inch to 1 mile.

King, E.R., and Zietz, I. 1971. Aeromagnetic study of the midcontinent gravity high of central United States. Geological Society of America Bulletin, v. 82, pp. 2187-2208.

Klasner, J.S., Cannon, W.F., and Van Schmus, W.R. 1982. The pre-Keweenawan tectonic history of southern Canadian shield and its influence on formation of the Midcontinent Rift. In Wold, R.J., and Hinze, W.J., (eds.), Geology and Tectonics of the Lake Superior Basin: Geological Society of America Memoir 156, pp. 27-46.

Koide, H., and Bhattacharji, S. 1975. Formation of fractures around magmatic intrusions and their role in ore localization. Economic Geology, v. 70, pp. 781-799.

Konda, T. 1970. Pyroxenes from the Beaver Bay gabbro complex of Minnesota. Contributions to Mineralogy and Petrology, v. 29, pp. 338-344.

Konda, T. and Green, J.C. 1974. Clinopyroxenes from the Keweenawan lavas of Minnesota. American Mineralogist, v. 59, pp. 1190-1197.

Kretz, R., Hartree, R., Garret, D., and Cermignani, C. 1985. Petrology of the the Grenville swarm of gabbro dikes, Canadian Precambrian Shield. Canadian Journal of Earth Sciences, v. 22, pp. 53-71.

Kushiro, I. 1972. Determination of liquidus relations in synthetic silicate systems with electron probe analysis. The system forsterite-diopside-silica at 1 atmosphere. American Mineralogist, v. 57, pp. 1260-1271.

Leaman, D.E. 1974. Form, mechanism and control of dolerite intrusion near Hobart, Tasmania. Journal of the Geological Society of Australia, v. 22, pp. 175-186.

Lindsley, D.H. 1983. Pyroxene thermometry. American Mineralogist, v. 68, pp. 477-493.

Lofgren, G. 1980. Experimental studies on the dynamic crystalization of silicate melts. In Hargraves, R.B. (editor, Physics of Magmatic Processes. Princeton University Press, pp. 487-552.

Longhi, J. 1981. Multicomponent phase equilibria of basalts. In Workshop on Magmatic Processes of Early Planetary Crusts, LPI Technical Report Number 82-01, pp. 90-94.

Mackasey, W.O. 1970. Eva Township, District of Thunder Bay; Ontario Department of Mines, Preliminary Geological Map P. 601, scale 1 inch to 1/4 mile. Geology, 1969.

Mackasey, W.O. 1975. Geology of Dorothea, Sandra, and Irwin Townships, District of Thunder Bay; Ontario Division of Mines, Geological Report 122, 83 p. Accompanied by Map 2294, scale 1 inch to 1/2 mile.

Massey, N.W.D. 1979. Keweenawan paleomagnetic reversals at Mamainse Point, Ontario: Fault repetition or three reversals? Canadian Journal of Earth Sciences, v. 16, pp. 373-375.

McBirney, A.R. 1979. Effects of assimilation. In Yoder, H.S. (editor), The Evolution of the Igneous Rocks: Fiftieth Anniversary Perspectives, Princeton University Press, pp. 307-338.

McBirney, A.R. and Noyes, R.M. 1979. Crystallization and layering of the Skaergaard Intrusion. Journal of Petrology, v. 20, pp. 487-554.

Morse, S.A. 1980. Basalts and phase diagrams. Springer-Verlag, New York, 493 p.

Muir, I.D. and Tilley, C.E. 1964. Iron enrichment and pyroxene fractionation in tholeiites. Geological Journal, v. 4, pp. 143-156.

Neumann, E.R. 1976. Two refinements for the calculation of structural formulae for pyroxenes and amphiboles, Norsk Geologisk Tidsskrift, v. 56, pp.1-6.

Neumann, E.-R., and Ramberg, I.B., 1978, Paleorifts - concluding remarks. In Neumann, E.-R., and Ramberg, I.B., (eds.), Tectonics and Geophysics of Continental Rifts: NATO Advanced Study Institute, Series C., v. 37, D. Reidel, Boston, pp. 409-424.

Norrish, K. and Hutton, J.T. 1969. An accurate X-ray sepctrographic method for the analysis of a wide range of geologic samples, Geochemica et Cosmochimica Acta, v. 33, pp. 431-455.

Ocola, L.C., and Meyer, R.P. 1973. Central North American rift system 1. Structure of the axial zone from seismic and gravimetric data. Journal of Geophysical Research, v. 78, pp. 5173-5194.

Ojakangas, R.W., and Morey, G.B. 1982. Keweenawan sedimentary rocks of the Lake Superior region: A summary. in Wold, R.J., and Hinze, W.J., (eds.), Geology and Tectonics of the Lake Superior Basin: Geological Society of America Memoir 156, pp. 157-164.

Ontario Department of Mines-Geological Survey of Canada. 1962. Nipigon Sheet. Ontario Department of Mines-Geological Survey of Canada, Aeromagnetic Map 7103G, scale 1 inch to 4 miles. Survey flown 1962.

Palmer, H.C. 1970. Paleomagnetism and correlation of some middle Keweenawan rocks, Lake Superior. Canadian Journal of Earth Sciences, v. 7, pp. 1410-1436.

Pasteris, J.D. 1981. Kimberlites: Strange bodies? EOS, v. 62, pp. 713-714.

Pasteris, J.D. 1985. Relationships between temperature and oxygen fugacity among Fe-Ti oxides in two regions of the Duluth Complex. Canadian Mineralogist, v. 23, pp. 111-127.

Pearce, T.H. 1970. Chemical variations in the Palisade Sill, Journal of Petrology, v. 11, pp. 15-32.

Percival, J.A., and Card, K.D. 1983. Archean crust as revealed in the Kapuskasing uplift, Superior province, Canada. Geology, v. 11, pp. 323-326.

Phillips, W.J. 1974. The dynamic emplacement of cone sheets. Tectonophysics, v. 24, pp. 69-84.

Platt, R.G., and Mitchell, R.H. 1982. The Marathon Dikes: ultrabasic lamprophyres from the vicinity of McKellar —

Harbour, N.W. Ontario. American Mineralogist, v. 67, pp. 907-916.

Pollard, D.D., Muller, O.H., and Dockstader, D.R. 1975. The form and growth of fingered sheet intrusions. Geological Society of America Bulletin, v. 86, pp. 351-363.

Pye, E.G. 1953. A petrographic study of the textures of basic and ultrabasic igneous rocks. Unpublished Ph.D. Thesis, University of Toronto, 93 p.

Pye, E.G. 1965. Geology and lithium deposits of the Georgia Lake area, District of Thunder Bay. Ontario Department of Mines, Geological Report 31, 113p.

Pye, E.G. 1968. Geology of the Lac des Iles area, District of Thunder Bay. Ontario Department of Mines, Geological Report 64, 47 p.

Ringwood, A.E. 1975. Composition and petrology of the Earth's Mantle, McGraw-Hill, 618p.

Roberts, J.L. 1970. The intrusion of magma into brittle rocks, in Newall, G. and Rast, R., (eds.), Mechanisms of Igneous Intrusion: Gallery Press, Liverpool, pp. 339-362.

Robertson, W.A. and Fahrig, W.F. 1971. The great Logan paleomagnetic loop - the polar wandering path from Canadian Shield Rocks during the Neohelikian Era. Canadian Journal of Earth Sciences, v. 8, pp. 1355-1372.

Robson, G.R., and Barr, K.G. 1964. The effect of stress on faulting and minor intrusions in the vicinity of a magma body. Bulletin Volcanol. v. 27, pp. 315-330.

Robson, D., and Cann, J.R. 1982. A geochemical model of mid-ocean ridge magma chambers. Earth and Planetary Science Letters, v. 65, pp. 93-104.

Rock, N.M.S. 1977. The nature and origin of lamprophyres: Some definitions, distinctions, and deviations. Earth-Science Reviews, v. 13, pp.123-169.

Roeder, P.L., and Emslie, F.R. 1970. Olivine-liquid equilibrium, Contributions to Mineralogy and Petrology, v. 29, pp. 275-289.

Ruzicka, V., and LeCheminant, G.M. 1984. Uranium deposit research, 1983. in Current Research, Part A: Geological Survey of Canada, Paper 84-1A, pp. 39-51.

Sage, R.P., Breaks, F.W., Stott, G., McWilliams, G., and Bowen, R.P. 1974. Operation Ignace-Armstrong, Caribou Lakes - Pashkokogan Lake Sheet, District of Thunder Bay. Ontario Division of Mines, Preliminary Map P. 962, Geological Series, scale 1:126 720 or 1 inch to 2 miles, Geology 1973.

Sawkins, F.J. 1976. Widespread continental rifting: some considerations of timing and mechanism. Geology, v. 4, pp. 427-430.

Shaw, H.R. 1965. Comments on viscosity, crystal settling and convection in granitic magmas. American Journal of Science, v. 263, pp. 120-152.

Shaw, H.R. 1972. Viscosities of magmatic silicate liquids. An empirical method of prediction. American Journal of Science, v. 272, pp. 870-893.

Silver, L.T., and Green, J.C. 1963. Zircon age for middle Keweenawan rocks of Lake Superior region (abs.). American

Geophysical Union Transactions, v. 44, p. 107.

Silver, L.T., and Green, J.C. 1972. Time constants for Keweenawan igneous activity (abs.): Geological Society of America Abstracts with Programs, v. 4, p. 665-666.

Silver, L.T., Bickford, M.E., VanSchmus, W.R., Anderson, J.T., and Medaris, L.G. jr. 1977. The 1.4 to 1.5 b.y. transcontinental perforation of North America (abs.). Geological Society of America Abstracts with Programs, v. 9, pp. 1176-1177.

Simkin, T. 1967. Flow differentiation in the picritic sills of North Skye. In Wyllie, P.J. (editor), Ultramafic and Related Rocks. J. Wiley and Sons, Inc., New York.

Smith, D. and Lindsley, D.H. 1971. Stable and metastable augite crystallization trends in a single basalt flow. American Mineralogist, v. 56, pp. 225-233.

Smith, E.I. 1983. Geochemistry and evolution of the early Proterozoic, post-Penokean rhyolites, granites and related rocks of south-central Wisconsin, U.S.A. Geological Society of America Memoir 160, pp.113-128.

Sparks, R.S.J. 1986. The role of crustal contamination in magma evolution through geological time. Earth and Planetary Science Letters, v. 78, pp. 211-223.

Sparks, R.S.J., Meyer, P., and Sigurdsson, H. 1980. Density variation amongst mid-ocean ridge basalts: Implications for magma mixing and the scarcity of primitive magmas. Earth and Planetary Science Letters, v. 46, 419-430.

Spencer, K.J. and Lindsley, D.H. 1981. A solution model for co-existing iron-titanium oxides. American Mineralogist, v. 66, pp. 1189-1201.

Spry, A.H. 1958. Some observations of the Jurassic dolerite of the Eureka Cone-Sheet near Zeehan, Tasmania. University of Tasmania, Geology Department, Dolerite Symposium, pp 93-129.

Stockwell, C.H., McGlynn, J.C., Emslie, R.F., Sanford, B.V., Norris, A.W., Donaldson, J.A., Fahrig, W.F., and Currie, K.L. 1972. Geology of the Canadian Shield, in Douglas, R.J.W. (ed.), Geology and Economic Minerals of Canada: Geological Survey of Canada, Economic Geology Report No. 1, 838 p.

Stolper, E. and Walker, D. 1980. Melt density and the average composition of basalt. Contributions to Mineralogy and Petrology, v. 74, pp. 7-12.

Stormer, J.C., and Nicholls, J. 1978. XLFRAC: A program for the inter-active testing of magmatic differentiation models. Computers and Geosciences, v. 4, pp. 143-159.

Streckeisen, A. 1976. To each plutonic rock its proper name. Earth Science Reviews, v. 12, pp. 1-33.

Sutcliffe, R.H. 1981. Geology of the Wabigoon-Quetico Subprovince Boundary in the Lake Nipigon Area, District of Thunder Bay, in Summary of Field Work 1981, by the Ontario Geological Survey, edited by John Wood, O.L. White, R.B. Barlow and A.C. Colvine, Ontario Geological Survey, Miscellaneous Paper 100, 26-29.

Sutcliffe, R.H. 1982. Precambrian Geology of the Wabigoon Quetico Subprovince Boundary, District of Thunder Bay. Ontario

Geological Survey, Preliminary Maps 2528, 2529, 2530, 2531, scale 1:50 000.

Sutcliffe, R.H. 1984. Geology of the Fletcher Lake Area, District of Thunder Bay: Ontario Geological Survey, Open File Report 5497, 119p.

Sutcliffe, R.H. and Greenwood, R.C. 1982. Geology of the Lake Nipigon Area. in Summary of Field Work, 1982, by the Ontario Geological Survey, edited by John Wood, Owen L. White, R.B. Barlow, and A.C. Colvine, Ontario Geological Survey, Miscellaneous Paper 106, p.19-23.

Sutcliffe, R.H. and Greenwood, R.C. 1985. Precambrian Geology of the Lake Nipigon area, District of Thunder Bay. Ontario Geological Survey, Preliminary Maps 2836, 2837, 2838, 2839. Scale 1:50,000.

Taylor, S.R. and Gorton, M.P. 1978. Geochemical applications of spark source mass spectrometry:III Element sensitivity, precision and accuracy. Geochimica et Cosmochimica Acta, v. 41, pp. 1375-1380.

Thorarinsson, S. 1970. The Lakagigar eruption of 1783. Bulletin Volcanologique, v. 10, pp. 157-168.

Upton, B.G.J., and Blundell, D.J. 1978. The Gardar igneous province: Evidence for Proterozoic continental rifting. in Neumann, E.-R., and Ramberg, I.B., (eds.), Tectonics and Geophysics of Continental Rifts: NATO Advanced Study Institute, Series C., v. 37, D. Reidel, Boston, pp. 163-172.

Van Schmus, W.R., Green, J.C., and Halls, H.C. 1982. Geochronology of Keweenawan rocks of the Lake Superior region: A summary. *in* Wold, R.J., and Hinze, W.J. (eds.), Geology and tectonics of the Lake Superior Basin: Geological Society of America Memoir 156, pp. 165-171.

Wager, L.R. and Brown, G.M. 1968. Layered igneous rocks. W.H. Freeman and Co. San Francisco, 588p.

Walker, F. 1958. Recent work on the form of dolerite intrusions in sedimentary terrains. University of Tasmania, Geology Department, Dolerite Symposium, p. 92.

Walker, G.P.L. 1975. A new concept of the evolution of the British Tertiary intrusive centers. Journal of the Geological Society of London, v. 131, pp. 121-141.

Walker, K.R. 1970. The Palisades Sill, New Jersey: A reinvestigation, Geological Society of America, Special PapIII, 178p.

Wallace, Henry. 1972. Differentiation trends in Osler volcanics, Shesheeb Bay Section, unpublished M.Sc. thesis, University Toronto, Toronto, Ontario, 109p.

Wallace, H. 1981. Keweenawan geology of the Lake Superior region. *in* Campbell, F.H.A. (ed.) Proterozoic Basins of Canada: Geological Survey of Canada, Paper 81-10, p. 399-417.

Weiblen, P.W., Mathez, E.A., and Morey, G.B. 1972. Logan intrusions. *in* Sims, P.K. and Morey, G.B. (editors), Geology of Minnesota: a centennial volume: Minnesota Geological Survey, p. 394-406.

Weiblen, P.W. 1982. Keweenawan intrusive igneous rocks. Geological Society of America, Memoir 156, pp. 57-82.

Wells, P.R.A., 1977. Pyroxene thermometry in simple and complex systems, Contributions to Mineralogy and Petrology, v. 62, pp.129-139.

Wilbrand, J.T., Gaudette, H.E., and Olszewski, W.J. 1984. Age and source variation of volcanics associated with Keweenawan rifting (abs.). Eos, v.65, p.1122.

Williams, R.J. 1971. Reaction constants in the system Fe - MgO - SiO_2 - O_2 at 1 atm between 900° and 1300°C: experimental results. American Journal of Science, v. 270, pp. 321-330.

Williams, R.J. 1972. Activity - composition relations in the fayalite-forsterite solid solution between 900° and 1300°C at low pressures. Earth and Planetary Science Letters, v. 15, pp. 296-300.

Williams, H. and McBirney, A.R. 1979. Volcanology. Freeman, Cooper and Co., San Francisco, 397p.

Wilson, A.W.G. 1910. Geology of the Nipigon Basin. Geological Survey of Canada, Memoir 1, 152 p. Accompanied by Map 8A.

Winkler, H.G.F. 1976. Petrogenesis of Metamorphic Rocks. Springer-Verlag, New York, 334 p.

Wood, B.J. and Banno, S. 1973. Garnet-orthopyroxene and orthopyroxene-clinopyroxene relationships in simple and complex systems. Contributions to Mineralogy and Petrology, v. 42, pp.109-124.

Wu, T.W. 1984. Geochemistry and petrogenesis of some granitoids in the Grenville Province of Ontario and their tectonic implications. Unpublished PhD Thesis, University of Western Ontario, London, Canada, 623p.

Yamakawa, M. 1971. Two different crystallization trends of pyroxene in a tholeiitic dolerite, Semi, Northern Japan. Contributions to Mineralogy and Petrology, v. 33, pp. 232-238.

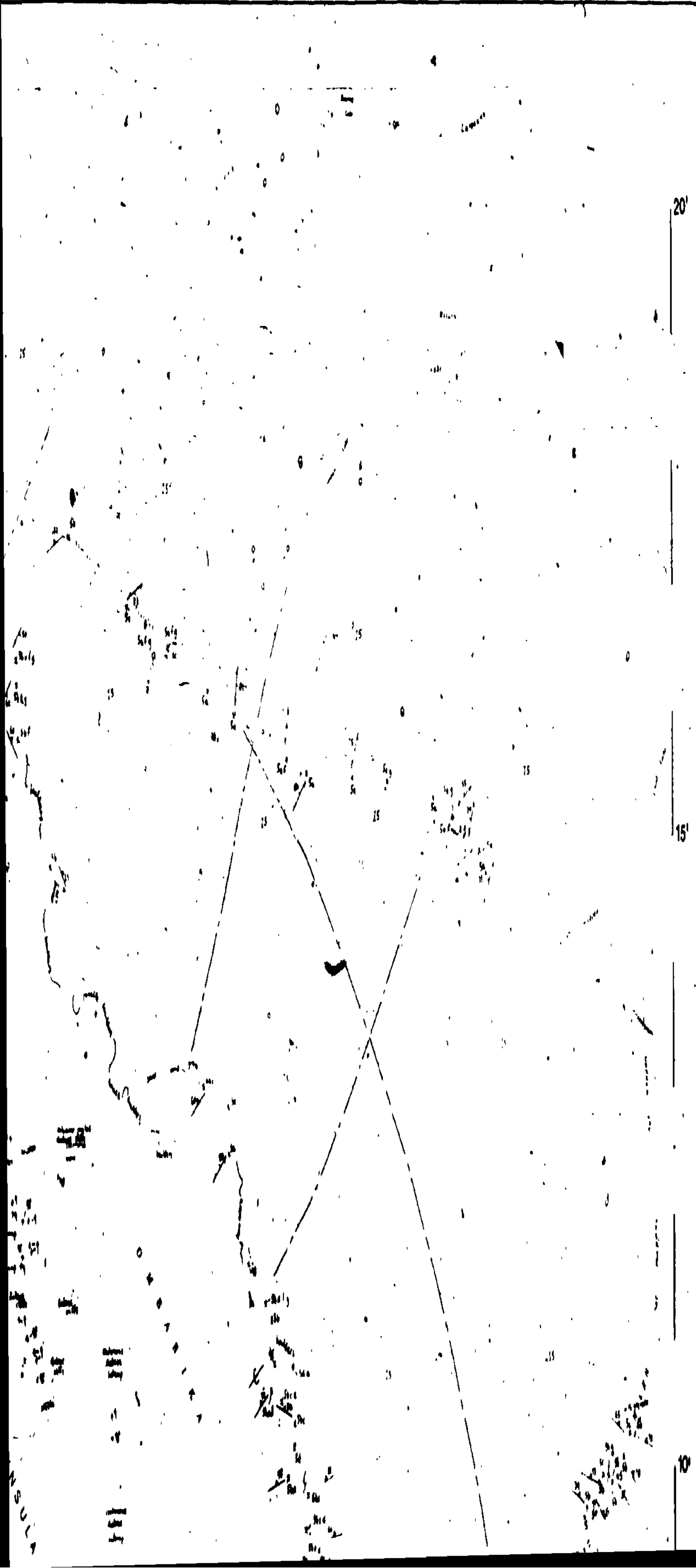

GEOLOGY
OF THE
LAKE NIPIGON AREA
NORTHERN PART

Scale 1:100 000

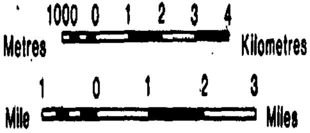
1000
0
1
2
3
4
Metres
Kilometres
1
0
1
2
3
Mile
Miles

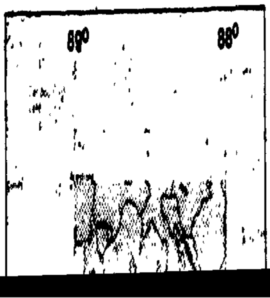

LEGEND[a]

PHANEROZOIC
CENOZOIC
QUATERNARY
PLEISTOCENE AND RECENT
Till, esker deposits, glaciolacustrine deposits, swamp, stream and lake deposits

UNCONFORMITY

PRECAMBRIAN[b]

MARGINAL NOTES

LOCATION AND ACCESS

The map area is bounded by Latitudes 49°45'N to 50°20'N and Longitudes 88°00'W to 89°00'W. In addition, Late Precambrian igneous rocks in the following areas were also investigated: the Eva and Kitto Townships area southwest of Beardmore (see Map P.2839, Figure 1); and the area west of Armstrong bounded by Latitudes 50°00'N to 50°30'N and Longitudes 89°00'W to 90°00'W (see Map P.2836, Figure 2).

Access to the map area is primarily by Lake Nipigon. Maintained access points to the northern part of the lake are located at Humboldt Bay on the eastern shore and at Gull Bay on the western shore.

MINERAL EXPLORATION

Within the map area, mineral exploration has primarily been in areas of Early Precambrian rocks.

Exploration for gold and base-metals has been centred on Early Precambrian supracrustal rocks. North of Lake Nipigon the Caribou Lake - Pikitigushi River metavolcanic-metasedimentary belt has been investigated since the 1930s. The most recent exploration was from 1980 to 1982. In the Humboldt Bay area of Lake Nipigon at the western end of the Onaman Rivers metavolcanic-metasedimentary belt, sulphide mineralization within the metavolcanic rocks has been investigated as recently as 1975. During 1970 and 1971, the Canadian Nickel Company Limited examined lenses of pyroxene-hornblendite within gneissic granitoids east of Ombabika Bay of Lake Nipigon.

The area north of Lake Nipigon has been explored for rare-element spodumene bearing pegmatites (Pye 1968; Breaks 1981).

GENERAL GEOLOGY

Previous mapping of Lake Nipigon was reported by Wilson (1910). Collins (1906) mapped the area northwest of Lake Nipigon as part of a survey of the area adjacent to the railway. More recent work was done by Pye (1968) in the Crescent Lake area, northeast of Lake Nipigon, by Sage *et al.* (1974), west of Lake Nipigon and by Sutcliffe (1981) to the south of the present area.

EARLY-PRECAMBRIAN

Early Precambrian rocks of the map area consist mainly of granitoid rocks and lesser metavolcanic and metasedimentary rocks of the Wabigoon Subprovince.

The Early Precambrian rocks occur around the margin of Lake Nipigon and are intruded by Late Precambrian Logan diabase sills and associated dikes. The Early Precambrian rocks are predominantly exposed under the sills but are also locally found on top of the sills.

Biotite tonalite to granodiorite is the most widespread Early Precambrian lithology in the area. The tonalite consists of several phases ranging in texture from gneissic to foliated and commonly contains amphibolite and pyroxene-amphibolite enclaves. Locally, such as on the Britannia Islands of Lake Nipigon, the tonalite is discordantly intruded by mafic dikes which have subsequently been deformed and metamorphosed. Hornblende diorite is locally associated with the tonalite and is particularly common on the

shore of Lake Nipigon south of Castle Bay and on the eastern shore of Lake Nipigon in Humboldt Bay. Numerous large blocks of tuff-breccia occur on the Mountain Islands and are probably not far removed from their source. A fluorite-bearing, quartz-feldspar porphyry to equigranular granite intrusion, centred on English Bay on the western side of Lake Nipigon is older than the diabase sills. This intrusion is considered to be the centre of felsic volcanism since it contains numerous inclusions of felsite, porphyry, flow banded, and pumiceous fragments. The felsic volcanic and subvolcanic rocks may have originally covered the northern part of Lake Nipigon and may still be preserved beneath the diabase.

In the northern part of Lake Nipigon, sedimentary rocks are present under the diabase sheet and consist predominantly of quartz arenite. Minor conglomerate is present at the base of the sequence in the vicinity of English Bay and contains clasts of porphyry and felsite in a quartz arenite matrix. The quartz arenite reaches a maximum thickness of 25 m as indicated by sections on Humboldt Bay of Lake Nipigon and Castle Lake. The quartz arenite consists of well sorted and rounded quartz grains. Cross-beds of up to 1.8 m in thickness are a conspicuous feature of the unit, along with ripplemarks.

The presence of ultramafic rocks within the Nipigon Plate was reported by Sutcliffe (1981). During the present mapping the ultramafic rocks were found to be intruded by the diabase sills, but the relationship with the Sibley sedimentary rocks was not established. The ultramafic intrusion in Kitto and Eva Townships (see Figure 1) is a circular ring dike or cone sheet, 6 km in diameter, which ranges in composition from olivine gabbro to peridotite (lherzolite). Within the map area an olivine gabbro intrusion of this suite occurs on Jackfish and Birch Islands in the western part of Lake Nipigon.

Diabase sills are the most extensive rock type in the area. In the northern part of Lake Nipigon, evidence indicates that only 1 sill is exposed. Sections on the Barn Islands and Livingstone Point indicate that this sill has a thickness of approximately 200 m. This sill grades, from base to top as follows: a lower chill zone, coarse ophitic diabase, to medium-grained diabase, to medium-grained diabase with coarse pegmatitic patches. Locally the medium-grained zone displays igneous layering and contains zones of anorthositic diabase. The upper 2 m of the sill is fine grained to aphanitic with polygonal fractures and is locally vesicular. Minor late granophyre veins cross-cut the diabase sills.

Diabase dikes and cone sheets which appear to have been feeders for the sills are coarser grained and have less well developed chill zones than the sills.

On the Rabbit Islands, in central Lake Nipigon, a possible carbonatite diatreme, 20 m wide, was found to cross-cut the diabase.

STRUCTURE

EARLY PRECAMBRIAN

The Early Precambrian tonalite-granodiorite has been moderately to highly deformed. Two periods of deformation within the tonalitic rocks are indicated by the presence of amphibolite dikes which cross-cut the tonalite gneissosity and have subsequently been deformed.

The late granites are massive and have caused brittle fragmentation of the tonalitic rocks into which they were emplaced.

The presence of conglomerate with tonalitic clasts, at the inferred base of the Onaman River supracrustal belt at Humboldt

untested and warrant investigation for copper, nickel and possibly chrome and platinum group mineralization. In the Leckie Lake Intrusion (see Sutcliffe 1981) up to 5% disseminated chalcopyrite was found in a pegmatitic gabbro phase of the olivine melagabbro south of the ultramafic core of the intrusion.

In the Early Precambrian rocks north of Lake Nipigon, and outside of the map area a lense of massive pyrite with minor chalcopyrite was found immediately south of the bridge where the Pikitigushi road crosses the Pikitigushi River. The lens is over 4 m wide and has a strike length in excess of 50 m.

URANIUM

Uranium mineralization in the Sibley basin, documented by Franklin (1978), is associated with fractures in Early Precambrian - Late Precambrian unconformity. To the south of the present map area, mineralization of this type was found in the vicinity of the Black Sturgeon Fault (Sutcliffe 1981). Exploration in 1982 by Uranerz Exploration and Mining Limited has revealed several mineralized fractures in this area, the largest of which is 40 cm wide (John Scott, Resource Geologist, Ontario Ministry of Natural Resources, Thunder Bay, personal communication, 1982). The fault on the western side of the Ombabika South Peninsula and exposures of the unconformity near Humboldt Bay, Lake Nipigon, warrant investigation for this type of mineralization. Hematized fractures near the contact of the English Bay porphyry and overlying sedimentary rocks may also warrant investigation for uranium.

LITHOPHILE MINERALIZATION

Spodumene-bearing dikes with columbite-tantalite mineralization occur north of the map area and were not examined during the survey. The economic potential of these dikes has been recently assessed by Breaks (1981).

GOLD-MOLYBDENUM

The fluorite-bearing, subvolcanic porphyry to granite intrusion on English Bay has not been previously recognized and warrants exploration for gold.

In the Collins Lake area, west of Armstrong, numerous quartz veins are present in the tonalite-granodiorite. Some of these veins contain molybdenite mineralization and may also warrant investigation for gold.

REFERENCES

Breaks, F.W.

1981: Lithophile Mineralization in Northwestern Ontario: Rare Element Granitoid Pegmatites; p. 19-21 *in* Summary of Field Work, 1981, by the Ontario Geological Survey, edited by John Wood, O.L. White, R.B. Barlow, and A.C. Colvine, Ontario Geological Survey, Miscellaneous Paper 100, 255 p.

Collins, W.H.

1906: Surveys along the National Transcontinental Railway Location between Lake Nipigon and Lac Seul; Geological Survey of Canada, Summary Report for 1906, p. 103-109.

Franklin, J.M.

1978 Uranium Mineralization in the Nipigon Area, Thunder Bay District, Ontario; Current Research, Part A, Geological Survey of Canada, Paper 78-1A, p. 275-282.

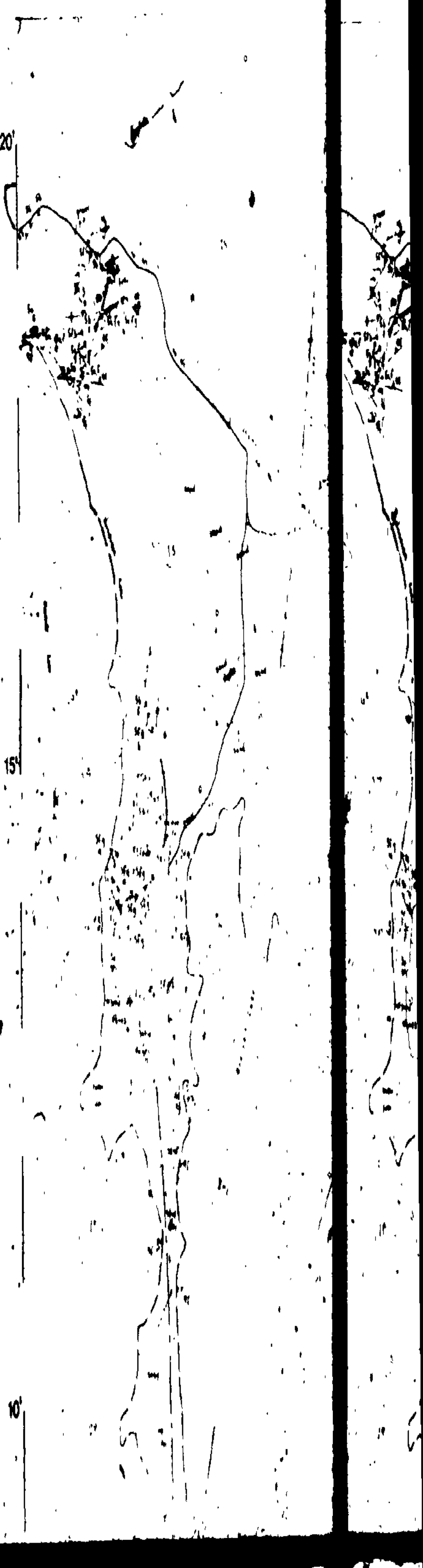

Biotite tonalite to granodiorite is the most widespread Early Precambrian lithology in the area. The tonalite consists of several

rocks are indicated by the presence of amphibolite dikes which cross-cut the tonalite gneissosity and have subsequently been

1906 Surveys along the National Transcontinental Railway Location between Lake Nipigon and Lac Seul; Geological Survey

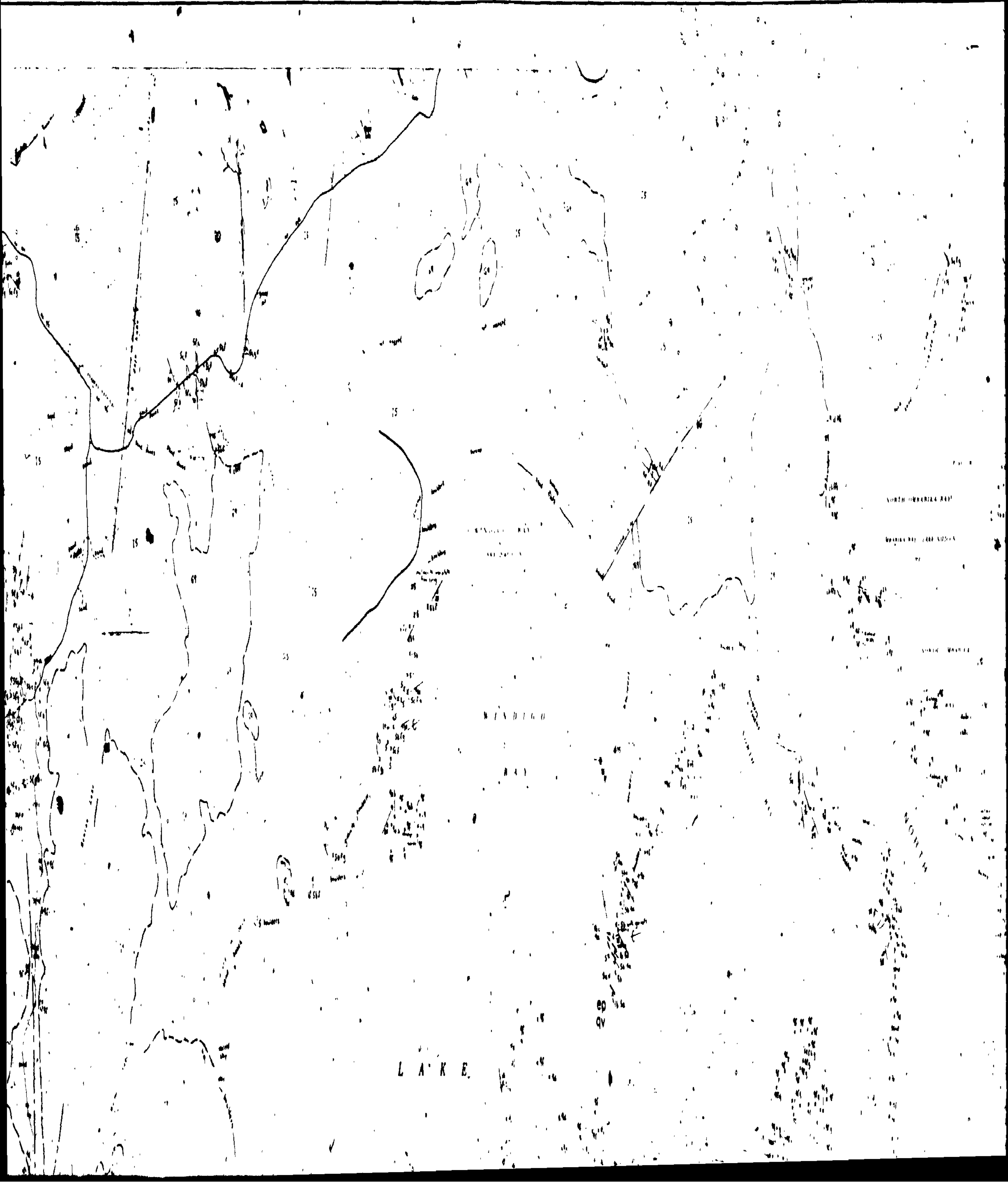
WINDIGO
BAY
LAKE
ep
qv

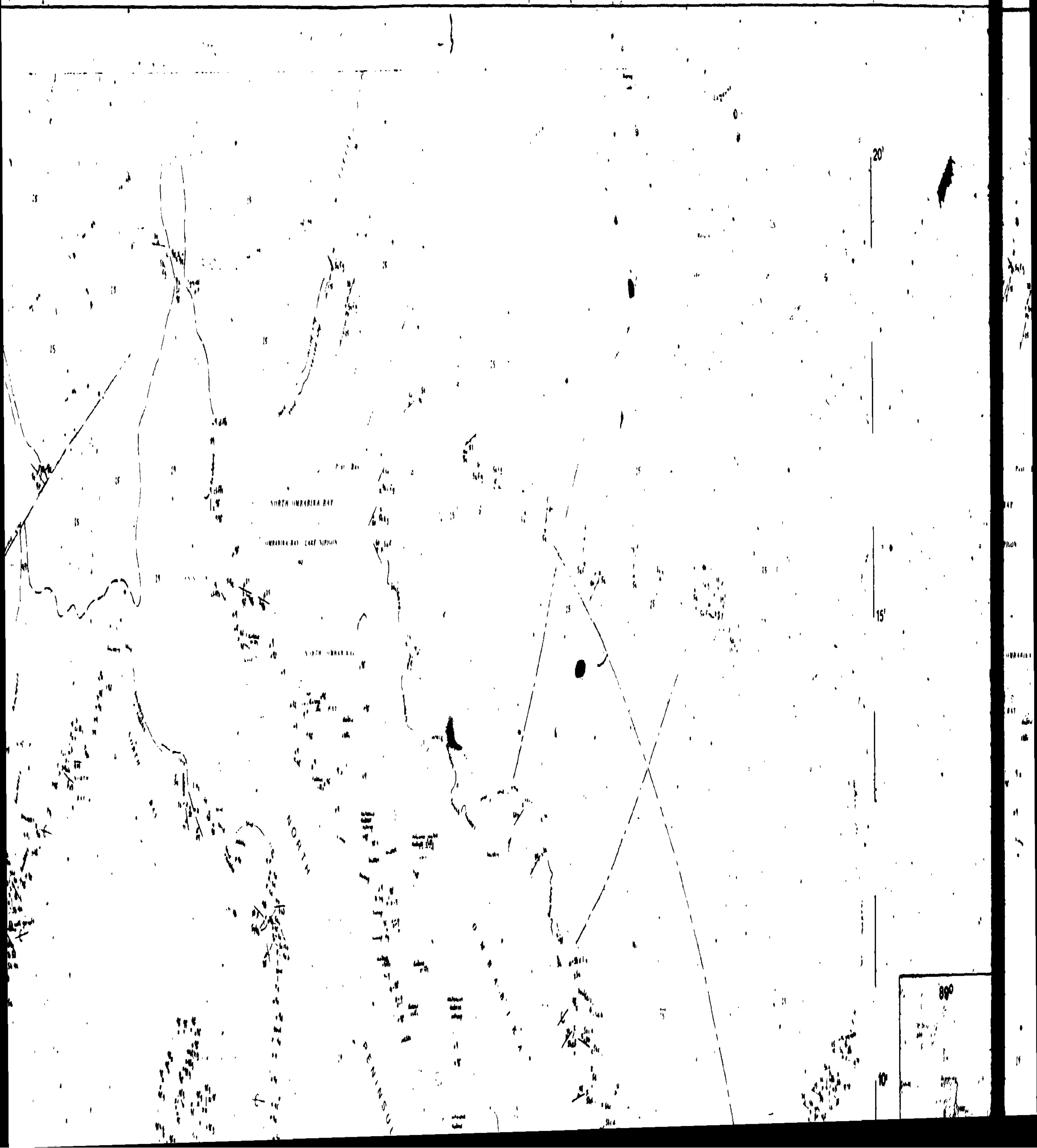
20'
NORTH OMBABIKA BAY
OMBABIKA BAY LAKE NIPIGON
NORTH OMBABIKA
15'
NORTH
PENINSU
10'
89°

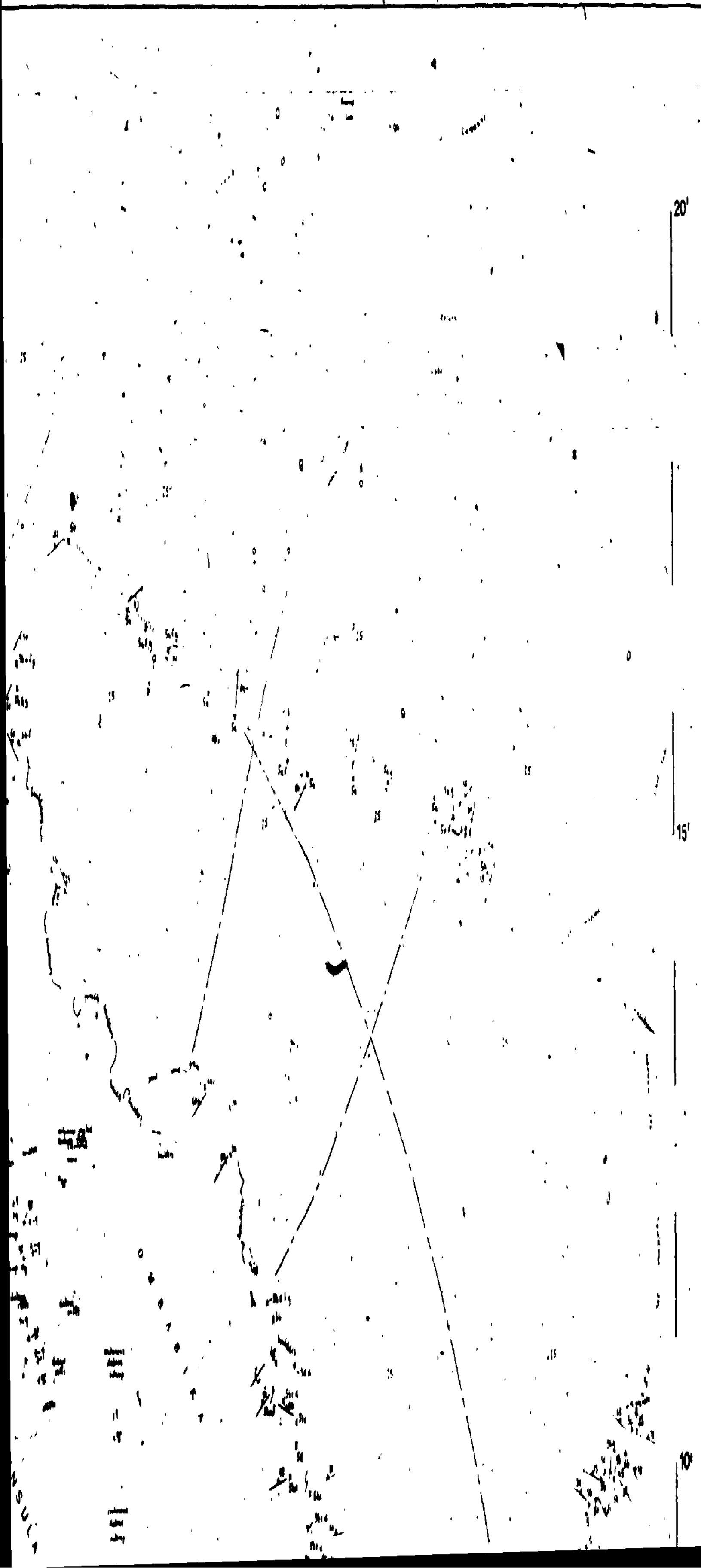

GEOLOGY
OF THE
LAKE NIPIGON AREA
NORTHERN PART

Scale 1:100 000

1000 0 1 2 3 4
Metres Kilometres

1 0 1 2 3
Mile Miles

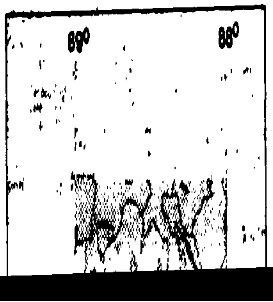

LEGEND[a]

PHANEROZOIC
CENOZOIC
QUATERNARY
PLEISTOCENE AND RECENT
Till, esker deposits, glaciolacustrine deposits, swamp, stream and lake deposits

UNCONFORMITY

PRECAMBRIAN[b]

MARGINAL NOTES

LOCATION AND ACCESS

The map-area is bounded by Latitudes 49°15' to 49°45'N and Longitudes 88°00' to 89°00'W, and covers four NTS map sheets (Grand Bay, Shakespeare Island, Orient Bay and Black Sturgeon Lake). It is approximately 130 km northeast of the city of Thunder Bay. Road access to the area is available via Highway 11 along the eastern margin of the map-area, Highway 585 in the south-central part of the area, and the Black Sturgeon gravel road in the southwest part of the area. Lake Nipigon can be reached by access points on Chief Bay, the Pashkokogan River, McIntyre Bay, South Bay, Pijitawabik Bay, High Hill Harbour, and Poplar Lodge.

MINERAL EXPLORATION

Within the map-area, mineral exploration has been primarily focused on the Early Precambrian rocks. The area east of Lake Nipigon in the Wabigoon-Quetico Subprovince boundary area has been extensively explored for gold. Exploration work prior to the 1970s has been reported by Mackasey (1970a, 1970b, 1975). The Leitch Gold Mine was in production from 1936 to 1965, and the adjacent property of the Sand River Gold Mines was in production from 1937 to 1942. In 1954 the Sand River property was purchased by Leitch Gold Mines Limited (Mackasey 1970a). A total of 847 291 ounces of Au and 31 775 ounces of Ag was produced from 920 745 tons of ore at the Leitch Mine and 50 065 ounces of Au and 3 628 ounces of Ag from 157 870 tons of ore at the Sand River Mine (Mackasey 1970a). High gold prices have resulted in considerable recent exploration activity in this region.

The Quetico Subprovince east of Lake Nipigon contains extensive rare element pegmatites. The area was explored for spodumene in the 1950s (Pye 1965) but recent activity has been minimal (Breaks 1980).

West of Lake Nipigon, Early Precambrian rocks have been prospected for gold and base metals (Pye 1968, Kaye 1969).

Relatively minor exploration has been directed towards the Late Precambrian rocks of the Nipigon Plate. Recently, however, there has been considerable interest in uranium mineralization associated with the Sibley Group sediments. Base-metal exploration has delineated minor occurrences of copper near the diabase-sediment interface such as the Disraeli Lake occurrences (Coates 1972).

GENERAL GEOLOGY

The map-area includes Early Precambrian supracrustal and plutonic rocks of the Wabigoon and Quetico Subprovinces and Late Precambrian sedimentary and intrusive rocks of the Nipigon Plate. The previous mapping of Lake Nipigon is reported by Wilson (1910). Coates (1972) mapped the area to the south containing Late Precambrian sediments

ECONOMIC GEOLOGY

Gold

Early Precambrian metavolcanics and metasediments southwest of Lake Nipigon can be correlated with the supracrustal rocks containing gold mineralization east of the lake. Both sequences appear to be similar in lithology, metamorphic grade, alteration and tectonic environment. This suggests that the sequence southwest of the lake and outside of the map area should be favourable for gold mineralization as indicated by Pye (1968). In this zone, numerous quartz veins are present and are associated with carbonatization of the mafic metavolcanics. This alteration appears to be commonly associated with northeast trending sheared zones.

Archean supracrustal rocks to the east of Black Sturgeon Lake contain numerous quartz veins and pods but these rocks appear to be of higher metamorphic grade than those on either side of the Nipigon Plate and therefore may have lower potential for gold mineralization.

Base Metals

Occurrences of copper at Disraeli Lake to the south of the map area are associated with Late Precambrian diabase sills and underlying Sibley Group stromatolitic carbonates. Coates (1972) considers these occurrences to be due to metasomatism related to diabase intrusion or by later supergene processes.

The intrusion of large amounts of tholeiitic magma into the sulphate rich Sibley sediments indicates an environment favourable for copper and nickel mineralization. Prospecting within the diabase for this type of mineralization should be concentrated on the basal portions of the sheets.

Ultramafic rocks within the area are largely untested and warrant investigation for copper, nickel, and possibly chrome and platinum group elements. The presence of a major ultramafic ring dike in Eva Township indicates a tectonic environment favourable for kimberlites, but none have been detected in this zone to date.

Uranium

Uranium mineralization in the Sibley basin has been described by Franklin (1970) and is associated with northwest trending fractures in Early Precambrian rocks near the Early Precambrian-Late Precambrian unconformity. Early Precambrian rocks in the vicinity of the Black Sturgeon Fault warrant investigation for this type of mineralization. In this zone, radioactive fractures were discovered by the field party approximately 1 km east of the south end of Black Sturgeon Lake.

REFERENCES

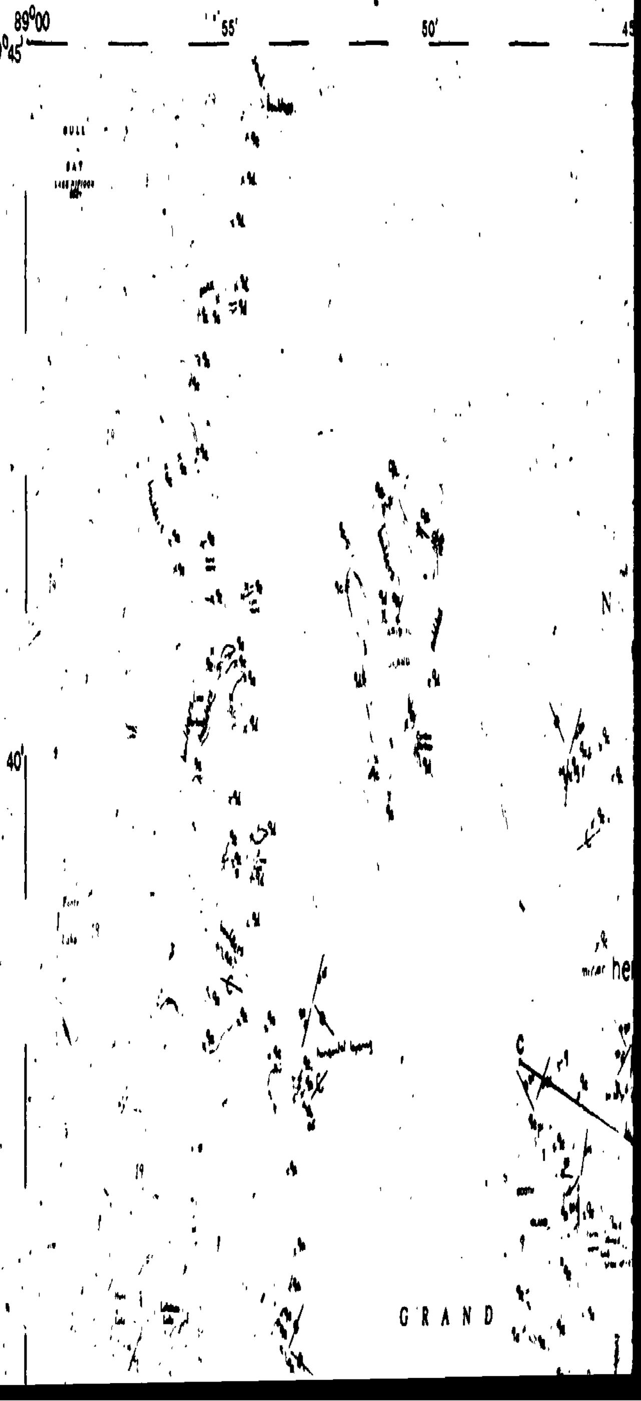

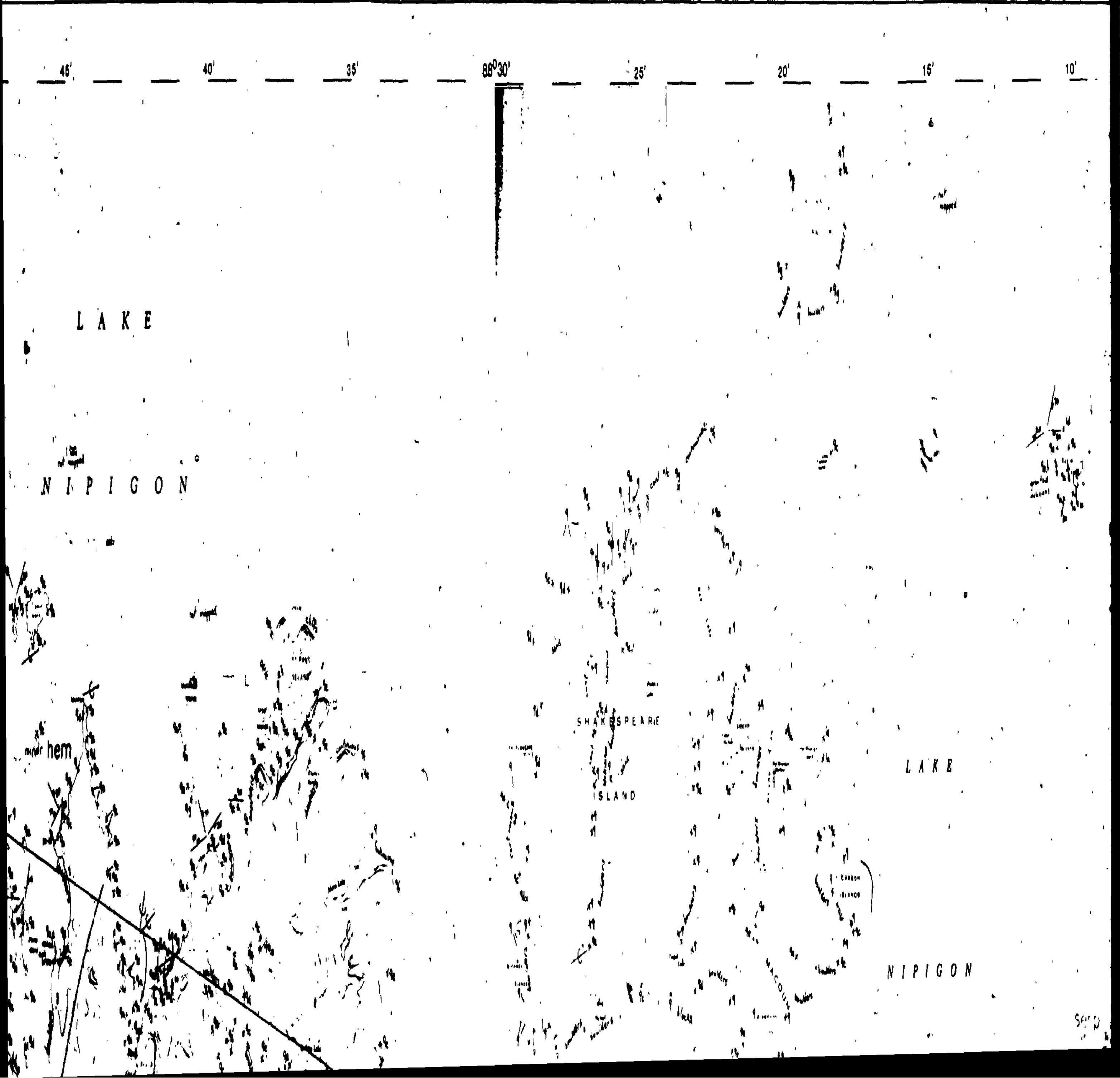
45'
40'
35'
88°30'
25'
20'
15'
10'
LAKE
NIPIGON
not mapped
not mapped
not mapped
hem
SHAKESPEARE
ISLAND
CARSON
ISLANDS
LAKE
NIPIGON

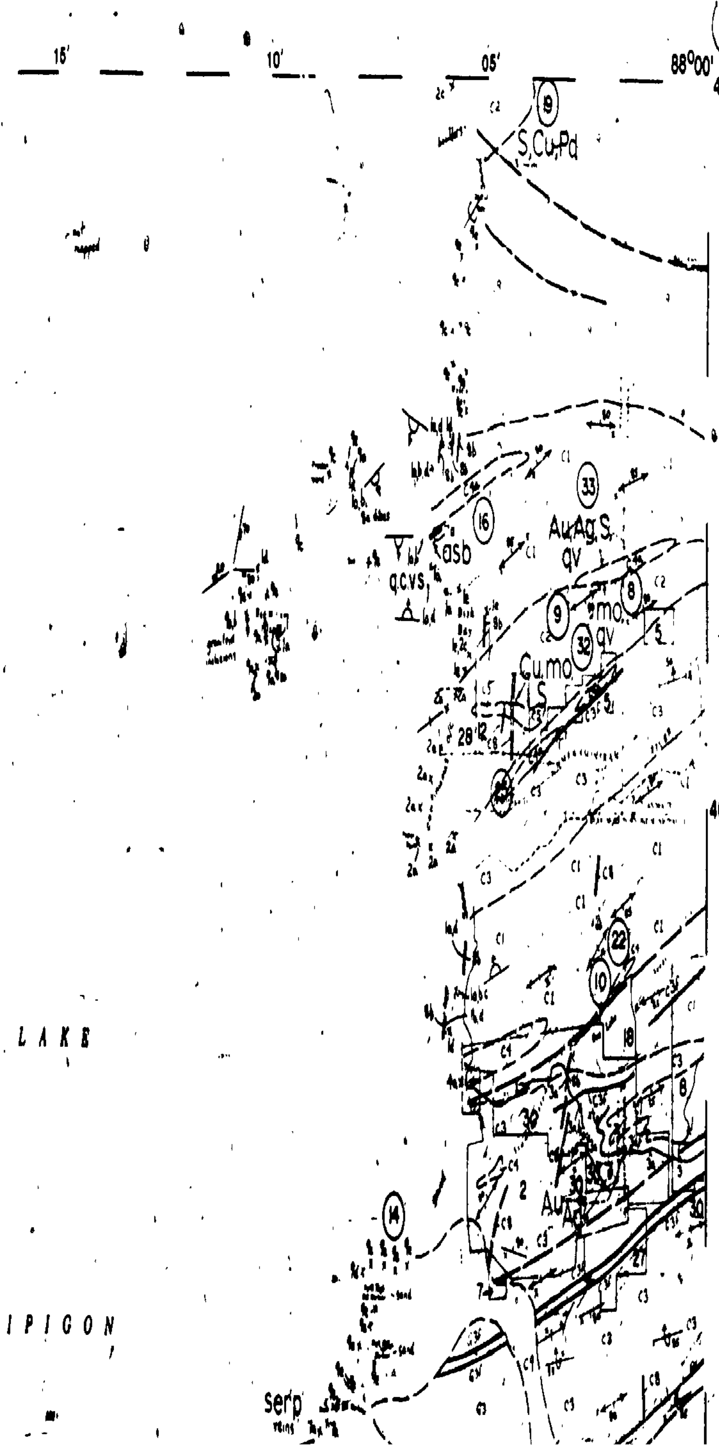
15'
10'
05'
88°00'
49°45'
40'
S,Cu,Pd
Au,Ag,S
qv
asb
q,c,v,s
mo
qv
Cu,mo
Au
serp
LAKE
NIPIGON

GEOLOGY

OF THE

LAKE NIPIGON AREA

SOUTHERN PART

Scale 1:100 000

Metres 1000 0 1 2 3 4 Kilometres

Mile 1 0 1 2 3 Miles

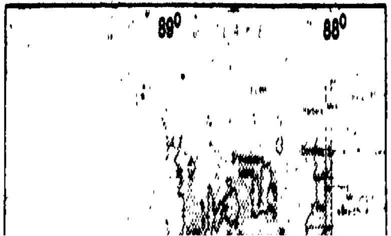

LEGEND

PHANEROZOIC
CENOZOIC
QUATERNARY
PLEISTOCENE AND RECENT
Till, esker deposits, lacustrine deposits, swamp

Precambrian lithology in the area. The tonalite consists of several phases ranging in texture from gneissic to foliated and commonly contains amphibolite and pyroxene-amphibolite enclaves. Locally, such as on the Britannia Islands of Lake Nipigon, the tonalite is discordantly intruded by mafic dikes which have subsequently been deformed and metamorphosed. Hornblende diorite is locally associated with the tonalite and is particularly common on the northeastern shore of Ombabika Bay of Lake Nipigon.

Biotite granite and granite pegmatite dikes intrude the biotite tonalite throughout the area. East of Armstrong the biotite granite forms a late massive pluton which is intrusive into tonalite. Microcline megacrystic granodiorite forms a pluton peripheral to the supracrustal belt on the northeastern shore of Humboldt Bay of Lake Nipigon.

Early Precambrian metavolcanic and metasedimentary rocks within the map area are encountered mostly in the Humboldt Bay and East Bay area of Lake Nipigon. In this area, the metavolcanics consist of predominantly amphibolite facies mafic metavolcanics which display relict pillow, massive, flow breccia, and porphyritic textures. Minor units of interflow metasedimentary rocks are also locally preserved within the metavolcanic units.

Intermediate fragmental metavolcanic rocks are exposed on the eastern shore of Lake Nipigon north of Mungo Park Point and consist of andesitic flow breccia and debris flow material. Minor units of argillite and meta-wacke are associated with the intermediate metavolcanic rocks.

On the northeastern shore of Humboldt Bay a unit of metaconglomerate with tonalite clasts occurs at what is interpreted to be the base of the supracrustal belt. Tonalite clasts in the conglomerate are similar in texture to outcrops of tonalite on the northwestern shore of the bay.

LATE PRECAMBRIAN

In the area investigated Late Precambrian rocks consist of: 1) felsic subvolcanic and volcanic rocks, 2) sedimentary rocks, probably of the Sibley Group; 3) a suite of predominately ultramafic intrusions; and 4) extensive diabase sills, sheets and dikes.

Felsic subvolcanic and volcanic rocks have not previously been reported within the Nipigon Plate. The volcanic rocks include debris flow, welded tuff and tuff-breccia. At present only sparse remnants are preserved, probably, due to erosion during volcanism. Outcrops of the volcanic rocks occur on the western

by the presence of amphibolite dikes which cross-cut the tonalite gneissosity and have subsequently been deformed.

The late granites are massive and have caused brittle fragmentation of the tonalitic rocks into which they were emplaced.

The presence of conglomerate with tonalitic clasts at the inferred base of the Onaman River supracrustal belt at Humboldt Bay, suggests that the supracrustal rocks may unconformably overlie a tonalitic basement in this area.

LATE PRECAMBRIAN

The Nipigon Plate at the northern end of Lake Nipigon is a broad, shallow basin. In general, the diabase sill dips gently into the centre of the lake. Steeper dips and an abrupt flexure of the sill occur along the eastern shore, along the North and South Peninsulas, and to a lesser extent along the western side of the lake. These flexures in the sill are believed to reflect fault blocks in the basement extant prior to sill emplacement.

Mapping during this survey has shown that the diabase sills were fed by cone sheets which are on the order of 30 to 50 km in diameter. This relationship is well documented west of Armstrong (see Figure 2). A similar structure, inferred in the Macdiarmid area, contains the circular ultramafic ring dike in its centre. West of Armstrong, the dike forming the cone sheet has a minimum width of 100 to 150 m and dips inward at 50° to vertical. On the northern and western parts of the structure, the erosional level corresponds to the level at which the dike becomes more gently dipping and makes the transition to a sill.

Subsidence of the northern part of Lake Nipigon during emplacement of the diabase sheets may explain the preservation of a thicker Late Precambrian section in this area. Reverse faulting on western side of the South Peninsula in which Early Precambrian tonalite overlies Late Precambrian sedimentary rocks may be related to this subsidence.

ECONOMIC GEOLOGY

BASE METALS

Mineralization within the diabase sill was observed predominantly in the pegmatitic patches near the top of the sill. These zones contain sparsely disseminated chalcopyrite.

The ultramafic to mafic intrusions of the area are largely

Survey along the National Transcontinental Railway Location between Lake Nipigon and Lac Seul. Geological Survey of Canada, Summary Report for 1906, p. 103-109

Franklin, J.M.

1978 Uranium Mineralization in the Nipigon Area, Thunder Bay District, Ontario. Current Research, Part A. Geological Survey of Canada, Paper 78-1A, p. 275-282

Franklin, J.M., McIlwaine, W.H. Poulsen, K.H., and Wanless, R.K.

1980 Stratigraphy and Depositional Setting of the Sibley Group, Thunder Bay District, Ontario, Canada. Canadian Journal of Earth Sciences, Volume 17, p. 633-651

ODM-GSC

1962 Nipigon Sheet, Ontario Department of Mines - Geological Survey of Canada, Aeromagnetic Map 7103G, scale 1:253 440 or 1 inch to 4 miles. Survey flown 1962

1962 Armstrong Sheet, Ontario Department of Mines - Geological Survey of Canada, Aeromagnetic Map 7121G, scale 1:253 440 or 1 inch to 4 miles. Survey flow 1962.

Pye, E.G.

1968 Geology of the Crescent Lake Area, District of Thunder Bay. Ontario Department of Mines, Geological Report 55, 66 p. Accompanied by Map 2100, scale 1:63 360 or 1 inch to 1 mile.

Sage, R.P., Breaks, F.W., Stott, G., McWilliams, G., and Bowen, R.P.

1974 Operation Ignace-Armstrong, Pashkokogan - Caribou Lakes Sheet, District of Thunder Bay. Ontario Division of Mines, Preliminary Map, P. 962, Geological Series, scale 1:126 720 or 1 inch to 2 miles. Geology 1973

Streckeisen, A.

1976 To Each Plutonic Rock its Proper Name. Earth-Science Reviews, Volume 12, p. 1-33

Sutcliffe, R.H.

1981 Geology of the Wabigoon - Quetico Subprovince Boundary in the Lake Nipigon Area, District of Thunder Bay, p. 26-29 in Summary of Field Work, 1981, by the Ontario Geological Survey, edited by John Wood, O.L. White, R.B. Barlow, and A.C. Colvine. Ontario Geological Survey, Miscellaneous Paper 100, 255 p.

Wilson, A.W.G.

1910 Geology of the Nipigon Basin Ontario. Geological Survey of Canada, Memoir 1, 152 p.

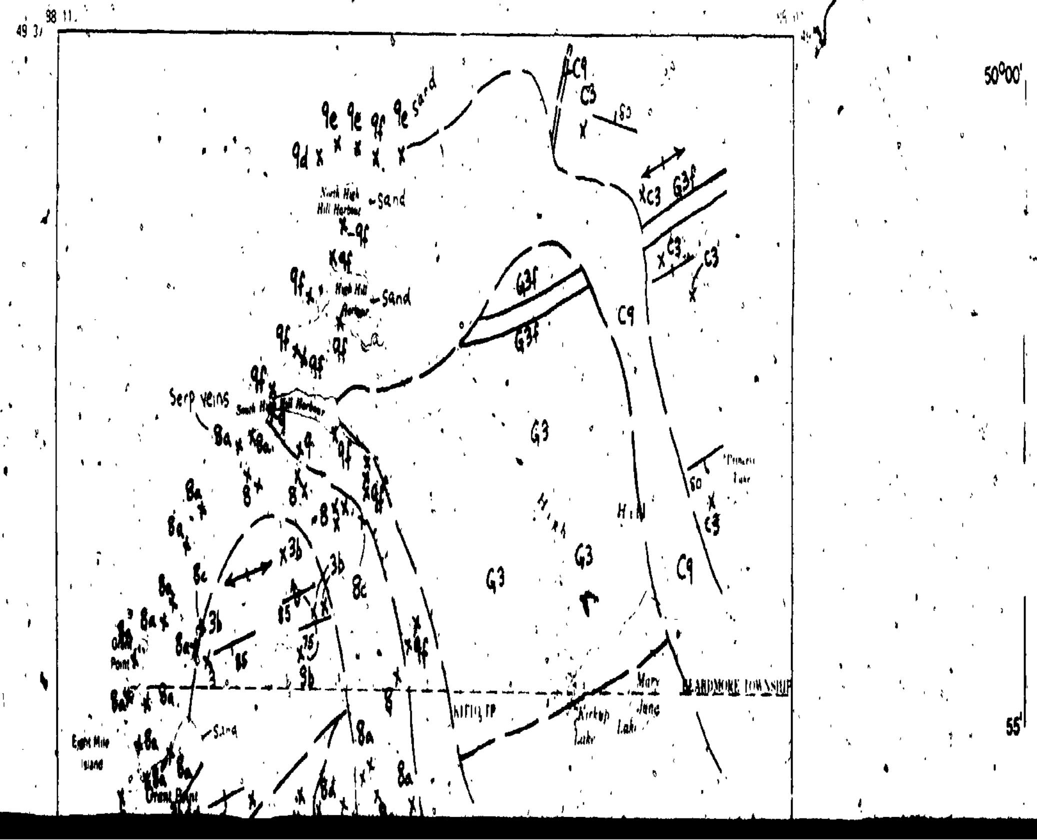

LAKE
NIPIGON
LAKE
NIPIGON
HURON
ISLAND
hem
corb
po py
LAKE

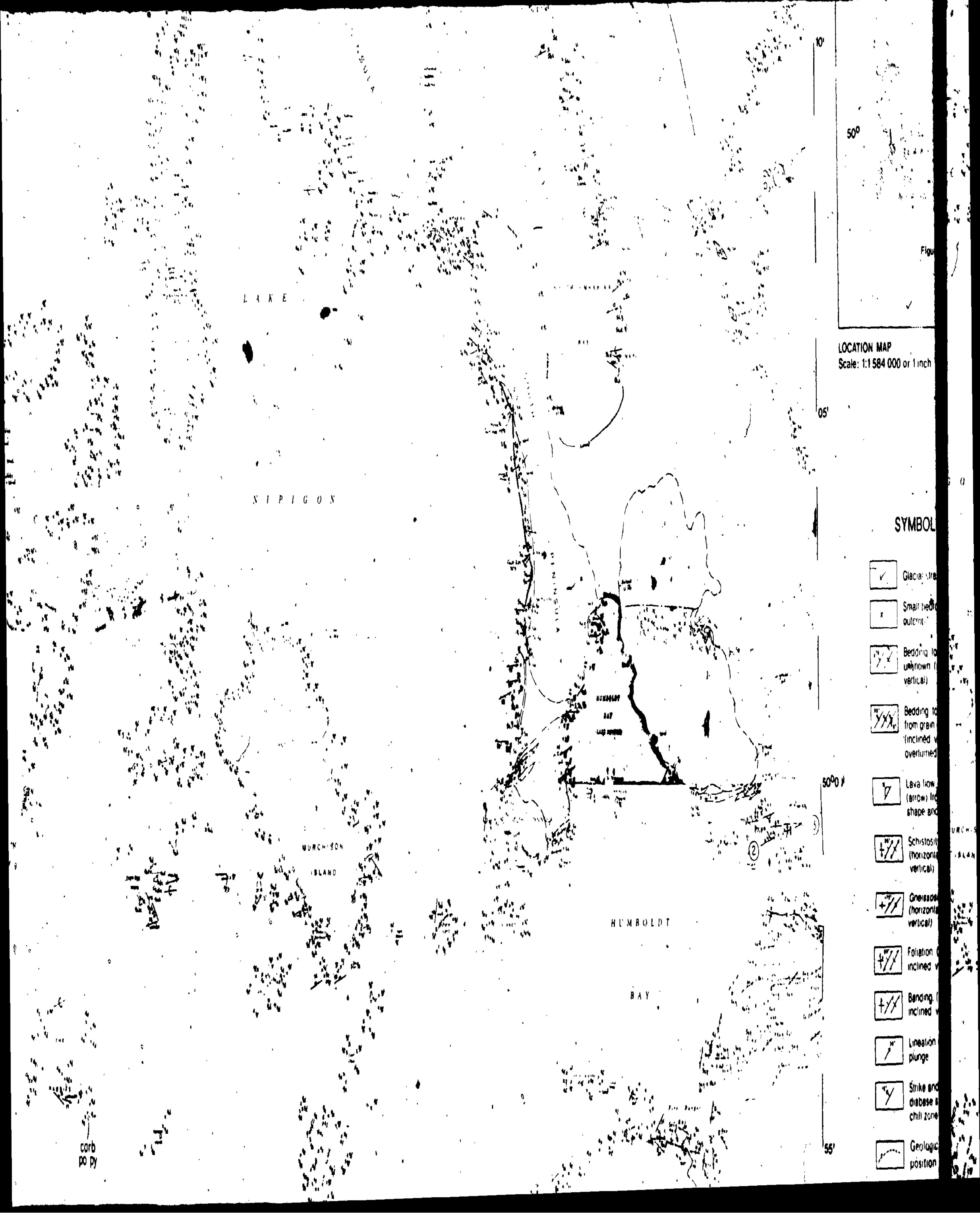
LAKE
NIPIGON
MURCHISON
ISLAND
HUMBOLDT
BAY
HUMBOLDT
BAY
LAKE NIPIGON
10'
05'
50⁰0'
55'
50⁰
LOCATION MAP
Scale: 1:1 584 000 or 1 inch
SYMBOL
Glacial stri
Small bedro
outcrop
Bedding to
unknown (
vertical)
Bedding to
from grain
(inclined v
overturned)
Lava flow,
(arrow) fro
shape and
Schistosit
(horizonta
vertical)
Gneissose
(horizonta
vertical)
Foliation
inclined v
Banding
inclined v
Lineation
plunge
Strike and
diabase
chill zone
Geologic
position
2
3
carb
po py

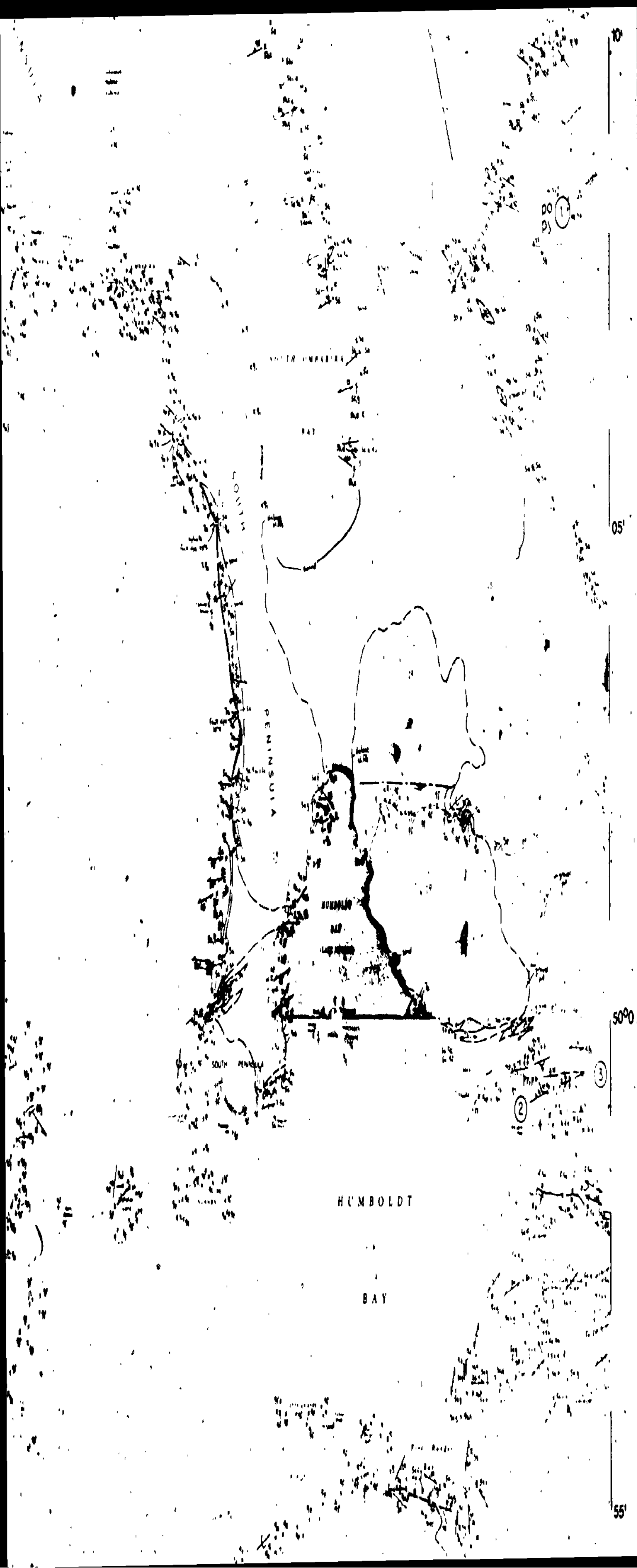

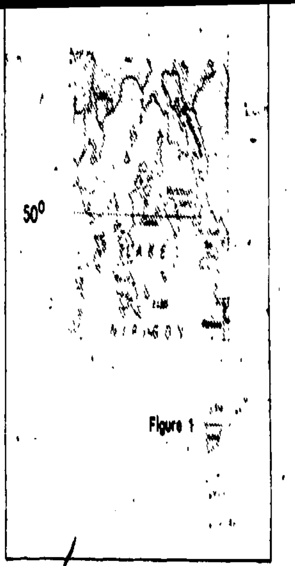

LOCATION MAP
Scale: 1:1 584 000 or 1 inch to 25 miles

SYMBOLS

- Glacial striae
- Small bedrock outcrop
- Bedding, top unknown, (inclined, vertical)
- Bedding, top (arrow) from grain gradation, (inclined, vertical, overturned)
- Lava flow, top (arrow) from pillow shape and packing
- Schistosity, (horizontal, inclined, vertical)
- Gneissosity, (horizontal, inclined, vertical)
- Foliation, (horizontal, inclined, vertical)
- Banding, (horizontal, inclined, vertical)
- Lineation with plunge
- Strike and dip of diabase sheet from chill zone
- Geological boundary, position interpreted.

swamp, stream and lake deposits

UNCONFORMITY

PRECAMBRIAN[c]
LATE PRECAMBRIAN (PROTEROZOIC)
MAFIC INTRUSIVE ROCKS
LOGAN DIABASE SILLS, SHEETS AND DIKES

9
- 9 Unsubdivided
- 9a Aphanitic to fine-grained diabase
- 9b Polygonally fractured diabase
- 9c Vesicular or amygdaloidal diabase
- 9d Quartz amphibole diabase, coarse-grained
- 9e Diabase with pegmatitic patches or veins
- 9f Medium-grained diabase
- 9g Layered diabase
- 9h Anorthositic diabase
- 9i Ophitic diabase
- 9k Granophyre veins related to diabase
- 9m Carbonate-diabase breccia

ULTRAMAFIC TO MAFIC INTRUSIVE ROCKS

8
- 8 Unsubdivided
- 8a Peridotite
- 8b Pyroxenite
- 8c Olivine metagabbro
- 8d Olivine gabbro

SEDIMENTARY ROCKS (SIBLEY GROUP)

7
- 7 Unsubdivided
- 7a Quartz arenite[d]
- 7b Conglomerate[d]
- 7c Calcareous mudstone[d]

FELSIC SUBVOLCANIC TO VOLCANIC ROCKS

6
- 6 Unsubdivided
- 6a Quartz-feldspar porphyry,
- 6b Granite
- 6c Welded tuff and tuff breccia
- 6d Volcanic conglomerate (debris flow)

UNCONFORMITY

EARLY PRECAMBRIAN (ARCHEAN)[c]
FELSIC TO INTERMEDIATE INTRUSIVE ROCKS

5
- 5 Unsubdivided
- 5a Tonalite to granodiorite, foliated
- 5b Tonalite to granodiorite, gneissic
- 5c Tonalite to granodiorite with amphibolite inclusions
- 5d Hornblende diorite
- 5e Microcline megacrystic granodiorite
- 5f Biotite granite
- 5g Pegmatite
- 5h Quartz-feldspar porphyry

MAFIC INTRUSIVE ROCKS

4
- 4a Amphibolite dikes
- 4b Pyroxene-amphibolite

METAVOLCANIC AND METASEDIMENTARY ROCKS
METASEDIMENTARY ROCKS

3
- 3 Unsubdivided
- 3a Conglomerate
- 3b Feldspathic wacke
- 3c Lithic wacke
- 3d Argillite and slate

ped the area to the south containing Late Precambrian sediments be

[illegible]

[illegible] associated with the Sibley Group sediments. Base metal exploration has [illegible] occurrences of copper near the diabase sediment interface such as the Disraeli Lake occurrences (Coates 1972)

GENERAL GEOLOGY

The map area includes Early Precambrian supracrustal and plutonic rocks of the Wabigoon and Quetico Subprovinces and Late Precambrian sedimentary and intrusive rocks of the Nipigon Plate. The previous mapping of Lake Nipigon is reported by Wilson (1910). Coates (1972) mapped the area to the south containing Late Precambrian sediments between Lake Nipigon and Lake Superior. Pye (1965, 1968), Kaye (1969) and Mackasey (1970, 1975) have mapped Early Precambrian rocks around the margin of the plate in the vicinity of the Subprovince boundary.

Early Precambrian

Early Precambrian rocks occur around the margin of the Nipigon Plate and within the Plate as uplifted fault blocks and as outliers overlying the Late Precambrian igneous rocks. During the present survey, previously unreported Early Precambrian metavolcanics were found on Hat Mountain Island and Red Willow Island in Lake Nipigon.

The stratigraphic assemblage of Early Precambrian rocks is similar on either side of the Nipigon Plate. The rocks are

1) a northern metavolcanic sequence consisting of mafic metavolcanics and lesser intermediate fragmental rocks;
2) a metasedimentary unit 1 to 2 km wide of polymictic conglomerate, quartz wacke, lithic wacke and argillite;
3) a thin, 1 km wide unit of mafic metavolcanics, and
4) a southern metasedimentary sequence.

The southern metasedimentary sequence increases in metamorphic grade to the south and eventually becomes migmatized. Unit 1 is assigned to the Wabigoon Subprovince, units 2 and 3 form the boundary zone and unit 4 is assigned to the Quetico Subprovince (Mackasey *et al.* 1974).

Early Precambrian metavolcanics and metasediments are exposed on the uplifted block east of the Black Sturgeon Fault. These rocks are of medium metamorphic grade and appear to be part of the subprovince boundary zone.

Mackasey *et al.* (1974) consider the subprovince boundary to be stratigraphic and to be a diffuse zone which represents a facies change from predominately volcanic to predominately sedimentary assemblages. According to their definition, the northern metavolcanic sequence is part of the Wabigoon Subprovince and the southern metasedimentary sequence part of the Quetico Subprovince. In the transition zone between these facies, the sediments show a progressive decrease in grain size to the south suggesting that the conglomerate represents a proximal facies of the Quetico Subprovince.

Late Precambrian

In the map area, the Late Precambrian rocks of the Nipigon Plate consist of

1) Sibley Group sediments which unconformably overlie the Early Precambrian rocks,
2) an ultramafic intrusion, and
3) extensive diabase sills and sheets with minor diabase dikes.

The Sibley Group sediments within the area are more extensive than previously recognized. New areas found to be underlain by Sibley Group rocks occur between Black Sturgeon and Forgan Lakes, where the sediments overlie a diabase sill. The sediments are predominantly white calcareous mudstone and carbonate and are probably part of the Rossport Formation (Franklin *et al.* 1980). Red mudstone, quartz arenite, and locally conglomerate are also present throughout the Sibley Group.

Ultramafic intrusions which have not been reported in the previous mapping have been delineated in the map area and to the south during the present survey. They are interpreted to intrude the Sibley sediments but have uncertain age relations with respect to the diabase. The ultramafic intrusion in Eva Township is a circular ring dike with an outside diameter of approximately 6 km and ranges in composition from peridotite to metagabbro.

Olivine diabase sills are the most extensive rock type in the area. Two sills are present in the map-area. The lower sill has a thickness of approximately 200 m and grades from coarse grained ophitic diabase to medium-grained diabase, to diabase with coarse pegmatitic patches containing quartz. The upper 2 m of the sill are fine grained to aphanitic with polygonal fractures. A zone of amygdaloidal diabase 10 to 20 cm below the chill is locally present. Late veins containing prehnite, carbonate, epidote, amphibole, tourmaline, and analcime are abundant near the top of the sheet. The overlying calcareous sediments of the Sibley Group exhibit contact metamorphic effects including the [illegible]

[illegible] Precambrian rocks near the Early Precambrian-Late Precambrian unconformity. Early Precambrian rocks in the vicinity of the Black Sturgeon Fault warrant investigation for this type of mineralization. In this zone, radioactive fractures were discovered by the field party approximately 1 km east of the south end of Black Sturgeon Lake.

REFERENCES

[illegible]
1981 [illegible] Rare Element Granitic Pegmatites [illegible] 1981 by the Ontario Geological Survey, [illegible] R.B. Barlow, A. Roberts [illegible] Ontario Geological Survey, Miscellaneous Paper 96 [illegible]

Coates, M.E.
1972 Geology of the Black Sturgeon River Area, District of Thunder Bay, Ontario Department of Mines and Northern Affairs, Geological Report 98, [illegible] Accompanied by Maps 2233, 2234, 2235, 2236, Scale 1 inch to 1 mile.

Franklin, J.M.
1970 Metallogeny of the Proterozoic Rocks of Thunder Bay District [illegible] Thesis [illegible] University of Western Ontario [illegible]

Franklin, J.M., [illegible]
1980 Stratigraphy and Depositional Setting of the Sibley Group, Thunder Bay District, Ontario, Canada [illegible]

Kaye, L.
1969 Geology of the Eayrs Lake-Starnes Lake Area, District of Thunder Bay, Ontario Department of Mines, Geological Report 77, 29p. Accompanied by Map 2172, Scale 1 inch to 1 mile.

Mackasey, W.O.
1970a Eva Township, District of Thunder Bay, Ontario Department of Mines, Preliminary Map P.601, Scale 1 inch to 1/4 mile. Geology 1969.
1970b Summers Township, District of Thunder Bay, Ontario Department of Mines, Preliminary Map P.602, Scale 1 inch to 1/4 mile. Geology 1970.
1975 Geology of Dorothea, Sandra and Irwin Townships, District of Thunder Bay, Ontario Division of Mines, Geological Report 122, 83p. Accompanied by Map 2294, Scale 1 inch to 1/4 mile.

Mackasey, W.O., Blackburn, C.E., and Trowell, N.F.
1974 A Regional Approach to the Wabigoon-Quetico Belts and its Bearing on Exploration in Northwestern Ontario, Ontario Division of Mines, Miscellaneous Paper 58, 30p.

ODM-GSC
1962 Nipigon Sheet, Ontario Department of Mines-Geological Survey of Canada, Aeromagnetic Map [illegible] Scale [illegible] Survey [illegible] 1962.

Pye, E.G.
1965 Geology and Lithium Deposits of Georgia Lake Area, District of Thunder Bay, Ontario Department of Mines, Geological Report 31, [illegible] Accompanied by Map 2056, Scale 1 inch to 1 mile.
1968 Geology of the Lac des Iles Area, District of Thunder Bay, Ontario Department of Mines, Geological Report 64, 47p. Accompanied by Maps 2135, 2136, Scale 1 inch to 1 mile.

Steckeisen, A.
1976 To Each Plutonic Rock its Proper Name, Earth Science Reviews, Vol. 12, p. 1-33.

Wilson, A.W.G.
1910 Geology of the Nipigon Basin, Ontario, Geological Survey of Canada, Memoir 1, 152p.

LIST OF PROPERTIES AND OCCURRENCES

1) Avalanche River Mines Limited (1956)
2) Camel Resources Limited (1980)
3) Caral Lithium Deposit (1960)
4) Conway, E.S. (1958)
5) Craig, C.L. (1967)
6) Dunning Lithium Deposit
7) Elcamber Resources (1980)
8) Falconbridge Nickel Mines Limited (1963)
9) Gunnex Limited (1971)
10) Gustafson, T.A. (?)
11) Harricana Lithium Deposit (1956)
12) Hopkins, A.P.E. (1967)
13) Hudson Bay Exploration and Development Company Limited (1981)
14) International Nickel Limited (1972)
15) [illegible] Lithium Deposit (1959)
[illegible]

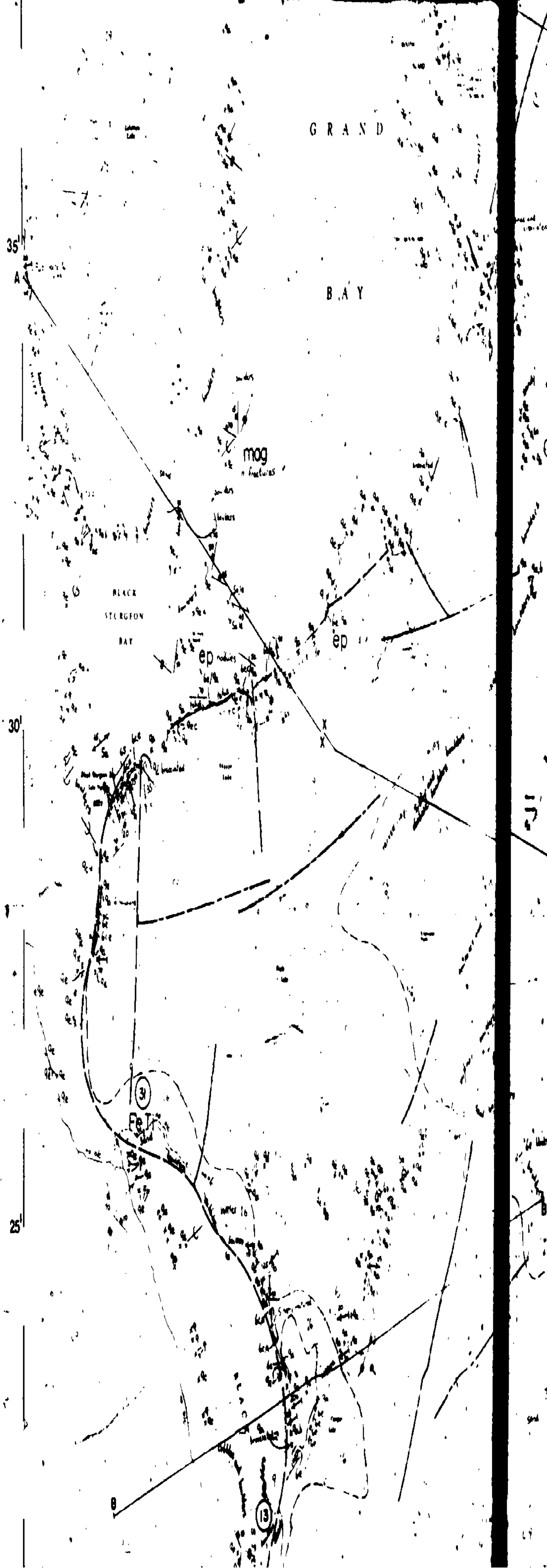

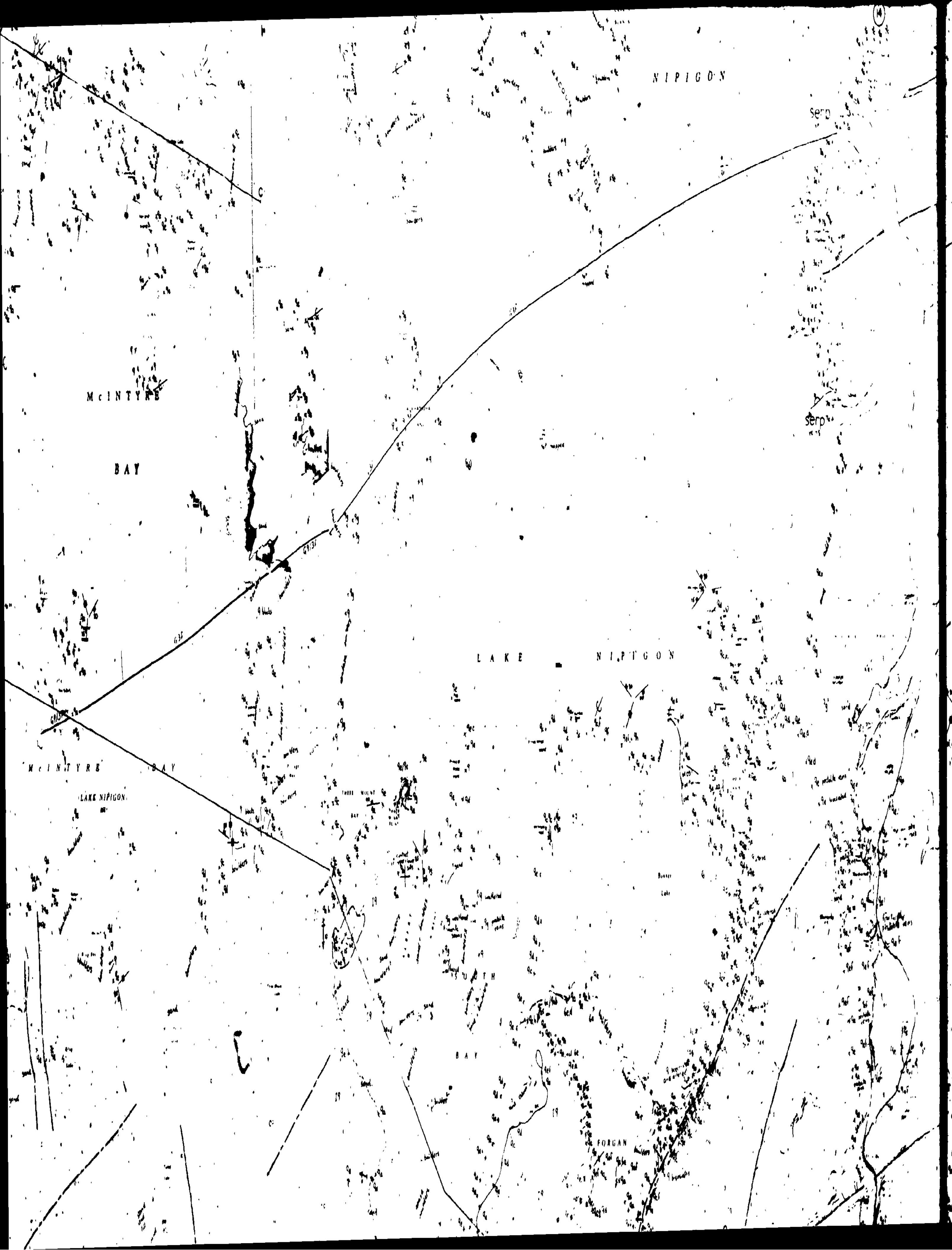

14
NIPIGON
serp
McINTYRE
BAY
LAKE NIPIGON
McINTYRE BAY
LAKE NIPIGON
serp
FORGAN
BAY

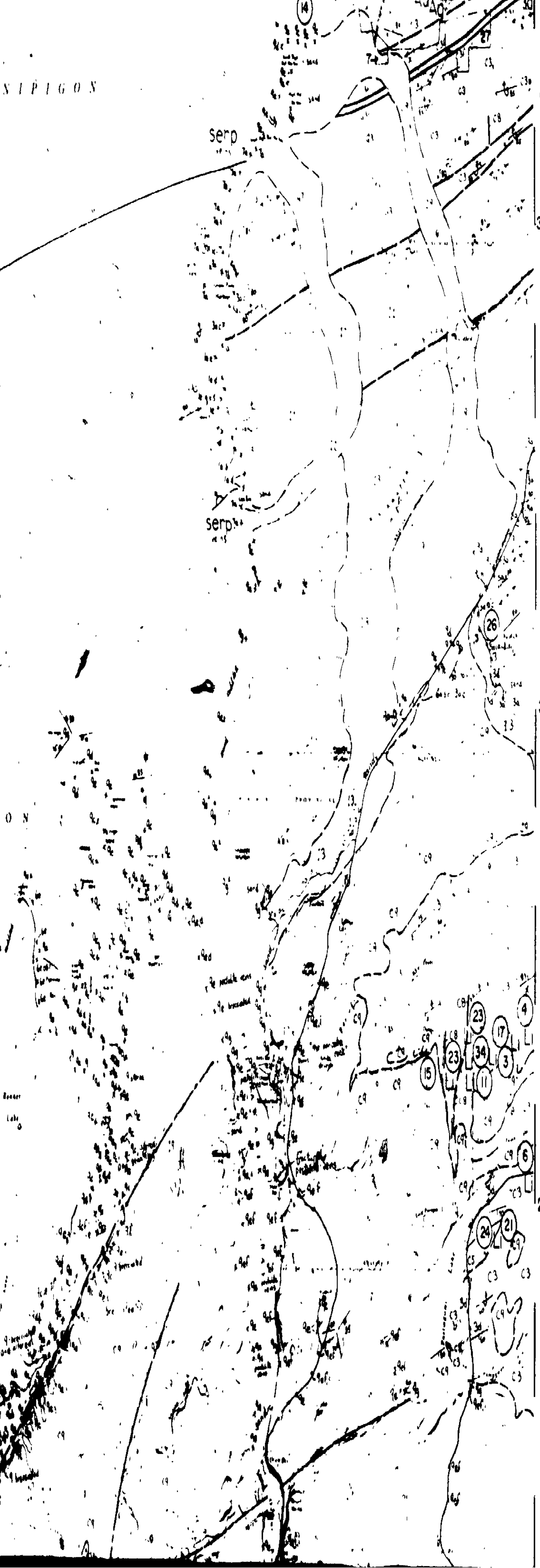

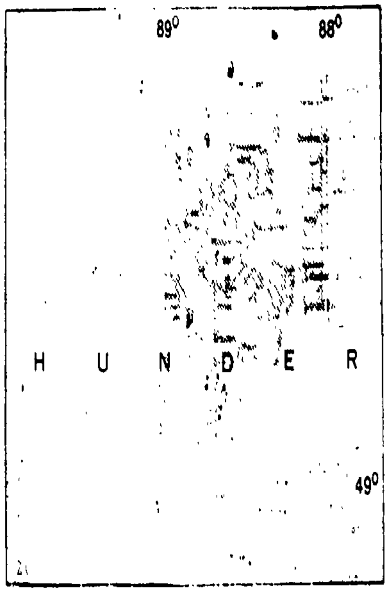

LOCATION MAP Scale: 1:1 584 000 or 1 inch to 25 miles

SYMBOLS

Glacial striae

Esker

Small bedrock outcrop

Bedding, horizontal

Bedding, top unknown (inclined, vertical)

Bedding, top [illegible] from grain gradation (inclined, vertical, overturned)

Bedding, top [illegible] from cross bedding (inclined, vertical, overturned)

Schistosity (horizontal, inclined, vertical)

Gneissosity (horizontal, inclined, vertical)

[illegible] with [illegible]

Geological boundary, [illegible] interpreted

Fault (observed, assumed). Spot indicates downthrow side. [illegible] indicate [illegible] movement

Lineament

[illegible] (horizontal, inclined, vertical)

[illegible] (depth in feet)

[illegible]

[illegible] (horizontal, inclined, vertical)

Cleavage (vertical, inclined)

[illegible] diabase sheet [illegible] zone

METAL AND MINERAL ABBREVIATIONS

Ag	Silver
asb	Asbestos
Au	Gold
Cu	Copper
ep	Epidote
Fe	Iron
hem	Hematite
Li	Lithium
mag	Magnetite
mo	[illegible]

LEGEND[a]

PHANEROZOIC
CENOZOIC
QUATERNARY
PLEISTOCENE AND RECENT
[illegible]
[illegible]

UNCONFORMITY

PRECAMBRIAN
LATE PRECAMBRIAN (PROTEROZOIC)
MAFIC INTRUSIVE ROCKS
[illegible] Sills and Sheets

9
9 Unsubdivided
9a [illegible]
9b [illegible]
9c [illegible]
9d [illegible]
9e [illegible]
9f [illegible]
9g [illegible] diabase
9h Feldspar porphyritic [illegible] diabase
9i Diabase with [illegible]

[illegible]

8
8 Unsubdivided
8a [illegible]
8b [illegible]

ULTRAMAFIC TO MAFIC INTRUSIVE ROCKS
7 Unsubdivided
7a Peridotite
7b [illegible]

SEDIMENTARY ROCKS [illegible]

6
6 Unsubdivided
6a [illegible]
6b Arkose
6c [illegible]
6d Red [illegible]
6e [illegible] siltstone
6f [illegible]

UNCONFORMITY

EARLY PRECAMBRIAN (ARCHEAN)
FELSIC TO INTERMEDIATE INTRUSIVE ROCKS

5
5 Unsubdivided
5a Tonalite [illegible] gneiss
5b Biotite [illegible] massive to foliated
5c Pegmatite

MAFIC INTRUSIVE ROCKS

4
4 Unsubdivided
4a Diorite
4b Amphibolite

METAVOLCANICS AND METASEDIMENTS
METASEDIMENTS

3
3 Unsubdivided
3a [illegible]
3b Conglomerate
3c Argillite, slate
3d Biotite schist derived from metasediments
3e Migmatite [illegible] derived from metasediments
3f [illegible]

INTERMEDIATE METAVOLCANICS

2
2 Unsubdivided
2a Tuff [illegible]
2b [illegible]

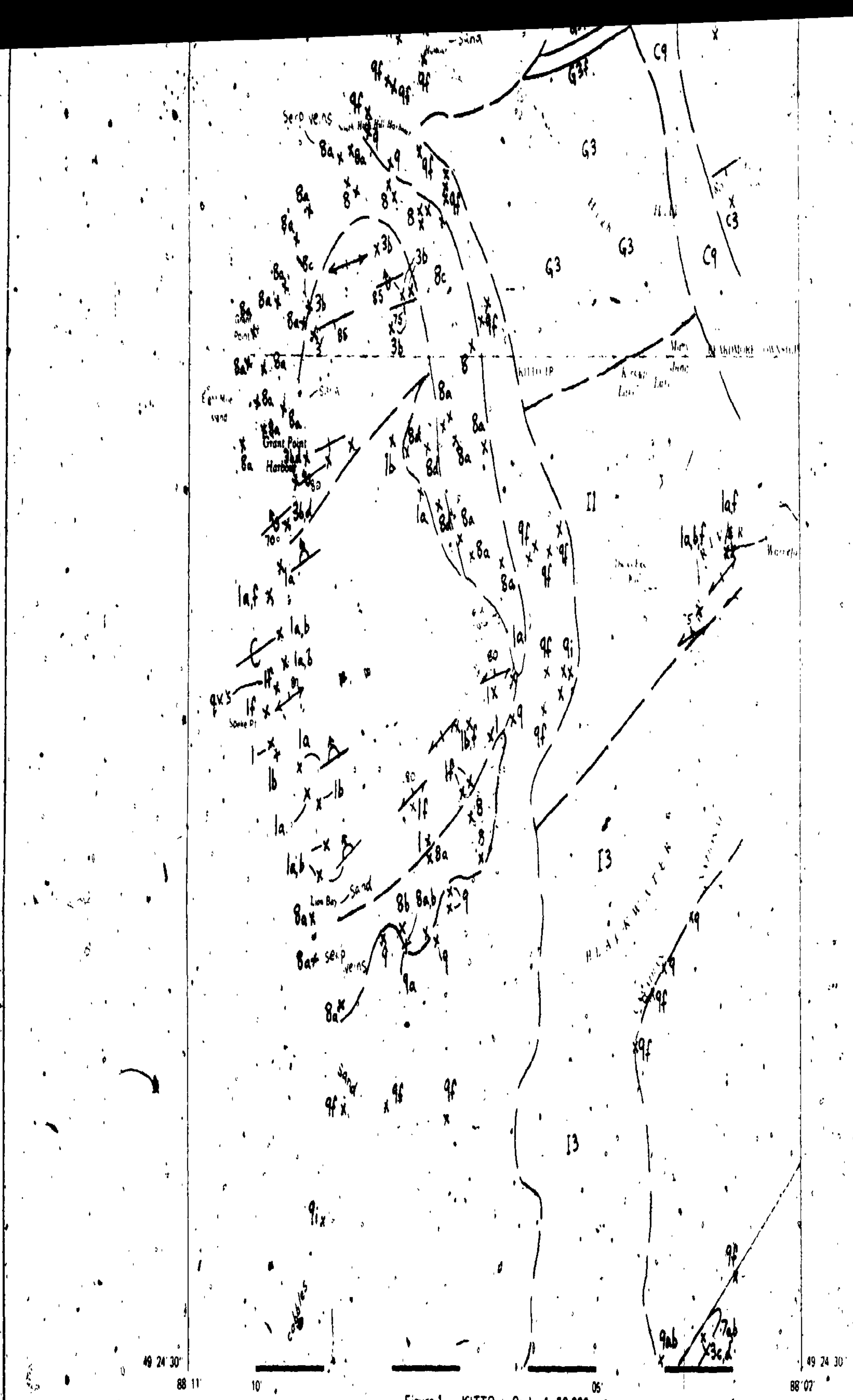
Sand
9f
G3
C9
Serp veins
8a
3b
3c
G3
C3
C9
G3
Grant Point Harbour
1b
1a
8d
I1
1a,f
1a,b
1f
Sand
Lone Bay
8b
8ab
9
9a
I3
9f
9ab
7ab
3c,d
cobbles
I3
49 24 30
88 11'
10'
05'
88 02'

Figure 1 KITTO Scale: 1: 50 000

55'
50'
89°45'
89°00'
56'

LAKE
LAKE
NIPIGON
N I P
55'
50'
45'
40'
35'
88°30'
25'
20'

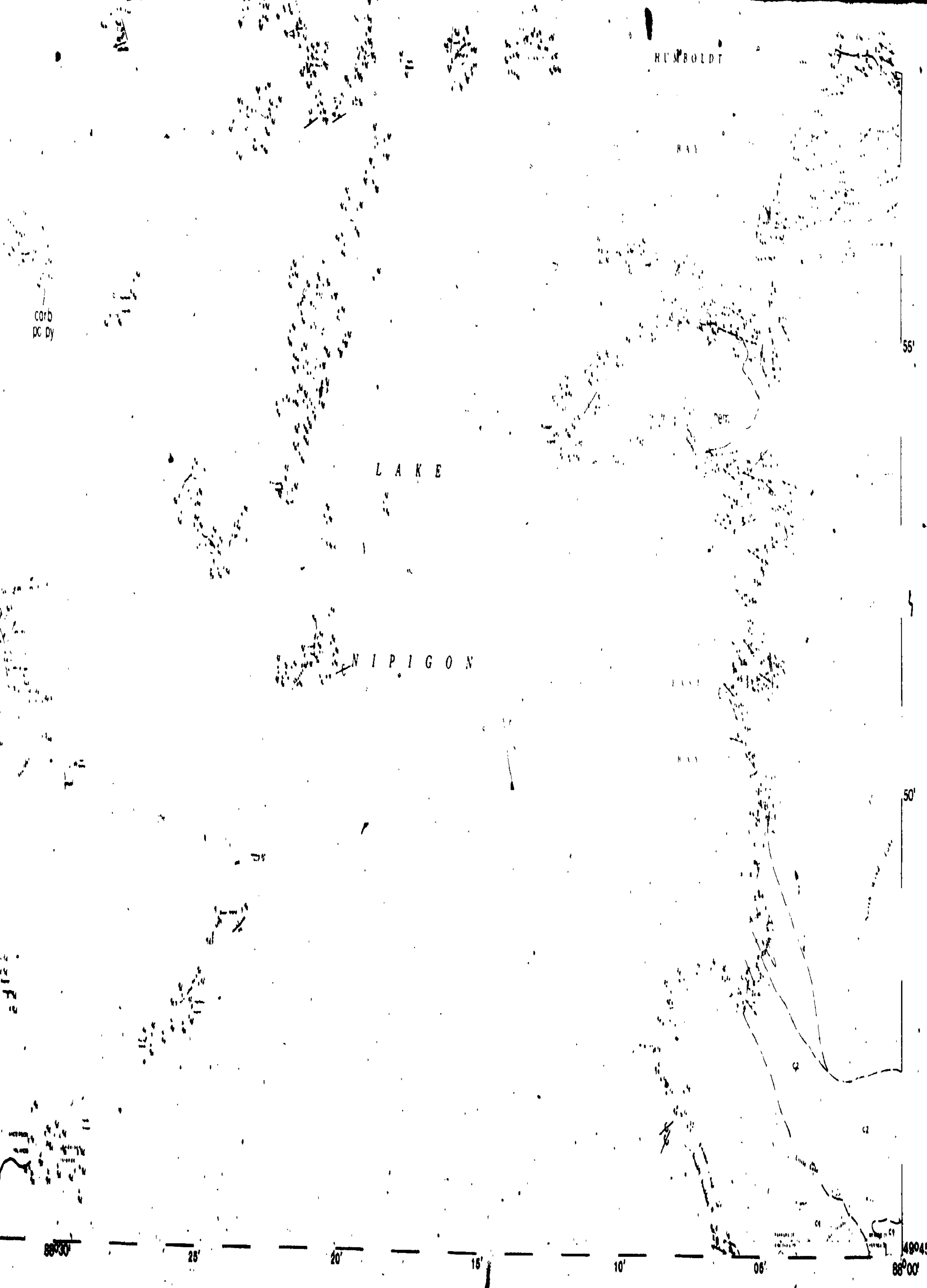
HUMBOLDT
BAY
LAKE
NIPIGON
BAY
carb
pc py
hem
55'
50'
49°45'
88°30'
25'
20'
15'
10'
05'
88°00'

Gneissosity (horizontal inclined vertical)

Foliation (horizontal inclined vertical)

Banding (horizontal inclined vertical)

Lineation with plunge

Strike and dip of diabase sheet from chill zone

Geological boundary position interpreted

Fault, (observed assumed) Spot indicates downthrown side arrows indicate horizontal movement

Lineament

Jointing, (horizontal inclined, vertical)

Drillhole, (vertical inclined)

LIST OF PROPERTIES

1 Canadian Nickel Company Limited (
2 Duval International Corporation (197
3 Zmudzinski, Jan and Clarke Loen (

METAL AND MINERAL ABBREVIATIONS

carb	ca
ep	
hem	h
mo	moly
po	py
py	
qv	quar
serp	ser

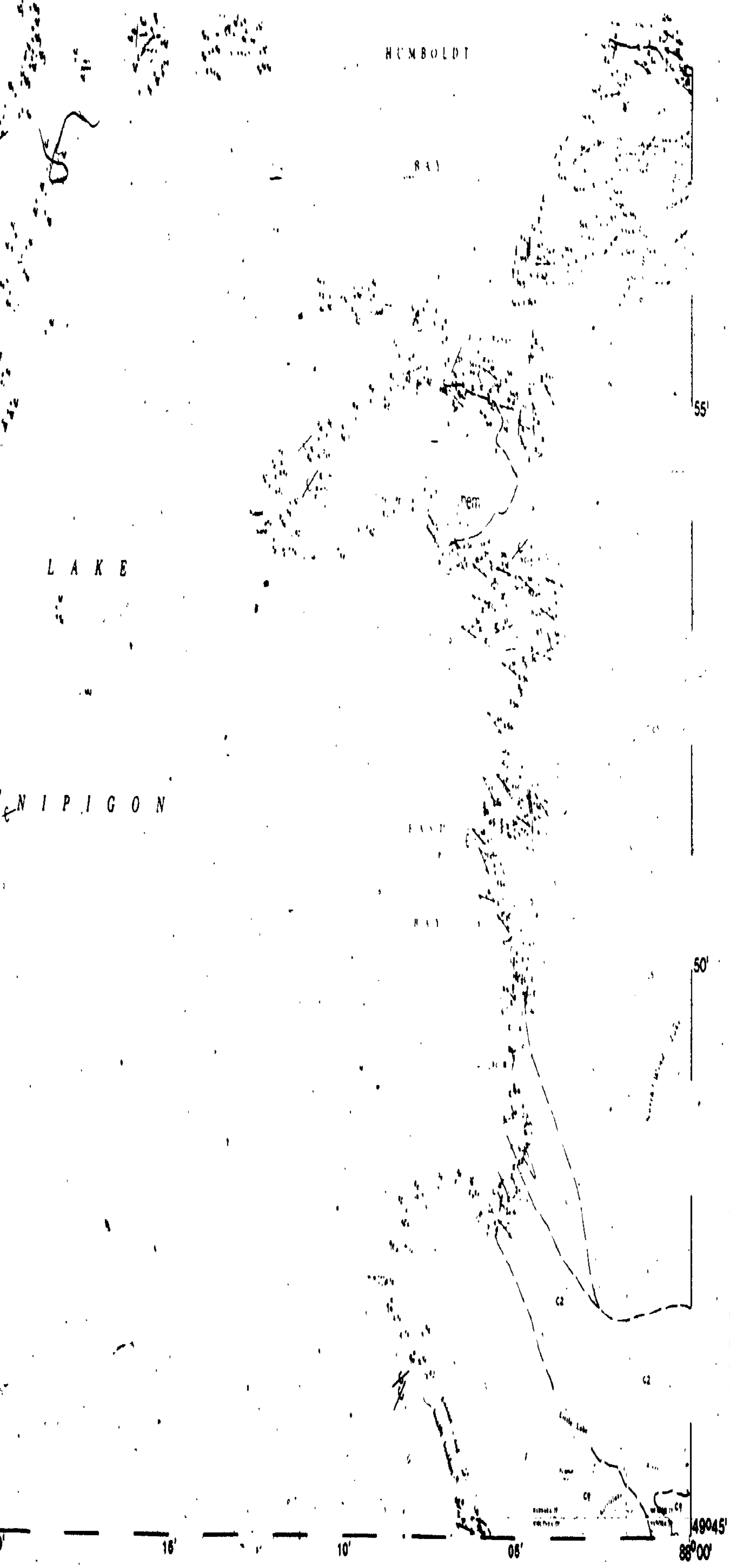

Gneissosity, (horizontal, inclined, vertical)

Foliation, (horizontal, inclined, vertical)

Banding, (horizontal, inclined, vertical)

Lineation with plunge

Strike and dip of diabase sheet from chill zone

Geological boundary, position interpreted.

Fault, (observed, assumed) Spot indicates downthrown side, arrows indicate horizontal movement

Lineament

Jointing, (horizontal, inclined, vertical)

Drillhole, (vertical, inclined)

LIST OF PROPERTIES

1. Canadian Nickel Company Limited (1971)
2. Duval International Corporation (1975)
3. Zmudzinski, Jan and Clarke, Loen (1972)

METAL AND MINERAL ABBREVIATIONS

carb	carbonate
ep	epidote
hem	hematite
mo	molybdenite
po	pyrrhotite
py	pyrite
qv	quartz vein
serp	serpentine

5d Hornblende diorite
5e Microcline megacrystic granodiorite
5f Biotite granite
5g Pegmatite
5h Quartz-feldspar porphyry

MAFIC INTRUSIVE ROCKS

4

4a Amphibolite dikes
4b Pyroxene-amphibolite

METAVOLCANIC AND METASEDIMENTARY ROCKS

METASEDIMENTARY ROCKS

3

3 Unsubdivided
3a Conglomerate
3b Feldspathic wacke
3c Lithic wacke
3d Argillite and slate
3e Chert, siliceous interflow metasedimentary rocks
3f Iron stone (oxide facies)

INTERMEDIATE METAVOLCANIC ROCKS

2

2 Unsubdivided
2a Tuff-breccia
2b Schistose fragmental rocks

MAFIC METAVOLCANIC ROCKS

1

1 Unsubdivided
1a Pillowed flow
1b Massive flow
1c Flow breccia
1d Porphyritic flow
1e Plagioclase-hornblende gneiss
1f Foliated to schistose flow

NOTES

a) This is a field legend and may be changed as a result of laboratory investigations
b) Plutonic rock classification follows the International Union of Geological Sciences Subcommission on the Systematics of Igneous Rocks (Streckeisen 1976)
c) Subdivision of rock units does not imply age relations
d) Probably correlates with the Pass Lake Formation (Franklin et al 1980).
e) Probably correlates with the Rossport Formation (Franklin et al 1980).
G) The letter "G" preceding a rock unit number indicates that the interpretation is based on geophysical data.
C) The letter "C" preceding a rock unit number indicates that the data is compiled from previous mapping.
I) The letter "I" preceding a rock unit number indicates that the interpretation is based on extrapolation of data.
/ Rock unit numbers separated by a "/" indicates that the first rock unit overlies the second rock unit.

[illegible] have been delineated in the map area [illegible] the present survey. They are interpreted to intrude the Sibley sediments but have uncertain age relations with respect to the diabase. The ultramafic intrusion in Eva Township is a circular ring dike with an outside diameter of approximately 6 km and ranges in composition from [illegible] to metagabbro.

[illegible] diabase sills are the most [illegible] in the area. [illegible] sills are present in the map area. The [illegible] has a thickness of approximately 200 m and grades from [illegible] diabase to medium grained diabase to [illegible] containing quartz. The upper 2 m [illegible] with polygonal fractures. A zone of [illegible] diabase [illegible] below the [illegible] is locally present [illegible] carbonate, epidote, amphibole [illegible] near the top of the sheet. The overlying [illegible] sediments of the Sibley Group exhibit contact metamorphic effects including the development of skarns and the growth of metamorphic epidote, amphibole [illegible] and serpentine. Remnants of Early Precambrian [illegible] the lower diabase.

The upper diabase sill is the highest stratigraphic unit of the Nipigon Plate within the map area. The upper contact of this sill was not observed and therefore the original thickness of the sheet [illegible]. The sill has a minimum thickness of approximately 100 m and ranges from ophitic to medium grained.

STRUCTURE

Early Precambrian

In the Nipigon area the Wabigoon-Quetico Subprovince boundary appears to be stratigraphic and no evidence is present to indicate a major structural break between the Subprovinces. East of Lake Nipigon the sequence is predominantly north facing and metavolcanics of the Wabigoon Subprovince appear to overlie metasediments of the Quetico Subprovince. West of Lake Nipigon, however, the opposite relationship is observed. In both sequences the sediments become fine grained and therefore appear to be more distal towards the south.

Insufficient outcrop of Early Precambrian rock occurs within the Nipigon Plate to trace the boundary zone through Lake Nipigon. A pronounced magnetic high (ODM-GSC 1962) associated with ironstone in the boundary zone indicates that the boundary passes through McIntyre Bay, and is offset sinisterally by the Black Sturgeon Fault Zone.

Nipigon Plate

Observations of the present survey support the hypothesis of Franklin *et al.* (1980) that the Nipigon Plate occupies a failed arm which extends north from a major flexure in the Keweenawan Lake Superior rift. The Black Sturgeon Fault and other parallel faults such as the Nipigon River Fault appear to have been the loci of tectonism in the Nipigon Plate during this event. Vertical movement along the Black Sturgeon Fault was contemporaneous with sedimentation. This has resulted in a thickening of Sibley sediments towards the fault and exposure of Early Precambrian rocks along the east side of the structure (Coates 1972).

Preliminary data suggests that the diabase sills may have been fed by cone sheets such as the cone sheet in Eva Township on the east shore of Lake Nipigon. Two concentric rings of diabase surround a central peridotite ring which may be a cumulate phase derived from the diabase. Mackasey (1975) has noted that the outer diabase sheet dips gently inward toward the center of the structure.

Over most of the map-area the diabase sills and sediments form a series of shallow basins and arches with dips ranging from subhorizontal to less than 15°. The sills are broadly conformable to the Sibley sediments but are markedly discordant to the Early Precambrian rocks. Steep dips of 40° to 80° occur in Sibley sediments and diabase sills associated with the northerly terminations of the Black Sturgeon and Nipigon River Faults.

[illegible]
4. [illegible] 196[illegible]
5. Craig, [illegible] 1967
6. [illegible] Deposit
7. [illegible] Resources 196[illegible]
8. [illegible] Mines Limited 1968
9. [illegible]
10. [illegible]
11. [illegible]
12. [illegible] 1967
13. [illegible] Bay [illegible] Development [illegible] Limited 1968
14. [illegible] Limited 1972
15. [illegible] Deposit 1964
16. [illegible] Mines Limited 1958
17. [illegible] Deposit 1968
18. [illegible] Mines Limited 196[illegible]
19. [illegible]
20. [illegible] Mines Limited 196[illegible]
21. [illegible] Deposit 1958
22. [illegible] 197[illegible]
23. [illegible] Mines Limited 1956
24. [illegible] Exploration Company Limited 197[illegible]
25. [illegible] Explorations Limited 1957
26. Pressman, B. 196[illegible]
27. Raynor, G.W. [illegible]
28. [illegible]
29. [illegible]
30. [illegible]
31. [illegible] Mines Limited 1959
32. Tyson, A.E. 196[illegible]
33. Tyson, [illegible] 196[illegible]
34. West [illegible] Deposit [illegible]
35. West St[illegible]

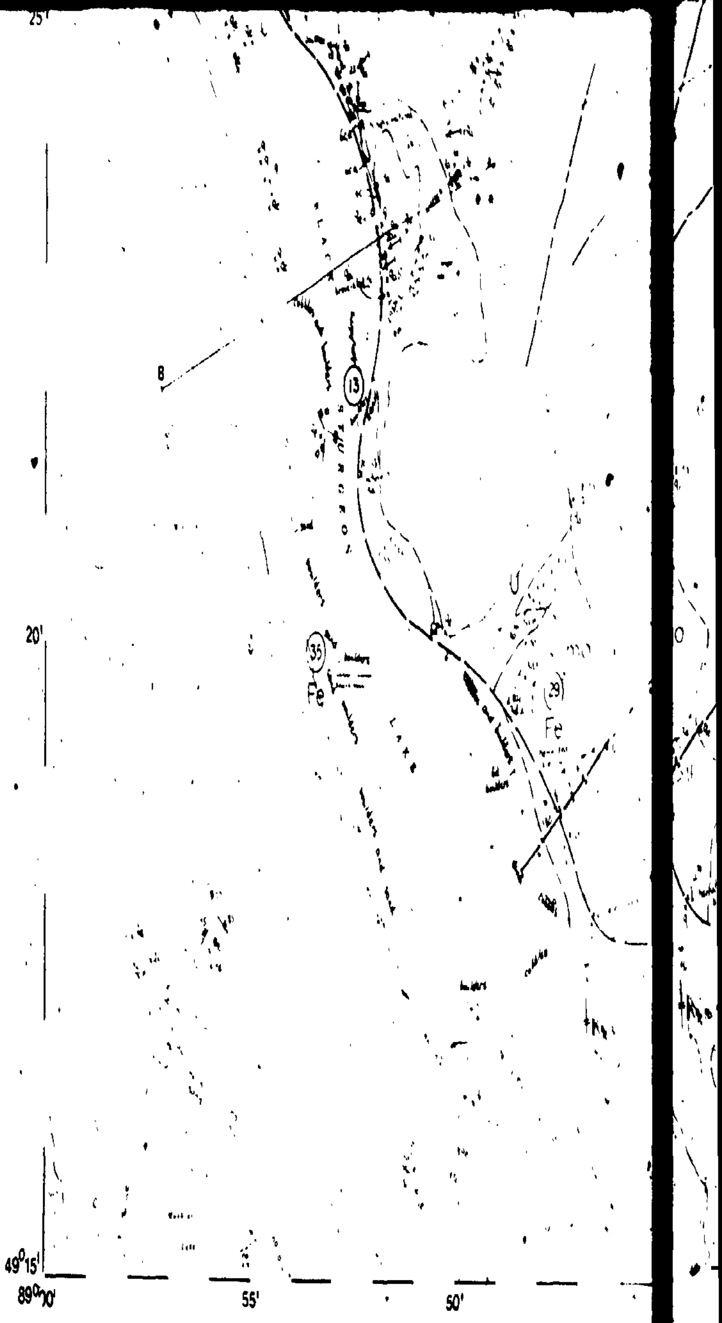

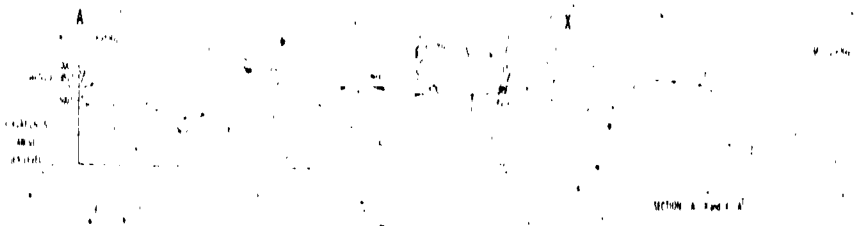

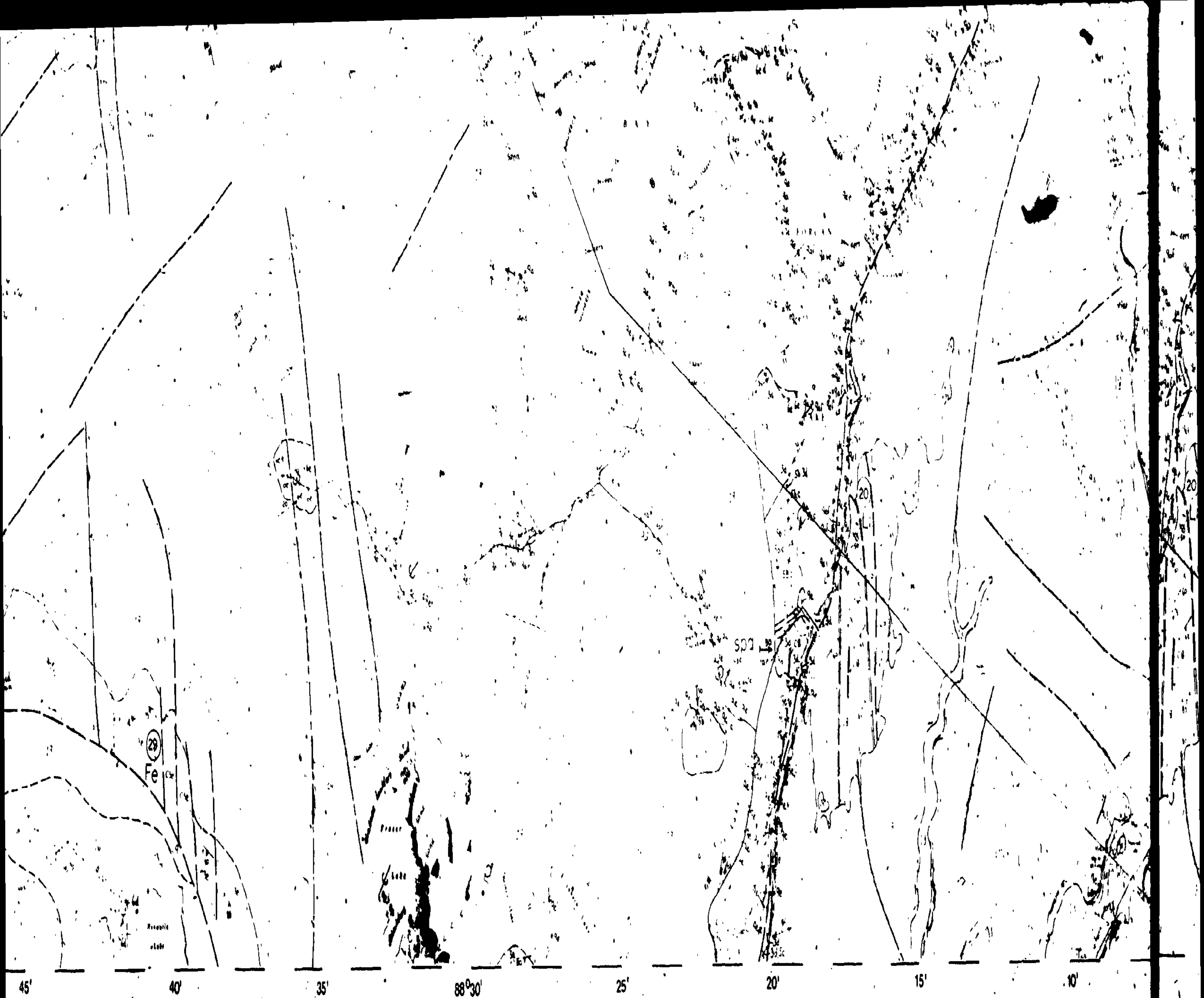
29
Fe
20
L
SPQ
45'
40'
35'
88°30'
25'
20'
15'
10'

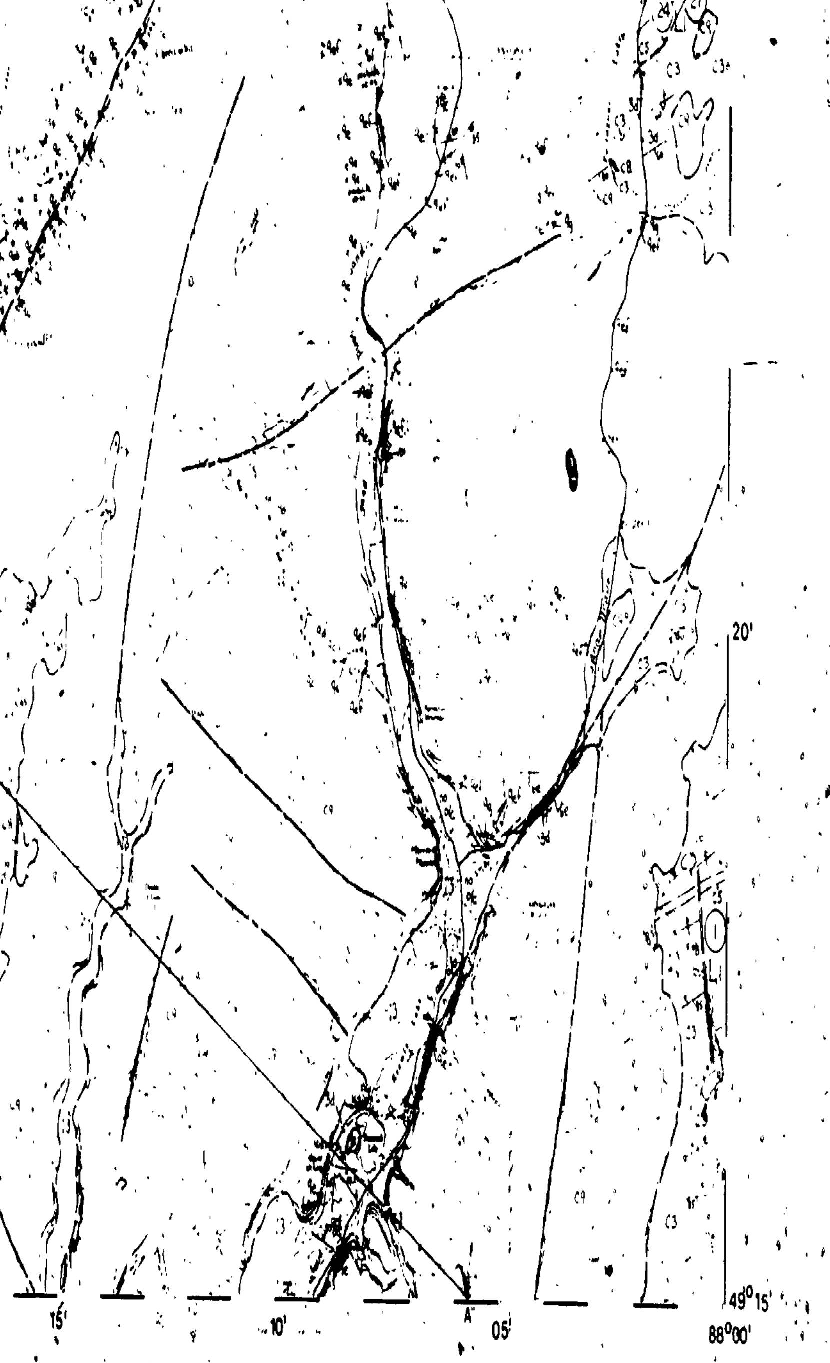

C3
C9
20'
49°15'
88°00'
15'
10'
05'
A'

METAL AND MINERAL ABBREVIATIONS

Ag
asb
Au
Cu
ep
Fe
hem
Li
mag
mo
Pd
qcv
qv
S
serp
spd
Ti
U

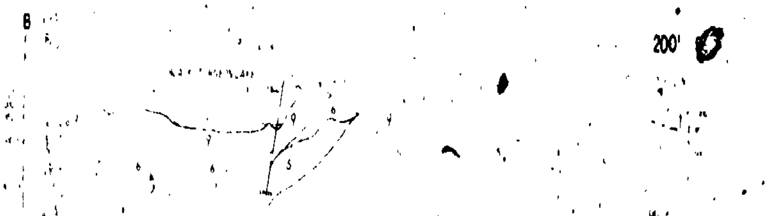

SECTION B B'

SECTION C C'